NASA CR-174799
PWA-5594-271

ENERGY EFFICIENT ENGINE

EXHAUST MIXER MODEL TECHNOLOGY REPORT ADDENDUM

PHASE III TEST PROGRAM

by

M. J. Larkin and J. R. Blatt

UNITED TECHNOLOGIES CORPORATION
Pratt & Whitney
Engineering Division

Prepared for

NATIONAL AERONAUTICS AND SPACE ADMINISTRATION

Lewis Research Center
Cleveland, Ohio 44135

Contract NAS3-20646

1. Report No.	2. Government Accession No.	3. Recipient's Catalog No.
NASA CR-174799		

4. Title and Subtitle	5. Report Date
Energy Efficient Engine Exhaust Mixer Model Technology Report Addendum; Phase III Test Program	April 1984 6. Performing Organization Code
7. Author(s)	8. Performing Org. Rept. No.
M. J. Larkin J. R. Blatt	PWA-5594-271
9. Performing Organization Name and Address	10. Work Unit No.
UNITED TECHNOLOGIES CORPORATION Pratt & Whitney, Engineering Division East Hartford, Connecticut 06108	11. Contract or Grant No. NAS3-20646
12. Sporsoring Agency Name and Address	13. Type Rept./Period Covered
NATIONAL AERONAUTICS AND SPACE ADMINISTRATION Lewis Research Center 21000 Brookpark Road; Cleveland, Ohio 44135	Technology Report 14. Sponsoring Agency Code

15. Supplementary Notes

Project Manager, Mr. C. C. Ciepluch
NASA Lewis Research Center, Cleveland, Ohio 44135

16. Abstract

The Phase III exhaust mixer test program was conducted to explore the trends established during previous Phases I and II. Combinations of mixer design parameters (which Phase I and II testing indicated could result in further improvement in overall performance) were tested. Phase III testing showed that the best performance achievable within tailpipe length and diameter constraints is 2.55 percent better than an optimized separate flow base line. A reduced penetration design achieved about the same overall performance level at a substantially lower level of excess pressure loss but with a small reduction in mixing. This low level of excess pressure loss confirmed Phase II trends.

Accuracy implied by test data repeatability is ±0.2 percent TSFC. To improve reliability of the data, the hot and cold flow thrust coefficient analysis used in Phases I and II was augmented by calculating percent mixing from traverse data. Relative change in percent mixing between configurations was determined from thrust and flow coefficient increments. The calculation procedure developed was found to be a useful tool in assessing mixer performance.

Additionally, detailed flow field data were obtained to facilitate calibration of computer codes such as those being developed under NASA Contract NAS3-23039.

17. Key Words [Suggested by Author(s)]	18. Distribution Statement
Energy Efficient Engines Forced Exhaust Mixers Reduced Mixer Losses	[redacted]

19. Security Class (This Rept)	20. Security Class (This Page)	21. No. Pgs	22. Price *
UNCLASSIFIED	UNCLASSIFIED	197	

*[redacted]

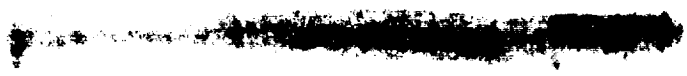

FOREWORD

The Energy Efficient Engine Component Development and Integration program is being conducted under parallel National Aeronautics and Space Administration contracts with Pratt & Whitney and General Electric Company. The overall project is under the direction of Mr. Carl C. Ciepluch. The Pratt & Whitney effort is under Contract NAS3-20646, and Mr. Edward Meleason is the NASA Project Engineer responsible for the portion of the project described in this report. Mr. David E. Gray is Manager of the Energy Efficient Engine Program at Pratt & Whitney. This report was prepared by Mr. M. J. Larkin and Mr. J. R. Blatt of Pratt & Whitney.

TABLE OF CONTENTS

LIST OF ILLUSTRATIONS

LIST OF ILLUSTRATIONS (Continued)

LIST OF ILLUSTRATIONS (Continued)

LIST OF TABLES

SECTION 1.0

1.0 SUMMARY

The Phase III exhaust mixer test program was conducted to explore the trends established during Phases I and II (Ref. 1). Combinations of mixer design parameters, which Phase I and II testing indicated could result in a further improvement in overall performance, were tested. Phase III testing proved that the best performance achievable within the stated tailpipe length and diameter constraints is 2.55 percent better than an optimized separate flow base line. This performance was achieved with approximately 82 percent mixing and 0.27 percent excess pressure loss. A reduced penetration design achieved about the same overall performance improvement (2.53 percent TSFC) at a substantially lower level of excess pressure loss (0.04 percent) but with a small reduction in mixing (76 percent). This low level of excess pressure loss confirmed the Phase II trend that longer, more gentle turning mixers would achieve reduced loss.

The accuracy implied by the data repeatability of this test is $\pm$0.2 percent TSFC. In order to improve the reliability of the data, the hot and cold flow thrust coefficient analysis was augmented by calculating percent mixing from the traverse data. In addition, relative changes in percent mixing between configurations was determined from thrust and flow coefficient increments. This additional procedure for calculating percent mixing from traverse data was found to be a useful tool in assessing mixer performance.

The Phase III program also included testing to obtain flow field information for use in the calibration of computer codes such as those being developed under Contract NAS3-23039. Two different unscalloped Phase II mixer configurations; a deep penetration design and a shallow penetration design, were traversed at the lobe exit to record stagnation temperature, pressure, and flow angle distributions. The lobes and tailpipes were also instrumented with static pressure taps to obtain velocity distributions through the lobes. During Phase II, these same configurations were traversed at the tailpipe exit at these same thermodynamic state points. Consequently, the combination of Phases II and III testing provides flow field data at the entrance to the lobes, through the lobes, at the lobe exit, and at the exit of the mixing chamber.

SECTION 2.0

INTRODUCTION

The Energy Efficient Engine Component Development and Integration Program, sponsored by the National Aeronautics and Space Administration (NASA), is directed toward demonstrating the technology to improve fuel efficiency and to reduce operating economics of future commercial gas-turbine engines. The program goals include a reduction in fuel consumption by a least 12 percent and a reduction in direct operating cost by at least 5 percent relative to a base Pratt & whitney JT9D-7 turbofan engine. To demonstrate the technology to accomplish these goals, the program is organized into two main technical tasks:

Task 1 - Flight Propulsion System Analysis, Design, and Integration;

Task 2 - Component Analysis, Design, and Development.

The work described in this report is a technology program conducted as part of the exhaust mixer system effort in Task 2. This activity was aimed at establishing the basic technology required to define a high performance mixed flow exhaust system for high bypass ratio engines. The performance objective was to demonstrate overall mixed flow exhaust system performance which is equivalent to a reduction of 3.3 percent thrust specific fuel consumption, compared to an optimized separate flow exhaust system equivalent to the Preliminary Design base-line engine of September, 1978. This technology would directly support the design of the Energy Efficient Engine flight propulsion system and the integrated core/low spool engine.

During the detail design of the mixed flow flight propulsion system, the engine became longer and its flow path was modified. The optimized separate flow exhaust system used for comparative purposes, in the mixer technology test program, was unchanged. This resulted in the performance benefit for the mixed flow configuration being reduced to 3.1 percent. The data presented in this report is in the context of the 3.1 percent benefit.

The mixer technology test program itself consisted of three phases spanning the years shown in Figure 1. The first phase employed 28 test configurations covering a wide range of design variables such as tailpipe length, mixer lobe details, turbine swirl, and integration of the structural pylon. After coordinating the results from Phase I with the updated engine design requirements, Phase II was conducted employing 16 test configurations to evaluate additional mixer refinements. the Phase I and II results are presented in NASA Report NASA CR-165459 (Ref. 1). The Phase III work which is described in this report, was conducted employing ten performance configurations aimed at the evaluation of performance improvement trends observed in Phases I and II. Two additional configurations were instrumented to obtain code verification data for use in computer codes such as those being developed under NASA Contract NAS3-23039.

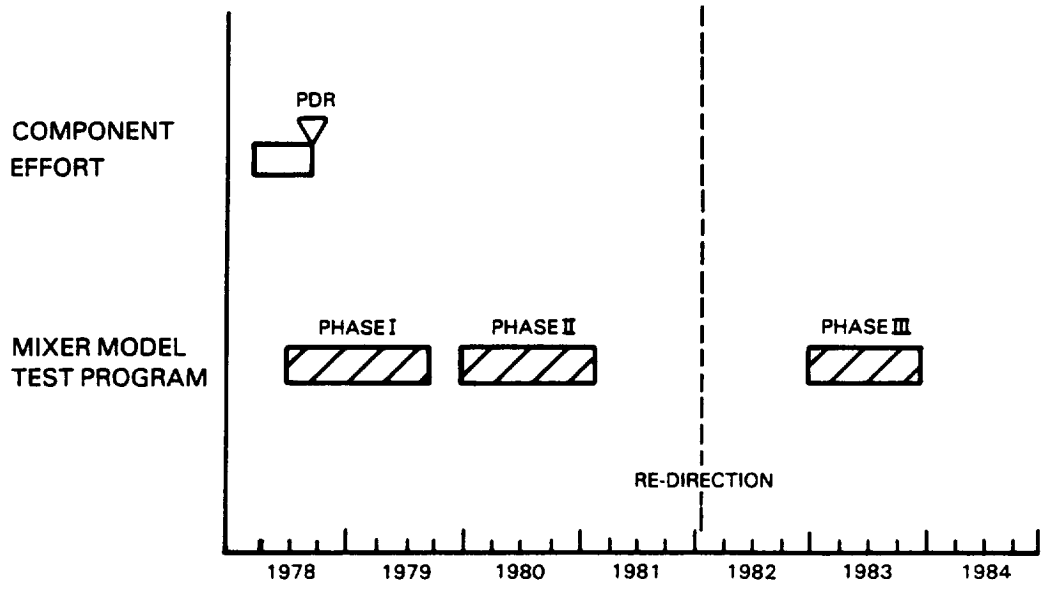

Figure 1 Exhaust Mixer Program

The testing was conducted in the Channel 11 static thrust facility at FluiDyne Engineering Corporation, Minneapolis, Minnesota. Nozzle gross thrust and flow coefficients were measured at both "hot" and "cold" conditions. The "hot" conditions simulated the Energy Efficient Engine flow conditions with a fan/primary total pressure ratio (PT7/PT8) of approximately 1.1 and primary/fan total temperature ratio (TRAT) of approximately 2.5. The "cold" conditions used uniform flow conditions (i.e., PT7/PT8 = 1.0 and TRAT = 1.0). This allowed mixing levels to be calculated and total pressure loss characteristics to be defined for each test configuration, providing important diagnostic information. In addition, total pressure and temperature traverses were taken at the exit of the tailpipe for all of the test configurations, along with oil smear photographs to provide flow visualization in interesting regions of the exhaust system.

This report contains a description of the mixer model aeromechanical design, a description of the test facility and test program, and a discussion of the test results. Major conclusions are also included. Finally, a complete tabulation of the measured data, the exit traverses, and flow visualization photographs are presented in the Appendices.

The mixer model aeromechanical design (Section 3.0) contains the requirements and criteria used in the model design, definition of the test configurations for Phase III, and mixer model fabrication techniques.

The test facility and test program description (Section 4.0) includes detailed test conditions, data acquisition techniques and data reduction methods, and data repeatability characteristics.

Phase III test results (Section 5.0) are discussed in detail, and this section includes test summaries which identify the more significant geometric variables for all configurations tested.

SECTION 3.0

MIXER MODEL AEROMECHANICAL DESIGN

3.1 LIST OF SYMBOLS

a_t	Speed of Sound
A	Cross Sectional Area
A_F	Fan Stream Flow Area
A_P	Primary Stream Flow Area
AGAP	Mixer/Plug Gap Area
AMIX	Mixing Plane Area
APEN	Penetration Area
BPR	Bypass Ratio - Ratio of Measured Fan to Primary Flow
Cf	Skin Friction Coefficient
CDMIX	Mixed Model Flow Coefficient
C_P	Specific Heat
CV'	Full Scale Model Thrust Coefficient
CV"	Overall Gross Thrust Coefficient
CVMIX	Mixed Model Thrust Coefficient
CVEXIT	Exit Plane Thrust Coefficient
DELA	Angular Increment
dl	Incremental Duct Length
D	Tailpipe Diameter at the Mixing Plane
F_x	Axial Momentum
Fg	Gross Thrust
h	Enthalpy
H2	Forced Balance Axial Thrust component
L	Tailpipe Length Measured From Mixing Plane to Exit
MIXP	Ideal Nozzle Performance Gain Available From Mixing
Mn	Mach Number
MnFAN	Mixing Plane Fan Stream Mach Number
MnPRI	Mixing Plane Primary Stream Mach Number
P	Static Pressure
PAM	Ambient Pressure
PRAT	Ratio of Mixing Plane Fan to Primary Stream Total Pressure
P_T	Total Pressure
PTEPAM	Mixing Plane Primary Stream Total to Ambient Nozzle Pressure Ratio
PTFPAM	Mixing Plane Fan Stream Total to Ambient Nozzle Pressure Ratio
PTMPA	Fully Mixed Total to Ambient Nozzle Pressure Ratio
PT7PAM	Charging Station Fan Stream Total to Ambient Nozzle Pressure Ratio
PT8PAM	Charging Station Primary Stream Total to Ambient Nozzle Pressure Ratio

LIST OF SYMBOLS (Cont'd)

R	1/2 Diameter at Mixing Plane
r	Radius
2r	Equivalent Duct Diameter
T	Static Temperature
To	Balance Temperature
TRAT	Ratio of Primary to Fan Stream Total Temperature
T_T	Total Temperature
TTMIX	Full Mixed Total Temperature
TT7	Charging Station Fan Stream Total Temperature
TT8	Charging Station Primary Stream Total Temperature
V	Velocity
W	Flow
WaFAN	Fan Stream Flow
WaPRI	Primary Stream Flow
Y/X	Primary Stream Flow Turning Parameter

Greek Letters:

α	Angle Between Engine Lobe Peak and Mixer Side Wall
β	Average Swirl Angle
γ	Ratio of Specific Heats
Δ	Difference in Levels
ϵ	Angle Between Radial Axis and Absolute Velocity
η_m	Mixer Efficiency
θ	Angle Between Engine Lobe Peak and Fan Valley
λ	Lobe Discharge Angle
μ	Radial Flow Angle
ν	Circumferential Flow Angle
π	Geometric Constant
ρ	Density
ϕ	Local Flow Angle
ψ	Mixer Cutback Angle
ω	Nonaxial Velocity Flow Angle

Subscripts:*

abs	Absolute
C-D	Convergent Divergent Nozzle Effect
F	Fan Stream
i	Traverse Integration Increment
j	Jet
M-FS	Model Full Scale Correction
M	Number of Traverse Probe Positions in the Primary Flow
mix	A Term Based on Mixed Conditions
mix-t	A Mixed Term Evaluated from Nozzle Exit Traverse Data
N	Total Number of Traverse Postions
o	Effective Momentum-Weighted Flow Property for the Unmixed Fan and Primary Flow
P	Primary Stream
partial	Partially Mixed Term
7	Fan Stream Charging Station
8	Primary Stream Charging Station
9	Nozzle Exit
100	Approximated Fully Mixed Flow Property at the Nozzle Exit

* For simplicity, subscripts may be written "on the line" of type, especially in text.

3.2 DESIGN REQUIREMENTS AND CRITERIA

The design criteria used in the Phase III model design are the same as those described in Section 3.2 of NASA CR-165459, except for slight modifications to the mixing plane design areas. In order to better match the Flight Propulsion System bypass ratio, the following areas were used:

Mixing Plane Area (AMIX)	= 276.45 cm^2 (42.85 $in.^2$)
At Mixing Plane -- Primary Stream Area (A_P)	= 68.97 cm^2 (10.69 $in.^2$)
At Mixing Plane -- Fan Stream Area (A_F)	= 207.48 cm^2 (32.16 $in.^2$)

These areas also correspond to the best Phase II configuration (49) which is the base-line for Phase III.

The requirements of Phase III were to capitalize on trends established during Phases I and II and evaluate parameters which would further improve overall performance. The trends were applied to the best Phase II model configuration. That configuration incorporated 18 lobes, a tailpipe length to diameter ratio of 0.61, and scallops and hoods. These parameters were held constant while lobe mixer length, penetration, and lobe discharge angle were evaluated. A sketch defining the major design variables is shown in Figure 2.

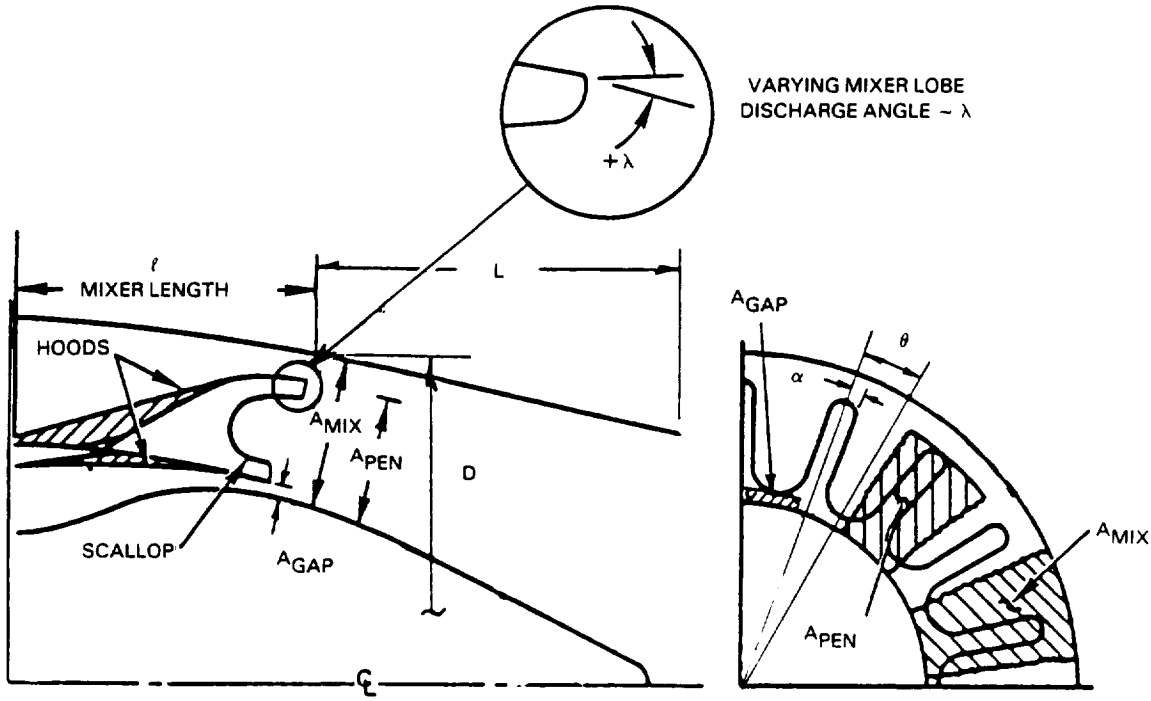

PENETRATION = A_{PEN}/A_{MIX}

TAILPIPE LENGTH/DIAMETER = L/D

MIXER/PLUG GAP = A_{GAP}/A_P

Figure 2 Mixer Test Variables

3.3 MIXER TEST CONFIGURATIONS

Definition of the test configurations for Phase III is provided in this section. The test configurations included are a free mixer in addition to 12 forced mixers. Major design variables are outlined and variations from the baseline design requirements are identified.

Thirteen mixer configurations were tested in the Phase III program. Their configuration numbers and key design parameters are given in Table I. Seven were new configurations, two were made by modifying a Phase II configuration, and the remaining four configurations consisted of a free mixer nozzle (configuration 1) and configurations 49, 29 and 34 from the Phase II program. Retest of the free mixer and configuration 49 provided reference conditions for data repeatability and accuracy. Configurations 34 and 29 were instrumented and used to obtain flow properties through the lobes for codes being developed under NASA Contract NAS3-23039. They were not retested for performance.

TABLE I

PHASE III MIXER DESIGN VARIABALES

Lobe No. = 18; Tailpipe L/D = 0.61

Configuration Type	Conf. No.	Special Features	Penetration	A_{GAP}/A_P	α/θ	Discharge Angle, (degrees)
Performance Test Phase II Design	49	Scalloped, Lobe Hoods	0.72	0.24	0.26	+4
	50	↓	0.72	0.24	0.26	0
	51		0.72	0.24	0.26	-1.5
High Penetration	53	Scalloped, Lobe Hoods, Increased Length	0.75	0.24	0.25	+8
	54	↓	0.75	0.24	0.25	+4
	55		0.75	0.24	0.25	+2
	59		0.75	0.24	0.25	0
	60	Scalloped, Lobe Hoods, Alternating Cut-back, Fan Valley Ramps	0.75	0,0.24	0.25	0,-9
Reduced Penetration	56	Scalloped, Lobe Hoods	0.65	0.24	0.31	+4
	57	↓	0.65	0.24	0.31	-2
Lobe Instrumentation Test	29		0.51	0.22	0.50	-8
	34		0.75	0.22	0.26	0

NOTE: Configurations 52 and 58 were not tested.

The configurations tested for performance had variations in length, penetration, and lobe discharge angle. Test parameters held constant were lobe number (18) and mixing length to diameter ratio (L/D = 0.61). In addition, performance configurations had hoods and scallops while the instrumented mixer did not. These designs along with the free mixers are illustrated in Figures 3 through 9.

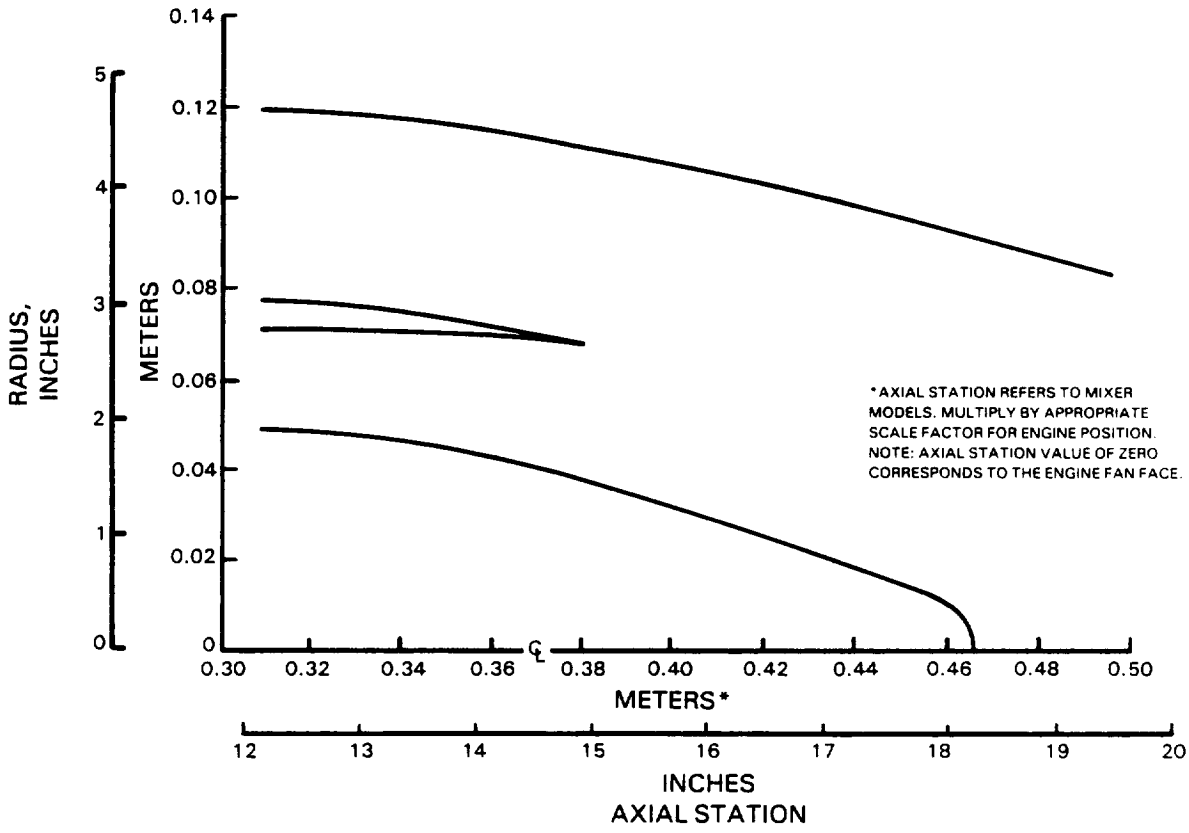

Figure 3 Free Mixer, Configuration 1

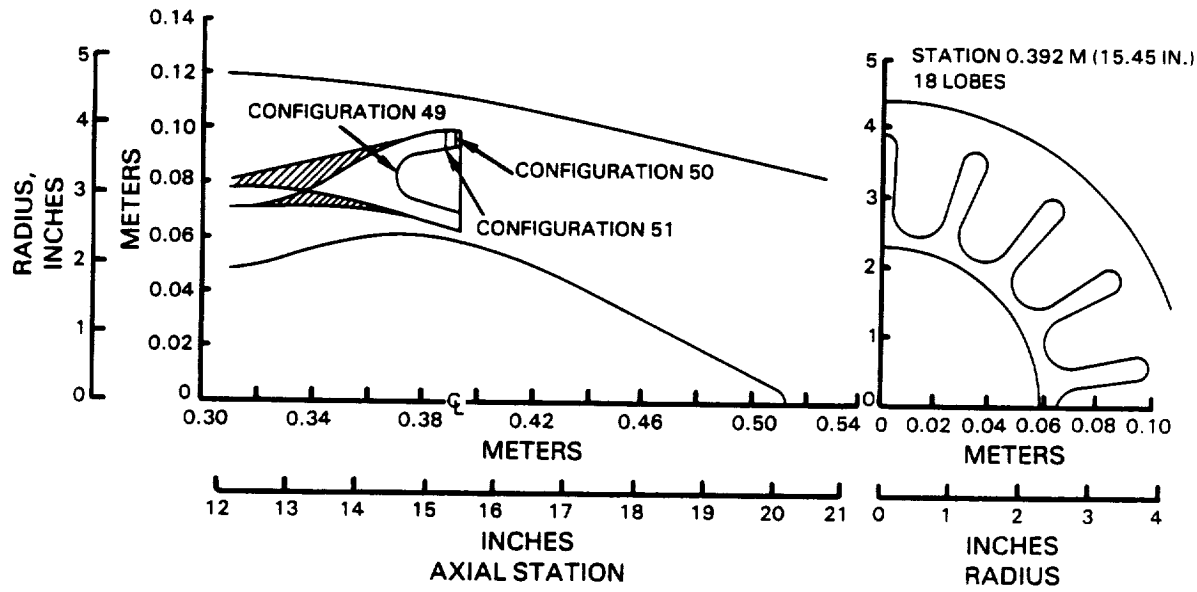

Figure 4 Configurations 49, 50, and 51

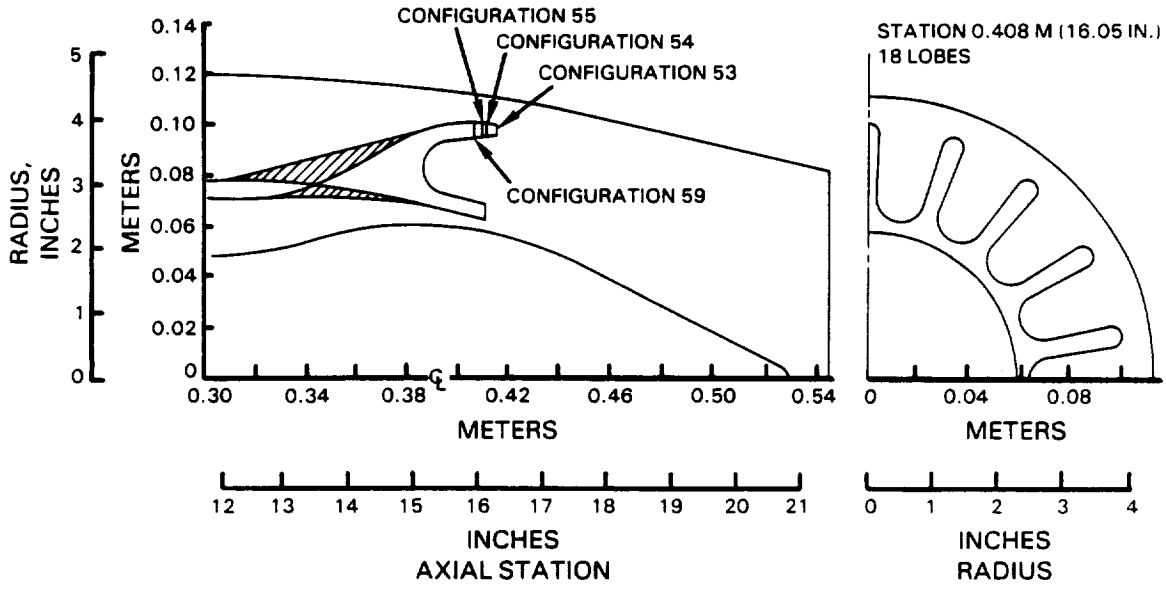

Figure 5 Configurations 53, 54, 55, and 59

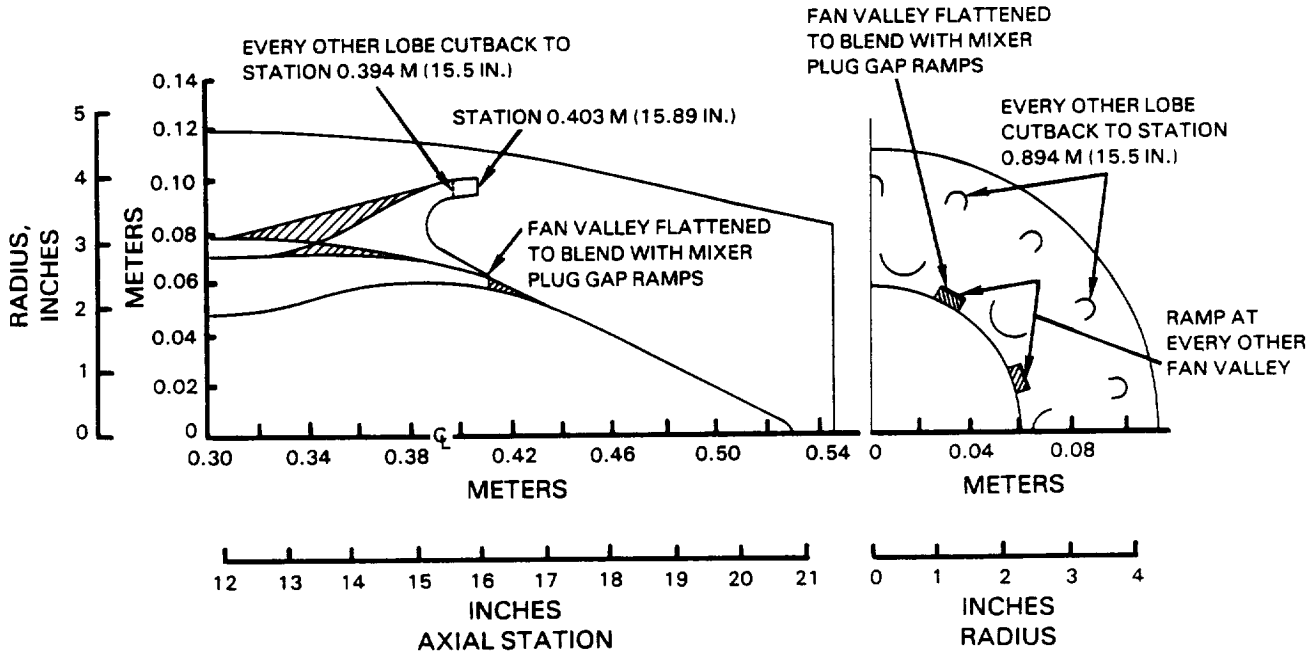

Figure 6 Configuration 60

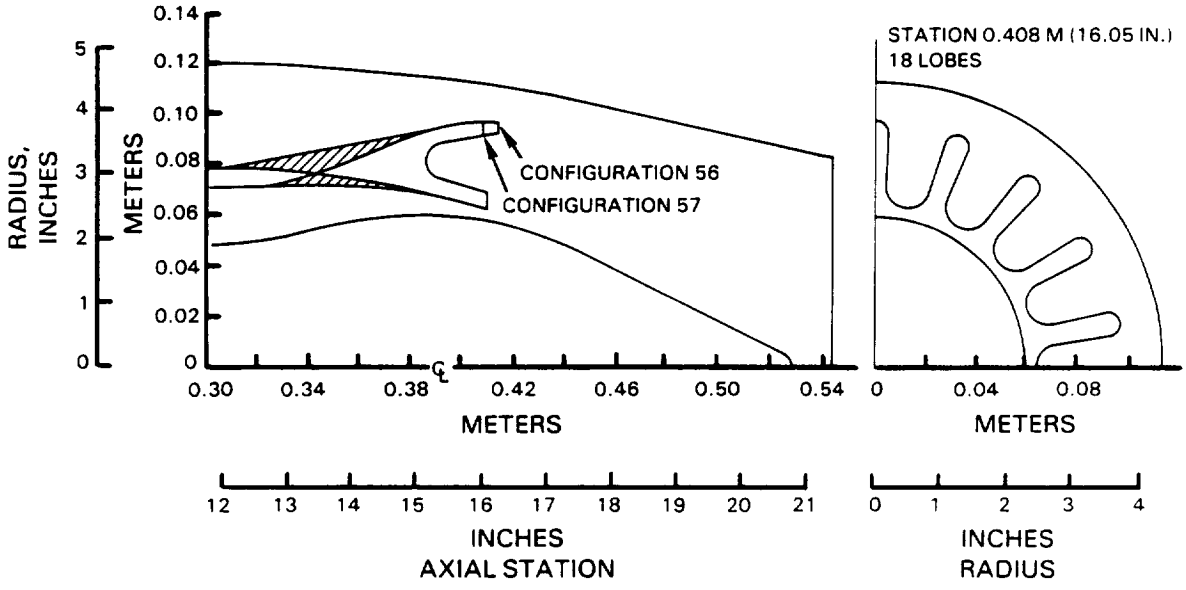

Figure 7 Configurations 56 and 57

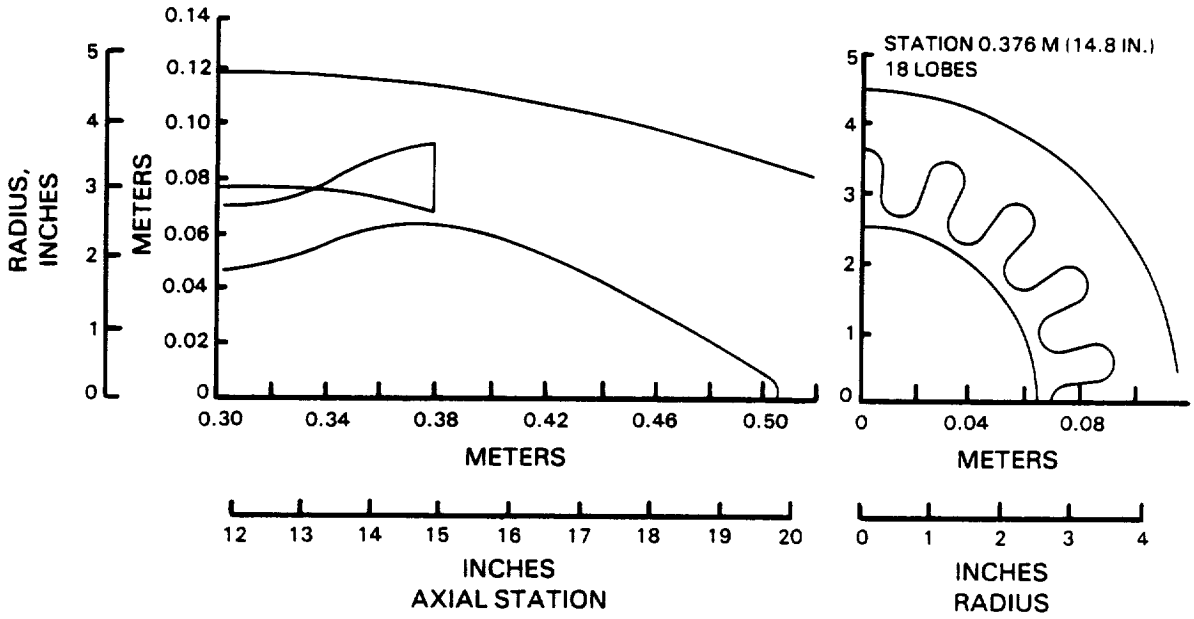

Figure 8 Configuration 29

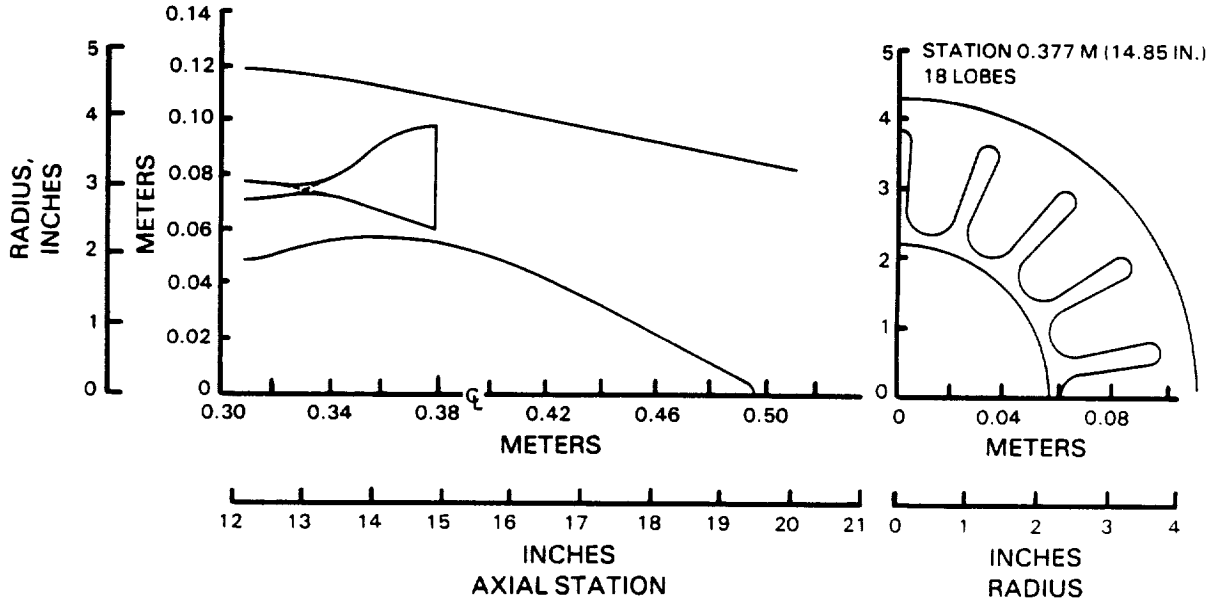

Figure 9 Configuration 34

Performance testing of mixer length variations consisted of one mid-length (configuration 49) and two long mixers (configurations 53 and 56). The mid-length mixer is the best performing mixer from Phase II. The longer mixers, +0.152m (+6 in.) full-scale, provide an improved flowpath with more gentle turning through the lobe.

The importance of lobe discharge angle was investigated with configurations 49 through 51 where the discharge angle was varied by cutting back the mixer lobe. This series provided guidance to cutting back the longer mixers.

The importance of lobe discharge angle for the longer, high penetration mixer was determined with configurations 53, 54, 55 and 59 and for the longer, reduced penetration mixer with configurations 56 and 57. Lobe discharge angle optimization and penetration trades for the long mixer designs can be made by comparing these two series.

In addition, the longer, high penetration mixer (configuration 59) was modified to make a unique configuration (configuration 60). This was done by cutting back every other mixer lobe a significant amount (λ = -9 degrees) and introducing fairings or ramps (reducing the plug gap to zero) between every other fan valley and the plug. This configuration determined the effect of large variations in lobe discharge angle (λ) and the impact of reducing the hot spot associated with the mixer plug gap.

Two short mixers from Phase II (configurations 29 and 34) were used to obtain pressure, temperature, and flow angle data through the lobes to aid in the development of mixer codes such as those being developed under NASA Contract NAS3-23029. Performance, tailpipe exit surveys, and flow visualization tests were completed in Phase II on these two unscalloped mixer designs. Detail geometry definition of these two configurations appears in Appendix D.

3.4 MODEL FABRICATION

Model hardware for both test phases was fabricated at Fluidyne Engineering Corporation. The mixers and plugs were fabricated from 416 stainless steel, and tailpipes from mild steel. The mixers were machined from solid steel blanks to 0.00086 m (0.034 in.) wall thickness. The trailing edge of the mixers was handworked to 0.00025 m (0.010 in.).

Several Phase III configurations were obtained by modifying the original mixers. Mixer number 12 was modified twice by cutting back the mixer lobe to change the discharge angle (λ). This same modification was performed four times on mixer number 13 and once on mixer number 14. In addition, mixer number 13 had every other fan valley flattened to blend with mixer plug gap ramps that were installed on plug number 19.

The mixer, tailpipe, and plug components, identified by number, for each test configuration are summarized in Table II. This table, when used with Figures 3 through 9, identifies the tailpipe and plug used with each mixer modification.

TABLE II

PHASE III TEST CONFIGURATION COMPONENTS

Configuration	Mixer	Tail-Pipe	Plug	Modification
1	1	1	1	
29	6	5	5	
34	10	11	11	
49	12	13	15	
50	12	13	15	Mixer Cutback, λ = 0°
51	12	13	15	Mixer Cutback, λ = -1.5°
53	13	15	19	
54	13	15	19	Mixer Cutback, λ = +4°
55	13	15	19	Mixer Cutback, λ = +2°
59	13	15	19	Mixer Cutback, λ = 0°
60	13	15	19*	Mixer Cutback, λ = 0,-9°
56	14	15	20	
57	14	15	20	Mixer Cutback, λ = -2°

* Ramps Added To Plug

SECTION 4.0

TEST FACILITY AND TEST PROGRAM

4.1 TEST FACILITY

The test program was conducted in the Channel 11 static mixed flow facility at the Medicine Lake laboratory of Fluidyne Engineering Corporation (FEC). This facility is described in Section 4.1 of NASA CR-165459. The multiple-tubed mercury manometer boards used by FEC in the Phase I and II tests to measure static and total pressures were replaced with individual solid state transducers for Phase III testing. There was one transducer for each pressure measurement. This approach, along with a remote communication terminal, reduced performance and survey data reduction turn-around time.

4.2 TEST INSTRUMENTATION

Phase III testing used the same common adapting hardware and instrumentation described in Section 4.2 of Ref. 1, and shown in Figure 10.

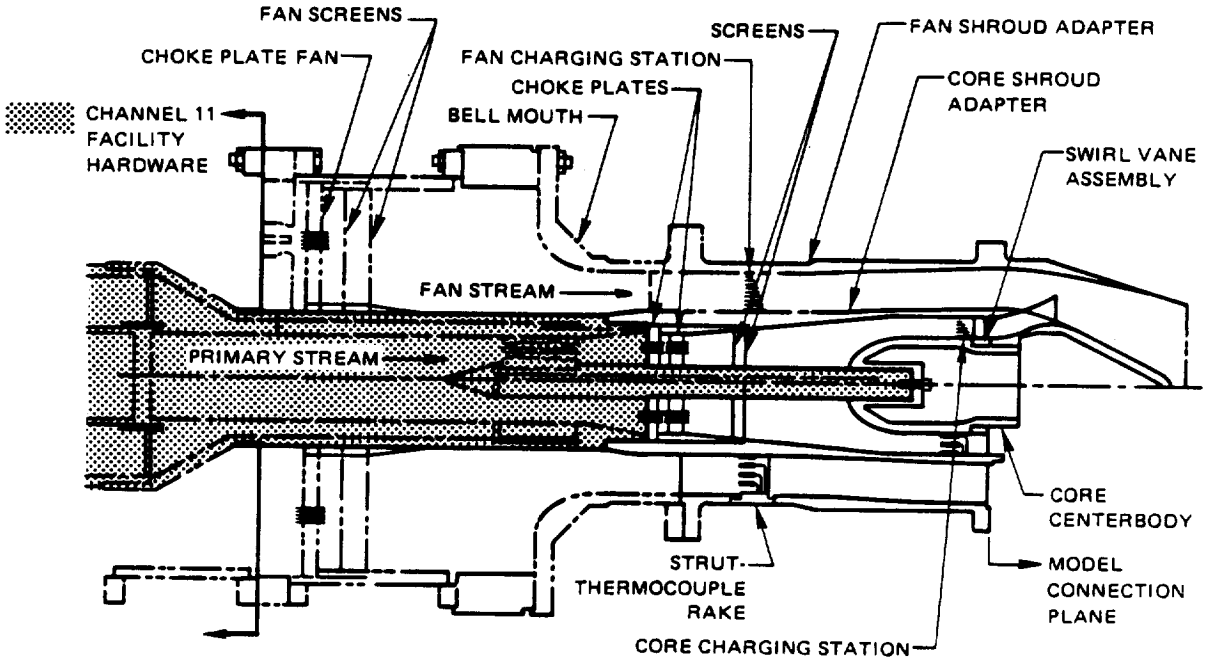

Figure 10 Charging Station Instrumentation Housed in the Model Adapter Section

Also included was a mixer exit survey rake shown in Figure 11, which consists of one 15-probe total temperature rake and a combination 15-probe total pressure/10-probe flow angle survey rake. The temperature and combination pressure/flow angle rake were separated by a 40-degree angle. During each test, pressure and temperature data were acquired at 2.0-degree angular intervals covering a 40-degree segment of the mixer exit for a total of 315 TT and 315 PT data points per test. Flow angle data were acquired in the radial and circumferential directions at 2.0-degree angular intervals over a 40-degree segment for a total of 210 pitch and 210 yaw angle data points per test. A detailed description and the calibration of the flow angle probes is contained in Appendix E.

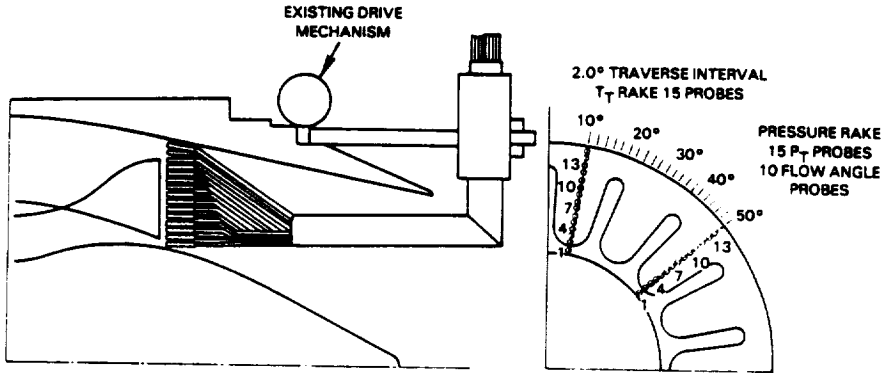

T_T PROBE NO.	P_T PROBE NO.	FLOW ANGLE PROBE NO.	CONFIGURATION 29 RADIUS METERS	CONFIGURATION 29 RADIUS INCHES	CONFIGURATION 34 RADIUS METERS	CONFIGURATION 34 RADIUS INCHES
1	1	1	0.0658	2.590	0.0564	2.220
2	2	2	0.0692	2.723	0.0598	2.353
3	3	3	0.0725	2.856	0.0631	2.486
4	4		0.0759	2.989	0.0665	2.619
5	5	4	0.0793	3.122	0.0699	2.752
6	6		0.0827	3.255	0.0733	2.885
7	7	5	0.0861	3.388	0.0767	3.018
8	8		0.0894	3.521	0.0800	3.151
9	9	6	0.0928	3.654	0.0834	3.284
10	10		0.0962	3.787	0.0868	3.417
11	11	7	0.0996	3.920	0.0902	3.550
12	12	8	0.1029	4.053	0.0935	3.683
13	13	9	0.1063	4.186	0.0969	3.816
14	14	10	0.1096	4.316	0.1003	3.949
15	15		0.1131	4.452	0.1037	4.082

Figure 11 Mixer Exit Traverse Rake Assembly

In addition, surface pressures taps were installed on two Phase II configurations (29 and 34). Configuration 29 acquired a total of 156 model surface pressures through the mixer in the fan (36 tailpipe, 42 mixer) and primary streams (36 plug, 42 mixer). Configuration 34 acquired a total of 162 surface pressures through the fan (36 tailpipe, 45 mixer) and primary (36 plug, 45 tailpipe) streams. The surface pressure locations are shown in Figures 12 and 13 for these configurations. All performance and survey data were recorded by FEC and transmitted to Pratt & Whitney on 9-track static tape via a remote data communication terminal.

Finally, a flow visualization technique was also applied to all performance configurations. The surface of the model was first spray painted white and then a mixture of lampblack and glycerin was applied in an array of spots covering the region of interest. A cold flow test run was then made to establish the airflow pattern on the surface of the models; the model was then disassembled.

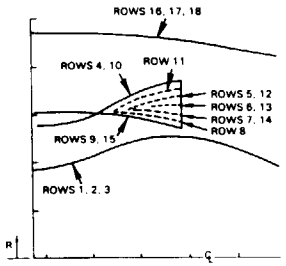

OUTER TAP LOCATION (FAN)

ROW	10	11	12	13	14	15		RADIUS METERS							RADIUS INCHES						
	TAP NUMBER																				
	θ 240°	258°	278°	298°	318°	330°	STATION	240°	258°	278°	298°	318°	330°	STATION	240°	258°	278°	298°	318°	330°
	351	---	367	---	---	383	.3098	.0777	---	.0777	---	---	.0777	12.195	3.059	---	3.059	---	---	3.059
	352	---	368	---	---	384	.3172	.0777	---	.0777	---	---	.0777	12.490	3.059	---	3.059	---	---	3.059
	353	---	369	---	---	385	.3247	.0775	---	.0775	---	---	.0775	12.785	3.050	---	3.050	---	---	3.050
	354	---	370	---	---	386	.3322	.0770	---	.0770	---	---	.0770	13.080	3.032	---	3.032	---	---	3.032
	355	361	371	---	---	387	.3397	.0799	.0788	.0777	---	---	.0762	13.375	3.145	3.104	3.059	---	---	2.999
	356	362	372	---	---	388	.3472	.0843	.0817	.0791	---	---	.0752	13.670	3.317	3.218	3.115	---	---	2.959
	357	363	373	---	---	389	.3547	.0878	.0841	.0803	---	---	.0736	13.965	3.456	3.311	3.160	---	---	2.907
	358	364	374	377	380	390	.362	.0902	.0863	.0823	.0804	.0785	.0723	14.260	3.551	3.399	3.241	3.165	3.059	2.846
	359	365	375	378	381	391	.3697	.0919	.0880	.0839	.0803	.0766	.0706	14.555	3.618	3.464	3.303	3.161	3.016	2.778
	360	366	376	379	382	392	.3765	.0932	.0892	.0851	.0799	.0747	.0688	14.822	3.669	3.513	3.350	3.144	2.939	2.707

INNER TAP LOCATION (PRIMARY)

ROW	4	5	6	7	8	9		RADIUS METERS							RADIUS INCHES						
	TAP NUMBER																				
	θ 120°	138°	158°	178°	198°	210°	STATION	120°	138°	158°	178°	198°	210°	STATION	120°	138°	158°	178°	198°	210°
	301	---	---	317	---	333	.3098	.0707	---	---	.0707	---	.0707	12.195	2.784	---	---	2.784	---	2.784
	302	---	---	318	---	334	.3172	.0713	---	---	.0713	---	.0713	12.490	2.806	---	---	2.806	---	2.806
	303	---	---	319	---	335	.3247	.0724	---	---	.0724	---	.0724	12.735	2.850	---	---	2.850	---	2.850
	304	---	---	320	---	336	.3322	.0751	---	---	.0751	---	.0751	13.080	2.957	---	---	2.957	---	2.957
	305	---	---	321	327	338	.3397	.0789	---	---	.0777	.0764	.0752	13.375	3.105	---	---	3.059	3.008	2.963
	306	---	---	322	328	338	.3472	.0832	---	---	.0791	.0766	.0742	13.670	3.277	---	---	3.115	3.016	2.923
	307	---	---	323	329	339	.3547	.0868	--	---	.0800	.0764	.0729	13.965	3.418	---	---	3.148	3.007	2.871
	308	311	314	324	330	340	.3622	.0893	0823	.0804	.0785	.0749	.0714	14.260	3.515	3.241	3.165	3.089	2.947	2.810
	309	312	315	325	331	341	.3697	.0910	.0839	.0803	.0766	.0731	.0696	14.555	3.582	3.303	3.161	3.016	2.876	2.742
	310	313	316	326	332	342	.3765	.0923	0851	.0799	.0747	.0712	.0670	14.827	3.633	3.350	3.144	2.939	2.802	2.671

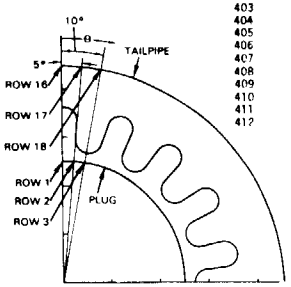

TAILPIPE/ROW

θ	16	17	18	STA. METERS	STA. INCHES
	TAD NUMBER				
0°	5°	10°			
401	413	425		.3023	11.90
402	414	426		.3098	12.195
403	415	427		.3172	12.490
404	416	428		.3247	12.785
405	417	429		.3322	13.080
406	418	430		.3397	13.375
407	419	431		.3472	13.670
408	420	432		.3547	13.965
409	421	433		.3622	14.260
410	422	434		.3697	14.555
411	423	435		.3772	14.850
412	424	436		.3810	15.000

PLUG ROW

θ	1	2	3	STA. METERS	STA. INCHES
	TAP NUMBER				
0°	5°	10°			
101	113	125		.3023	11.900
102	114	126		.3098	12.195
103	115	127		.3172	12.490
104	116	128		.3247	12.785
105	117	129		.3322	13.080
106	118	130		.3397	13.375
107	119	131		.3472	13.670
108	120	132		.3547	13.965
109	121	133		.3622	14.260
110	122	134		.3697	14.555
111	123	135		.3772	14.850
112	124	136		.3810	15.000

Figure 12 Configuration 29 Surface Pressure-Tap Locations

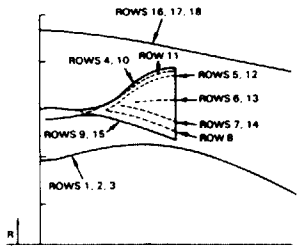

OUTER TAP LOCATION (FAN)

ROW	10	11	12	13	14	15		RADIUS METERS							RADIUS INCHES						
	TAP NUMBER																				
	θ 240°	258°	278	298°	316°	330°	STATION	240°	258°	278°	298°	318°	330°	STATION	240°	258°	278°	298°	318°	330°
	351	----	367	----	----	386	.3098	.0777	---	.0772	---	---	.0772	12.195	3.041	---	3.041	---	---	3.041
	352	----	368	----	----	387	.3172	.0766	---	.0766	---	---	.0766	12.490	3.015	---	3.015	---	---	3.015
	353	----	369	----	----	388	.3247	.0759	---	.0757	---	---	.0755	12.785	2.990	---	2.980	---	---	2.971
	354	----	370	----	----	389	.3322	.0766	---	.0760	---	---	.0741	13.080	3.015	---	2.992	---	---	2.917
	355	361	371	----	----	390	.3397	.0792	.0783	.0769	---	---	.0723	13.375	3.120	3.082	3.029	---	---	2.847
	356	362	372	----	381	391	.3472	.0843	.0825	.0800	---	0791	.0703	13.670	3.317	3.240	3.150	---	3.115	2.766
	357	363	373	377	382	392	.3547	.0899	.0878	.0854	.0811	.0768	.0680	13.965	3.541	3.458	3.362	3.191	3.024	2.678
	358	364	374	378	383	393	.3622	.0946	.0974	.0898	.0815	.0740	.0655	14.260	3.725	3.637	3.535	3.210	2.915	2.577
	359	365	375	379	384	394	.3697	.0975	.0953	.0927	.0818	.0710	.0628	14.555	3.838	3.752	3.650	3.219	2.795	2.472
	360	366	376	380	385	395	.3765	.0984	.0962	.0935	.0808	.0678	.0601	14.822	3.875	3.786	3.680	3.130	2.670	2.365

INNER TAP LOCATION (PRIMARY)

ROW	4	5	6	7	8	9		RADIUS METERS							RADIUS INCHES						
	TAP NUMBER																				
	θ 120°	138°	158°	178°	198°	210°	STATION	120°	138°	158°	178°	198°	210°	STATION	120°	138°	158°	178°	198°	210°
	301	----	----	320	----	336	.3078	.0706	---	---	.0706	---	.0706	12.195	2.781	---	---	2.781	---	2.781
	302	----	----	321	----	337	.3172	.0712	---	---	.0712	---	.0712	12.490	2.802	---	---	2.502	---	2.802
	303	----	----	322	----	338	.3247	.0724	---	---	.0724	---	.0724	12.785	2.852	---	---	2.552	---	2.852
	304	----	----	323	----	339	.3322	.0747	---	---	.0740	---	.0726	13.080	2.940	---	---	2.912	---	2.860
	305	----	----	324	330	340	.3397	.0782	---	---	.0759	.0740	.0714	13.375	3.080	---	---	3.029	2.915	2.811
	306	311	----	325	331	341	.3472	.0831	.0800	---	.0791	.0739	.0693	13.670	3.273	3.150	---	3.115	2.911	2.730
	307	312	316	326	332	342	.3547	.0888	.0854	.0811	.0768	.0718	.0671	13.965	3.497	3.362	3.191	3.024	2.825	2.642
	308	313	317	327	333	343	.3622	.0936	.0898	.0815	.0740	.0691	.0645	14.260	3.685	3.535	3.210	2.915	2.720	2.541
	309	314	318	328	334	344	.3697	.0966	.0927	.0818	.0710	.0662	.0619	14.565	3.802	3.650	3.219	2.795	2.608	2.436
	310	315	319	329	335	345	.3765	.0975	.0935	.0808	.0678	.0633	.0592	14.822	3.839	3.680	3.100	2.670	2.492	2.329

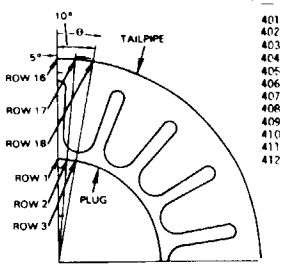

TAILPIPE/PDM

16	17	18			
	TAP NUMBER				
θ 0°	5°	10°	STA. METERS	STA. INCHES	
401	413	425	.3023	11.90	
402	414	426	.3098	12.195	
403	415	427	.3172	12.490	
404	416	428	.3247	12.785	
405	417	429	.3322	13.080	
406	418	430	.3397	13.375	
407	419	431	.3472	13.670	
408	420	432	.3547	13.965	
409	421	433	.3622	14.260	
410	422	434	.3617	14.556	
411	423	435	.3772	14.850	
412	424	436	.3810	15.000	

PLUG ROW

1	2	3		
TAP NUMBER				
θ 0°	5°	10°	STA. METERS	STA. INCHES
101	113	125	.3023	11.900
102	114	126	.3098	12.195
103	115	127	.3172	12.490
104	116	128	.3247	12.785
105	117	129	.3322	13.080
106	118	130	.3397	13.375
107	119	131	.3472	13.670
108	120	132	.3547	13.965
109	121	133	.3622	14.260
110	122	134	.3697	14.555
111	123	135	.3772	14.850
112	124	136	.3810	15.000

Figure 13 Configuration 34 Surface Pressure-Tap Locations

4.3 TEST PROGRAM

This section discusses the actual test conditions, data acquisition and reduction, and an evaluation of the data repeatability. The test conditions were based on simulation of Energy Efficient Engine Flight Propulsion System flow conditions. The data acquisition and reduction section describes the aerodynamic performance parameters acquired, the mixer and exit plane traverse measurements which were made, and the flow visualization information which was obtained. Finally, data repeatability is evaluated with a statistical evaluation of the free mixer test data, which represents the largest sampling of data available.

4.3.1 Test Conditions

The test conditions covered in the Phase III program simulated a range of cruise power settings for the Flight Propulsion System, at Mach 0.8, 10,668 m (35,000 feet). Each performance evaluation covered a range of cruise power settings(from approximately 88 to 110 percent) as defined in Table III. Each hot flow test point is defined by a primary stream pressure ratio (PT8/PAM), a fan to primary stream total pressure ratio (PT7/PT8) and a primary to fan stream total temperature ratio (TRAT). The cold flow test consisted of a range of pressure ratios which duplicate the range of mixed pressure ratios associated with the engine power setting variation. Hot and cold flow condition number 2, which corresponds to the maximum cruise condition, was repeated twice to provide data reliability and accuracy. This procedure facilitates calculation of the level of mixing and the amount of excess pressure loss exhibited by the test configuration.

The nozzle and mixer exit traverses were made at condition number 2 of the hot flow test; the flow visualization tests were conducted at the comparable cold flow condition.

TABLE III

PHASE III TEST CONDITIONS

Condition Number	Primary Stream Pressure Ratio PT8PAM	Fan to Primary Stream Pressure Ratio (PT7/PT8)	Primary to Fan Stream Temperature Ratio (TRAT)
Hot Flow Tests			
1	2.2	1.11	2.44
2	2.35	1.10	2.50 (Repeat Twice)
3	2.4	1.09	2.56
Cold Flow Tests			
1	2.4	1.00	1.00
2	2.5	1.00	1.00 (Repeat Twice)
3	2.6	1.00	1.00
Nozzle and Mixer Exit Traverse	(see condition 2 of the hot flow test series)		
Flow Visualization			
PT8PAM = PT7PAM = 2.5 TRAT = 1.0			

4.3.2 Data Acquisition and Reduction

The experimental data produced during the Phase III program are described in this section. This includes several new methods used to determine the major aerodynamic performance parameters in addition to the one described in Section 4.3.2 of NASA CR-165459. Also included is the method used to determine the nonaxial velocity at the mixer exit plane for two previously tested Phase II configurations.

4.3.2.1 Traverse Integration Analysis

Two mixing functions were defined for calculating mixing efficiency from the nozzle exit traverse data: 1) a total temperature function, and 2) a gross thrust function. These methods for calculating mixing are independent of thrust balance force measurements and require only hot flow testing at simulated engine operating temperatures and pressures. Both mixing functions were used to minimize the possibility that definitional assumptions would bias the result. Percent mixing is evaluated from gross thrust terms using the same fundamental definition that was applied to the thrust balance measurements. The mixing functions are distinguished by the rigor of the definitions. The temperature mixing function approximates the gross thrust terms. The thrust terms are assumed to be proportional to the root of total temperature ($\sqrt{TT}$). In the case of the thrust function, an exact definition of gross thrust is specified. The equations which define the temperature mixing and thrust mixing functions are described in the following paragraphs.

The fundamental definition of mixing efficiency (η_m) as defined by gross thrust terms is:

$$\eta_m = \frac{\left(\frac{F_{g\ partial}}{F_{g\ fully\ mixed}}\right)_{\substack{partially\\mixed\\term}} - \left(\frac{F_{g\ fan} + F_{g\ primary}}{F_{g\ fully\ mixed}}\right)_{\substack{unmixed\\term}}}{1 - \left(\frac{F_{g\ fan} + F_{g\ primary}}{F_{g\ fully\ mixed}}\right)_{\substack{unmixed\\term}}}$$

The unmixed term is an analytical construct in that the fan and primary stream gross thrust are determined by expanding the fan and primary stream through the nozzle without mixing, that is, the streams are separated by a slip line along which the streams are in local static pressure balance.

In the case of the temperature mixing function, the gross thrust terms are evaluated with the following approximations and assumptions:

1. $Fg \propto W\sqrt{TT}$;

2. The nozzle exit velocity is assumed to be parallel to the nozzle centerline;

3. Each streamtube of the flow is expanded to ambient. If the streamtube flow is supersonic, the Mach number is set equal to one; and

4. Cp = constant

The thrust terms are functions of venturi-measured flows (WaFAN and WaPRI), charging station pressures and temperatures (TT7, TT8, PT7 and PT8), and the nozzle exit total temperature and total pressure distributions (TTi and PTi). The partially mixed term is evaluated from the nozzle exit traverse measurements.

$$\left(\frac{F_{g\ partial}}{F_{g\ fully\ mixed}}\right)_{\substack{partially\\mixed\\term}} = \sum_{i=1,N}\left\{\frac{W_i}{\sum_{i=1,N} W_i}\sqrt{\frac{T_{T_i}}{T_{T_{mix-t}}}}\right\}$$

Where Wi is a local flow increment, defined as

$$Wi = f(PTi, TTi, PAM, Ai)$$

The mixed total temperature is evaluated from the traverse measurements.

$$T_{T_{mix-t}} = \frac{\sum_{i=1,N}\left(W_i\ T_{T_i}\right)}{\sum_{i=1,N} W_i}$$

The integration is conducted for N traverse probe positions, each of which is associated with an incremental area (Ai).

The unmixed term is evaluated from the charging station properties and venturi measured flows.

$$\left(\frac{F_{g\ fan} + F_{g\ primary}}{F_{g\ fully\ mixed}}\right)_{\substack{unmixed\\term}} = \left\{ \sqrt{\frac{T_{T_7}}{T_{T_{mix}}}}\left(1 - \frac{1}{(1+BPR)}\right) + \sqrt{\frac{T_{T_8}}{T_{T_{mix}}}}\left(\frac{1}{(1+BPR)}\right) \right\}$$

Where: $BPR = \frac{W_{a\ FAN}}{W_{a\ PRI}}$

The fully mixed total temperature (TTmix) is obtained from the mixing calculation procedure which is outlined in Appendix A of the Phase I and II report (NASA CR-165459).

In the case of the thrust mixing function, an exact definition of the gross thrust terms is specified. The gross thrust terms are evaluated with the following assumptions and approximations:

1. The fully mixed pressure at the nozzle exit is approximated;
2. Cp = constant; and
3. The nozzle exit local static pressure and radial flow angle are analytically estimated.

The partially mixed term in the fundamental mixing efficiency equation is evaluated from the venturi measured flows, the charging station measurements, the nozzle exit traverse measurements, an approximation of the fully mixed nozzle exit total pressure, and the estimated nozzle exit static pressure and flow angle distribution. The partially mixed term is a ratio of partial and fully mixed gross thrusts. This ratio is initially calculated as a function of the measured model jet area and then modified to reflect the thrust ratio that would be obtained with equal flows for both the partially mixed and fully mixed terms, that is, the fully mixed condition requires a relatively larger jet area to pass the same flow as the partially mixed condition.

$$\left(\frac{F_{g\ partial}}{F_{g\ fully\ mixed}}\right)_{\substack{partially\\mixed\\term}} = \left\{ \frac{\sum_{i=1,N}\left[\left(F_{x_i}\right)_{partial} + (P_i - PAM)A_i\right]}{\sum_{i=1,N}\left(F_{x_i}\right)_{mix-t}} \right\} \left\{ \frac{\sum_{i=1,N}\left(W_i\right)_{mix-t}}{\sum_{i=1,N}\left(W_i\right)_{partial}} \right\}$$

(Fxi)partial, (Wi)partial, and (Wi)MIX-T are local axial momentum and flow increments in the exhaust flow at the nozzle exit. The momentum of the fully mixed flow is determined by expanding the flow increments of the mixed flow to ambient pressure. Where:

$$\left(F_{x_i}\right) \text{ and } \left(W_i\right)_{\text{partial}} = f\left(P_{T_i},\ T_{T_i},\ P_i,\ A_i, \phi_j\right)$$

$$\left(W_i\right)_{\text{mix-t}} = f\left(P_{T100}, T_{T_{\text{mix-t}}}, P_i,\ A_i, \phi_j\right)$$

$$\left(F_{x_i}\right)_{\text{mix-t}} = f\left(W_{i\ \text{mix-t}},\ P_{T100},\ T_{T_{\text{mix-t}}},\ PAM\right)$$

$$T_{T_{\text{mix-t}}} = \frac{\sum_{i=1,N}\left[\left(W_i\right)_{\text{partial}}\ T_{T_i}\right]}{\sum_{i=1,N}\left(W_i\right)_{\text{partial}}}$$

Pi and ϕj are the nozzle exit local static pressure and flow angle, respectively, where:

$$Pi = PTi\ (P/PT)_{\text{analytical}}$$

Since only throat plane stagnation properties were measured during each nozzle traverse, local static pressure (P/PT) and radial variations in local flow angle were estimated with the VNAP II computer program. VNAP is a two-dimensional, time dependent, compressible, turbulent flow code developed at the Los Alamos Scientific Laboratory (Ref. 2). The VNAP prediction for the transonic flow field through the separate flow and mixed nozzles was made with no-slip walls and a free expansion plume. The estimated throat static pressure (P/PT) and flow angle (ϕj) contours are shown in Figure 14. Local flow angle variations resulting from mixer generated secondary flows are not predicted by this analysis.

The fully mixed total pressure at the nozzle exit (PT 100) is approximated by linear extrapolation from an effective partially mixed total pressure (PTpartial) as illustrated in Figure 15. This procedure is iterative since percent mixing is not initially known. The slope of the extrapolation is determined by the relationship between the effective unmixed total pressure (PTo) and the fully mixed total pressure at the mixing plane (PTmix). This relationship is assumed to be a linear function of percent mixing. In equation form, the fully mixed total pressure at the nozzle exit is:

$$P_{T\ 100} = P_{T\text{partial}} - \left\{\left(P_{To} - P_{T\text{mix}}\right)\left[(100 - \%\ \text{mix})/100\right]\right\}$$

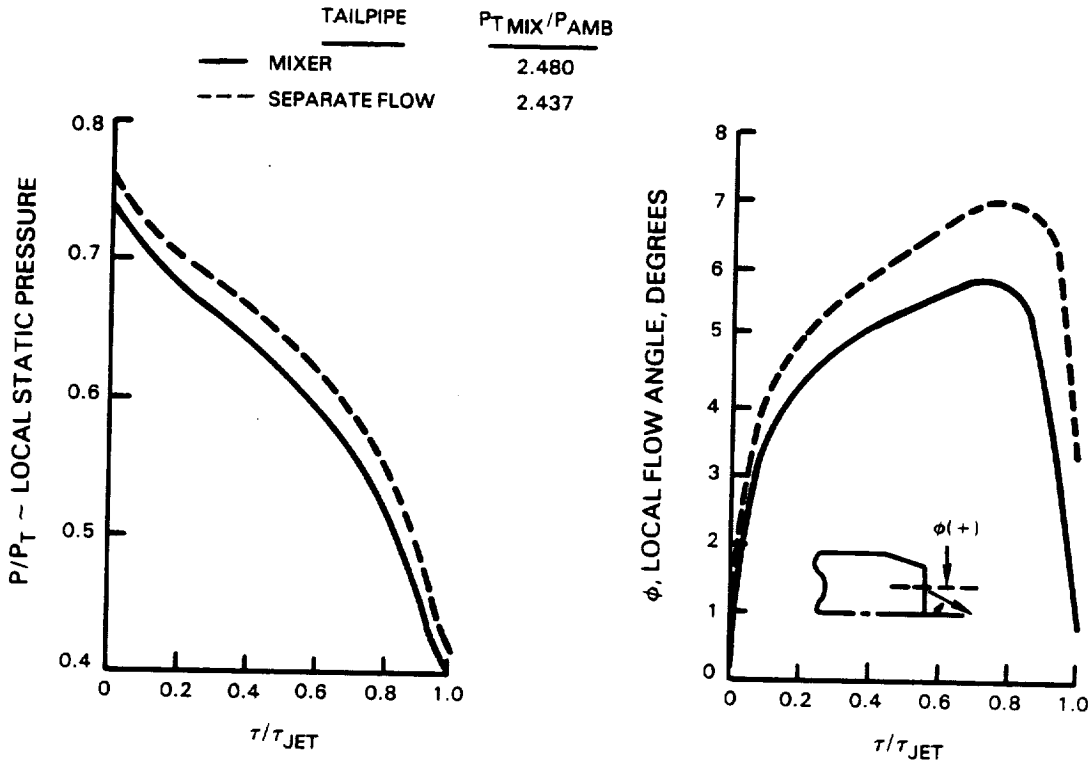

Figure 14 Estimated Throat Plane Static Pressure and Flow Angle Distribution

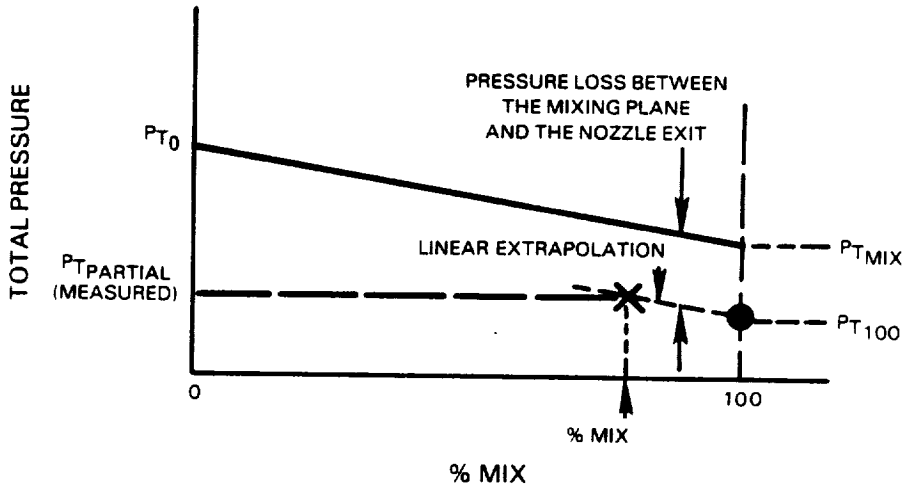

Figure 15 Calculation of the Fully Mixed Nozzle Exit Total Pressure (PT 100)

The fully mixed total pressure is obtained from the mixing calculation procedure. The unmixed total pressure (PTo) is defined as an effective momentum weighted total pressure which is a function of the mixer exit stagnation properties, venturi measured fan and primary flow, and the nozzle exit static pressure distribution.

$$P_{T_o} = \frac{P_{T_F} \int_{A_{F9}} (F_{x_i})_F + P_{T_p} \int_{A_{P9}} (F_{x_i})_p}{\int_{A_{F9}} (F_{x_i})_F + \int_{A_{P9}} (F_{x_i})_p}$$

where: $(F_{xi})_F = f(P_{TF}, T_{T7}, Pi, A_{F9}, \phi j)$
$(F_{xi})_P = f(P_{TP}, T_{T8}, Pi, A_{P9}, \phi j)$

Note that the fan and primary total pressures (PTF and PTP) are mixing plane pressures which are determined from the charging station measurements by accounting for the skin friction losses between the mixing plane and mixer exit. The flow areas of the unmixed fan and primary streams at the nozzle exit (AF9 and AP9) are determined iteratively.

$$A_{F9} + A_{P9} = f(P_{TF}, P_{TP}, T_{T7}, T_{T8}, P_j, WaFAN, WaPRI, \phi j, Aj)$$

The partially mixed total pressure (PTpartial) is defined as a momentum weighted total pressure which is a function of the nozzle exit traverse measurements.

$$P_{T\ partial} = \frac{\sum_{i=1,N} P_{T_i} \left(F_{x_i}\right)_{partial}}{\sum_{i=1,N} \left(F_{x_i}\right)_{partial}}$$

where $(F_{xi})_{partial} = f(P_{Ti}, T_{Ti}, P_j, A_i, \phi j)$

The unmixed term in the fundamental mixing efficiency equation is evaluated from the venturi measured flows, the charging station measurements, and the estimated nozzle exit static pressure and flow angle distribution. As in the case of the partially mixed term, the gross thrust ratio is initially calculated as a function of the measured nozzle exit area, and then modified to reflect the thrust ratio that would be obtained with equal flows for the mixed and unmixed terms.

$$\left(\frac{F_{g\ fan} + F_{g\ primary}}{F_{g\ fully\ mixed}}\right)_{\substack{unmixed\\term}} = \left\{\frac{\sum_{i=1,M}(F_{x_i})_{primary} + \sum_{i=M+1,N}(F_{x_i})_{fan} + \sum_{i=1,N}(P_i - PAM)A_i}{\sum_{i=1,N}(F_{x_{i_{mix}}})}\right\}\left\{\frac{\sum_{i=1,N}(W_i)_{mix}}{\sum_{i=1,M}(W_i)_{primary} + \sum_{i=M,N}(W_i)_{fan}}\right\}$$

$(Fxi)primary$, $(Fxi)fan$, $(Wi)primary$, $(Wi)fan$, and $(Wi)mix$ are local axial momentum and flow increments in the exhaust flow at the nozzle exit. The fan stream and primary stream momentum and flow increments are summed for M increments of the primary flow and (N-M) increments of the fan flow. The momentum of the fully mixed flow, $(Fxi)mix$, is determined by expanding the flow increments of the mixed flow to ambient pressure, where:

$$(F_{x_i})_{primary} \text{ and } (W_i)_{primary} = f(P_{T_p}, T_{T_8}, P_i, \phi_j, A_{F_9})$$

$$(F_{x_i})_{fan} \text{ and } (W_i)_{fan} = f(P_{T_F}, T_{T_7}, P_i, \phi_j, A_{P_9})$$

$$(W_i)_{mix} = f(P_{T_{mix}}, T_{T_{mix}}, P_i, \phi_j, A_j)$$

$$(F_{x_i})_{mix} = f((W_i)_{mix}, P_{T_{mix}}, T_{T_{mix}}, PAM)$$

For both mixing functions, the integration is conducted for N traverse probe positions, each of which is associated with an incremental area (Ai). Local area increments were calculated for each rake position as shown below.

$$Ai = \left\{[(ri+1)^2 - (ri)^2] + [(ri)^2 - (ri-1)^2]\right\}[(\pi/2)\ (DELA/360)]$$

where: r = temperature probe radius, and
DELA = angular increment

For the first and last rake positions: $Ai = Ai/2.0$.

The total number of increments in the integration procedure was equal to the number of temperature probe positions. The radial positions of the temperature and pressure probes were identical except for the inner temperature probe where there was no corresponding pressure probe. The total pressure at this position was obtained by extrapolation. The nozzle exit static pressure values were interpolated from a cubic spline fit of the predicted static pressure distribution.

4.3.2.2 Secondary Methods for Calculating Percent Mixing

Percent mixing was evaluated by a third (III) and forth (IV) method in addition to the hot and cold flow thrust and traverse mixing function approaches. These methods utilize increments of thrust coefficient (ΔCVmix) and/or flow coefficient (ΔCDmix) to evaluate changes in mixing and pressure loss relative to a base.

A thrust coefficient increment may be considered as a sum of skin friction, mixing, and excess pressure loss components. The contribution of mixing and excess pressure loss to the increment were isolated by analytically estimating the impact of skin friction on the increment. The mixing and excess pressure loss components were then determined by solving two independent linear equations derived from the thrust coefficient increments.

In the case of Method III, two hot flow performance coefficient increments (ΔCVmix and ΔCDmix) were used to define two independent linear equations which relate excess pressure loss ($\Delta(\Delta PT/PT)$ and percent mixing increments. These relationships were assumed to be linear, since the influence of pressure loss or mixing increments on thrust or flow coefficient are essentially constant for any two configurations tested at similar conditions. A root of these two linear equations approximates the solution for the excess pressure loss and percent mixing increments between the two configurations.

In the case of the fourth method, increments of flow coefficient (hot flow) and cold flow thrust coefficient are used to estimate an increment in percent mixing relative to the base configuration.

These two methods are illustrated in Figure 16. Method III is shown as a typical solution for a decrease in thrust coefficient and an increase in flow coefficient relative to the base. Method IV is shown as a typical solution for an increase in flow coefficient and increase in thrust coefficient relative to the base.

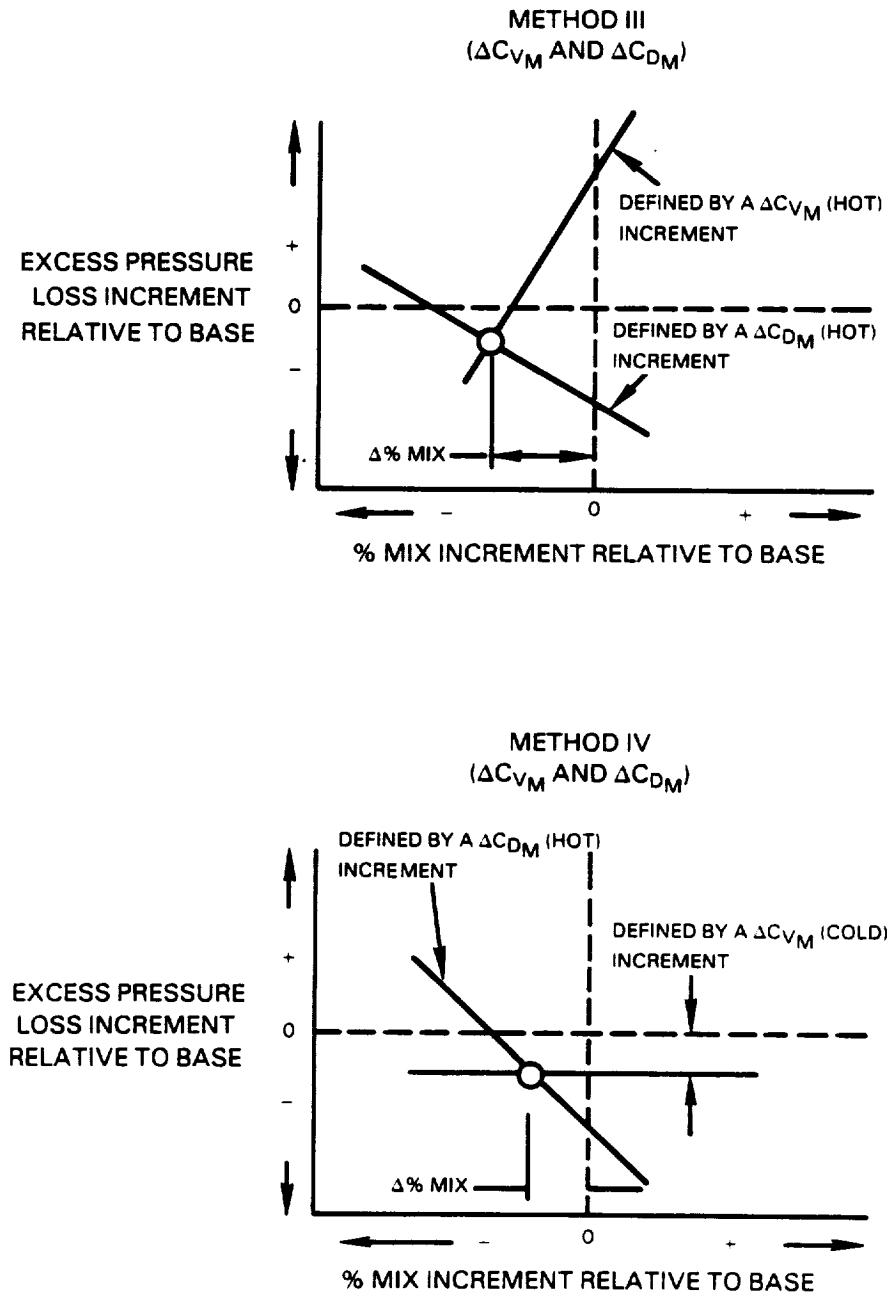

Figure 16 Illustration of Secondary Methods For Calculating percent Mix

4.3.2.3 Velocity Vectors At Mixer Exit Plane

Two Phase II mixer designs (configurations 29 and 34) were surveyed at the mixer exit plane to obtain pressure, temperature, and flow angle data through the lobes for codes such as those being developed under NASA Contract NAS3-23039. In addition, these data were used to determine the velocity vectors and the flow angles at selected circumferential locations using the following procedure.

The procedure begins with the measured static and total pressures, total temperature, and calculated radial (pitch, μ) and circumferential (yaw, ν) flow angles. The absolute velocity and the pitch and yaw angles are shown in the diagram below,

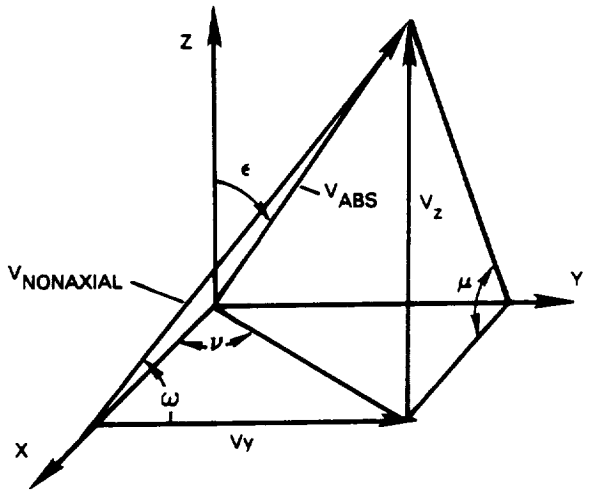

where x is in the axial, z is in the radial, and y is in the circuferential direction. The absolute velocity at a given radial and circumferential location can be calculated by:

$$V_{abs} = (a_t)\ Mn\ /\ \sqrt{1 + [(\gamma - 1)/2]\ Mn^2}$$

where (a_t) is the speed of sound based on measured total temperature, and Mach number is a function of measured values of static and total pressure at a given radial and circumferential survey position. The angle (ϵ) between the radial axis (z) and the absolute velocity can be defined as:

$$\epsilon = \tan^{-1}[\ 1\ /\ (\cos\nu\ \tan\mu)]$$

The radial component of velocity, Vz, is defined as:

$$Vz = Vabs\ (\sin\epsilon\ \cos\nu\ \tan\mu)$$

and the circumferential component of velocity, Vy, is defined as:

$$V_y = Vabs\ (\sin\epsilon\ \sin\nu)$$

combining these components of velocity results in the nonaxial velocity and its angle (ω) in the mixing plane:

$$V_{nonaxial} = \sqrt{Vz^2 + Vy^2}$$

$$\omega = \tan^{-1} (Vz/Vy) = \tan^{-1} (\tan \mu / \tan \nu)$$

The pitch (μ) and yaw (ν) angles that were used in the above equations were calculated with a dynamic pressure that was based on measured local conditions (at a given survey position) instead of a free stream condition. A table containing Vabs, Vnonaxial, ω , μ , and ν for both configurations, at selected locations, appears in Appendix D. In addition to correcting the pitch and yaw angles for local flow conditions, a second order least squares curve fit was used to fit the flow angle calibration data. These curves also appear in Appendix D.

4.3.2.4 Nozzle Exit Plane Traverses

Traverse plots were obtained by surveying the nozzle exit plane of all new configurations. At a single simulated engine operating point, total pressure and total temperature were measured and nondimensionalized relative to the corresponding ideal mixed property. A sample of the resultant plots is shown in Figures 17 and 18. The charging station conditions for each stream (fan stream = Station 7 and primary stream = Station 8) are identified. The absolute level of the fully mixed reference is also identified. A complete presentation of all the traverse plots is included in Appendix B. The location of the primary lobe peaks are indicated by arrows.

4.3.2.5 Mixer Exit Plane Traverses and Surface Pressures

Total pressure and total temperature traverse plots were obtained by surveying the lobe exit plane, and the same method was used as described in Section 4.3.2.4 for two previously tested unscalloped Phase II configurations (Configurations 29 and 34). In addition, model surface pressures were nondimensionalized by charging station total pressure (in each stream), and Mach numbers were computed. A complete (mixer, plug, tailpipe) tabulation of these pressures and corresponding Mach numbers is presented in Appendix D, along with total pressure and temperature traverse results in the form of tables.

Finally, lobe exit plane flow angle data were reduced using two approaches. The first involved FEC reduced data using a linear curve fit of the flow angle calibration data using free stream values of dynamic pressure. A complete tabulation of the 40-degree traverse segment for both configurations is presented in Appendix E. The second approach considered the impact variations in dynamic pressure (due to changing gas properties across the mixing plane) on flow angle. In addition, the flow angle calibration data were reduced using a second order least squares curve fit. This approach was used to calculate velocity vectors at selected traverse positions, and complete data tabulations of these results are shown in Appendix D.

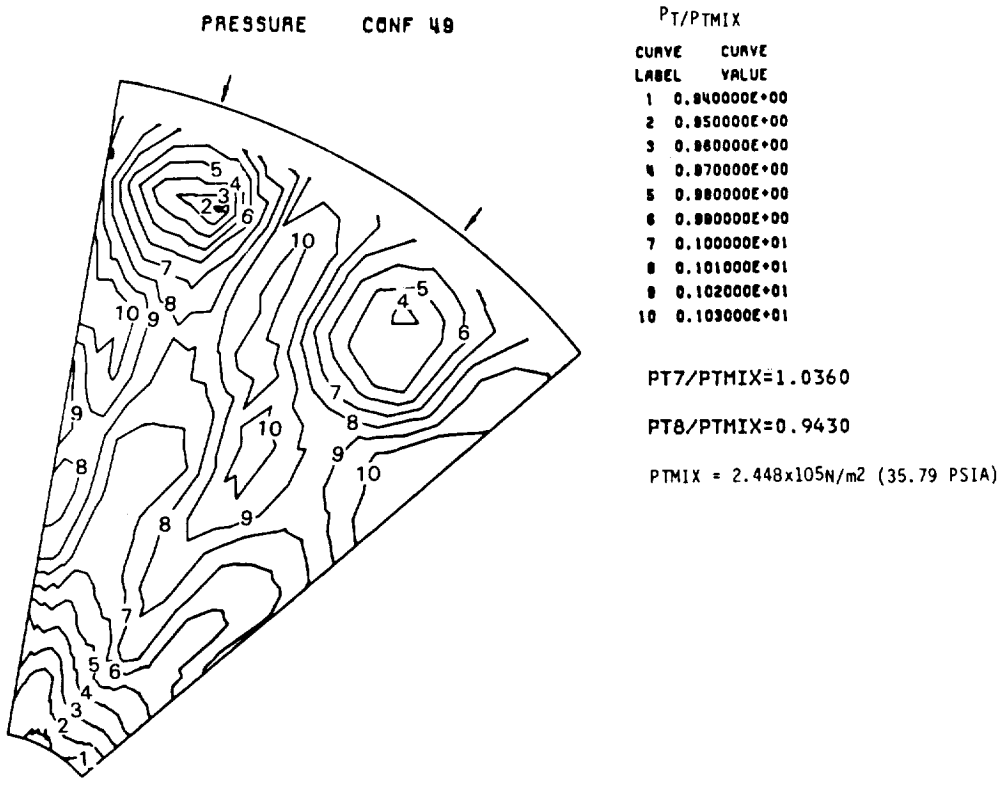

Figure 17 Resultant Pressure Plot Sample

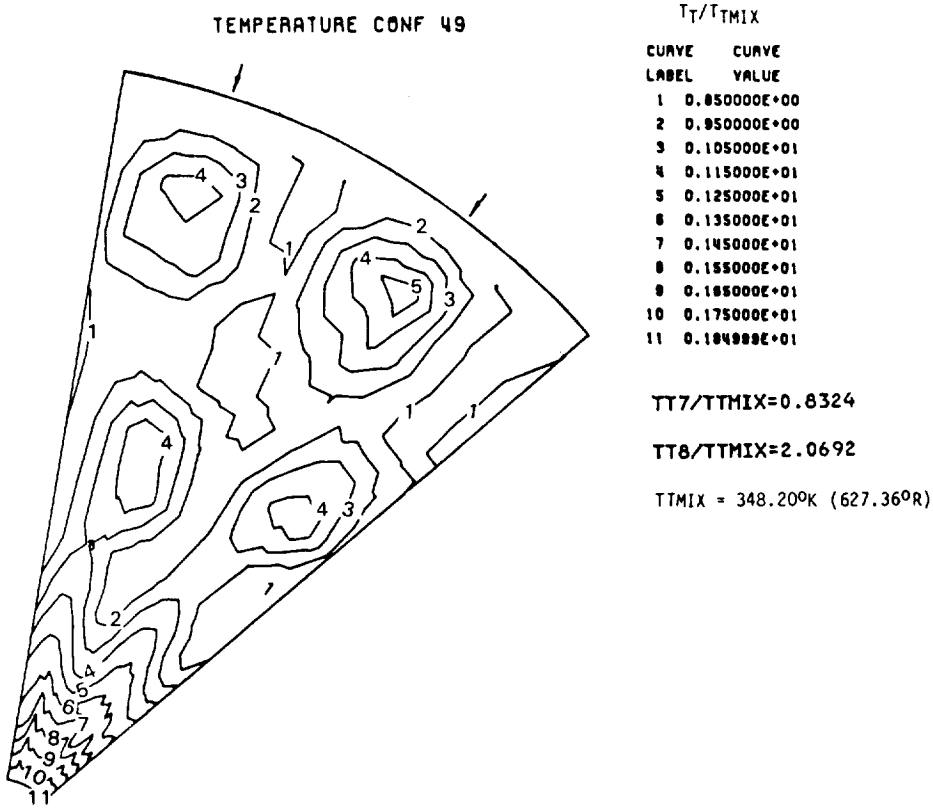

Figure 18 Resultant Temperature Plot Sample

4.3.2.6 Flow Visualization Photographs

Flow visualization tests were made for all configurations. These tests were conducted with uniform cold flow at a nozzle pressure ratio of 2.5 to provide a general indication of the flow field through the exhaust system. A sample photograph is presented in Figure 19. The streaks result from placing an array of dots (using a lampblack/glycerine mixture) on the painted surface of the model prior to a test run. A complete set of photographs is presented in Appendix C.

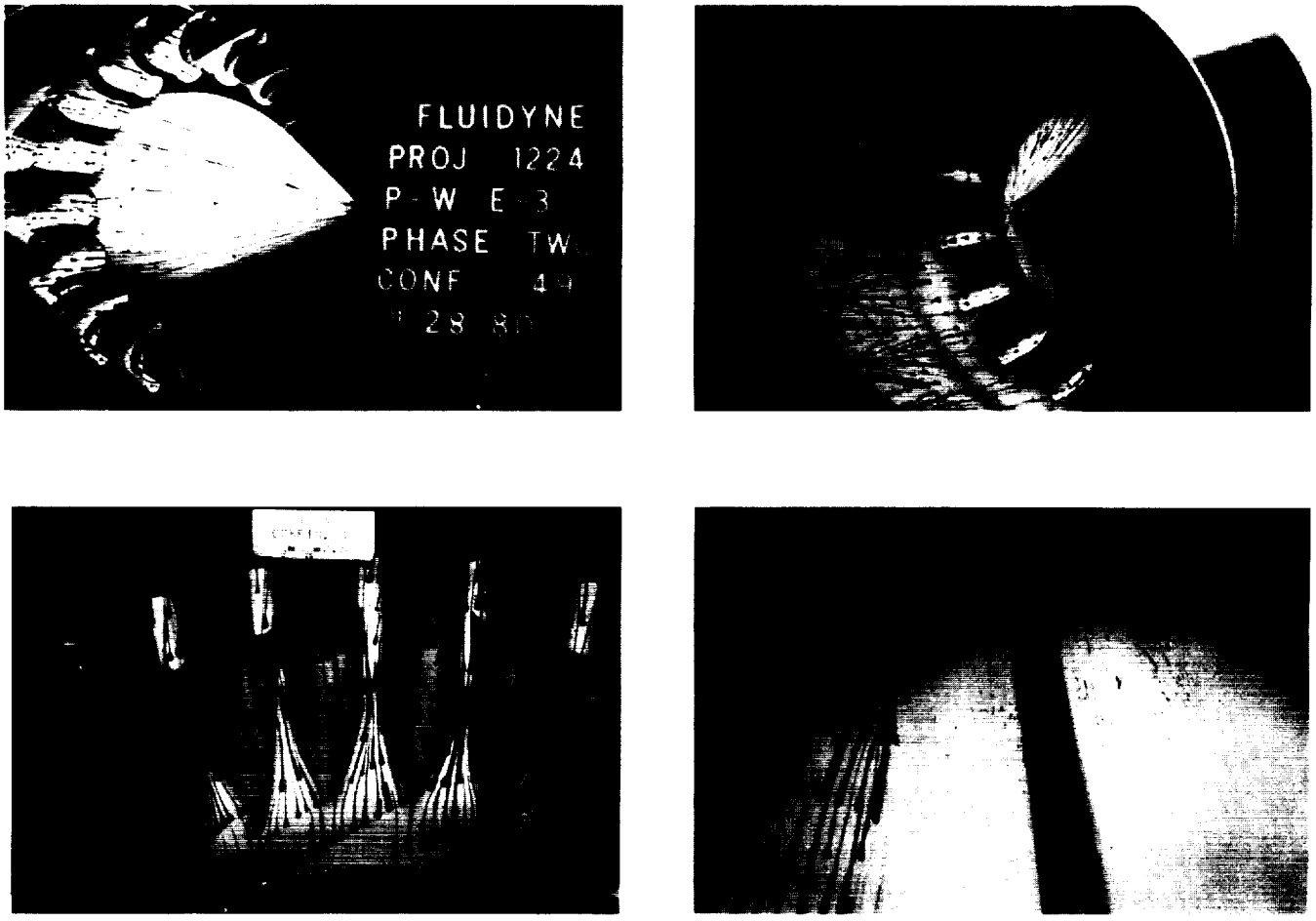

Figure 19 Flow Visualization Photographs, Configuration 49

4.3.3 Date Repeatability

The free mixer configuration was tested at the beginning, several times during, and at the end of the Phase III test program to establish data repeatability with Phase II. The repeatability of thrust coefficient (CVMIX) data was analyzed at relatively high nozzle pressure ratio, spanning the principal pressure ratio of 2.5 used in the parametric evaluations.

The Phase III "cold" flow test had a standard deviation equal to ±0.0008 as illustrated in Figure 20. The "hot" flow test also had a standard deviation equal to ±0.0008. During Phase II, the "cold" flow tests had a standard deviation equal to ±0.0006 as illustrated in Figure 21. The "hot" flow tests had a standard deviation equal to ±0.0004. In general, the repeatability for Phase II was somewhat better than that for Phase III. However, Phase III results are typical of the repeatability observed during a previous experimental program in the Channel 11 test facility at Fluidyne Engineering Corporation.

Although the amount of available data is relatively small, an indication of the amount of data bias between Phase II and Phase III testing is provided by comparing the mean hot and cold thrust coefficient levels of the free mixer configuration. At a mixed nozzle pressure ratio of 2.5, the cold flow bias shift is 0.0007 and the hot flow bias shift is 0.0002. In general, the trends from each phase of the program were used independently. Therefore, this bias is not particularly troublesome.

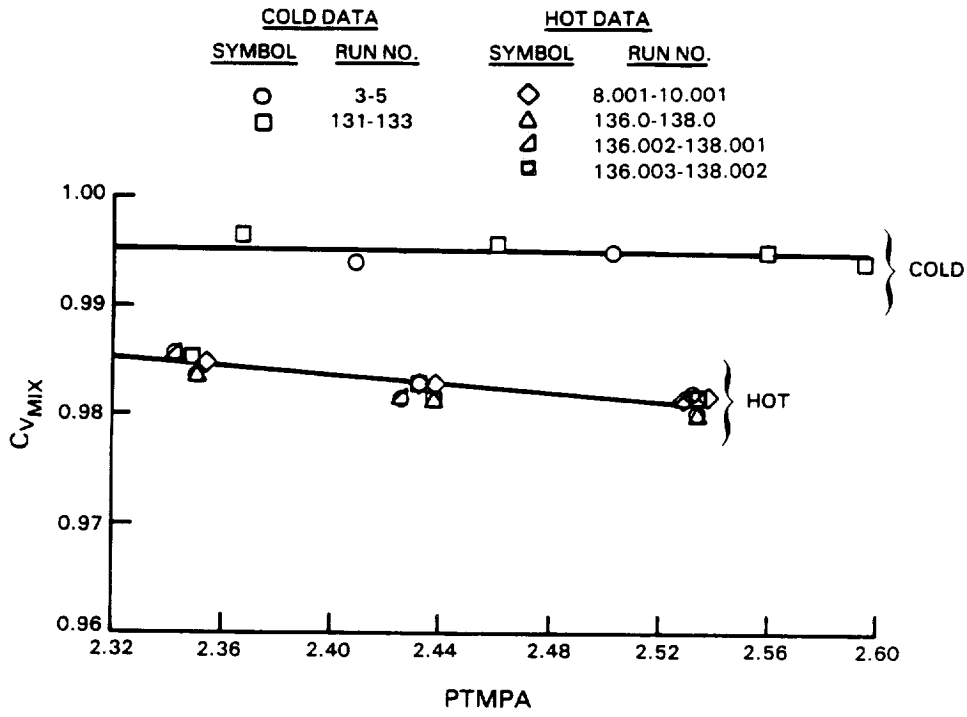

Figure 20 Phase III Mixer Data, Configuration 1

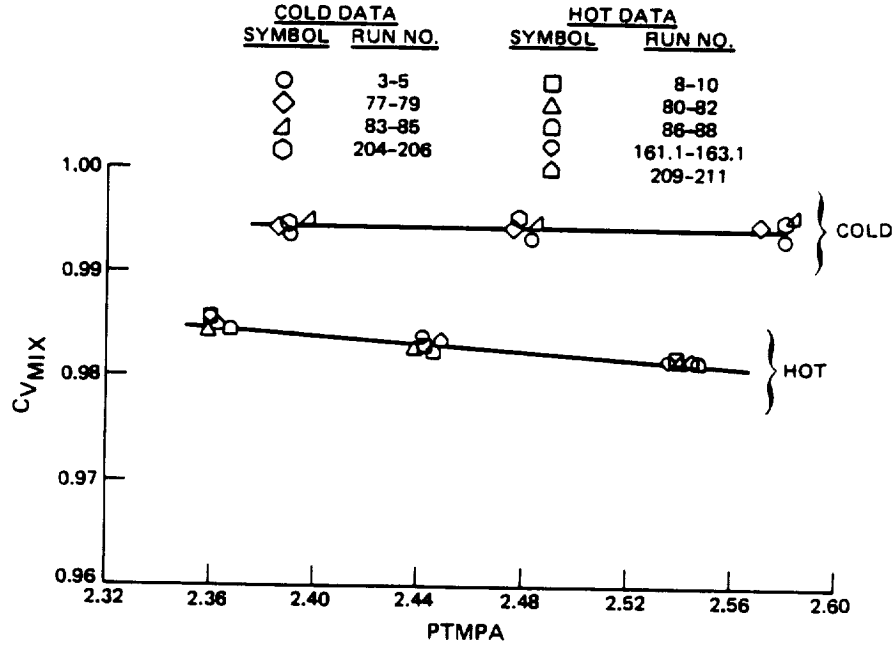

Figure 21 Phase II Free Mixer Data, Configuration 1

SECTION 5.0

TEST RESULTS AND ANALYSIS

5.1 TEST SUMMARY AND CONCLUSIONS

Ten scale model mixer configurations were performance tested during Phase III. These configurations were essentially variations on the best performing Phase II model, configuration 49. The performance test was conducted to determine if the best overall performance demonstrated in Phases I and II could be improved by exploiting two performance trends observed during these tests. A tabular summary of the performance characteristics of the configurations tested in Phase III is presented in Table IV.

TABLE IV

PHASE III MIXER CONFIGURATION PERFORMANCE CHARACTERISTICS SUMMARY

Lobe No. = 18; Tailpipe L/D = 0.61; Scalloped, Hooded Lobes

Configuration Type	Conf. No.	Exhaust System Length Relative to Config. 49 cm (inch)	Penetration	Lobe Discharge Angle, λ (degrees)	Percent Mixing	Excess Pressure Loss $\Delta(\Delta PT/PT)$*	Thrust Coefficient CV'	ΔTSFC** (%)
Base-Line Mixer, Best Phase II Configuration	49		0.72	+4	81.3	0.0033	0.9873	-2.45
Discharge Angle Variations	50	No Change	0.72	0	82.2	0.0027	0.9877	-2.55
	51	No Change	0.72	-1.5	74.0	0.0035	0.9862	-2.19
	51				[81.3]#		[0.9872]#	[-2.43]#
Extended Exhaust System, High Penetration, Discharge Angle Variations	53	+1.524 (+0.61)	0.75	+8	75.3	0.0016	0.9872	-2.36
	54	+1.524 (+0.61)	0.75	+4	75.1	0.0025	0.9868	-2.26
	55	+1.524 (+0.61)	0.75	+2	85.6	0.0032	0.9879	-2.53
	55				[77.2]		[0.9867]	[-2.24]
	59	+1.524 (+0.61)	0.75	0	74.7	0.0024	0.9868	-2.26
	60@	+1.524 (+0.61)	0.75	0 & -9	88.8	0.0063	0.9869	-2.29
	60@				[85.2]		[0.9864]	[-2.16]
Extended Exhaust System, Reduced Penetration, Discharge Angle Variations	56	+1.524 (+0.61)	0.65	+4	63.9	0.0004	0.9862	-2.12
	56				[76.0]		[0.9879]	[-2.53]
	57	+1.524 (+0.61)	0.65	-2	--	0.0004##	0.9870	-2.31
	57				[75.2]		[0.9878]	[-2.50]

* In Excess of Skin Friction Losses.
** Relative to the Optimized Separate Flow System.
\# In Each Case where the Data Assessment Procedure Indicated that the Thrust Balance Data was Significantly Affected by Data Scatter, an Alternate Performance Assessment, Indicated by [ ], was Made Based on the Traverse Integration Results as Described in Section 5.2.
Excess Pressure Loss was Assumed to be the Same as that for Configuration 56.
@ Special Features Included a Bilevel Discharge Angle and Mixer-Plug Gap Ramps.

In addition, two scale model configurations were tested to obtain flow field information which could be used for computer code calibration. Two different mixer configurations, a high penetration design and a low penetration design, were instrumented and flow field data was obtained at the entrance to the lobes, through the lobes, at the lobe exit, and at the exit of the mixing chamber as shown in Figure 22. These configurations were performance tested in Phase II. The combination of Phase II performance data and Phase III flow field data will benefit codes such as those being developed under Contract NAS3-23029.

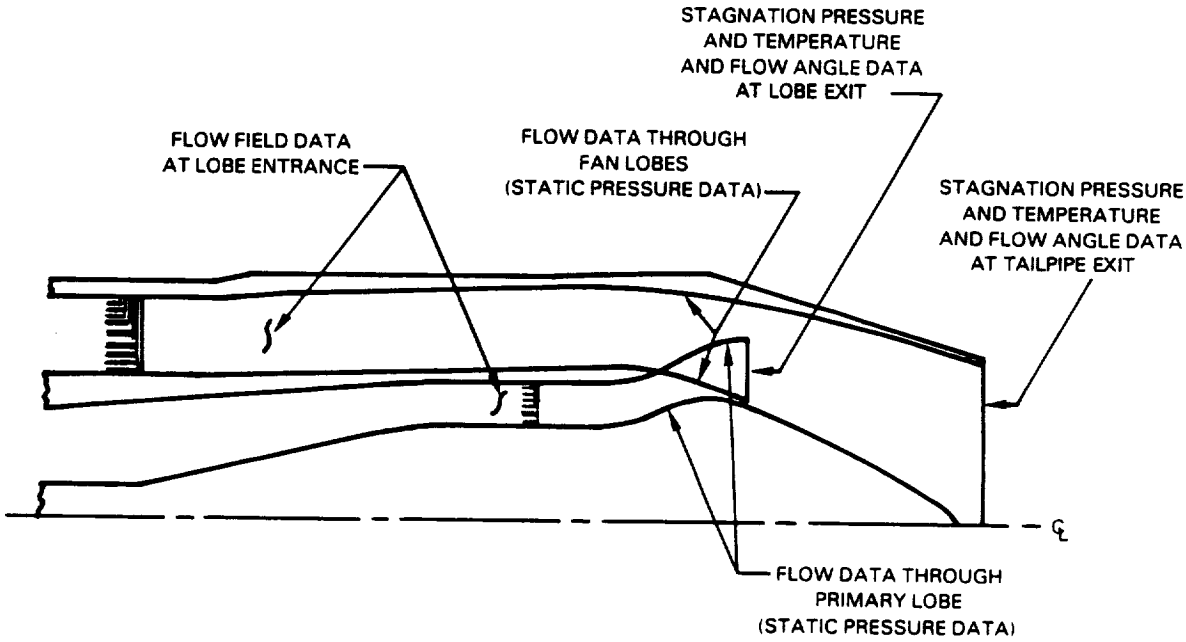

Figure 22 Lobe and Tailpipe Flow Field Data

A summary performance comparison in terms of percent mixing, excess pressure loss, and TSFC increments is shown in Figure 23. This comparison shows the shortfall in performance relative to the program goal, and the size of the shortfall relative to the guaranteed accuracy of the facility (±0.25 percent CV or ±0.6 percent TSFC) and the accuracy implied by the data repeatability of this test (±0.2 percent TSFC). Because the performance shortfall is not large in comparison to the accuracy of the facility, the data analysis of this test was expanded relative to the Phase I and II tests. This additional analysis included evaluations of percent mixing based on integration of the nozzle exit traverse data. In some cases, the traverse results were assessed to be more accurate than the thrust balance measurements and this is reflected in the summary table.

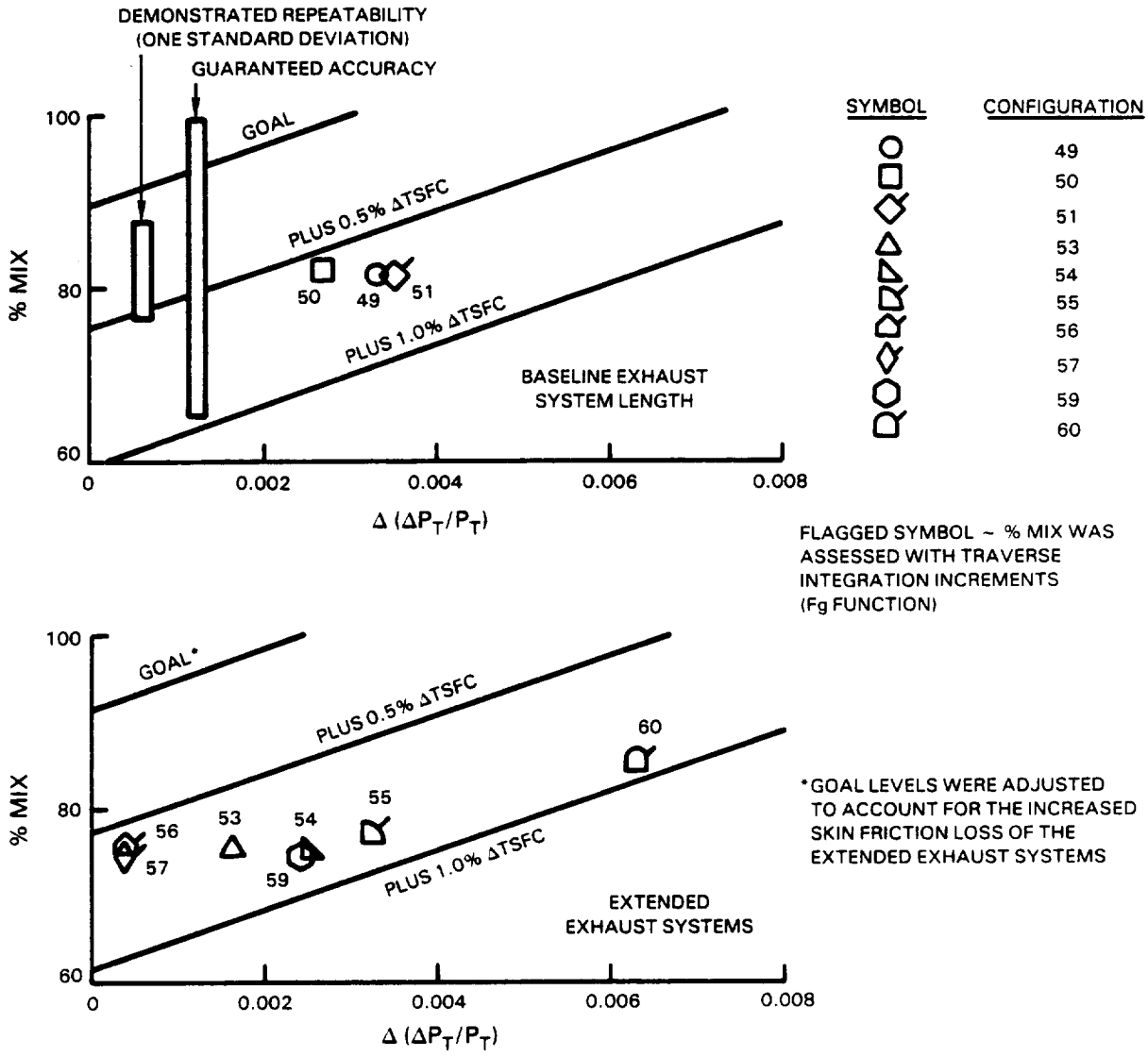

Figure 23 Performance Relative to the TSFC Goal

The test results obtained support the following conclusions:

1. The best measured TSFC improvement relative to the optimized separate flow exhaust system was 2.55 percent, which is 0.55 percent below the program goal of 3.1 percent. This was obtained by modifying the discharge angle of configuration 49 from +4 to 0 degrees.

2. There was no major overall performance peak within the lobe discharge angle range between +4 and -2 degrees. The best overall performance was obtained with a zero degree discharge angle.

3. Percent mixing and excess pressure losses were found to be interdependent in that both are sensitive to the degree of lobe flowpath turning. As a consequence, the extended and reduced penetration mixers did not increase overall performance above the level demonstrated by configuration 49. Excess pressure loss was significantly reduced by decreasing flowpath turning; however, this performance gain was negated because mixing was also reduced by a reduction in flowpath turning.

4. The use of integrated nozzle exit survey data was found to be a useful tool in assessing mixer performance.

5. Performance and flow field data were obtained for two different mixer lobe configurations. Codes such as those being developed under Contract NAS3-23039 can be calibrated with these data.

5.2 DATA PRESENTATION AND ANALYSIS

The experimental data obtained during the test are presented as two distinct groups: mixer instrumentation test data and performance results. The mixer instrumentation data were obtained to provide a mixer flow-path data base. These data consist of lobe exit traverse data (stagnation properties and local flow angle) and lobe surface static pressure data for two mixer configurations. The mixer instrumentation data are described in Section 5.9. The performance results are based on thrust balance and nozzle exit traverse data. The nozzle traverse data were used to assess mixing by integrating the measured temperature and pressure stagnation profiles. In addition, isoparameter plots of the nozzle exit stagnation profiles and total temperature distribution plots are presented as a visual aid. Performance is presented in terms of thrust specific fuel consumption (TSFC), nozzle gross thrust coefficient (CVmix), excess pressure loss (Δ (Δ PT/PT), and percent mixing. The best measure of overall performance is the equivalent change in thrust specific fuel consumption. Percent mixing and excess pressure loss are key components of the overall performance.

The definition of parameters is the same as in the Phase I and II report except that additional data evaluation techniques were introduced as a means to enhance the accuracy of the performance assessments. Multiple evaluations of percent mixing were made. They were used to judge the accuracy of the thrust balance data. Four methods were used: Method I - Percent mixing was determined by integrating the traverse measurements; both a temperature mixing function

and thrust mixing function were evaluated. Method II - Percent mixing was evaluated using hot and cold flow thrust coefficients as in Phases I and II. Methods III and IV - Percent mixing was evaluated by two secondary methods which used increments in thrust coefficient and flow coefficient relative to a base configuration.

The Phase III test was designed to improve on the best performance obtained in Phases I and II by exploiting two data trends observed during those tests: 1) the performance of some mixer configurations was sensitive to the lobe discharge angle, and 2) excess pressure loss correlated with the degree of flow turning through the mixer flow path. Ten mixer configurations were tested with three degrees of "turning" through the mixer flow path. In order of decreasing flow turning, three types of mixers were investigated: 1) the best configuration from Phase II (configuration 49), which was used as a base line, 2) an extended flow path, high penetration mixer, and 3) an extended flow path, reduced penetration mixer. Lobe exit discharge angle (λ) variations were tested for all three types of mixers. In addition, a hybrid configuration was tested with two levels of discharge angle on alternating lobes and with plug gap inserts. The mixing length (L/D) was held constant for all of the mixer configurations. The free mixer exhaust system was tested four times at regular intervals through the program to demonstrate repeatability. The configurations are described in detail in Section 3.3.

Alternative methods for assessing performance were added to the test program to increase confidence in the results. The guaranteed repeatability of the facility is $\pm$0.25 percent CV. The accuracy demonstrated by repeat testing of the free mixer within the Phase III test program (one standard deviation) was 0.08 percent ΔCV or 0.2 percent ΔTSFC. This is equivalent to approximately 6 percent mixing and 0.17 percent pressure loss. In the extreme, the percent mixing uncertainty could be doubled since two thrust coefficient levels determine percent mixing. Since the magnitude of these uncertainties was large relative to the performance gap that this program was intended to close, the hot and cold thrust coefficient analysis was augmented by calculating percent mixing from the traverse data. Two mixing functions were defined for this purpose: a thrust mixing function and a temperature mixing function. In addition, percent mixing was determined from increments of thrust and flow coefficient relative to a base configuration (referred to as secondary methods).

The essentially independent evaluations of percent mixing from the thrust balance data and the traverse mixing functions were compared and used to judge the accuracy of the thrust data. In addition, all four of the methods for evaluating percent mixing are compared. In some cases, where the disagreement is sufficient to cause concern over the accuracy of data trends, an inspection of the multiple percent mixing evaluations serves to identify which parameters are most effected by data scatter. When the impact of data scatter is significant, an alternate evaluation of thrust specific fuel consumption is presented based on the traverse mixing function analysis.

For the sake of simplicity, absolute values of the traverse mixing functions are compared with the thrust data results (good agreement with the base configuration was demonstrated). When alternate evaluations of specific fuel consumption are presented, they are based on increments in the thrust function traverse results relative to the base configuration.

The mixing function increment was applied to the base configuration percent mixing determined from the thrust balance data to calculate the alternate percent mixing level and specific fuel consumption. Relative changes in the traverse integration results were considered to be the most accurate.

The traverse integration analysis and the secondary methods for calculating percent mixing are described in Sections 4.3.2.1 and 4.3.2.2. In addition, the method used to determine the traverse plots and flow angle at the lobe exit is described in Sections 4.3.2.3, 4.3.2.4 and 4.3.2.5.

5.3 BASE CONFIGURATION

Configuration 49 exhibited the best overall performance in Phase II and was selected as a base configuration for the Phase III testing. The Phase II and III test results for configuration 49 showed excellent agreement. At the maximum cruise test condition, the hot and cold flow thrust coefficients were repeated within 0.0002. The differences in excess pressure loss and percent mixing were negligible.

5.4 DISCHARGE ANGLE VARIATIONS ON THE BASE CONFIGURATION

Variations in discharge angle (λ) on the base configuration between +4 and -1.5 degrees produced no major improvements in thrust specific fuel consumption or clear trends in percent mixing or excess pressure loss. This is shown by the test results from configurations 49, 50 and 51 which are summarized in Figure 24. Note that this summary includes percent mixing evaluations based on both the thrust balance data and the traverse data, plus an alternate assessment of thrust specific fuel consumption for configuration 51. Both types of percent mixing evaluations agree within a range that is consistent with the demonstrated accuracy of the test facility; however, in the case of configuration 51, the data assessment procedure (that is, a comparison of four independent percent mixing evaluations) indicates that the traverse integration results for configuration 51 may more accurately predict percent mixing and thrust specific fuel consumption than the thrust balance data. A comparison of the independent percent mixing evaluations for configuraions 50 and 51 are shown in Figures 25 and 26, respectively. All of the evaluations show generally good agreement for configuration 50 and indicate that data scatter had no significant impact on the performance results. In the case of configuration 51, there is moderate disagreement, which indicates that the thrust balance data are probably less accurate than the traverse integration results.

The small effect on percent mixing of varying the discharge angle from +4 to -1.5 degrees is graphically illustrated by the lack of change in the nozzle exit total temperature distributions, as shown in Figure 27.

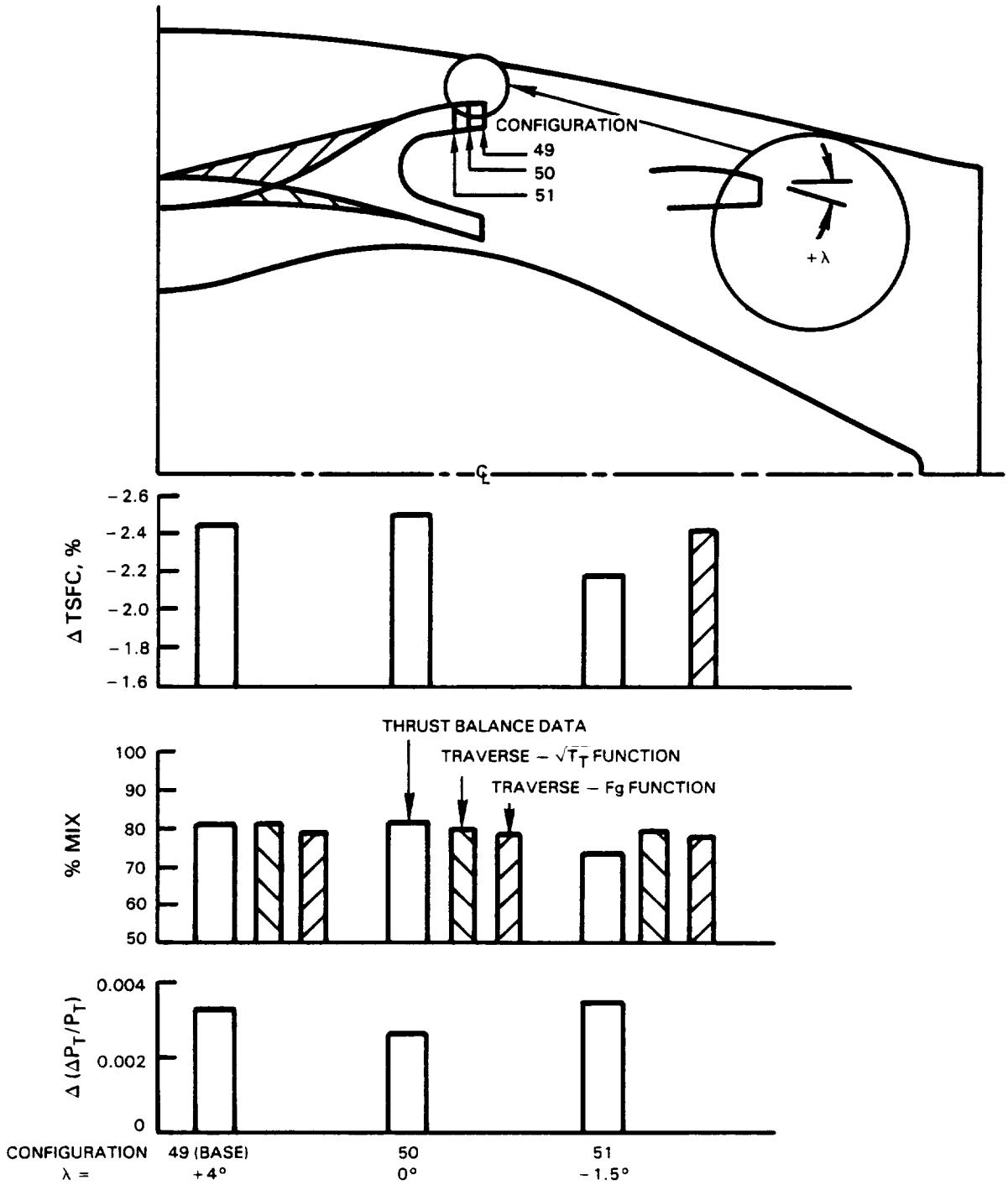

Figure 24 Performance Summary - Effect of Lobe Discharge Angle (λ) Variations on the Base Configuration

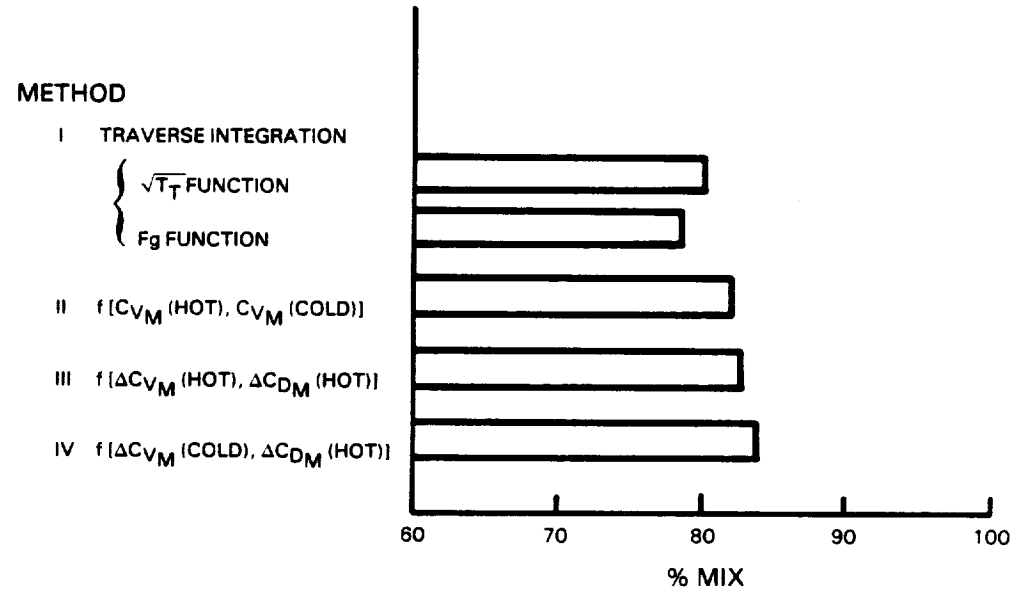

Figure 25 A Comparison of the Independent Percent Mixing Evaluations for Configuration 50

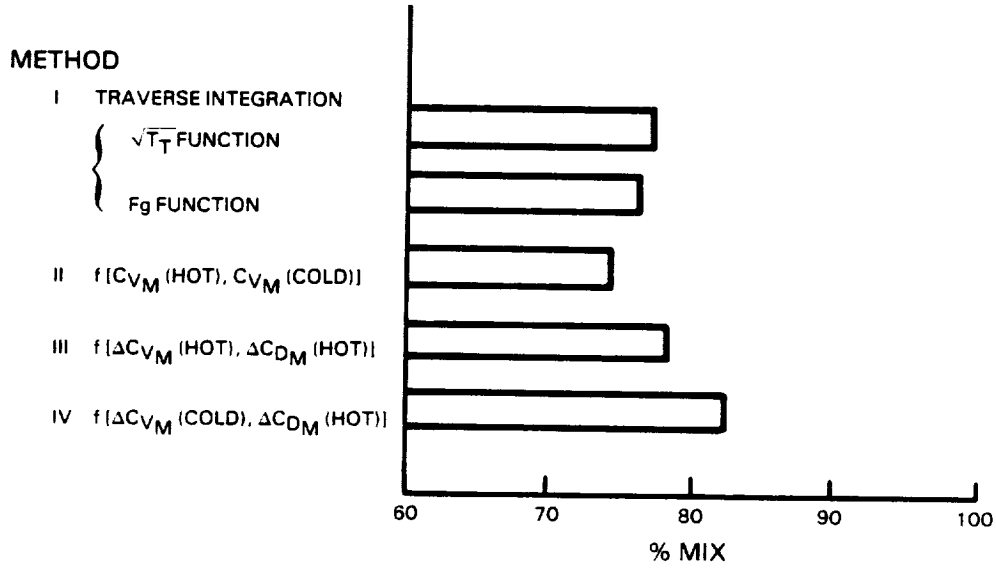

Figure 26 A Comparison of the Independent Percent Mixing Evaluations for Configuration 51

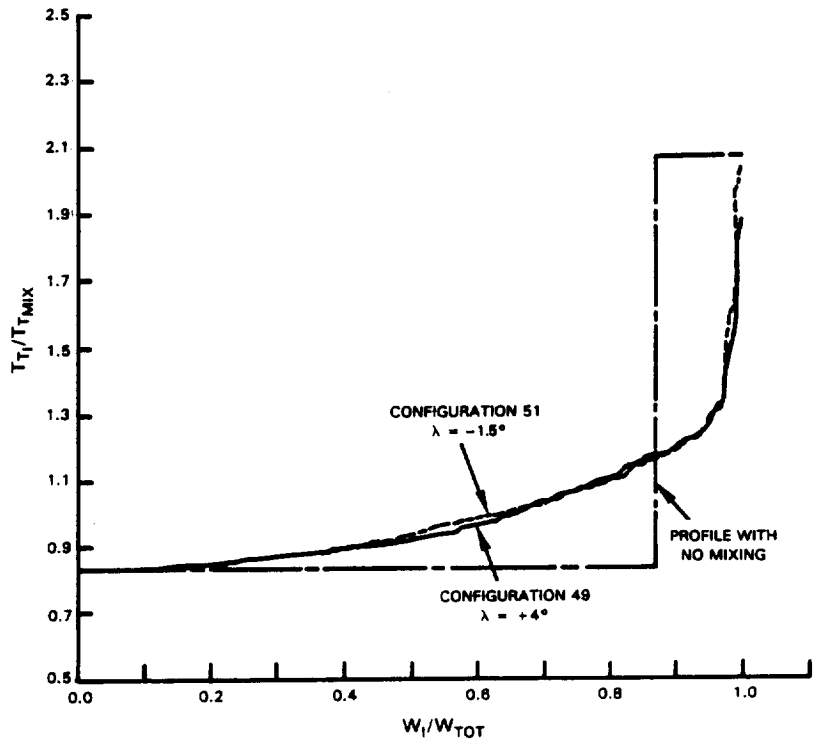

Figure 27 The Effect On Nozzle Exit Total Temperature Distribution of Varying the Lobe Discharge Angle

5.5 EXTENDED EXHAUST SYSTEM - HIGH PENETRATION MIXERS

An average reduction in overall performance, relative to the base-line configuration, of approximately 0.17 percent TSFC was measured for the high penetration, extended mixer series. This was due primarily to an unexpected lapse of approximately 5 percent mixing relative to the base-line configuration. In addition, there was no significant response in overall performance to variations in the discharge angle (λ) between zero and eight degrees, as shown in Figure 28. Percent mixing evaluations by both the thrust balance data and traverse results showed good agreement except in the case of configuration 55. The thrust balance data indicated that for configuration 55 there was a "spike" in the percent mixing trend; however, the data assessment procedure showed that this was the result of thrust balance data scatter. Therefore, an alternate assessment of thrust specific fuel consumption was made based on the traverse results.

The excess pressure loss ($\Delta(\Delta PT/PT)$ was reduced relative to the base-line configuration. this is consistent with a trend observed in Phase II testing in which a reduction in mixer flowpath turning resulted in a reduction in excess pressure loss. In the case of configurations 53, 54, and 59, the reduction in excess pressure loss exceeded the estimated increase in skin friction loss ($\Delta PT/PT=0.0006$) which resulted from extending the exhaust system. The measured variations in excess pressure loss due to changes in the discharge angle are relatively small and probably do not define a clear trend. A further discussion of the excess pressure loss trends is provided in Section 5.8.

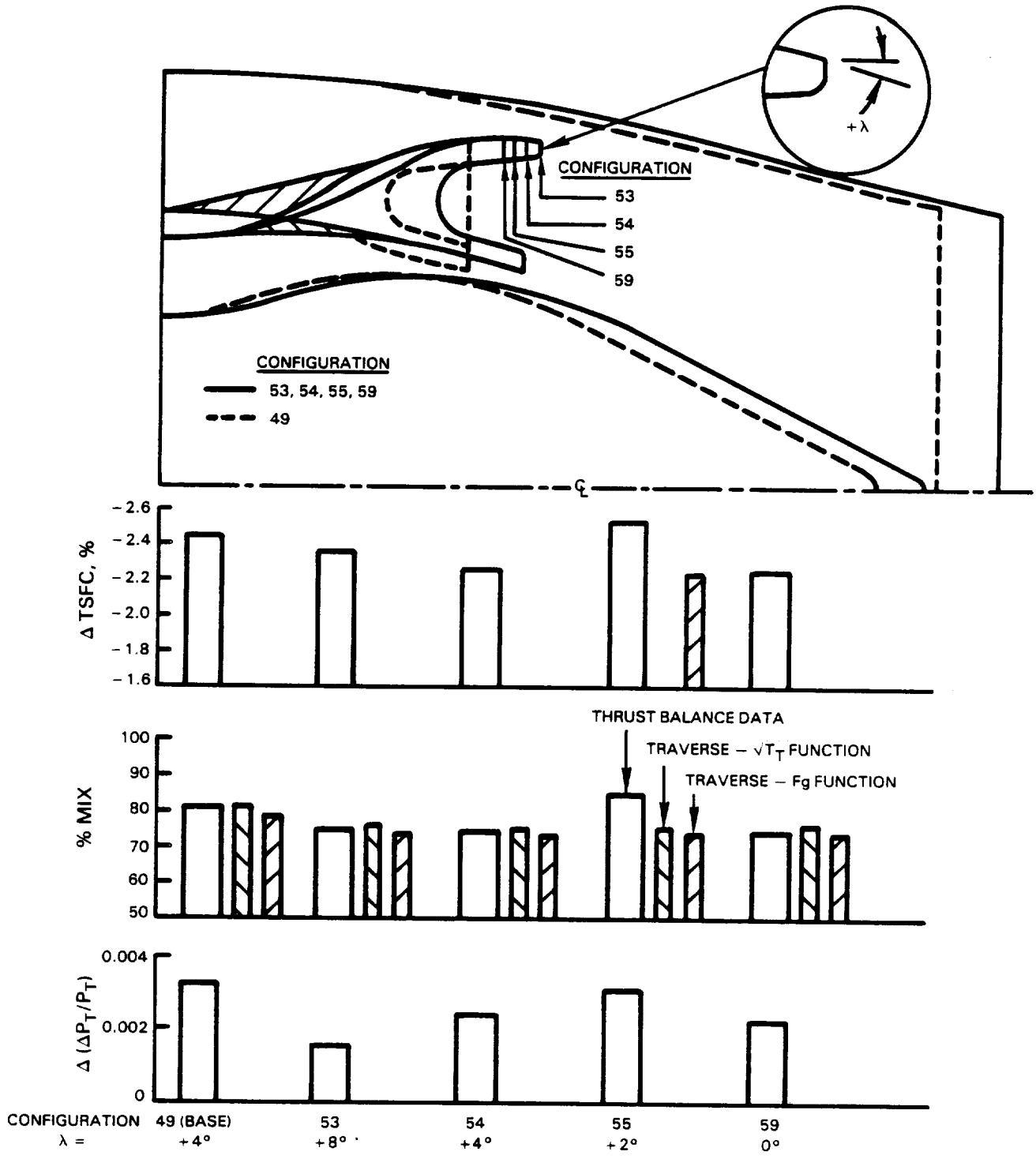

Figure 28 Performance Summary - Effect of High Penetration Extended Mixers With Discharge Angle Variations

A comparison of all four independent percent mixing evaluations shows good agreement for configurations 53, 54, and 59 as illustrated in Figures 29 through 31, respectively. In the case of configuration 55, the data assessment procedure indicates that the thrust balance results were less accurate than the traverse results due to an inaccurate force balance measurement which resulted in an elevated hot flow thrust coefficient (CVmix). This assessment is based on a comparison of all four independent methods for evaluating percent mixing which is shown in Figure 32. Note that the traverse and Method IV evaluations of percent mixing show good agreement. This is likely to occur only if the "cold" thrust coefficient and "hot" flow coefficient are not significantly affected by data scatter. If these coefficients are accurate, the lack of agreement in percent mixing evaluated by Methods II and III is due to the impact of data scatter on the "hot" thrust coefficient as illustrated in Figure 33. Note that only the force balance component of the "hot" thrust coefficient is completely independent of the measurements which determine the "hot" flow coefficient.

The consistent reduction in mixing observed for all four of the extended high penetration mixers relative to the base-line configuration was probably the result of reduced flow turning through the extended mixers and a reduction in the relative flow angles of the fan and primary streams at the mixing plane. These differences would tend to reduce the strength of the secondary flow systems in the wake of the extended mixers, which would tend to reduce mixing. These were the only significant geometry differences between the two types of mixers. Phase I and II testing showed that the number of lobes, penetration, and mixing length (L/D) were the primary geometric variables that affect percent mixing. The number of lobes and the mixing length were the same for the base-line and the extended mixers. The penetration of the extended mixers was slightly increased relative to the base-line configuration from 0.72 percent to 0.75 percent. Phase II testing indicated that this change would tend to slightly increase percent mixing.

A comparison of the nozzle exit total temperature distributions of configurations 49 and 54, as shown in Figure 34, graphically illustrates the reduction in percent mixing that occurred with the extended mixers which have reduced lobe flow path turning. Note that the total temperature distribution of configuration 54 is slightly closer to the unmixed total temperature profile over a considerable range of flow.

5.6 EXTENDED EXHAUST SYSTEM - REDUCED PENETRATION MIXERS

The extended, reduced penetration mixers were tested to determine if a more optimal combination of flow turning and penetration could be obtained by increasing the length of the base-line configuration and reducing the mixer penetration while maintaining the same number of lobes and mixing length. The reduction in penetration was used as a means to further decrease flow turning through the mixer primary stream without increasing skin friction or the overall length of the exhaust system. Phase II testing indicated that reducing penetration would result in a performance trade between decreased excess pressure loss ($\Delta(\Delta PT/PT)$ and decreased mixing. In addition, the impact of discharge angle variations was measured.

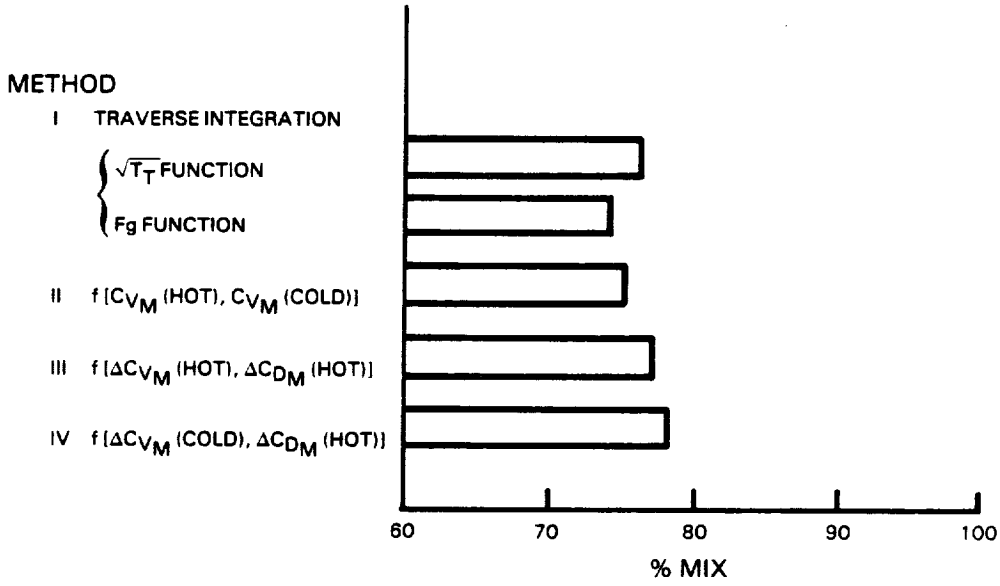

Figure 29 A comparison of the Independent Percent Mixing Evaluations for Configuration 53

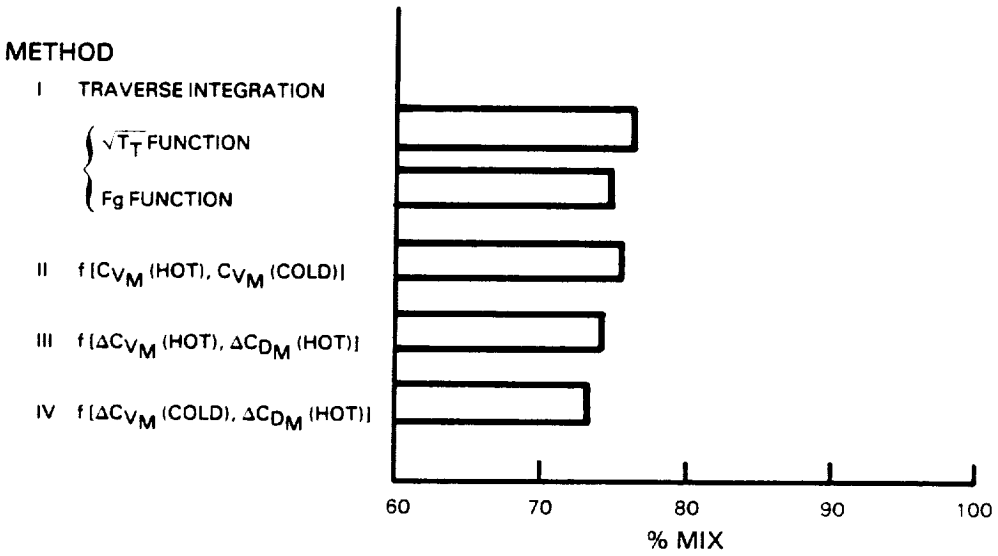

Figure 30 A Comparison of the Independent Percent Mixing Evaluations for Configuration 54

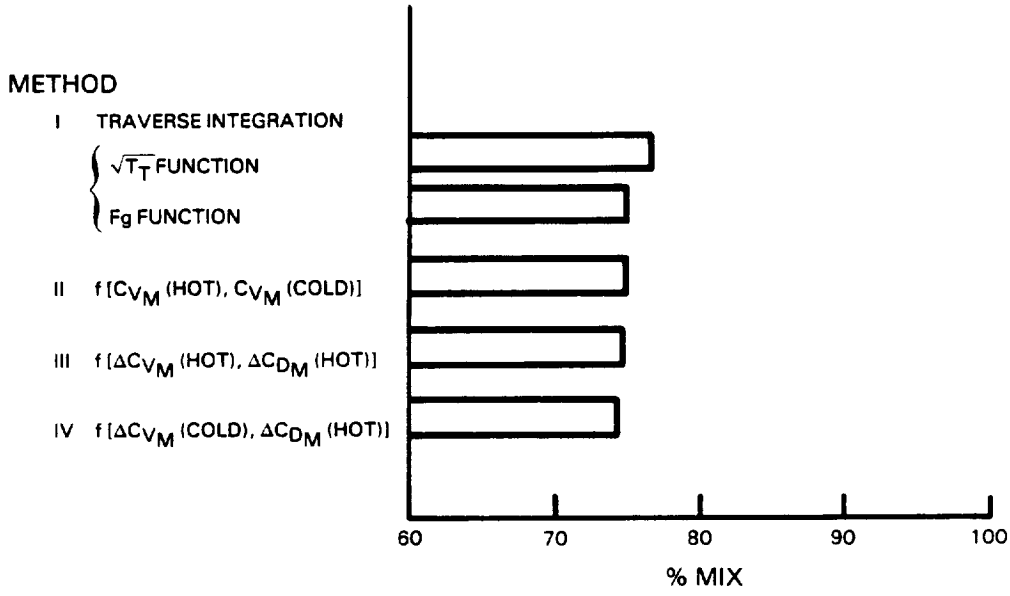

Figure 31 A Comparison of the Independent Percent Mixing Evaluations for Configuration 59

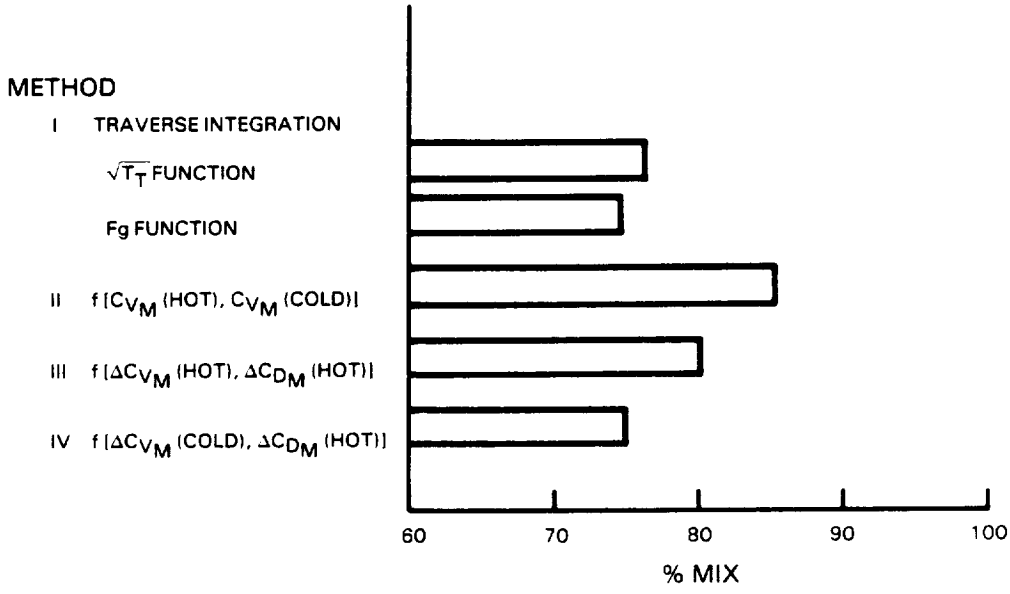

Figure 32 A Comparison of the Independent Percent Mixing Evaluations for Configuration 55

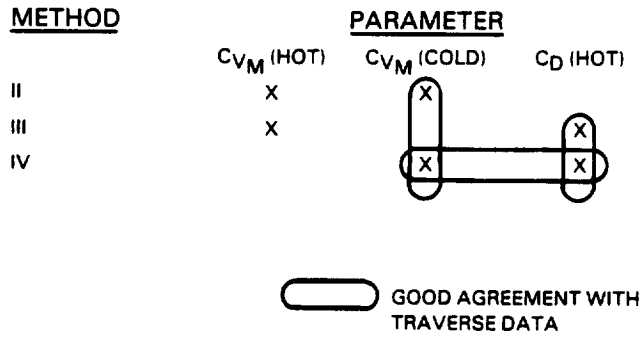

Figure 33 Accuracy Assessment for Configuration 55

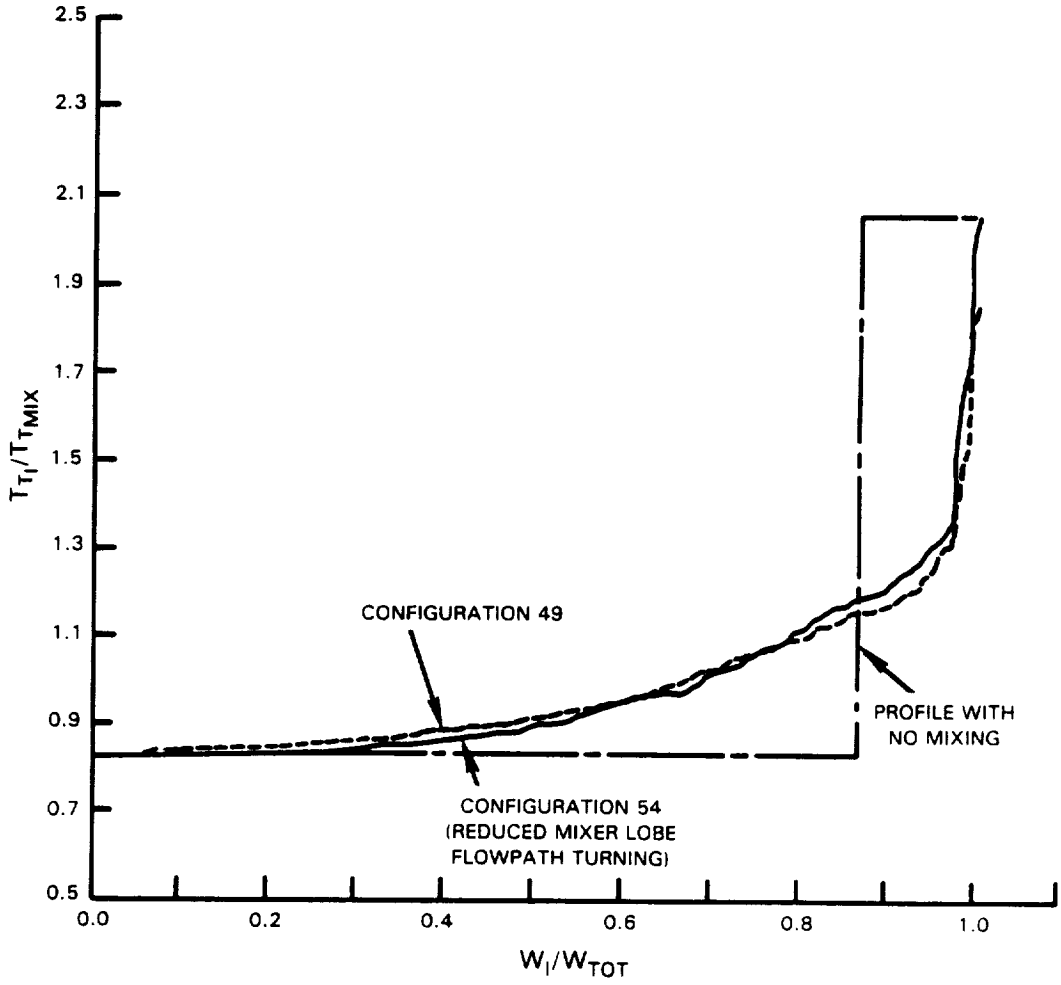

Figure 34 The Effect on Nozzle Exit Total Temperature Distribution of Reducing Mixer Lobe Flowpath Turning

The overall peformance of the extended exhaust system, reduced penetration mixers was assessed to be essentially the same as the performance of the base-line configuration as shown in Figure 35. Varying the mixer discharge angle (λ) between -2 and +4 degrees had no major impact on percent mixing or overall performance. A large reduction in excess pressure loss ($\Delta(\Delta PT/PT)$) of 0.0029 relative to the base-line configuration was measured. This reduction substantially exceeded the increase in skin friction pressure loss ($\Delta PT/PT$= 0.0006) which resulted from extending the exhaust system. However, the net gain in overall performance was small due to a reduction in percent mixing of approximately 5 percent. The mixing decreased as a result of decreasing the penetration relative to the base configuration from 72 to 65 percent. The excess pressure loss decreased due to a reduction in flow turning through the mixer. Although a significantly optimum combination of flow turning and penetration was not identified for a cruise power setting, it should be noted that essentially the same overall performance was obtained at a lower level of pressure loss.

The assessment of thrust specific fuel consumption and percent mixing was based on the cold flow thrust balance data and the traverse integration results, because the data assessment procedure indicated that the "hot" thrust coefficient was significantly affected by data scatter. In addition, the results based on the "hot" thrust coefficient indicated a severe drop in performance and percent mixing (17.4 percent for configuration 56) which was inconsistent with the data trends and performance levels observed in Phase I and II testing. Percent mixing could not be evaluated directly from the thrust data for configuration 57, since only hot flow data were taken. This economy in tests points made it possible to add configuration 60 to the test program. The excess pressure loss for configuration 57 was assumed to be equal to that of configuration 56. A comparison of all four percent mixing evaluations for configuration 56 shows considerable disagreement as illustrated in Figure 36. Note that the traverse and Method IV evaluations of percent mixing show good areement. As in the case of configuration 55, this indicates a significant inaccuracy in the hot flow force balance measurements as illustrated in Figure 37.

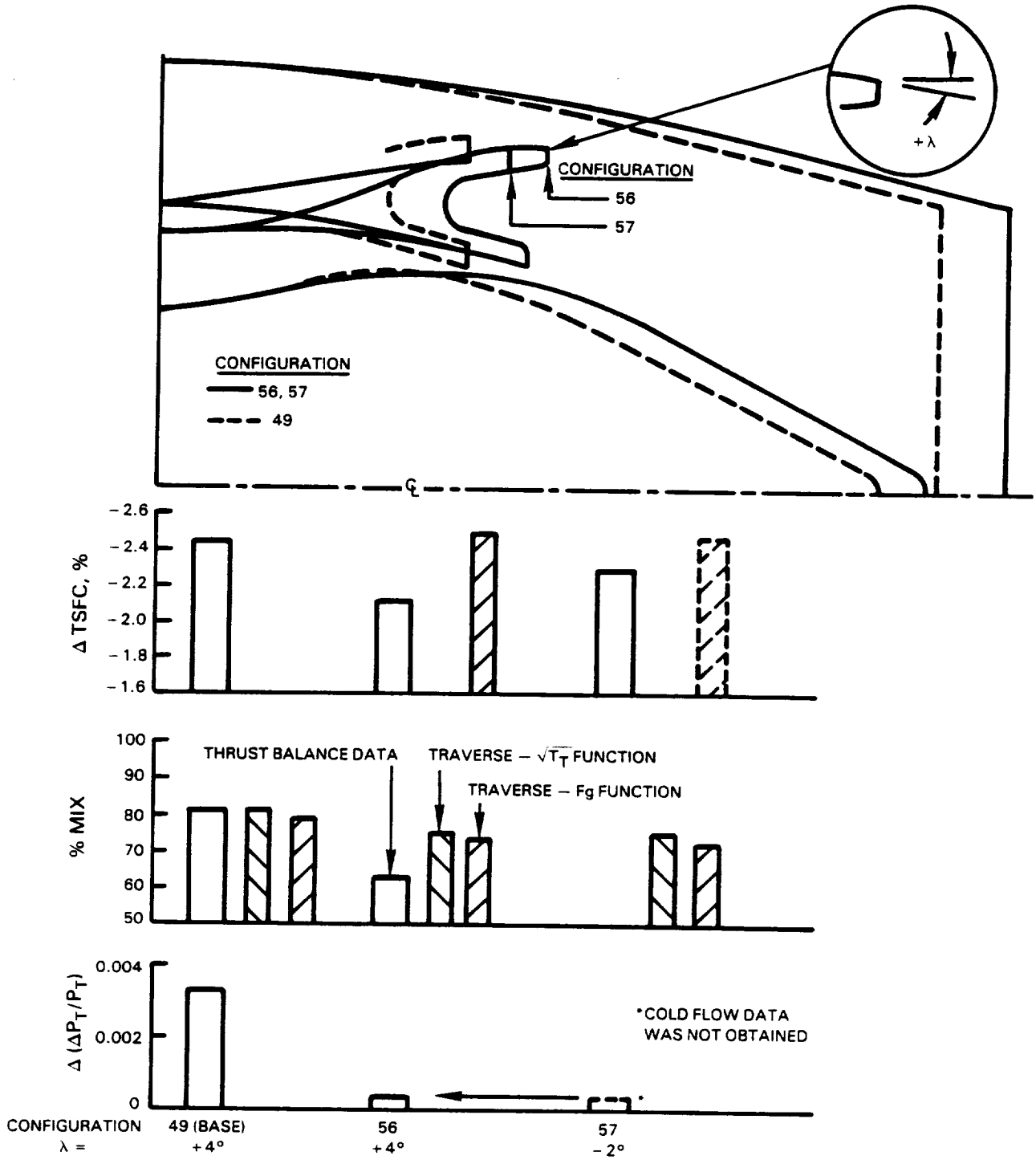

Figure 35 Performance Summary - Effect of Low Penetration, Extended Mixers with Discharge Angle Variations

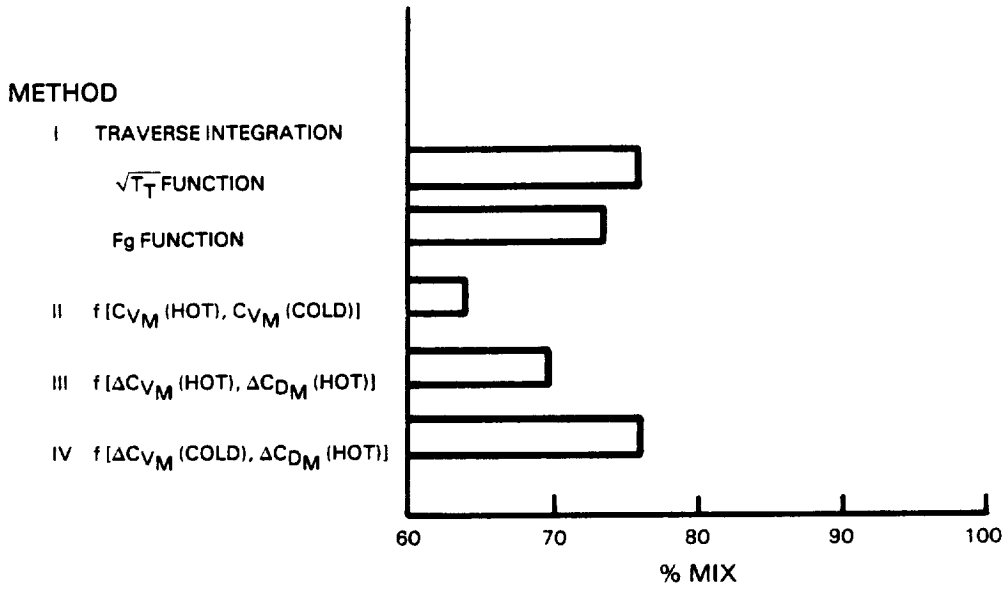

Figure 36 A Comparison of the Independent Percent Mixing Evaluations for Configuration 56

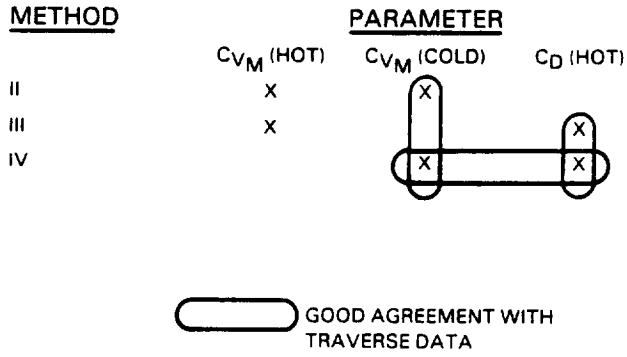

Figure 37 Accuracy Assessment for Configuration 56

5.7 ADDITIONAL MIXER MODIFICATIONS

An additional configuration was added to the test program to determine if an increase in mixing and overall performance could be obtained by two additional geometry changes: 1) a further lobe cutback and, 2) the addition of mixer/plug ramps. These modifications were made to configuration 59, and the modified design was identified as configuration 60. Both modifications were included in one configuration to avoid adding additional test points to the program. The additional cutback was selected to extend the test range for discharge angle (λ) to -9 degrees, since small discharge angle variations (λ = 2 to -4 degrees) were shown to have little impact on overall performance (Sections 5.4 through 5.6). Only every other lobe was modified to minimize changes in the primary and fan areas at the mixing plane. this produced a bilevel set of discharge angles (λ = 0 to -9 degrees). The mixer/plug ramp was selected as a novel method for influencing mixing in the central region of the mixing duct. In Phase II testing it was demonstrated that mixing was affected by the size of the mixer/plug gap. A gap size (Agap/Aprimary) of approximately 22 percent resulted in the best overall performance although a "hot spot" was present in the central region of the tailpipe. A smaller gap size increased mixing and removed the hot spot; however, overall performance was not improved due to a pressure loss penalty. The gap size was controlled by varying the proximity between the mixer and plug in the region of the mixing plane. The mixer/plug ramp was devised as an alternate method to reduce the gap size and inject more fan flow into the central "hot spot". As in the case of the lobe cutback, ramps were added to every other lobe.

The additional modifications resulted in a loss of overall performance of 0.29 percent TSFC (based on the traverse integration approach) relative to the baseline configuration, and no major change relative to configuration 59 as shown in Figure 38. The impact of the modifications is best illustrated by comparing configurations 59 and 60. The modifications produced a significant increase in mixing (7.8 percent based on the traverse integration increments); however, this improvement was negated by a 0.0039 increase in excess pressure loss ($\Delta(\Delta PT/PT)$).

The mixing improvement can also be seen in a comparison of the nozzle exit total temperature distributions of configurations 59 and 60 as shown in Figure 39. Note that the mixer/plug ramps eliminated the central "hot spot". In addition, the bilevel cutback modification appears to have increased mixing in the outer region of the tailpipe.

A comparison of all four percent mixing evaluations showed considerable disagreement as illustrated in Figure 40. Therefore, a performance assessment based on the traverse integration approach was considered more accurate. Note that an error in a single parameter is not clearly defined by the percent mixing comparisons. However, an inaccurately high "hot" flow coefficient for configuration 60 is the type of error that would cause Methods III and IV to predict low levels of percent mixing.

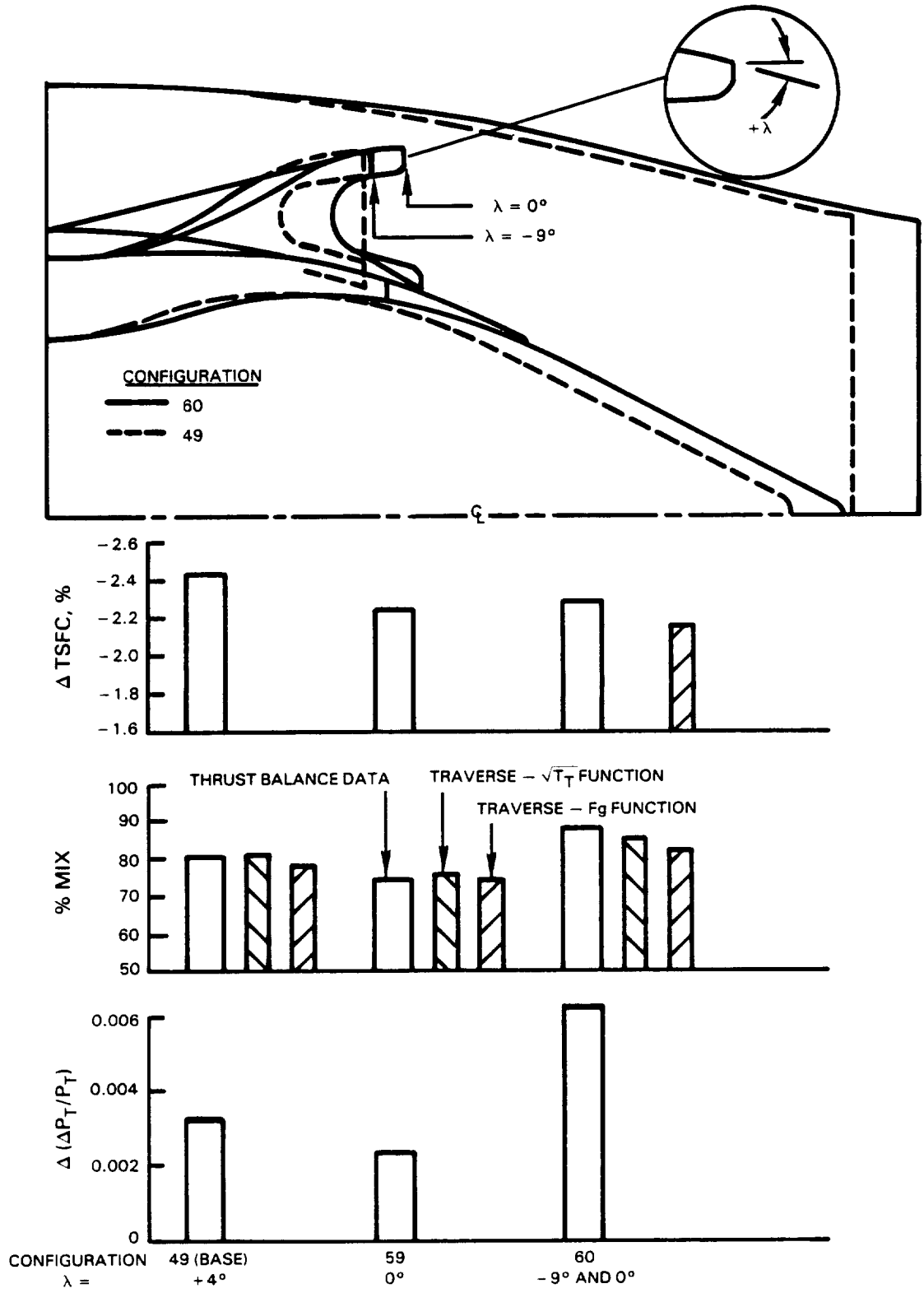

Figure 38 Performance Summary - Effect of Bilevel Discharge Angle and Mixer/Plug Ramps

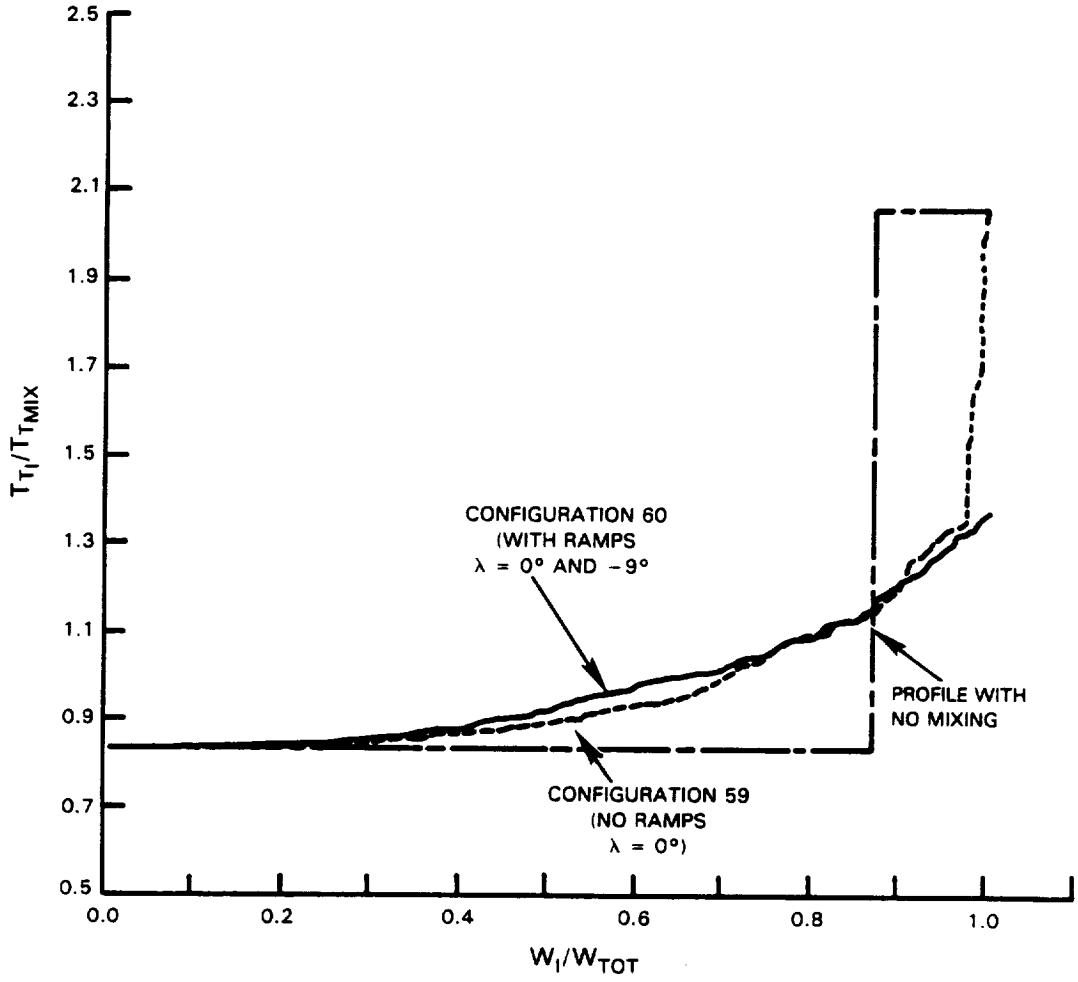

Figure 39 The Effect on Nozzle Exit Total Temperature Distribution of the Mixer/Plug Ramps and the Bilevel Lobe Discharge Angle

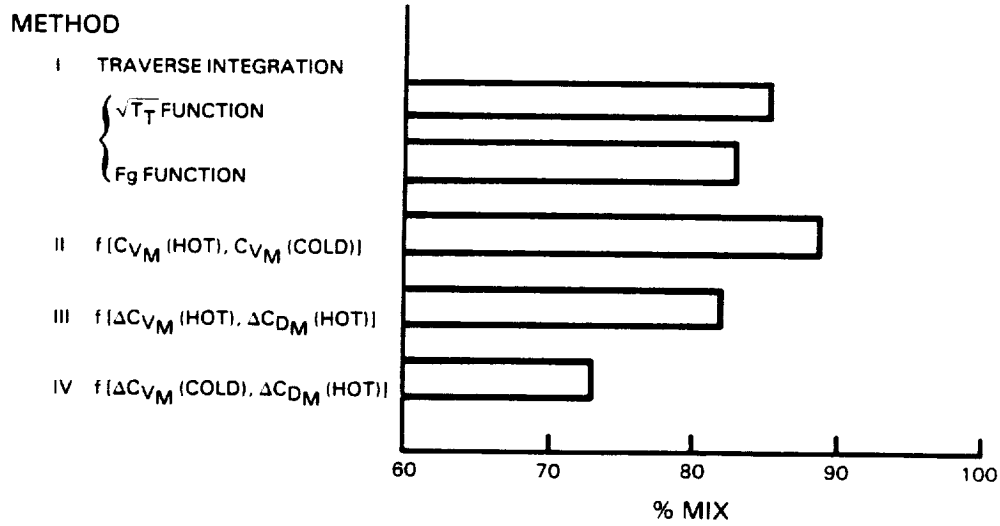

Figure 40 A Comparison of the Independent Percent Mixing Evaluations for Configuration 60

Since the plug/ramp and the lobe cutback modifications were tested as one configuration, the degree to which each modification affected overall performance could not be obtained from the thrust balance data. Integration of the nozzle survey data in regions behind individual lobes provided some insight into the impact of each modification on mixing; however, the excess pressure loss components of performance could not be accurately determined from the survey data. The lobe cutback was estimated to produce a 2 to 3 percent gain in mixing and the mixer/plug gap gain was estimated to be between 5 and 6 percent. Two comparisons were utilized to estimate mixing from the traverse data. First, the effect of the mixer/plug ramps on mixing was estimated by comparing traverse integration results from configurations 59 and 60 from regions where differences in the nozzle exit profiles were generated primarily by the ramps, that is, in regions where the discharge angles were the same (λ = 0 degrees). This approach indicated that the ramps improved mixing by 5.1 percent, and, since the total gain in mixing was 7.8 percent, the lobe modification gain was 2.7 percent. Similar results were obtained by comparing two integration regions from configuration 60 where differences in the nozzle exit profiles were generated primarily by differences in the discharge angles. This approach indicated that the discharge angle modification increased mixing by 2.1 percent and the ramps improved mixing by 5.7 percent. These results are illustrated graphically in Figure 41. The percent mixing increments are quoted on the basis of the gross thrust mixing function. Both the thrust function and temperature function produced essentially the same results.

Excess pressure loss increments for the individual lobe cutback and ramp modifications could not be reliably determined from the traverse data. It was observed that the total pressure levels determined by integrating in two adjacent regions behind similar lobes were different by approximately 0.25 percent for most of the configurations. Therefore, integrating behind individual lobes where the lobe geometry was different would not produce reliable results where the expected pressure loss differences were a few tenths of one percent. This problem is probably the result of the large degree of distortion in the nozzle exit total pressure profiles, which could not be integrated to the high degree of accuracy required without a substantial increase in the grid density of the total pressure survey.

5.8 EXCESS PRESSURE LOSS TRENDS

As in Phase I and II testing, excess pressure loss ($\Delta(\Delta PT/PT)$ was reduced by decreasing penetration or increasing mixer lobe length. In the case of the Phase III configurations, these changes predominately affected flow turning through the primary stream, and a strong correlation between primary stream flow turning and excess pressure loss was observed as illustrated in Figure 42. The primary stream flow turning was characterized by the degree of radial displacement of the lobe outer wall measured at the point of maximum displacement (y/x). Note, that in the case of the extended mixers (configurations 53, 54, 55, 59, and 56) excess pressure loss was almost eliminated by a reduction in penetration. This tends to indicate that for both the base-line and extended mixers, most of the excess pressure loss was generated by the primary stream flow turning.

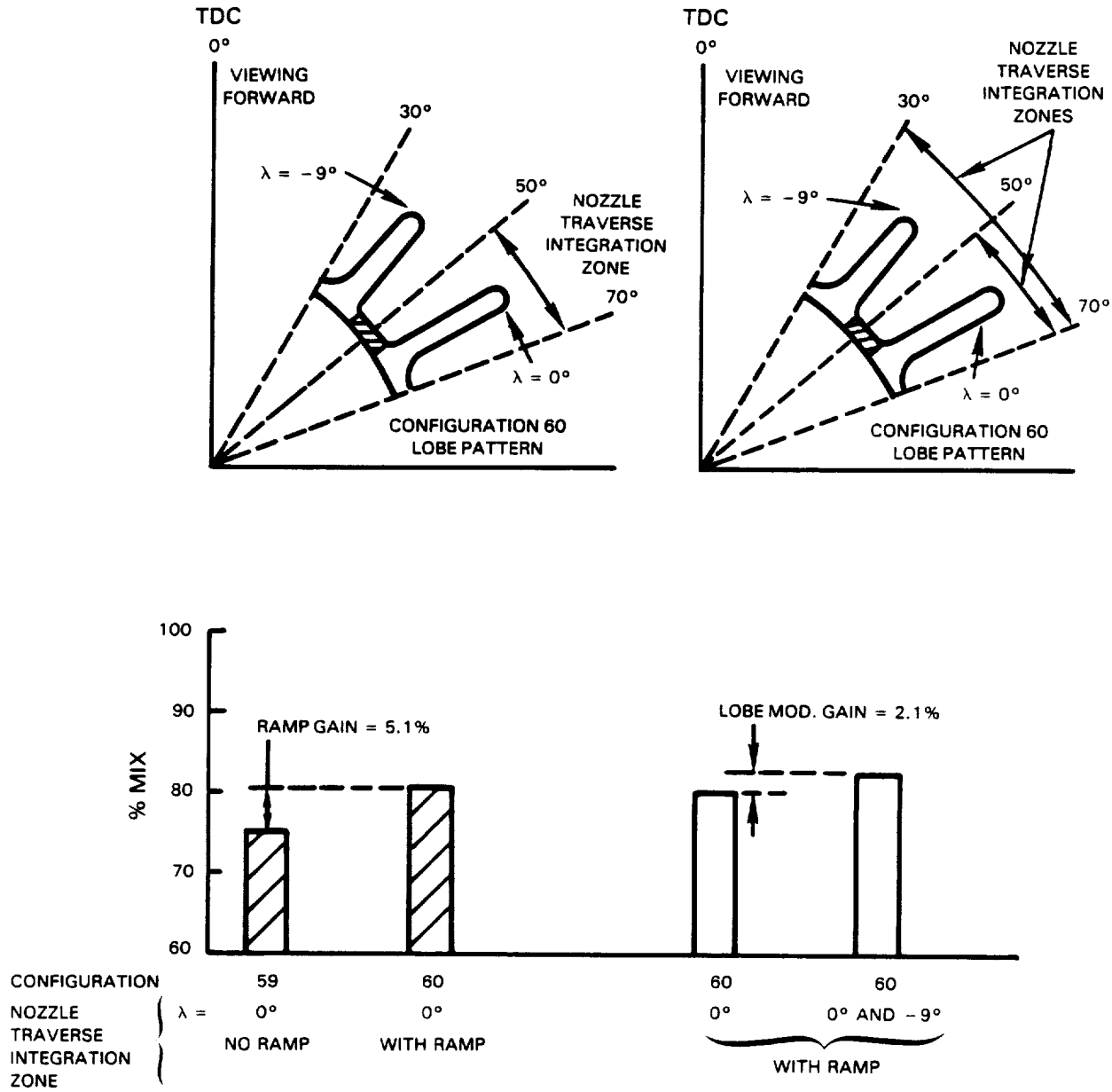

Figure 41 Traverse Integration Performance Assessment - The Impact on Mixing of the Lobe and Mixer/Plug Ramp Modifications

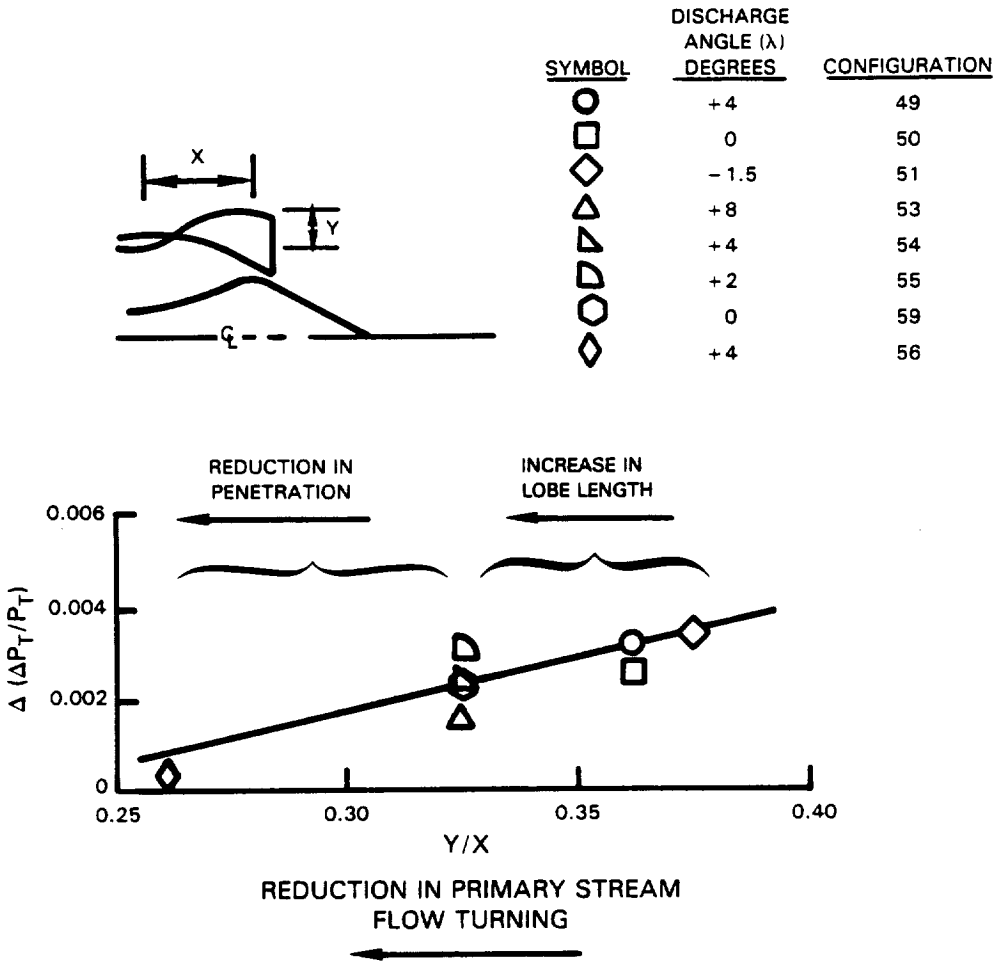

Figure 42 Effect of Mixer Flow Path Turning on Excess Pressure Loss

5.9 MIXER INSTRUMENTATION TEST RESULTS

Two unscalloped mixer configurations (29 and 34) that had been performance tested in Phase II were instrumented to obtain flow properties (in the form of pressure, temperature, and flow angle data) through the lobes for codes such as those being developed under NASA Contract NAS3-23039. Configuration 29 is a low penetration (0.51), low excess pressure loss [$\Delta(\Delta PT/PT)] < 0$ design, while configuration 34 has high penetration (0.75) and high loss (0.012). Even though configuration 19 had 30 percent less mixing than configuration 34, it had a resultant performance increase of 0.48 percent TSFC, that was primarily due to its low loss. A summary of these results is shown in Table V.

TABLE V

UNSCALLOPED CONFIGURATIONS PERFORMANCE TESTED IN PHASE II

		Conf. 29	Conf. 34
Geometry	Penetration	0.51	0.75
	Lobe Number	18	18
	Tailpipe L/D	0.61	0.61
Performance	% Mix	59	89
	Δ (ΔPT/PT)	< 0	0.012
	Δ TSFC	-2.11	1.63

Diagnostic testing of configurations 29 and 34 established the total pressure profiles (relative to the ideal fully mixed total pressure) at the exit of the lobes (see Figure 43) and identifies the actual loss regions of the lobe. The outline of the lobe is added for clarity. There is a concentrated low pressure region at the very top of the lobe that is associated with primary stream flow turning. The configuration 34 low pressure region is more severe than that for configuration 29 and is due to more flow turning. In addition, there are low pressure regions along the side of the lobe. The outermost low pressure regions are believed to be caused by the secondary flows within the lobe due to the static pressure gradients set up by the flow turning. The inner low pressure regions, near the centerbody, are a result of the interference between the lobe fan valley and centerbody. Finally, another low pressure region exists at the base of the fan valley and is due to an accumulation of the boundary layer from the upstream duct and the flow turning through the fan portion of the lobe.

Nonaxial velocities at the lobe exit plane were also calculated (at selected locations) for configurations 29 and 34. The major features of these radial-circumferential velocity fields are: a strong radial velocity directed toward the centerbody in the fan valley region, a slightly weaker radial velocity for configuration 29 but stronger velocity field for configuration 34 directed outward toward the tailpipe wall in the primary lobe region, and significant circumferential velocity components near the lobe side wall and lobe/centerbody regions for both configurations. These velocity fields, when combined, suggest a large-scale counterclockwise circulation region and is similar to those observed in other diagnostic mixer tests (Ref. 3). A description of those nonaxial velocities, in the form of velocity vectors, is shown in Figure 44 where numbers next to the vector are magnitudes of velocity in m/sec.

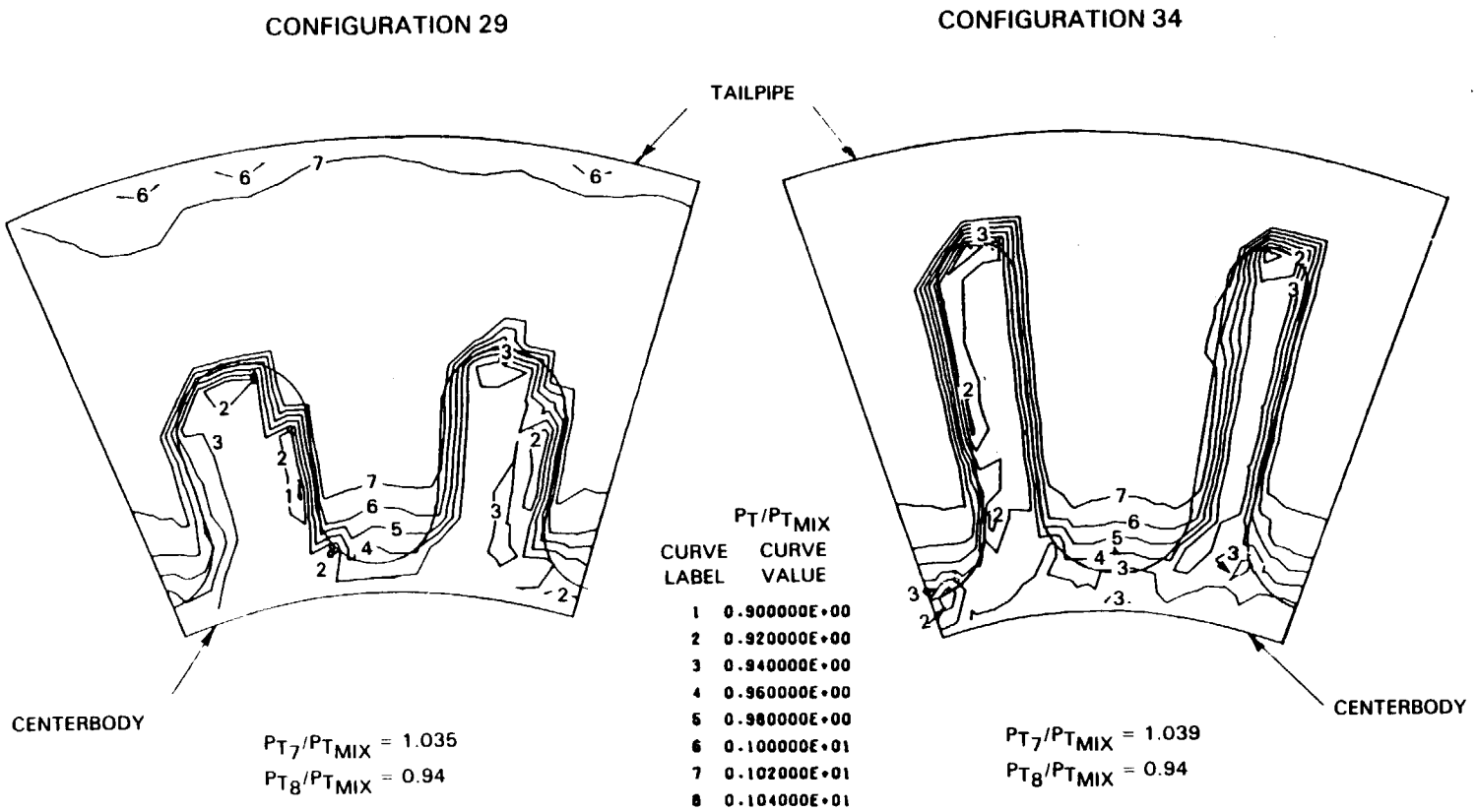

Figure 43 Pressure Patterns Measured at the Mixer Exit

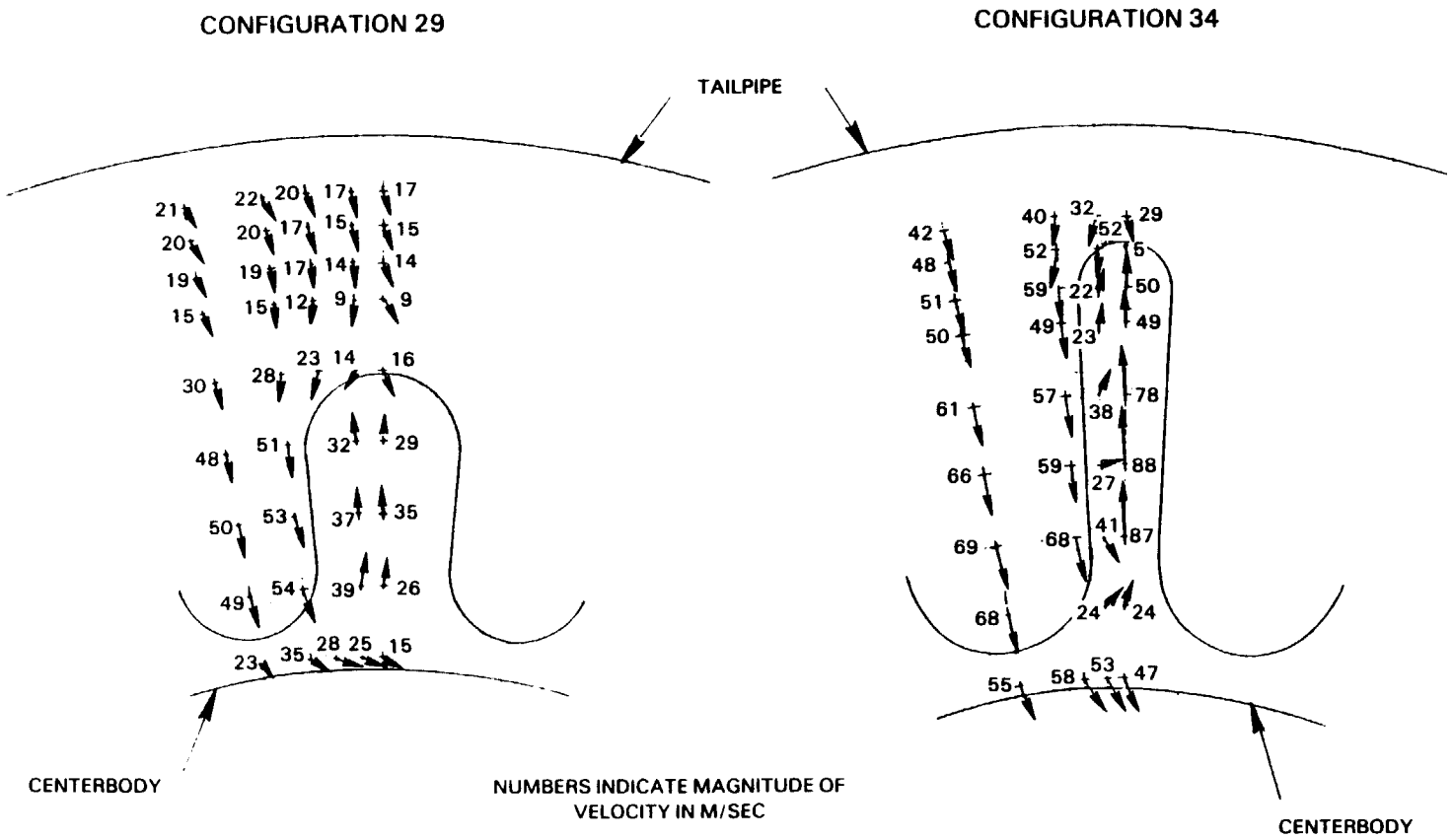

Figure 44 Nonaxial Velocity at the Mixing Plane

Total temperature profiles (relative to the ideal, fully mixed total temperature) were also established for configurations 29 and 34 at the exit of the lobe and tailpipe nozzle as shown in Figures 45 and 46. The low penetration, low loss design (configuration 29) exhibited a mixing level that was 30 percent less than the higher penetration, high loss configuration (34). This is evidenced by the increased gradients and reduced penetration of the primary flow into the fan stream as seen at the nozzle exit plane. The shaded areas on the traverse plots define the region where mixed temperatures exist and provides a guide to distinguish the primary from the fan stream. The lobe shape is clearly outlined at the mixer exit plane, and the steep gradients indicate that very little mixing has taken place.

Finally, lobes, tailpipe, and centerbody (plug) surface pressures were used to determine local Mach numbers which are based on measured charging total pressure in each stream. Figures 47 (configuration 19) and 48 (configuration 34) show the mixer surface Mach number contours in the fan and primary streams, where the flow direction is indicated by arrows. Fan flow that goes around the backside of the low penetration design (configuration 29) accelerates toward the fan valley and then diffuses slightly as it approaches the lobe trailing edge. In the primary stream, the flow accelerates around the fan valley and then diffuses slightly as it travels toward the inside lobe peak.

For the high penetration configuration, the flow field shows stronger gradients and slightly different trends. The fan flow accelerates rapidly around the lobe backside (due to the narrow lobe shape) and then diffuses slightly as it approaches the mixer trailing edge. A similar flow field occurs in the primary stream where the flow around the inside fan valley accelerates and then diffuses significantly, especially along the inside lobe peak. This diffusion is associated with the large primary flow turning of the high penetration design.

Figures 49 through 52 show the tailpipe and centerbody (plug) surface Mach numbers for configurations 29 and 34. Also shown are one-dimensional Mach number calculations which are based on the area distributions shown for each flow path. The one-dimensional Mach number calculations agree fairly well with the tailpipe data (Figures 50 and 52) but vary significantly with the centerbody data (Figures 49 and 51), especially at the lobe trailing edge. This disagreement is primarily due to the more severe flow turning that takes place in the primary stream.

A complete tabulation of all the data presented in this section can be found in Appendix D.

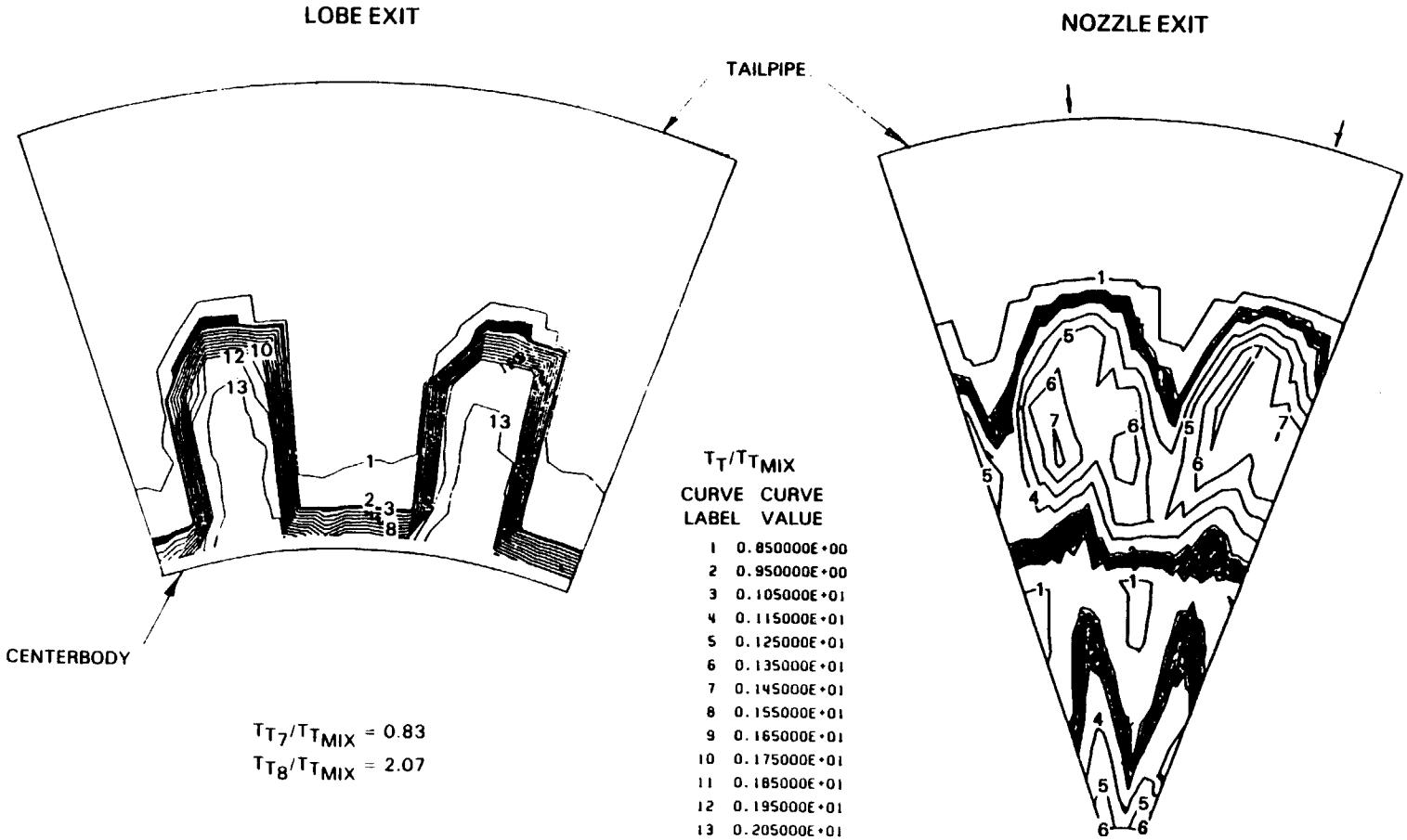

Figure 45 Configuration 29 Temperature Patterns

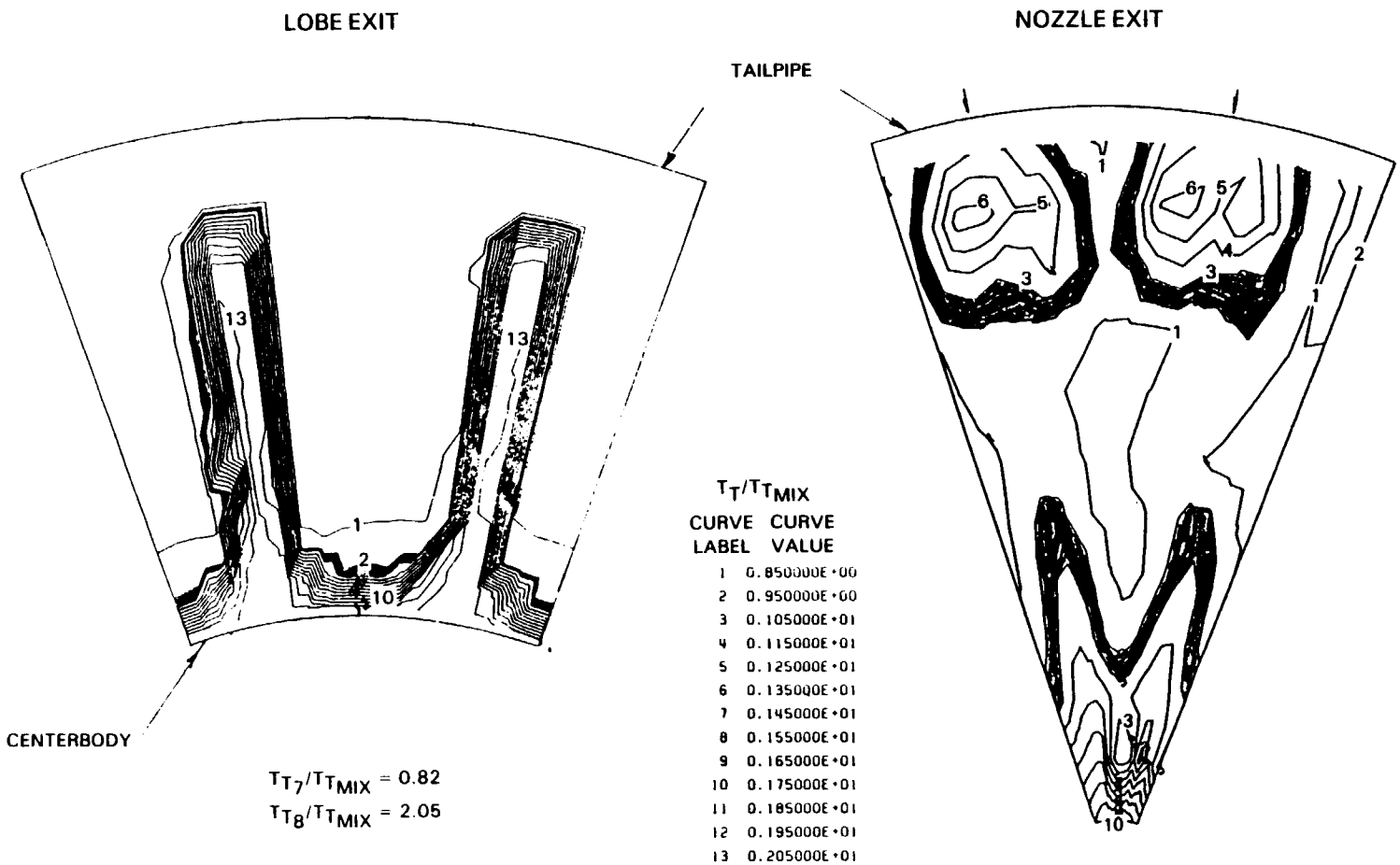

Figure 46 Configuration 34 Temperature Patterns

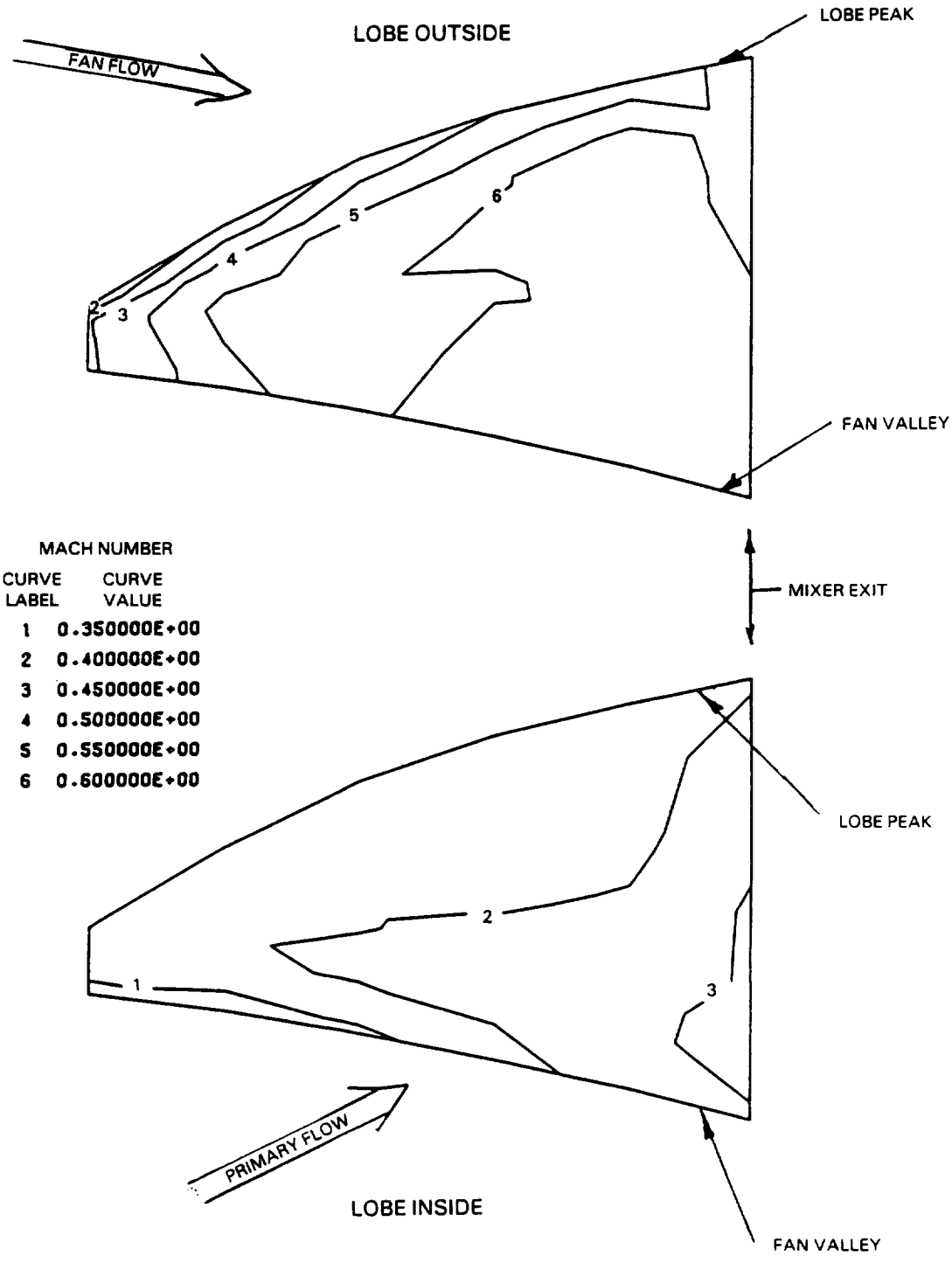

Figure 47 Configuration 29 Mixer Surface Mach Number Patterns

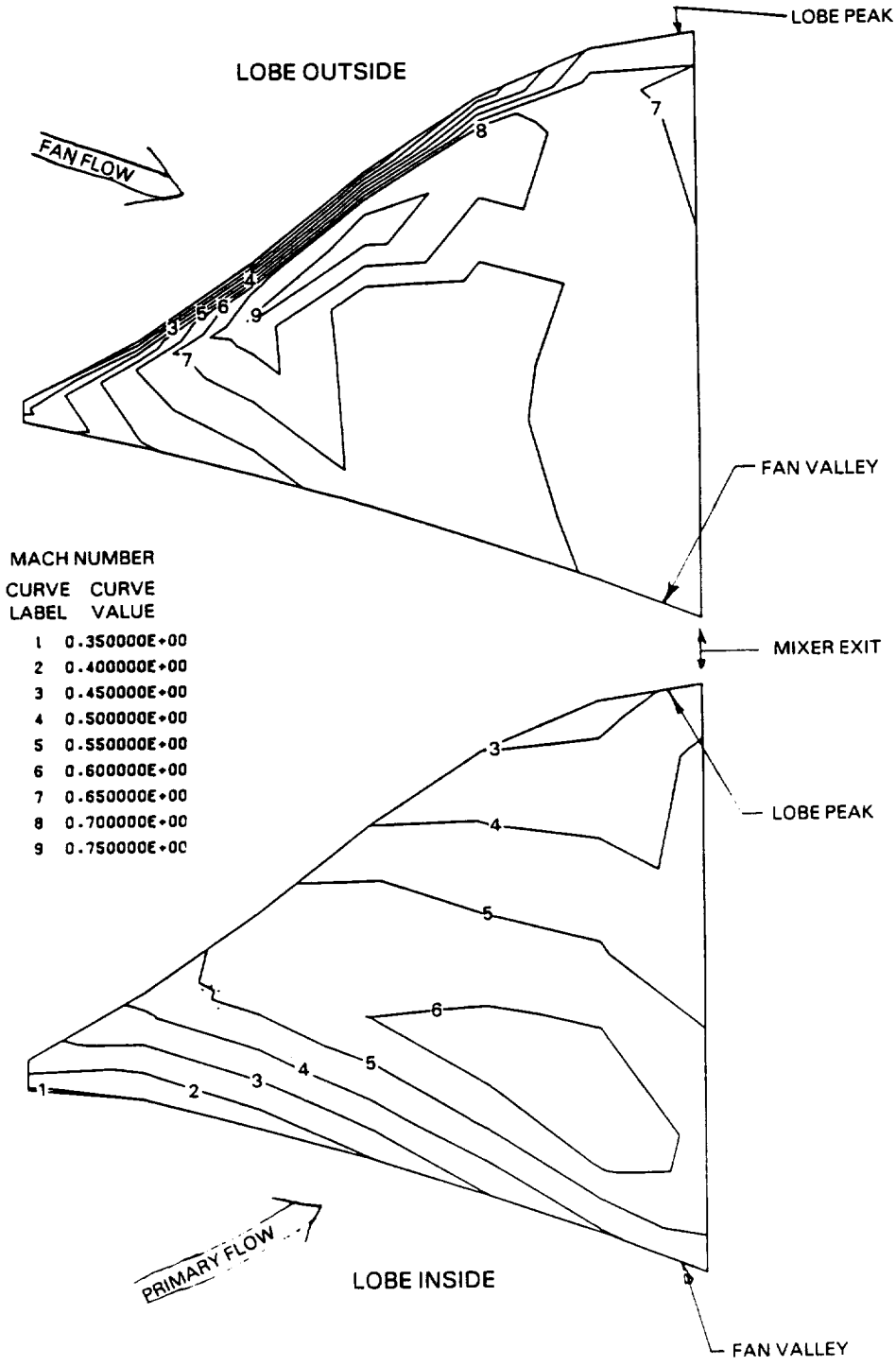

Figure 48 Configuration 34 Mixer Surface Mach Number Patterns

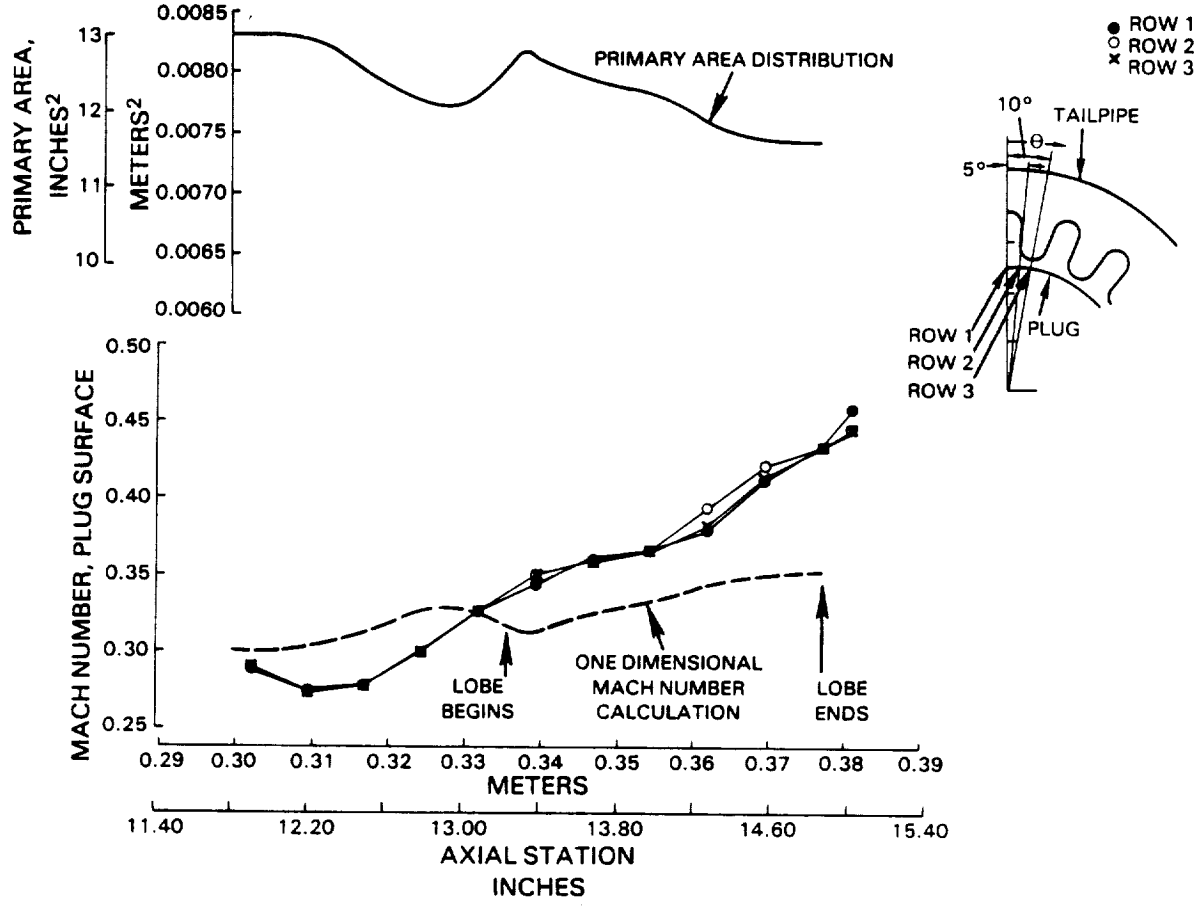

Figure 49 Configuration 29 Mixer Plug Surface Mach Number and Primary Stream Area Distributions

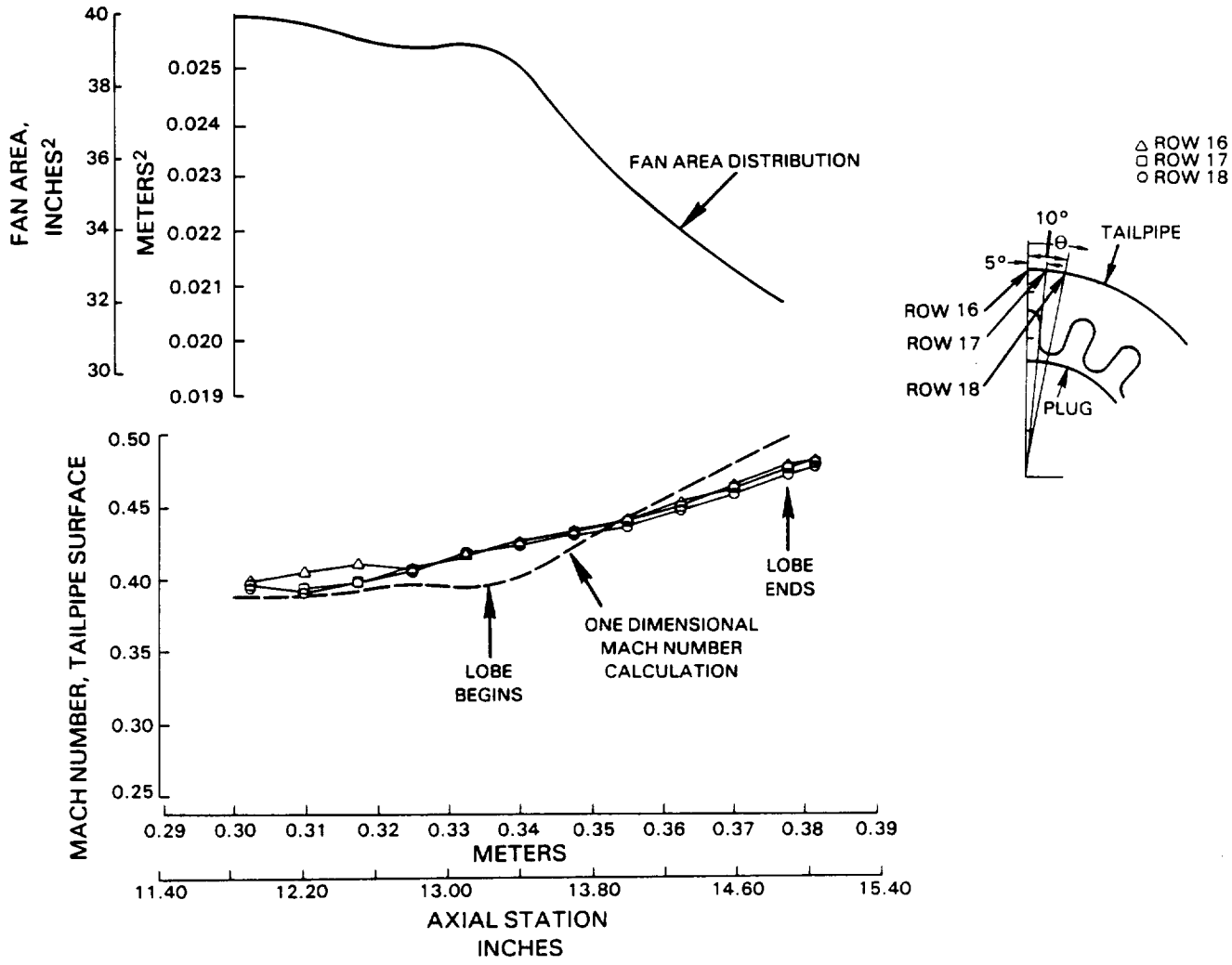

Figure 50 Configuration 29 Mixer Tailpipe Surface Mach Number and Fan Stream Area Distributions

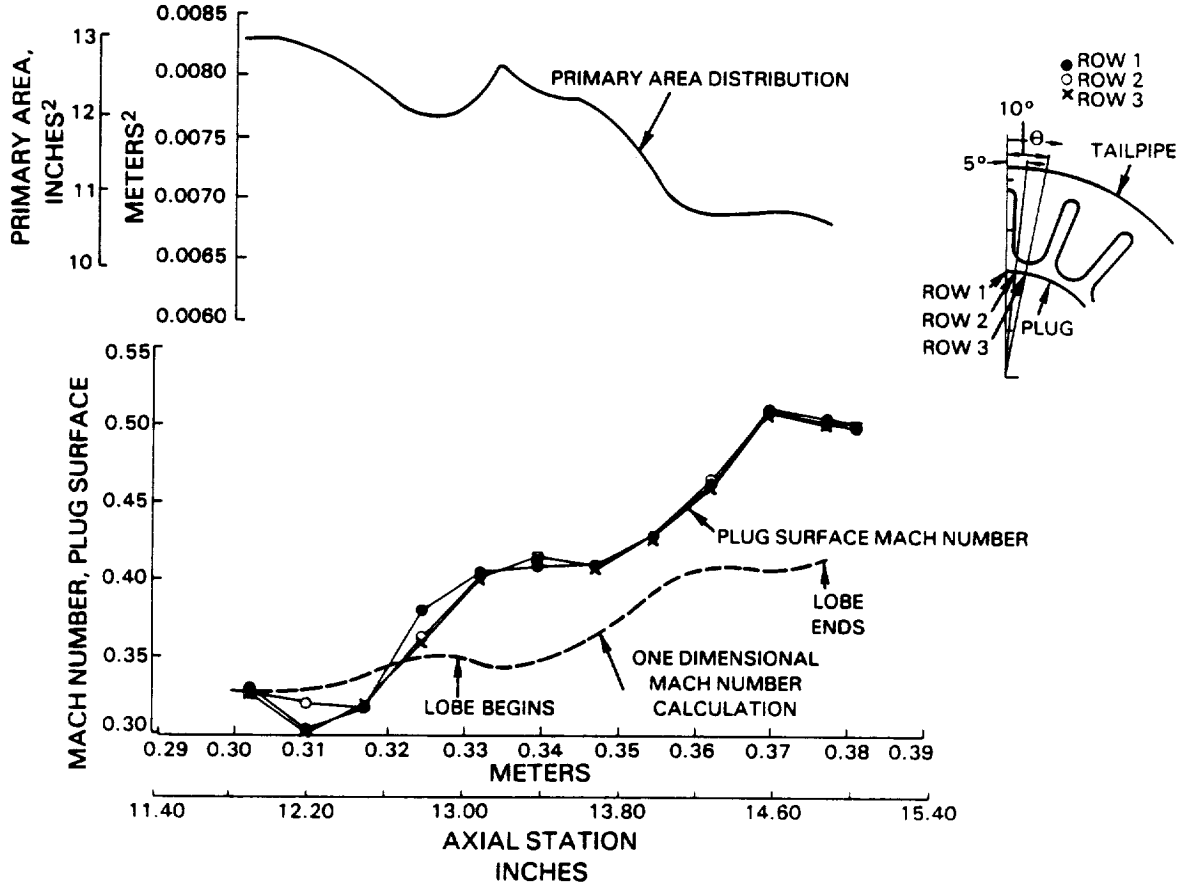

Figure 51 Configuration 34 Mixer Plug Surface Mach Number and Primary Stream Area Distributions

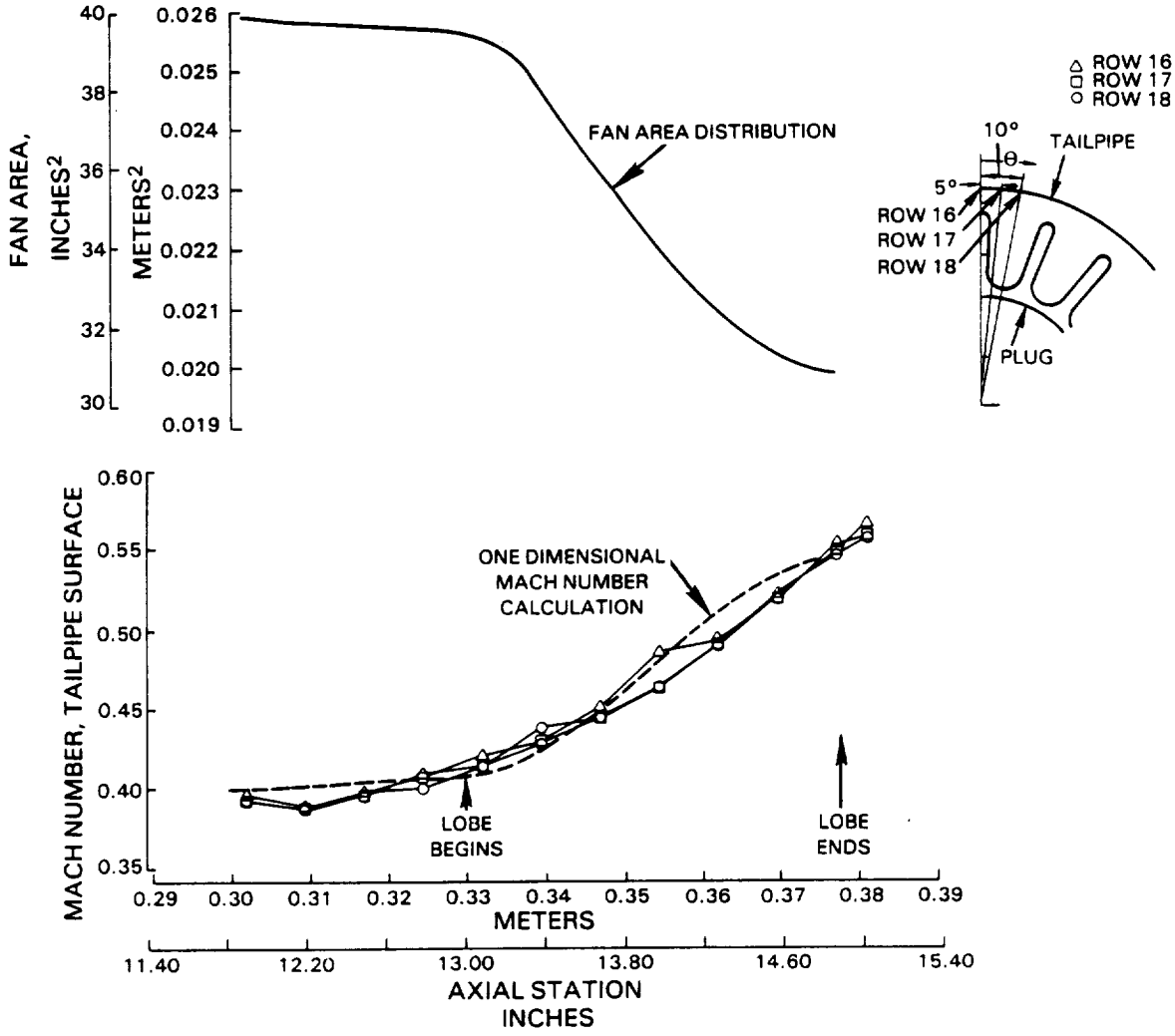

Figure 52 Configuration 34 Mixer Tailpipe Surface Mach Number and Fan Stream Area Distributions

REFERENCES

1. Kozlowski, H. and Larkin, M., "Energy Efficient Engine Exhaust Mixer Model Technology Report," NASA CR-165459, United Technologies Corporation, Pratt & Whitney, June 1981.

2. Cline, M. C., "A Computer Program for Computaton of Two-Dimensional, Time-Dependent, Compressible, Turbulent Flow," LA-8872, Los Alamos National Laboratory, August 1981.

3. Patterson, R. W., "Turbofan Forced Mixer-Nozzle Internal Flow Field I - A Benchmark Experimental Study," NASA Contractor Report 3492, April, 1982.

APPENDIX A

MODEL TEST DATA

Tabulations of the key model test data are presented in this appendix. The data are grouped in order of the test configuration number. The $C_{V\ MIX}$ and $C_{D\ MIX}$ data have been processed to reflect fully mixed flow properties for the reference ideal conditions.

A.1 DEFINITION OF SYMBOLS

Defined at Model Mixing Plane

$C_{V\ MIX}$ - Mixed Model Thrust Coefficient = $Fg_{\ MEASURED}/Fg_{\ \left.\begin{matrix}FULLY\\MIXED\end{matrix}\right)\ IDEAL}$

$C_{D\ MIX}$ - Mixed Model Flow Coefficient =

$$(Wa_{\ FAN} + Wa_{\ PRI})_{MEASURED}/Wa_{\left.\begin{matrix}FULLY\\MIXED\end{matrix}\right)IDEAL}$$

PTMPA - Fully Mixed Total to Ambient Nozzle Pressure Ratio

PTFPAM - Fan Stream Total to Ambient Nozzle Pressure Ratio

PTEPAM - Primary Stream Total to Ambient Nozzle Pressure Ratio

PRAT - Ratio of PTFPAM to PTEPAM

MIXP - Ideal Nozzle Performance Gain Available From Mixing =

$$\left[(Fg_{\begin{matrix}FULLY\\MIXED\end{matrix}} - Fg_{UNMIXED})\ /Fg_{\begin{matrix}FULLY\\MIXED\end{matrix}}\right]_{IDEAL}$$

$F_G(3)$ - Fully Mixed Ideal Thrust = $Fg_{\left.\begin{matrix}FULLY\\MIXED\end{matrix}\right)\ IDEAL}$ - lb

MN_{FAN} - Fan Stream Mach Number

MN_{PRI} - Primary Stream Mach Number

Defined at Model Charging Station

PT7PAM - Fan Stream Total to Ambient Nozzle Pressure Ratio

PT8PAM - Primary Stream Total to Ambient Nozzle Pressure Ratio

TT7 - Fan Stream Total Temperature - ^{o}R

TT8 - Primary Stream Total Temperature - ^{o}R

TRAT - Ratio of TT8 to TT7

PAM - Ambient Pressure - $lb/in.^2$

BPR - Bypass Ratio = $(Wa_{FAN}/Wa_{PRI})_{MEASURED}$

A.2 TEST DATA LISTING

E3 MIXER NO. 1 CONF 1,RUNS 1.002-5.0,COLD

RUN	1.0020	2.0020	3.0000	4.0000	5.0000
CVMIX	.99493	.99506	.99415	.99502	.99412
CDMIX	.96488	.96696	.96844	.96898	.97000
PTMPA	2.1964	2.2902	2.4078	2.5015	2.5940
PTFPAM	2.1934	2.2854	2.4105	2.5047	2.5969
PTEPAM	2.2034	2.3012	2.4012	2.4939	2.5869
PRAT	.99546	.99314	1.0039	1.0043	1.0039
MIXP	.39433E-05	.85102E-06	.84075E-05	.13882E-04	-.30546E-05
FG(3)	804.87	860.64	929.23	984.84	1039.0
MNFAN	.40473	.40462	.41112	.41169	.41194
MNPRI	.41295	.41687	.40412	.40380	.40494
PT7PAM	2.2041	2.2966	2.4227	2.5174	2.6101
PT8PAM	2.2191	2.3180	2.4176	2.5109	2.6046
TT7	530.93	529.06	517.19	524.94	512.79
TT8	532.12	530.70	519.98	526.76	515.78
TRAT	1.0022	1.0031	1.0054	1.0035	1.0058
PAM	14.118	14.118	14.106	14.116	14.106
BFR	2.3014	2.2792	2.3902	2.3932	2.3906

E3 MIXER NO. 1 CONF 1,RUNS 130.0-133.0,COLD

RUN	130.00	131.00	132.001	133.00
CVMIX	.99585	.99653	.99582	.99523
CDMIX	.96677	.96764	.96942	.97002
PTMPA	2.2467	2.3665	2.4592	2.5580
PTFPAM	2.2456	2.3701	2.4617	2.5626
PTEPAM	2.2492	2.3580	2.4533	2.5472
PRAT	.99844	1.0051	1.0034	1.0060
MIXP	.80779E-05	.66556E-05	.32616E-05	.52039E-05
FG(3)	846.25	917.05	973.08	1032.1
MNFAN	.40729	.41143	.41144	.41316
MNPRI	.41020	.40218	.40526	.40232
PT7PAM	2.2567	2.3819	2.4739	2.5755
PT8PAM	2.2654	2.3744	2.4708	2.5651
TT7	533.43	530.04	533.54	526.39
TT8	537.40	533.45	536.27	530.61
TRAT	1.0074	1.0064	1.0051	1.0080
PAM	14.301	14.301	14.299	14.301
BFR	2.3037	2.3662	2.3359	2.3747

E3 MIXER NO. 1 CONF 1,RUNS 6.001-10.001,HOT

RUN	6.0010	7.0000	8.0010	9.0020	10.001
CVMIX	.98826	.98636	.98500	.98317	.98191
CDMIX	.96837	.97303	.97544	.97963	.98184
PTMPA	2.1860	2.2755	2.3538	2.4380	2.5374
PTFPAM	2.2606	2.3498	2.4270	2.5070	2.6093
PTEPAM	1.9880	2.0893	2.1789	2.2882	2.3855
PRAT	1.1371	1.1247	1.1139	1.0956	1.0938
MIXP	.86031E-02	.10637E-01	.12110E-01	.14721E-01	.16171E-01
FG(3)	811.65	868.29	916.32	969.58	1031.6
MNFAN	.49046	.48215	.47458	.46227	.46125
MNPRI	.23003	.24757	.26169	.28569	.28835
PT7PAM	2.2759	2.3653	2.4426	2.5224	2.6253
PT8PAM	1.9931	2.0955	2.1862	2.2972	2.3952
TT7	533.36	534.49	529.77	535.51	525.04
TT8	1248.2	1267.6	1268.0	1308.3	1323.1
TRAT	2.3403	2.3715	2.3934	2.4430	2.5201
PAM	14.293	14.297	14.293	14.285	14.293
BFR	7.3449	6.7916	6.3838	5.9013	5.8256

E3 MIXER NO. 1 CONF 1,RUNS 136.0-138.0,HOT

RUN	136.00	137.00	138.00
CVMIX	.98378	.98168	.98025
COMIX	.97669	.98068	.98328
PTMPA	2.3501	2.4373	2.5334
PTFPAM	2.4230	2.5068	2.6041
PTEPAM	2.1761	2.2855	2.3857
PRAT	1.1135	1.0968	1.0915
MIXP	.12197E-01	.14815E-01	.16466E-01
FG(3)	905.63	960.43	1019.8
MNFAN	.47463	.46327	.45994
MNPRI	.26284	.28461	.29195
PT7PAM	2.4386	2.5223	2.6200
PT8PAM	2.1834	2.2944	2.3955
TT7	537.91	540.21	542.11
TT8	1286.9	1325.9	1364.4
TRAT	2.3923	2.4544	2.5168
PAM	14.142	14.141	14.143
BPR	6.3862	5.8818	5.7731

E3 MIXER NO. 1 CONF 1,RUNS 136.002,137.001,138.001,HOT

RUN	136.002	137.001	138.001
CVMIX	.98581	.98181	.98156
COMIX	.97476	.97964	.98099
PTMPA	2.3425	2.4251	2.5279
PTFPAM	2.4189	2.4961	2.6009
PTEPAM	2.1533	2.2667	2.3666
PRAT	1.1234	1.1012	1.0990
MIXP	.11365E-01	.14344E-01	.15355E-01
FG(3)	907.13	959.48	1021.8
MNFAN	.48151	.46621	.46436
MNPRI	.25000	.27871	.28122
PT7PAM	2.4348	2.5117	2.6172
PT8PAM	2.1599	2.2752	2.3755
TT7	536.67	535.72	532.31
TT8	1287.9	1313.7	1332.3
TRAT	2.3998	2.4523	2.5028
PAM	14.263	14.248	14.248
BPR	6.7687	6.0160	6.0724

E3 MIXER NO. 1 CONF 1,RUNS 135.001,136.003,137.002,138.002,HOT

RUN	135.001	136.003	137.002	138.002
CVMIX	.98628	.98550	.98311	.98219
COMIX	.97242	.97454	.97875	.98136
PTMPA	2.2730	2.3486	2.4318	2.5315
PTFPAM	2.3501	2.4257	2.5038	2.6076
PTEPAM	2.0725	2.1570	2.2719	2.3655
PRAT	1.1339	1.1245	1.1021	1.1024
MIXP	.97763E-02	.11099E-01	.14280E-01	.15492E-01
FG(3)	865.13	911.76	964.78	1026.6
MNFAN	.48901	.48256	.46678	.46749
MNPRI	.23614	.24883	.27764	.27846
PT7PAM	2.3659	2.4416	2.5194	2.6238
PT8PAM	2.0782	2.1636	2.2804	2.3745
TT7	534.52	537.97	537.03	541.82
TT8	1271.1	1283.6	1313.6	1358.9
TRAT	2.3780	2.3860	2.4461	2.5080
PAM	14.278	14.283	14.281	14.280
BPR	7.2229	6.7692	5.9807	6.0364

E3 MIXER NO.12 CONF 49,RUNS 11.001-15.001,COLD

RUN	11.001	12.000	13.001	14.000	15.001
CVMIX	.99035	.99085	.99067	.99062	.99068
CDMIX	.96986	.97003	.96983	.97093	.97032
PTMPA	2.3654	2.4766	2.4772	2.4754	2.5713
PTFPAM	2.3626	2.4734	2.4758	2.4735	2.5696
PTEPAM	2.3740	2.4868	2.4814	2.4813	2.5764
PRAT	.99519	.99459	.99777	.99685	.99737
MIXP	.15487E-04	.13955E-04	.21933E-04	.15696E-04	.12029E-04
FG(3)	914.34	979.74	979.54	979.93	1035.1
MNFAN	.51163	.51154	.51249	.51300	.51273
MNPRI	.51863	.51946	.51576	.51760	.51657
PT7PAM	2.3814	2.4930	2.4956	2.4932	2.5901
PT8PAM	2.3933	2.5071	2.5014	2.5014	2.5972
TT7	533.33	531.78	534.04	529.31	533.36
TT8	538.29	536.56	538.43	534.72	537.66
TRAT	1.0093	1.0090	1.0082	1.0102	1.0081
PAM	14.246	14.247	14.242	14.247	14.239
BPR	3.1754	3.1705	3.1953	3.1887	3.1932

E3 MIXER NO.12 CONF 49,RUNS 16.0-20.0,HOT

RUN	16.000	17.000	18.000	19.000	20.000
CVMIX	.98787	.98762	.98710	.98945	.98816
CDMIX	.97510	.97593	.97633	.97432	.97589
PTMPA	2.3357	2.4758	2.4746	2.4751	2.5080
PTFPAM	2.4029	2.5442	2.5425	2.5446	2.5735
PTEPAM	2.1671	2.3163	2.3171	2.3096	2.3659
PRAT	1.1088	1.0984	1.0973	1.1018	1.0878
MIXP	.12226E-01	.13961E-01	.14042E-01	.13742E-01	.15255E-01
FG(3)	900.45	983.59	983.29	981.44	1002.5
MNFAN	.54581	.54021	.53986	.54093	.53415
MNPRI	.38419	.39500	.39638	.39002	.40537
PT7PAM	2.4234	2.5655	2.5638	2.5660	2.5948
PT8PAM	2.1814	2.3324	2.3333	2.3253	2.3830
TT7	528.50	534.19	530.68	531.85	532.05
TT8	1283.6	1332.5	1326.6	1325.7	1355.7
TRAT	2.4287	2.4945	2.4998	2.4927	2.5482
PAM	14.225	14.226	14.226	14.224	14.226
BPR	6.8439	6.6642	6.6506	6.7514	6.5097

E3 MIXER NO.12 CONF 50,RUNS 21.0-25.0,COLD

RUN	21.000	22.000	23.000	24.000	25.000
CVMIX	.99109	.99109	.99121	.99080	.99176
CDMIX	.96954	.97015	.96995	.97017	.96993
PTMPA	2.3687	2.4801	2.4780	2.4702	2.5683
PTFPAM	2.3686	2.4804	2.4784	2.4694	2.5676
PTEPAM	2.3687	2.4792	2.4767	2.4724	2.5700
PRAT	.99995	1.0005	1.0007	.99876	.99908
MIXP	.11767E-04	.22203E-04	.14240E-04	.18066E-04	.11848E-04
FG(3)	912.90	978.61	977.25	973.01	1030.3
MNFAN	.51304	.51366	.51358	.51308	.51301
MNPRI	.51301	.51296	.51259	.51490	.51437
PT7PAM	2.3875	2.5002	2.4982	2.4891	2.5881
PT8PAM	2.3877	2.4990	2.4965	2.4924	2.5907
TT7	529.52	527.35	526.69	529.03	532.27
TT8	536.55	534.80	533.53	534.75	537.30
TRAT	1.0171	1.0141	1.0130	1.0108	1.0094
PAM	14.198	14.199	14.200	14.202	14.203
BPR	3.2261	3.2241	3.2230	3.2042	3.2037

E3 MIXER NO.12 CONF 50,RUNS 26.0-30.0,HOT

RUN	26.000	27.000	28.000	29.000	30.000
CVMIX	.98770	.98826	.98854	.98863	.98688
CDMIX	.97494	.97522	.97602	.97489	.97683
PTMPA	2.3318	2.4731	2.4719	2.4740	2.5036
PTFPAM	2.3990	2.5416	2.5394	2.5411	2.5705
PTEPAM	2.1639	2.3125	2.3159	2.3189	2.3580
PRAT	1.1086	1.0991	1.0965	1.0958	1.0901
MIXP	.12443E-01	.13983E-01	.14145E-01	.14031E-01	.15406E-01
FG(3)	899.08	982.31	982.22	982.07	1000.8
MNFAN	.54538	.54001	.53920	.53828	.53564
MNPRI	.38398	.39343	.39687	.39675	.40342
PT7PAM	2.4195	2.5630	2.5607	2.5623	2.5918
PT8PAM	2.1781	2.3284	2.3321	2.3351	2.3750
TT7	531.14	528.19	530.00	528.69	534.87
TT8	1297.9	1322.5	1327.4	1319.6	1371.6
TRAT	2.4436	2.5038	2.5046	2.4960	2.5644
PAM	14.242	14.240	14.238	14.234	14.225
BPR	6.8688	6.7103	6.6456	6.6257	6.5717

E3 MIXER NO.12 CONF 51,RUNS 33.0-37.0,COLD

RUN	33.000	34.000	35.000	36.000	37.000
CVMIX	.99021	.99000	.99076	.99104	.99034
CDMIX	.96987	.96989	.96937	.96976	.96971
PTMPA	2.3687	2.4758	2.4759	2.4757	2.5640
PTFPAM	2.3671	2.4757	2.4741	2.4758	2.5628
PTEPAM	2.3736	2.4761	2.4814	2.4753	2.5672
PRAT	.99727	.99983	.99707	1.0002	.99830
MIXP	.25211E-04	.17323E-04	.14321E-04	.13055E-04	.10245E-04
FG(3)	910.27	972.46	971.72	972.46	1024.7
MNFAN	.51237	.51325	.51189	.51329	.51259
MNPRI	.51625	.51351	.51619	.51299	.51508
PT7PAM	2.3860	2.4954	2.4938	2.4955	2.5832
PT8PAM	2.3929	2.4960	2.5016	2.4952	2.5880
TT7	532.64	531.75	529.73	533.15	532.46
TT8	541.01	538.52	536.20	538.24	536.95
TRAT	1.0157	1.0127	1.0122	1.0095	1.0084
PAM	14.152	14.150	14.146	14.153	14.164
BPR	3.1940	3.2115	3.1869	3.2110	3.1923

E3 MIXER NO.12 CONF 51,RUNS 38.0-42.0,HOT

RUN	38.000	39.000	40.000	41.000	42.000
CVMIX	.98670	.98685	.98725	.98698	.98655
CDMIX	.97452	.97537	.97481	.97499	.97544
PTMPA	2.3414	2.4817	2.4835	2.4786	2.5108
PTFPAM	2.4089	2.5518	2.5535	2.5462	2.5770
PTEPAM	2.1717	2.3152	2.3165	2.3223	2.3664
PRAT	1.1092	1.1022	1.1023	1.0964	1.0890
MIXP	.12252E-01	.13782E-01	.13687E-01	.14092E-01	.15235E-01
FG(3)	901.91	984.05	983.68	981.11	1000.9
MNFAN	.54562	.54177	.54156	.53864	.53444
MNPRI	.38319	.39045	.38999	.39627	.40365
PT7PAM	2.4295	2.5733	2.5750	2.5675	2.5983
PT8PAM	2.1859	2.3311	2.3323	2.3386	2.3835
TT7	528.97	528.66	532.02	534.70	530.66
TT8	1286.1	1320.5	1324.4	1334.5	1354.0
TRAT	2.4314	2.4978	2.4894	2.4958	2.5515
PAM	14.204	14.190	14.178	14.180	14.186
BPR	6.8606	6.7524	6.7471	6.6215	6.5375

E3 MIXER NO.13 CONF 53,RUNS 57.0-61.0,COLD

RUN	57.000	58.000	59.000	60.000	61.000
CVMIX	.99170	.99165	.99133	.99158	.99149
CDMIX	.97186	.97207	.97214	.97196	.97211
PTMPA	2.3654	2.4737	2.4748	2.4745	2.5584
PTFPAM	2.3649	2.4729	2.4741	2.4735	2.5581
PTEPAM	2.3666	2.4758	2.4766	2.4771	2.5593
PRAT	.99930	.99883	.99900	.99855	.99951
MIXP	.53268E-05	.74703E-05	.18659E-04	.13196E-04	.12555E-04
FG(3)	916.65	980.44	981.33	980.58	1030.6
MNFAN	.51652	.51652	.51663	.51634	.51679
MNPRI	.51756	.51822	.51810	.51844	.51751
PT7PAM	2.3844	2.4932	2.4945	2.4938	2.5791
PT8PAM	2.3894	2.4998	2.5007	2.5012	2.5841
TT7	530.55	529.41	528.22	532.40	531.27
TT8	538.04	535.45	533.74	536.70	536.35
TRAT	1.0141	1.0114	1.0104	1.0081	1.0096
PAM	14.247	14.247	14.249	14.244	14.250
BPR	3.0877	3.0745	3.0738	3.0641	3.0742

E3 MIXER NO.13 CONF 53,RUNS 62.0-66.0,HOT

RUN	62.000	63.000	64.000	65.000	66.000
CVMIX	.98864	.98819	.98805	.98781	.98759
CDMIX	.97667	.97768	.97784	.97792	.97826
PTMPA	2.3306	2.4692	2.4669	2.4673	2.5005
PTFPAM	2.3995	2.5390	2.5362	2.5365	2.5684
PTEPAM	2.1598	2.3082	2.3086	2.3103	2.3551
PRAT	1.1110	1.1000	1.0986	1.0979	1.0906
MIXP	.12471E-01	.14066E-01	.14189E-01	.14333E-01	.15481E-01
FG(3)	896.39	978.79	978.15	978.56	998.51
MNFAN	.54937	.54384	.54322	.54278	.53361
MNPRI	.38564	.39715	.39883	.39949	.40663
PT7PAM	2.4210	2.5613	2.5585	2.5587	2.5907
PT8PAM	2.1760	2.3265	2.3272	2.3289	2.3747
TT7	529.77	530.96	535.47	536.56	534.08
TT8	1297.4	1329.6	1340.7	1347.5	1369.5
TRAT	2.4489	2.5042	2.5038	2.5114	2.5643
PAM	14.180	14.182	14.190	14.191	14.192
BPR	6.8314	6.6196	6.5749	6.5768	6.4764

E3 MIXER NO.13 CONF 54,RUNS 69.0-73.0,COLD

RUN	69.000	70.000	71.000	72.000	73.000
CVMIX	.99112	.99080	.99144	.99091	.99075
CDMIX	.97177	.97179	.97199	.97187	.97229
PTMPA	2.3599	2.4701	2.4704	2.4696	2.5616
PTFPAM	2.3580	2.4678	2.4689	2.4686	2.5611
PTEPAM	2.3656	2.4767	2.4747	2.4723	2.5627
PRAT	.99676	.99643	.99767	.99849	.99938
MIXP	.99699E-05	.17865E-04	.24900E-04	.12838E-04	.21928E-04
FG(3)	906.05	970.29	970.68	969.86	1024.3
MNFAN	.51556	.51546	.51605	.51625	.51689
MNPRI	.52027	.52064	.51943	.51848	.51780
PT7PAM	2.3773	2.4880	2.4892	2.4889	2.5822
PT8PAM	2.3887	2.5009	2.4988	2.4964	2.5876
TT7	533.19	533.95	532.39	535.66	534.28
TT8	539.24	538.88	537.26	540.34	538.58
TRAT	1.0113	1.0092	1.0092	1.0087	1.0080
PAM	14.133	14.134	14.134	14.131	14.135
BPR	3.0549	3.0487	3.0598	3.0663	3.0694

E3 MIXER NO.13 CONF 54,RUNS 74.0-78.0,HOT

RUN	74.000	75.000	76.000	77.000	78.001
CVMIX	.98805	.98751	.98740	.98777	.98675
COMIX	.97664	.97865	.97815	.97831	.97877
PTMPA	2.3190	2.4685	2.4674	2.4797	2.5135
PTFPAM	2.3857	2.5388	2.5371	2.5504	2.5817
PTEPAM	2.1552	2.3056	2.3072	2.3148	2.3674
PRAT	1.1069	1.1011	1.0996	1.1018	1.0905
MIXP	.12372E-01	.14023E-01	.14145E-01	.13963E-01	.15466E-01
FG(3)	893.06	982.68	980.88	987.80	1007.7
MNFAN	.54763	.54499	.54387	.54517	.53896
MNFRI	.39023	.39691	.39800	.39592	.40723
PT7PAM	2.4071	2.5612	2.5595	2.5730	2.6041
PT8PAM	2.1717	2.3239	2.3256	2.3331	2.3871
TT7	536.82	541.32	541.61	541.04	541.69
TT8	1301.4	1352.4	1354.7	1349.9	1384.4
TRAT	2.4243	2.4983	2.5012	2.4950	2.5556
PAM	14.236	14.231	14.221	14.214	14.206
BPR	6.7045	6.6340	6.6097	6.6529	6.4659

E3 MIXER NO.13 CONF 55,RUNS 81.0-85.0,COLD

RUN	81.000	82.000	83.000	84.000	85.000
CVMIX	.99079	.99116	.99073	.99032	.99127
COMIX	.97188	.97175	.97159	.97212	.97240
PTMPA	2.3606	2.4680	2.4701	2.4657	2.5575
PTFPAM	2.3581	2.4653	2.4666	2.4622	2.5595
PTEPAM	2.3680	2.4758	2.4806	2.4760	2.5510
PRAT	.99582	.99578	.99435	.99444	1.0033
MIXP	.14219E-04	.72730E-05	.10027E-04	.65317E-05	.12611E-04
FG(3)	909.99	972.81	973.94	971.83	1026.0
MNFAN	.51529	.51518	.51456	.51500	.51839
MNFRI	.52138	.52133	.52278	.52310	.51355
PT7PAM	2.3774	2.4855	2.4867	2.4823	2.5806
PT8PAM	2.3913	2.5001	2.5051	2.5005	2.5755
TT7	525.00	526.31	531.34	534.08	532.31
TT8	530.78	530.84	534.46	536.64	535.28
TRAT	1.0110	1.0076	1.0059	1.0048	1.0056
PAM	14.186	14.189	14.190	14.189	14.190
BPR	3.0424	3.0391	3.0214	3.0215	3.0995

E3 MIXER NO.13 CONF 55,RUNS 86.0-90.0,HOT

RUN	86.000	87.000	88.000	89.000	90.000
CVMIX	.98827	.98951	.98780	.98864	.98728
COMIX	.97634	.97689	.97714	.97725	.97838
PTMPA	2.3265	2.4666	2.4650	2.4651	2.4961
PTFPAM	2.3950	2.5374	2.5359	2.5359	2.5635
PTEPAM	2.1553	2.3010	2.2984	2.2998	2.3509
PRAT	1.1112	1.1027	1.1033	1.1027	1.0904
MIXP	.12156E-01	.13911E-01	.13780E-01	.13904E-01	.15191E-01
FG(3)	899.63	982.87	982.20	982.42	1001.7
MNFAN	.54966	.54477	.54534	.54500	.53895
MNFRI	.38551	.39361	.39339	.39414	.40704
PT7PAM	2.4166	2.5598	2.5583	2.5583	2.5858
PT8PAM	2.1716	2.3191	2.3165	2.3179	2.3705
TT7	529.08	527.55	530.07	533.09	523.40
TT8	1283.4	1320.9	1322.4	1332.0	1335.5
TRAT	2.4257	2.5039	2.4947	2.4987	2.5516
PAM	14.274	14.274	14.275	14.276	14.272
BPR	6.7943	6.6774	6.6712	6.6554	6.4527

E3 MIXER NO.14 CONF 56,RUNS 93.0-97.0,COLD

RUN	93.000	94.000	95.000	96.000	97.000
CVMIX	.99238	.99205	.99215	.99209	.99195
CDMIX	.97372	.97292	.97293	.97275	.97313
PTMPA	2.3591	2.4721	2.4754	2.4756	2.5673
PTFPAM	2.3597	2.4733	2.4760	2.4770	2.5695
PTEPAM	2.3570	2.4684	2.4735	2.4713	2.5601
PRAT	1.0011	1.0020	1.0010	1.0023	1.0037
MIXP	.24144E-04	.12515E-04	.16240E-04	.15495E-04	.12315E-04
FG(3)	910.05	975.36	977.15	976.88	1030.9
MNFAN	.51580	.51552	.51517	.51552	.51631
MNPRI	.51420	.51260	.51368	.51213	.51095
PT7PAM	2.3787	2.4931	2.4958	2.4968	2.5901
PT8PAM	2.3794	2.4917	2.4970	2.4947	2.5843
TT7	537.45	539.29	540.54	543.85	543.77
TT8	542.08	543.88	543.96	546.87	546.57
TRAT	1.0086	1.0085	1.0063	1.0056	1.0051
PAM	14.174	14.174	14.172	14.169	14.168
BPR	3.0190	3.0201	3.0070	3.0142	3.0277

E3 MIXER NO.14 CONF 56,RUNS 98.0-102.,HOT

RUN	98.000	99.000	100.00	101.00	102.00
CVMIX	.98745	.98726	.98670	.98702	.98807
CDMIX	.97881	.97939	.97978	.97976	.97935
PTMPA	2.3337	2.4742	2.4785	2.4741	2.5107
PTFPAM	2.4037	2.5457	2.5510	2.5467	2.5814
PTEPAM	2.1645	2.3127	2.3131	2.3084	2.3585
PRAT	1.1105	1.1007	1.1028	1.1032	1.0945
MIXP	.12605E-01	.14167E-01	.14105E-01	.14109E-01	.15320E-01
FG(3)	899.76	983.01	985.90	983.43	1004.6
MNFAN	.54886	.54355	.54481	.54491	.53952
MNPRI	.38570	.39545	.39363	.39327	.40097
PT7PAM	2.4247	2.5675	2.5730	2.5687	2.6032
PT8PAM	2.1806	2.3309	2.3311	2.3264	2.3774
TT7	531.13	532.64	536.14	538.41	528.99
TT8	1295.4	1328.8	1337.3	1343.6	1349.9
TRAT	2.4389	2.4947	2.4943	2.4956	2.5518
PAM	14.174	14.175	14.175	14.177	14.177
BPR	6.6203	6.4466	6.4916	6.5020	6.3910

E3 MIXER NO.14 CONF 57,RUNS 110.0-114.0,HOT

RUN	110.00	111.00	112.00	113.00	114.00
CVMIX	.98764	.98763	.98801	.98773	.98734
CDMIX	.97740	.97916	.97914	.97893	.97899
PTMPA	2.3242	2.4609	2.4623	2.4639	2.4912
PTFPAM	2.3923	2.5316	2.5326	2.5352	2.5585
PTEPAM	2.1601	2.3001	2.3044	2.3012	2.3497
PRAT	1.1075	1.1007	1.0990	1.1017	1.0889
MIXP	.12510E-01	.14035E-01	.14333E-01	.14096E-01	.15403E-01
FG(3)	892.85	975.28	975.81	976.78	991.86
MNFAN	.54660	.54334	.54227	.54363	.53658
MNPRI	.38750	.39525	.39677	.39393	.40656
PT7PAM	2.4131	2.5534	2.5543	2.5571	2.5801
PT8PAM	2.1762	2.3179	2.3224	2.3190	2.3689
TT7	525.53	531.85	533.53	535.83	526.76
TT8	1276.4	1324.7	1335.9	1336.9	1340.5
TRAT	2.4287	2.4907	2.5039	2.4950	2.5448
PAM	14.172	14.180	14.176	14.180	14.165
BPR	6.5761	6.4775	6.4575	6.5005	6.2845

E3 MIXER NO.13 CONF 59,RUNS 141.0-145.0,COLD

RUN	141.00	142.00	143.00	144.00	145.00
CVMIX	.99105	.99120	.99048	.99161	.99102
CDMIX	.97207	.97214	.97210	.97192	.97234
PTMPA	2.3548	2.4690	2.4704	2.4743	2.5554
PTFPAM	2.3586	2.4724	2.4734	2.4768	2.5588
PTEPAM	2.3432	2.4582	2.4609	2.4663	2.5447
PRAT	1.0066	1.0058	1.0051	1.0042	1.0055
MIXP	.77794E-05	.69982E-05	.15735E-04	.11466E-04	.14496E-04
FG(3)	910.10	976.81	977.48	979.47	1027.3
MNFAN	.51930	.51908	.51879	.51835	.51915
MNPRI	.50974	.51066	.51139	.51219	.51110
PT7PAM	2.3781	2.4929	2.4939	2.4972	2.5799
PT8PAM	2.3655	2.4818	2.4846	2.4901	2.5692
TT7	524.08	528.28	527.09	530.97	532.47
TT8	531.77	533.76	531.61	535.13	536.12
TRAT	1.0147	1.0104	1.0086	1.0078	1.0069
PAM	14.238	14.233	14.231	14.230	14.226
BPR	3.1338	3.1168	3.1062	3.0979	3.1060

E3 MIXER NO.13 CONF 59,RUNS 146.0-150.0,HOT

RUN	146.00	147.00	148.00	149.00	150.00
CVMIX	.98812	.98776	.98738	.98763	.98650
CDMIX	.97707	.97818	.97823	.97787	.97903
PTMPA	2.3305	2.4676	2.4711	2.4758	2.4964
PTFPAM	2.4019	2.5379	2.5423	2.5468	2.5657
PTEPAM	2.1472	2.3039	2.3038	2.3106	2.3440
PRAT	1.1186	1.1016	1.1035	1.1022	1.0946
MIXP	.11929E-01	.13875E-01	.13740E-01	.13907E-01	.15053E-0
FG(3)	896.37	977.59	978.87	980.67	996.16
MNFAN	.55371	.54513	.54615	.54520	.54133
MNPRI	.37822	.39613	.39423	.39528	.40323
PT7PAM	2.4238	2.5604	2.5648	2.5693	2.5881
PT8PAM	2.1628	2.3222	2.3220	2.3290	2.3632
TT7	530.34	532.17	532.18	536.74	526.92
TT8	1292.2	1326.9	1325.6	1338.2	1345.2
TRAT	2.4365	2.4935	2.4909	2.4932	2.5529
PAM	14.175	14.171	14.159	14.150	14.181
BPR	6.9936	6.6255	6.6651	6.6334	6.5465

E3 MIXER NO.13 CONF 60,RUNS 153.0-157.0,COLD

RUN	153.00	154.00	155.00	156.00	157.00
CVMIX	.98839	.98872	.98953	.98947	.98902
COMIX	.96773	.96843	.96776	.96756	.96836
PTMPA	2.3551	2.4671	2.4639	2.4671	2.5541
PTFPAM	2.3585	2.4698	2.4680	2.4705	2.5582
PTEPAM	2.3444	2.4585	2.4507	2.4560	2.5406
PRAT	1.0060	1.0046	1.0071	1.0059	1.0069
MIXP	.20163E-04	.20045E-04	.47736E-05	.57686E-05	.12620E-0
FG(3)	908.12	974.39	971.72	973.41	1025.3
MNFAN	.51577	.51576	.51617	.51560	.51658
MNPRI	.50694	.50916	.50583	.50697	.50644
PT7PAM	2.3781	2.4904	2.4886	2.4911	2.5797
PT8PAM	2.3654	2.4806	2.4724	2.4779	2.5632
TT7	531.41	528.81	535.73	535.22	534.59
TT8	543.56	538.92	544.80	543.37	542.36
TRAT	1.0229	1.0191	1.0169	1.0152	1.0145
PAM	14.268	14.268	14.267	14.267	14.267
BPR	3.2440	3.2236	3.2491	3.2366	3.2449

E3 MIXER NO.13 CONF 60,RUNS 158.0-162.0,HOT

RUN	158.00	159.00	160.00	161.00	162.00
CVMIX	.98762	.98782	.98738	.98798	.98676
COMIX	.97364	.97473	.97474	.97402	.97506
PTMPA	2.3344	2.4772	2.4736	2.4759	2.5001
PTFPAM	2.4032	2.5474	2.5448	2.5466	2.5678
PTEPAM	2.1552	2.3060	2.2993	2.3021	2.3471
PRAT	1.1151	1.1047	1.1068	1.1062	1.0940
MIXP	.11875E-01	.13470E-01	.13500E-01	.13422E-01	.14913E-0
FG(3)	902.79	987.58	985.49	986.23	1001.8
MNFAN	.54932	.54408	.54500	.54434	.53813
MNPRI	.37821	.38940	.38708	.38706	.40001
PT7PAM	2.4251	2.5702	2.5676	2.5694	2.5903
PT8PAM	2.1703	2.3231	2.3162	2.3190	2.3654
TT7	536.81	540.67	540.98	538.65	534.29
TT8	1304.5	1343.6	1349.8	1341.0	1363.2
TRAT	2.4301	2.4850	2.4950	2.4896	2.5515
PAM	14.290	14.284	14.284	14.286	14.289
BPR	7.0895	6.9813	6.9361	6.9326	6.7090

APPENDIX B

NOZZLE EXIT PLANE TRAVERSES

Traverse plots were obtained by surveying the nozzle exit plane of all the configurations in Phase III. At a single simulated engine operating point, total pressure and total temperature were measured and nondimensionalized relative to the corresponding ideal mixed property. The charging station conditions for each stream (fan stream = station 7 and primary stream = station 8) are identified along with the absolute level of the fully mixed reference. The location of the primary lobe peaks is indicated by an arrow.

B.1 NOZZLE EXIT SURVEY

B.1.1 Pressure Traverse

B.1.2 Temperature Traverse

PRESSURE

CONFIGURATION 50

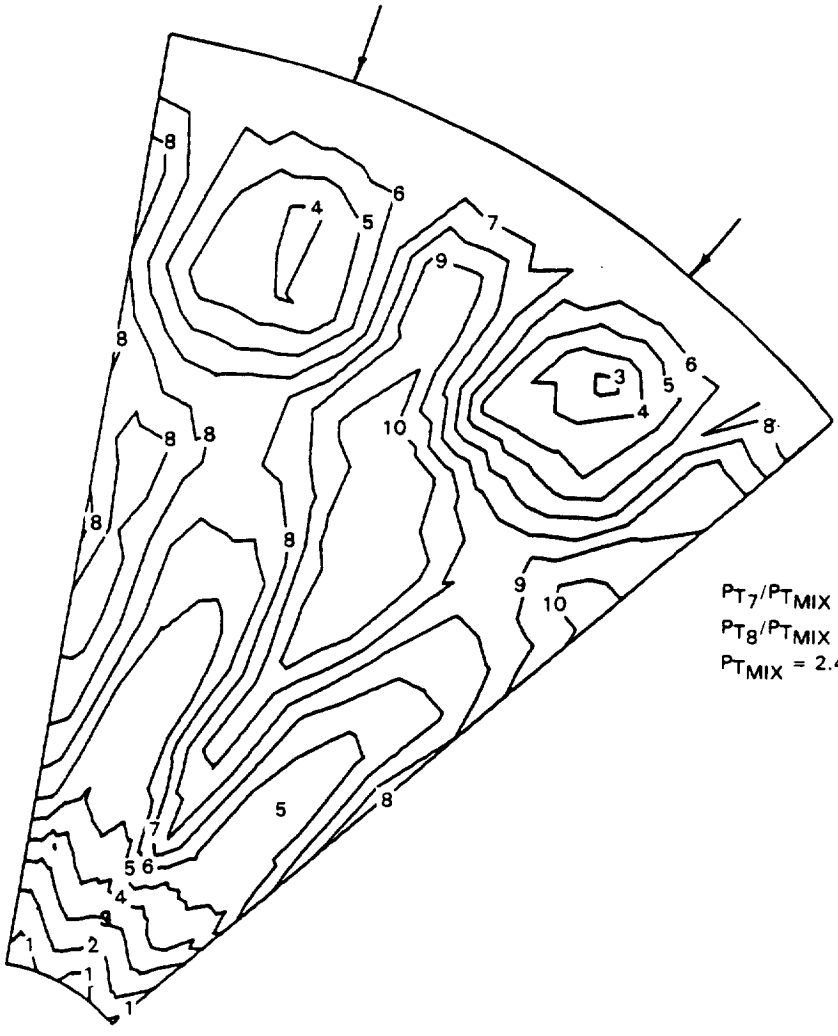

$P_T/P_{T_{MIX}}$

CURVE LABEL	CURVE VALUE
1	0.940000E+00
2	0.950000E+00
3	0.960000E+00
4	0.970000E+00
5	0.980000E+00
6	0.990000E+00
7	0.100000E+01
8	0.101000E+01
9	0.102000E+01
10	0.103000E+01

$P_{T_7}/P_{T_{MIX}} = 1.0364$

$P_{T_8}/P_{T_{MIX}} = 0.9397$

$P_{T_{MIX}} = 2.431 * 10^5 \text{ N/M}^2$ (35.25 PSIA)

PRESSURE

CONFIGURATION 51

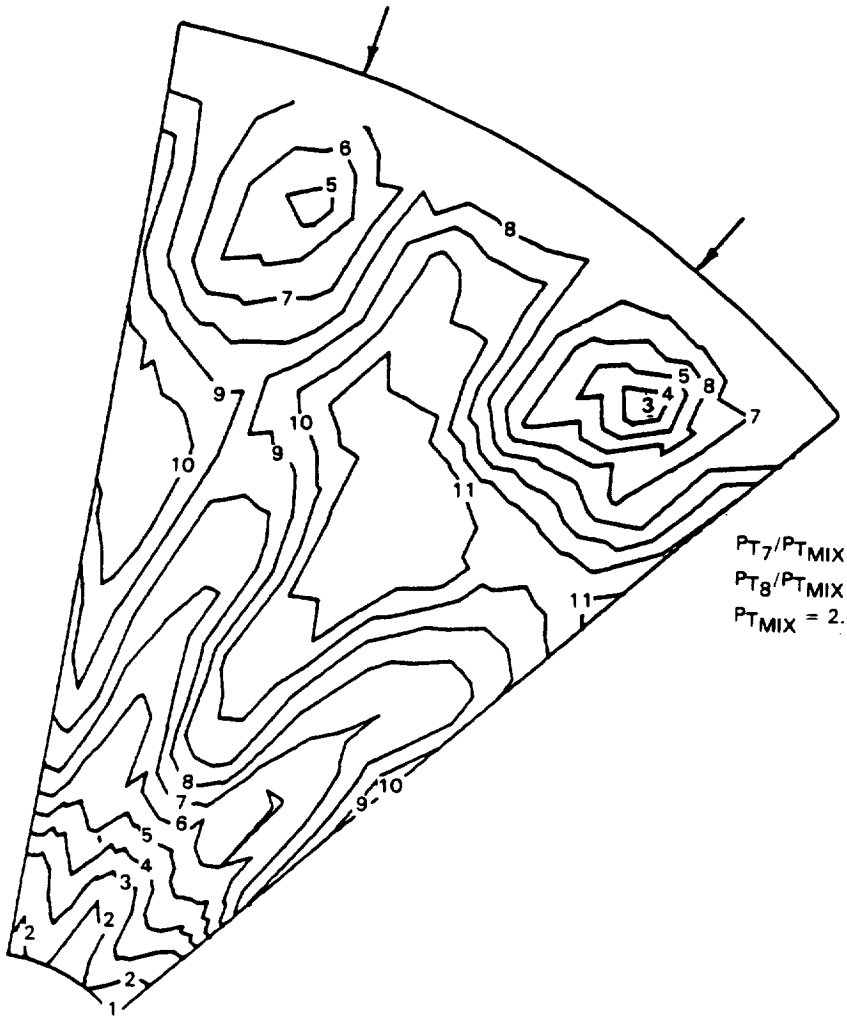

$P_T/P_{T_{MIX}}$ CURVE LABEL	CURVE VALUE
1	0.930000E+00
2	0.940000E+00
3	0.950000E+00
4	0.960000E+00
5	0.970000E+00
6	0.980000E+00
7	0.990000E+00
8	0.100000E+01
9	0.101000E+01
10	0.102000E+01
11	0.103000E+01

$P_{T_7}/P_{T_{MIX}} = 1.0362$

$P_{T_8}/P_{T_{MIX}} = 0.9404$

$P_{T_{MIX}} = 2.425 \cdot 10^5$ N/M^2 (35.18 PSIA)

C-2

PRESSURE

CONFIGURATION 53

CURVE LABEL	$P_T/P_{T_{MIX}}$ CURVE VALUE
1	0.940000E+00
2	0.950000E+00
3	0.960000E+00
4	0.970000E+00
5	0.980000E+00
6	0.990000E+00
7	0.100000E+01
8	0.101000E+01
9	0.102000E+01
10	0.103000E+01
11	0.104000E+01

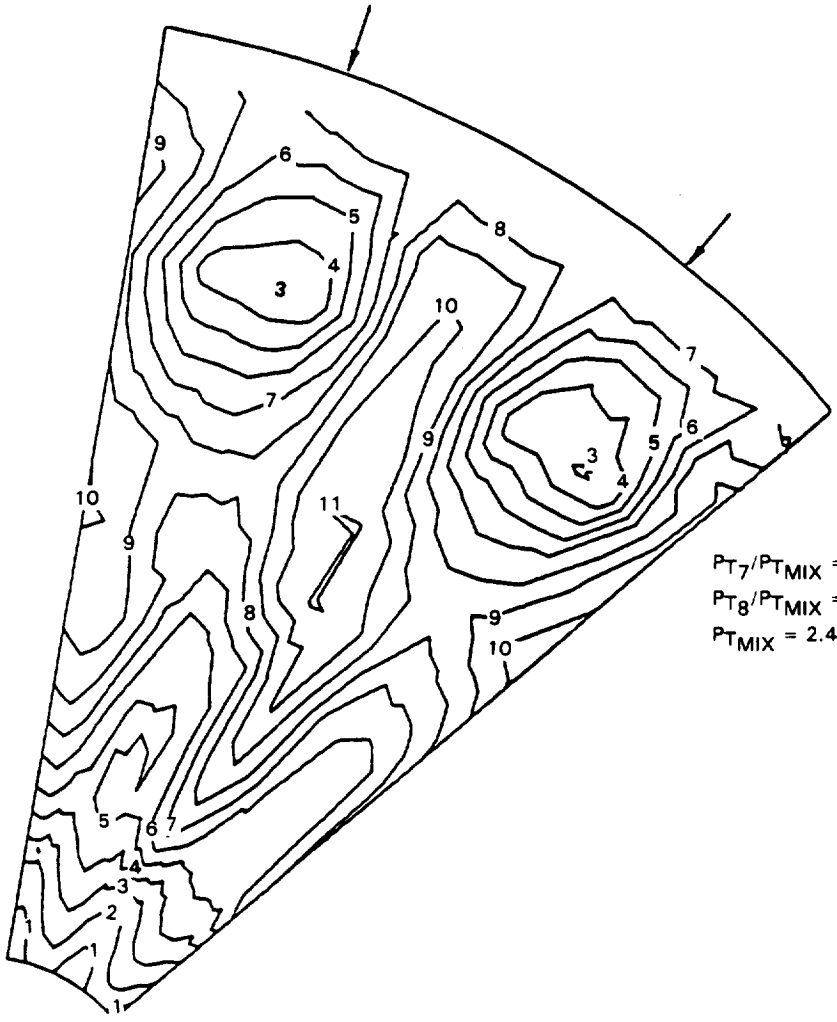

$P_{T_7}/P_{T_{MIX}} = 1.0370$

$P_{T_8}/P_{T_{MIX}} = 0.9420$

$P_{T_{MIX}} = 2.431 \cdot 10^5$ N/M^2 (35.26 PSIA)

PRESSURE

CONFIGURATION 54

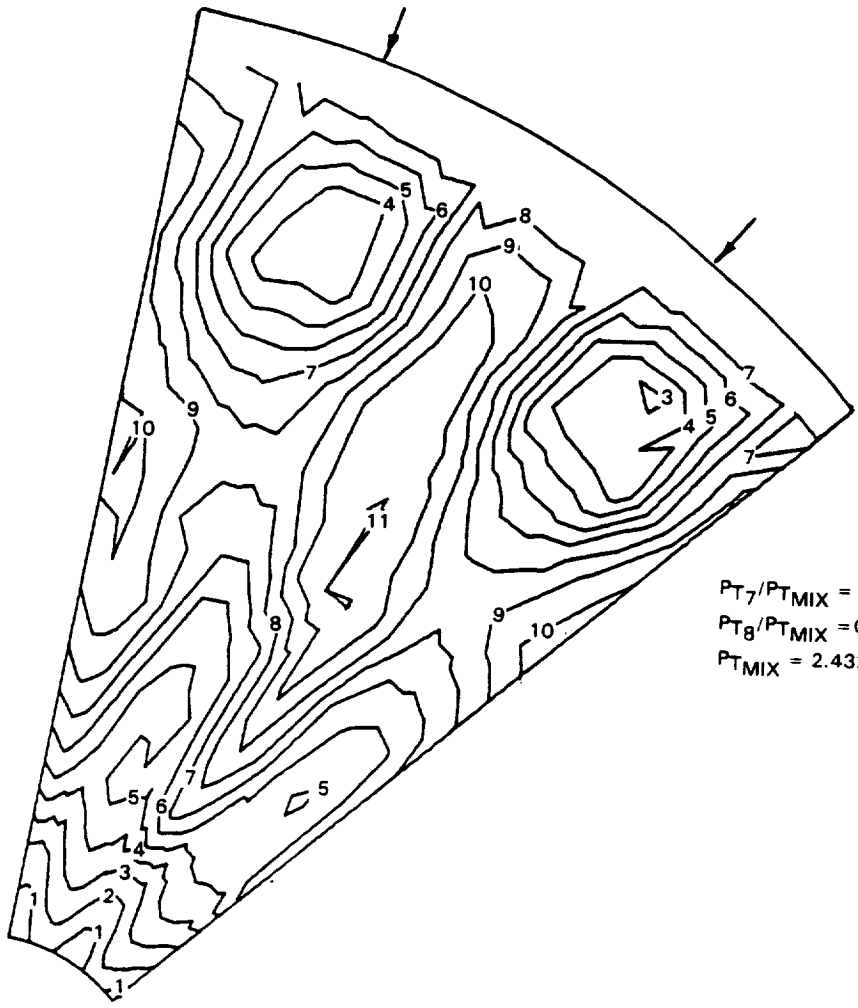

$P_T/P_{T_{MIX}}$

CURVE LABEL	CURVE VALUE
1	0.940000E+0
2	0.950000E+0
3	0.960000E+0
4	0.970000E+0
5	0.980000E+0
6	0.990000E+0
7	0.100000E+0
8	0.101000E+0
9	0.102000E+0
10	0.103000E+0
11	0.104000E+0

$P_{T_7}/P_{T_{MIX}} = 1.0372$

$P_{T_8}/P_{T_{MIX}} = 0.9414$

$P_{T_{MIX}} = 2.432 \cdot 10^5$ N/M^2 (35.27 PSIA)

PRESSURE

CONFIGURATION 55

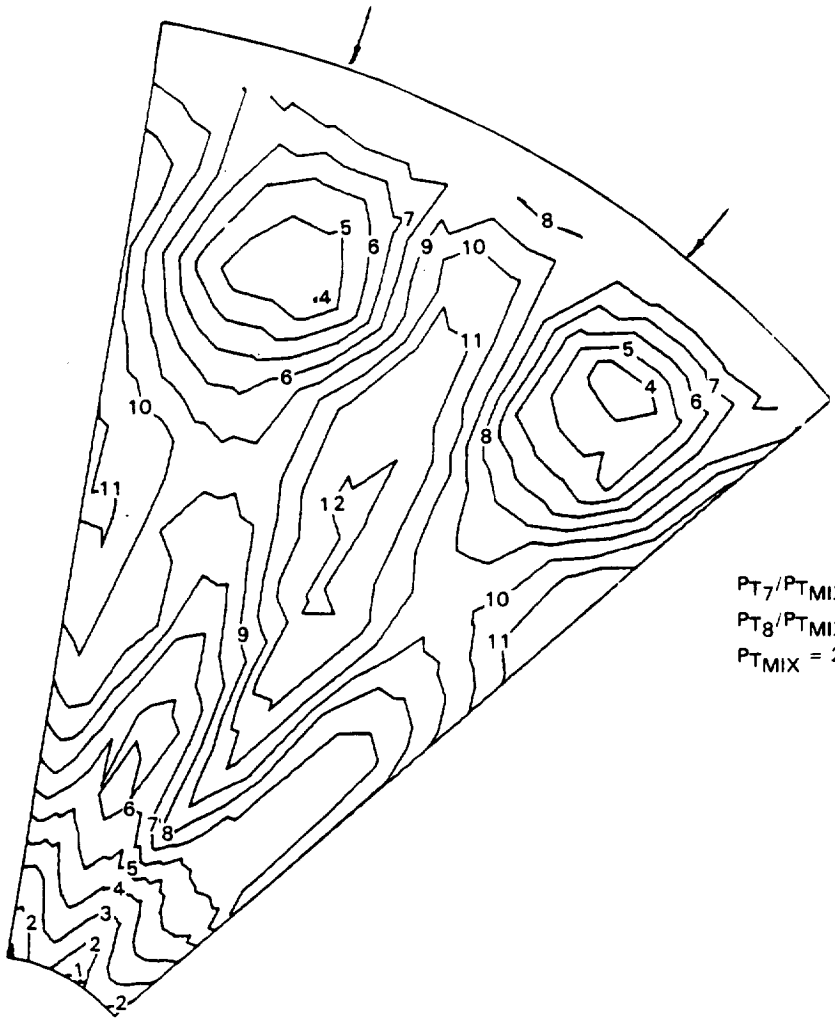

$P_T/P_{T_{MIX}}$

CURVE LABEL	CURVE VALUE
1	0.930000E+00
2	0.940000E+00
3	0.950000E+00
4	0.960000E+00
5	0.970000E+00
6	0.980000E+00
7	0.990000E+00
8	0.100000E+01
9	0.101000E+01
10	0.102000E+01
11	0.103000E+01
12	0.104000E+01

$P_{T_7}/P_{T_{MIX}} = 1.0373$

$P_{T_8}/P_{T_{MIX}} = 0.9408$

$P_{T_{MIX}} = 2.427 \cdot 10^5$ N/M^2 (35.21 PSIA)

PRESSURE

CONFIGURATION 56

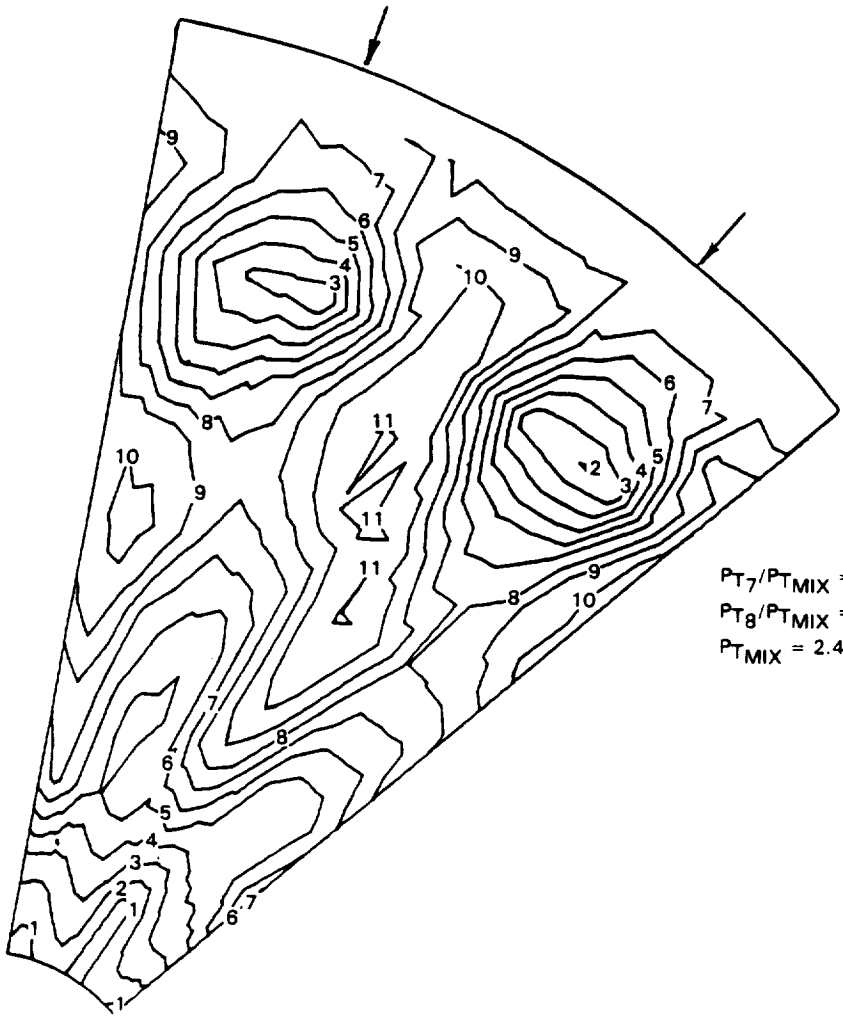

$P_T/P_{T_{MIX}}$

CURVE LABEL	CURVE VALUE
1	0.940000E+00
2	0.950000E+00
3	0.960000E+00
4	0.970000E+00
5	0.980000E+00
6	0.990000E+00
7	0.100000E+01
8	0.101000E+01
9	0.102000E+01
10	0.103000E+01
11	0.104000E+01

$P_{T_7}/P_{T_{MIX}} = 1.0378$

$P_{T_8}/P_{T_{MIX}} = 0.9407$

$P_{T_{MIX}} = 2.421 \cdot 10^5$ N/M^2 (35.11 PSIA)

PRESSURE

CONFIGURATION 57

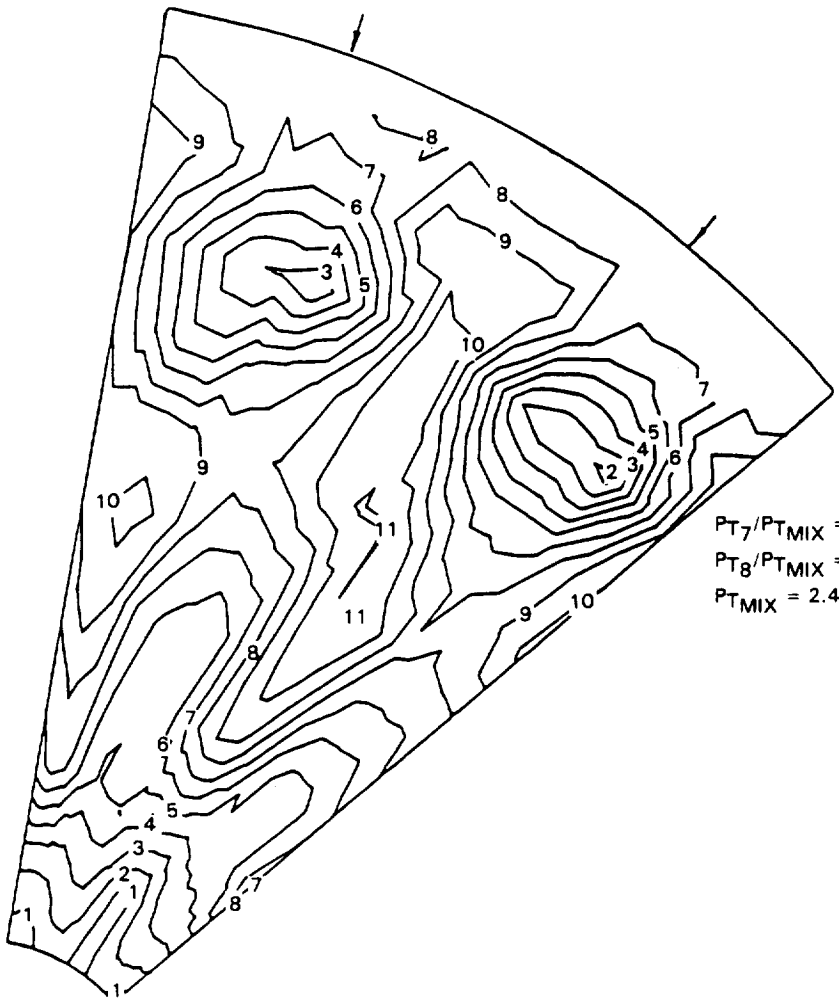

$P_T/P_{T_{MIX}}$

CURVE LABEL	CURVE VALUE
1	0.940000E+00
2	0.950000E+00
3	0.960000E+00
4	0.970000E+00
5	0.980000E+00
6	0.990000E+00
7	0.100000E+01
8	0.101000E+01
9	0.102000E+01
10	0.103000E+01
11	0.104000E+01

$P_{T_7}/P_{T_{MIX}} = 1.0376$

$P_{T_8}/P_{T_{MIX}} = 0.9409$

$P_{T_{MIX}} = 2.407 \cdot 10^5$ N/M^2 (34.91 PSIA)

PRESSURE

CONFIGURATION 59

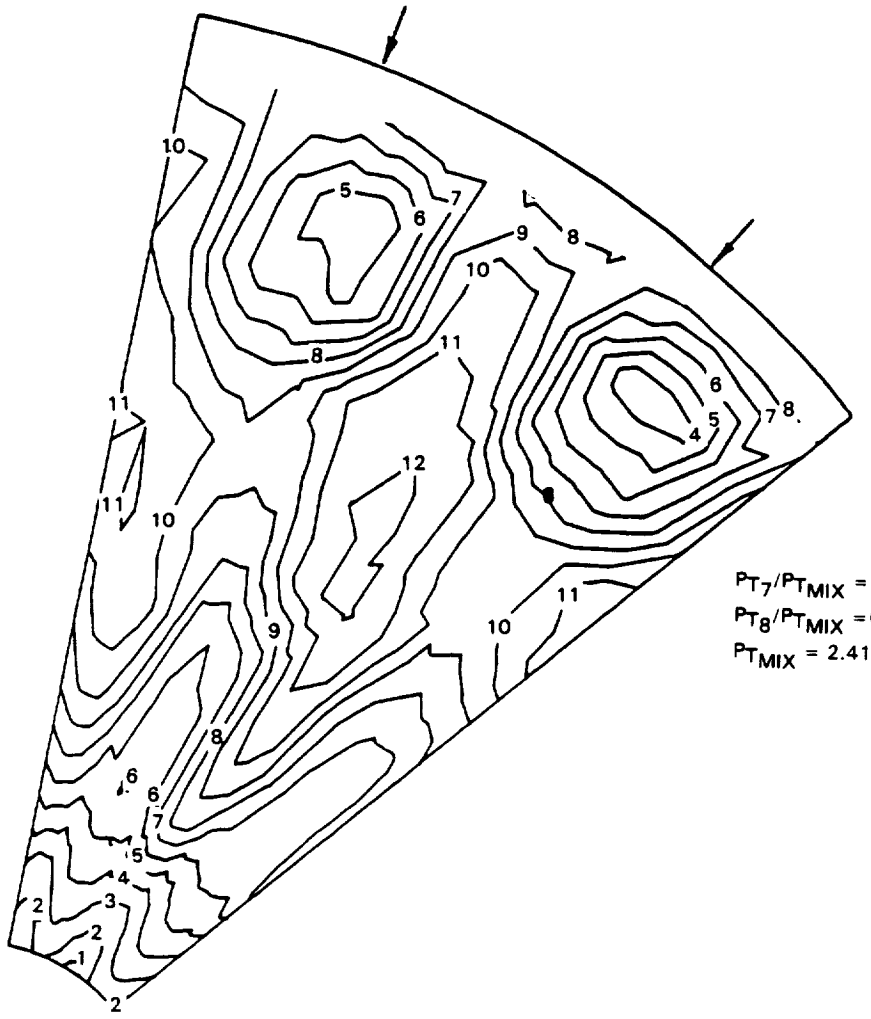

CURVE LABEL	$P_T/P_{T_{MIX}}$ CURVE VALUE
1	0.930000E+00
2	0.940000E+00
3	0.950000E+00
4	0.960000E+00
5	0.970000E+00
6	0.980000E+00
7	0.990000E+00
8	0.100000E+01
9	0.101000E+01
10	0.102000E+01
11	0.103000E+01
12	0.104000E+01

$P_{T_7}/P_{T_{MIX}} = 1.0374$

$P_{T_8}/P_{T_{MIX}} = 0.9407$

$P_{T_{MIX}} = 2.413 \cdot 10^5$ N/M^2 (35.00 PSIA)

PRESSURE

CONFIGURATION 60

CURVE LABEL	$P_T/P_{T_{MIX}}$ CURVE VALUE
1	0.940000E+00
2	0.950000E+00
3	0.960000E+00
4	0.970000E+00
5	0.980000E+00
6	0.990000E+00
7	0.100000E+01
8	0.101000E+01
9	0.102000E+01
10	0.103000E+01
11	0.104000E+01

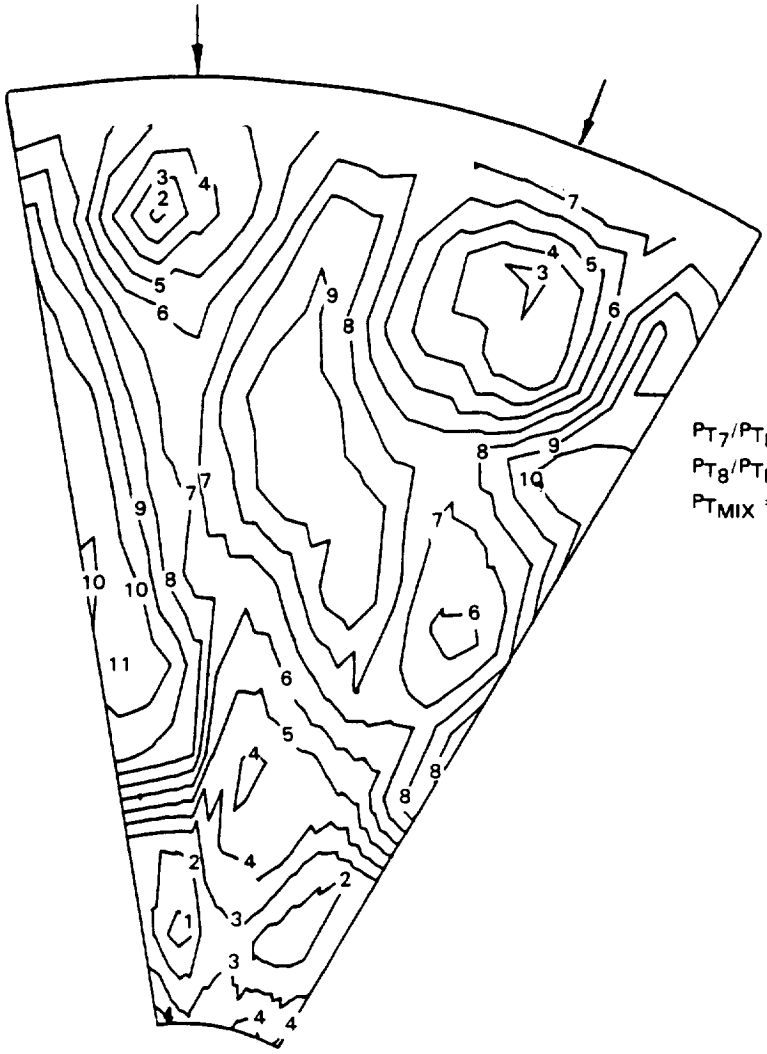

$P_{T_7}/P_{T_{MIX}} = 1.0374$

$P_{T_8}/P_{T_{MIX}} = 0.9372$

$P_{T_{MIX}} = 2.434 \cdot 10^5$ N/M^2 (35.31 PSIA)

TEMPERATURE

CONFIGURATION 50

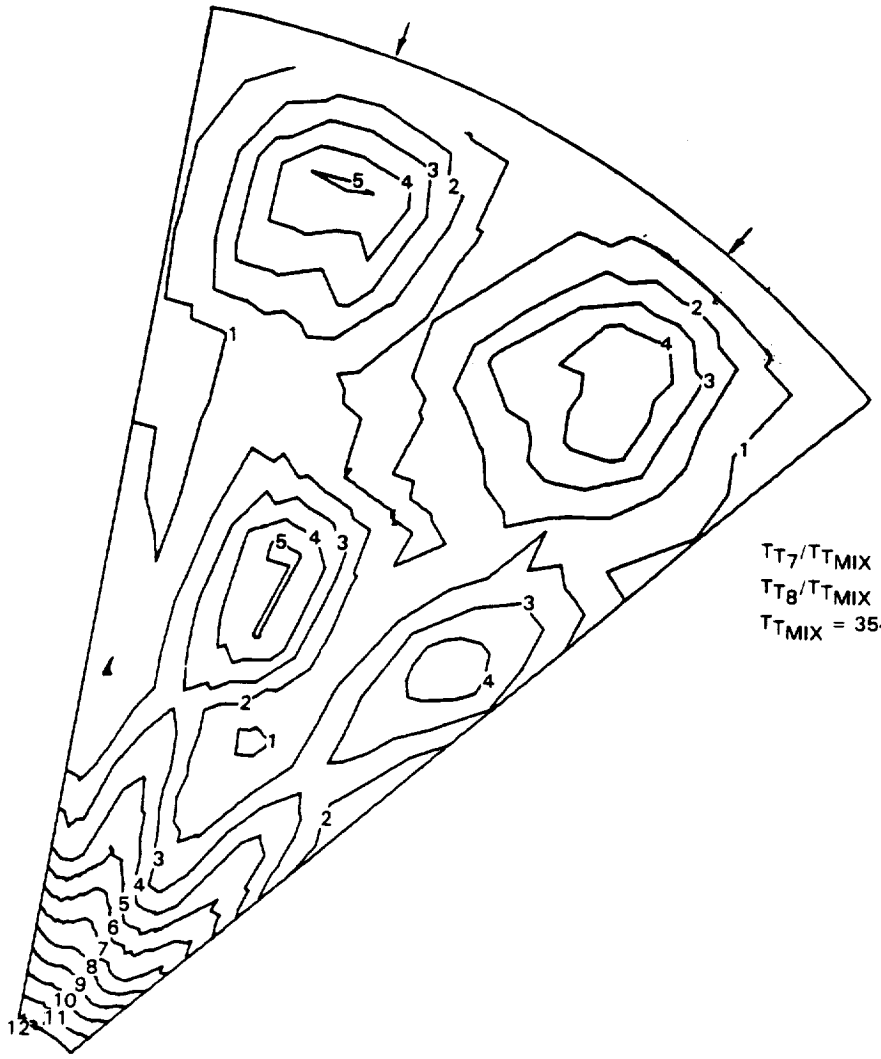

CURVE LABEL	$T_T/T_{T_{MIX}}$ CURVE VALUE
1	0.850000E+00
2	0.950000E+00
3	0.105000E+01
4	0.115000E+01
5	0.125000E+01
6	0.135000E+01
7	0.145000E+01
8	0.155000E+01
9	0.165000E+01
10	0.175000E+01
11	0.185000E+01
12	0.195000E+01

$T_{T_7}/T_{T_{MIX}} = 0.8344$

$T_{T_8}/T_{T_{MIX}} = 2.0858$

$T_{T_{MIX}} = 354.77°K\ (638.59°R)$

TEMPERATURE

CONFIGURATION 51

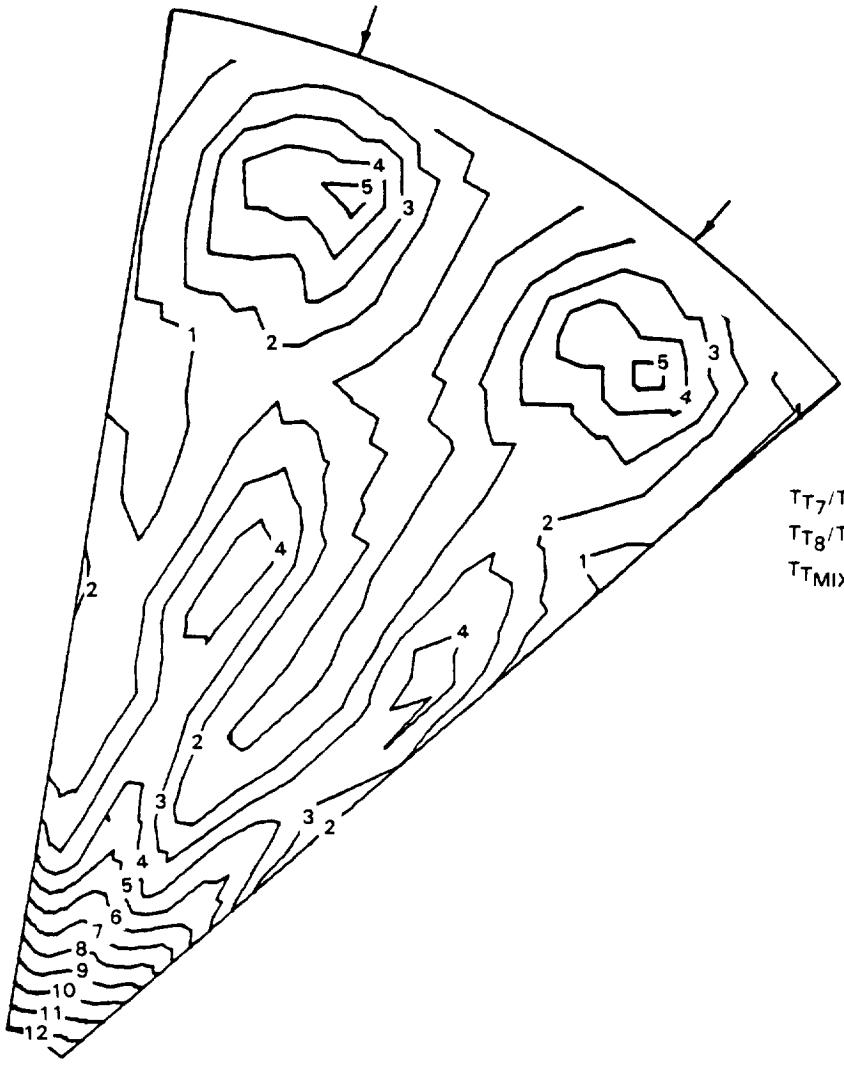

$T_T/T_{T_{MIX}}$

CURVE LABEL	CURVE VALUE
1	0.850000E+00
2	0.950000E+00
3	0.105000E+01
4	0.115000E+01
5	0.125000E+01
6	0.135000E+01
7	0.145000E+01
8	0.155000E+01
9	0.165000E+01
10	0.175000E+01
11	0.185000E+01
12	0.195000E+01

$T_{T_7}/T_{T_{MIX}} = 0.8340$

$T_{T_8}/T_{T_{MIX}} = 2.0839$

$T_{T_{MIX}} = 353.81°K\ (636.86°R)$

TEMPERATURE

CONFIGURATION 53

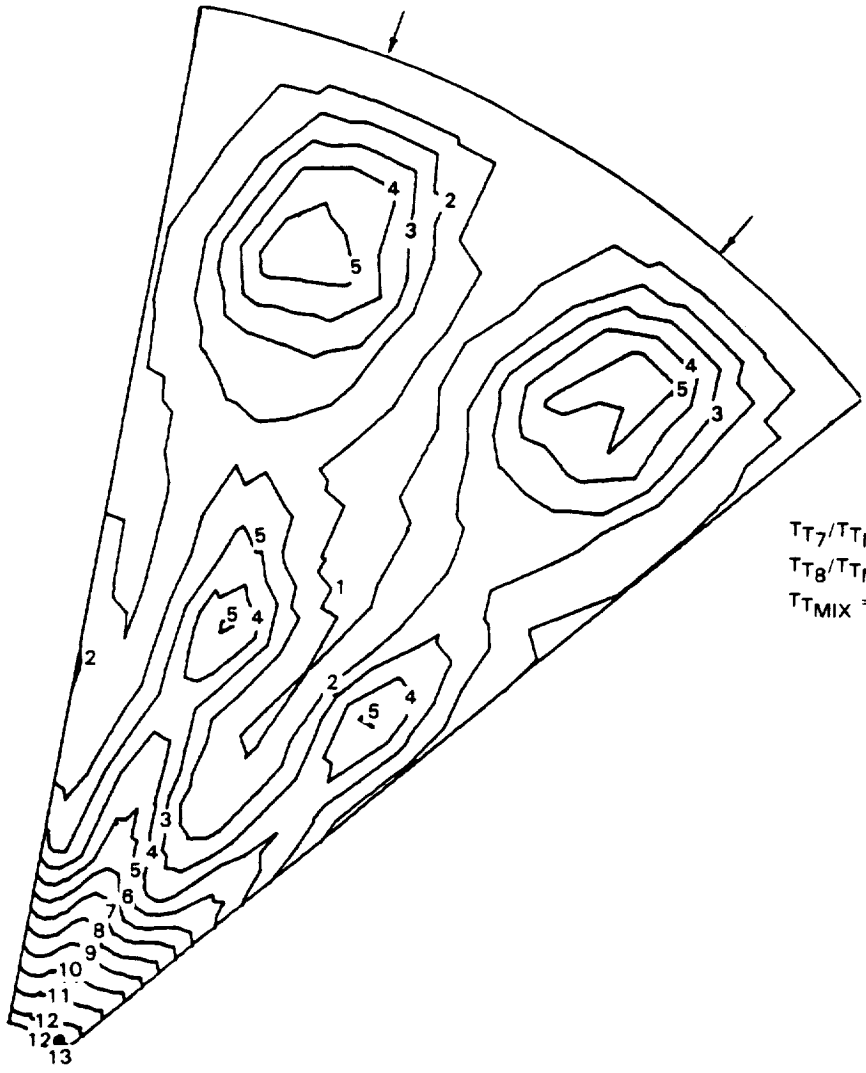

$T_T/T_{T_{MIX}}$

CURVE LABEL	CURVE VALUE
1	0.850000E+00
2	0.950000E+00
3	0.105000E+01
4	0.115000E+01
5	0.125000E+01
6	0.135000E+01
7	0.145000E+01
8	0.155000E+01
9	0.165000E+01
10	0.175000E+01
11	0.185000E+01
12	0.195000E+01
13	0.205000E+01

$T_{T_7}/T_{T_{MIX}} = 0.8318$

$T_{T_8}/T_{T_{MIX}} = 2.0791$

$T_{T_{MIX}} = 357.51°K\ (643.53°R)$

TEMPERATURE

CONFIGURATION 54

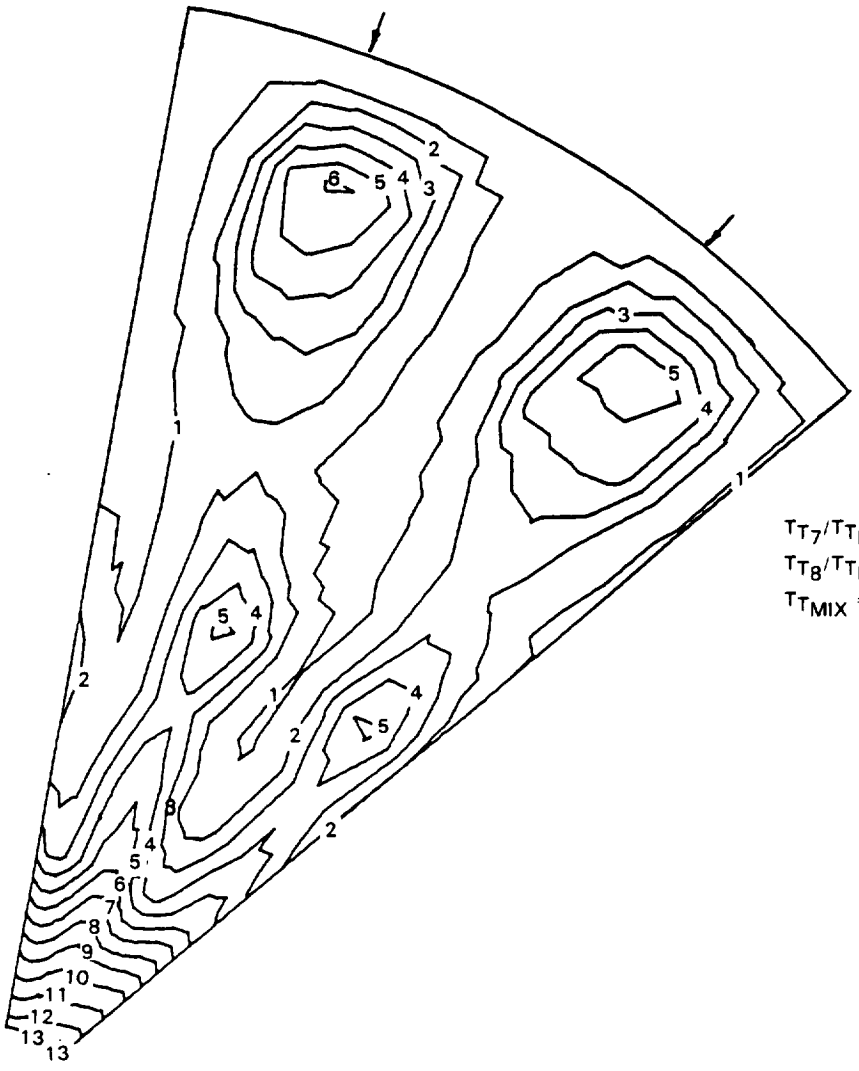

$T_T/T_{T_{MIX}}$

CURVE LABEL	CURVE VALUE
1	0.850000E+00
2	0.950000E+00
3	0.105000E+01
4	0.115000E+01
5	0.125000E+01
6	0.135000E+01
7	0.145000E+01
8	0.155000E+01
9	0.165000E+01
10	0.175000E+01
11	0.185000E+01
12	0.195000E+01
13	0.205000E+01

$T_{T_7}/T_{T_{MIX}} = 0.8322$

$T_{T_8}/T_{T_{MIX}} = 2.0797$

$T_{T_{MIX}} = 361.40°K\ (650.52°R)$

TEMPERATURE

CONFIGURATION 55

CURVE LABEL	$T_T/T_{T_{MIX}}$ CURVE VALUE
1	0.850000E+00
2	0.950000E+00
3	0.105000E+01
4	0.115000E+01
5	0.125000E+01
6	0.135000E+01
7	0.145000E+01
8	0.155000E+01
9	0.165000E+01
10	0.175000E+01
11	0.185000E+01
12	0.195000E+01
13	0.205000E+01

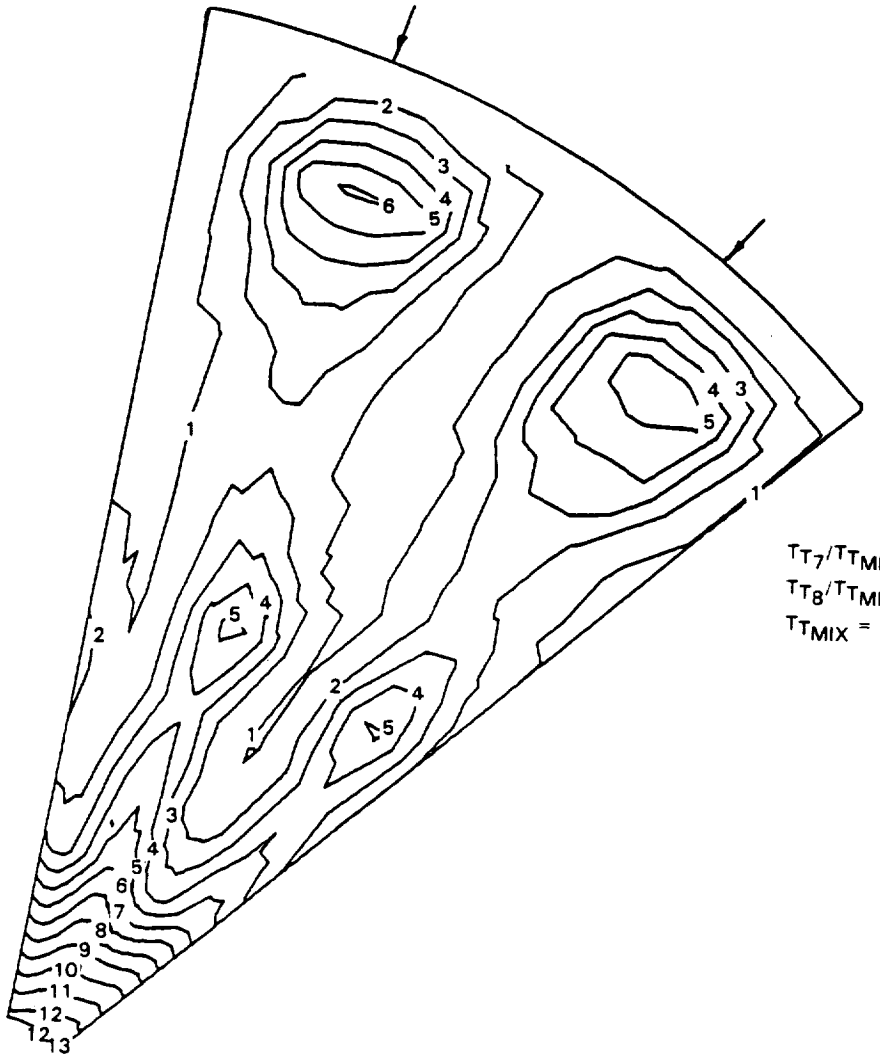

$T_{T_7}/T_{T_{MIX}} = 0.8327$

$T_{T_8}/T_{T_{MIX}} = 2.0774$

$T_{T_{MIX}} = 354.22°K\ (637.59°R)$

TEMPERATURE

CONFIGURATION 56

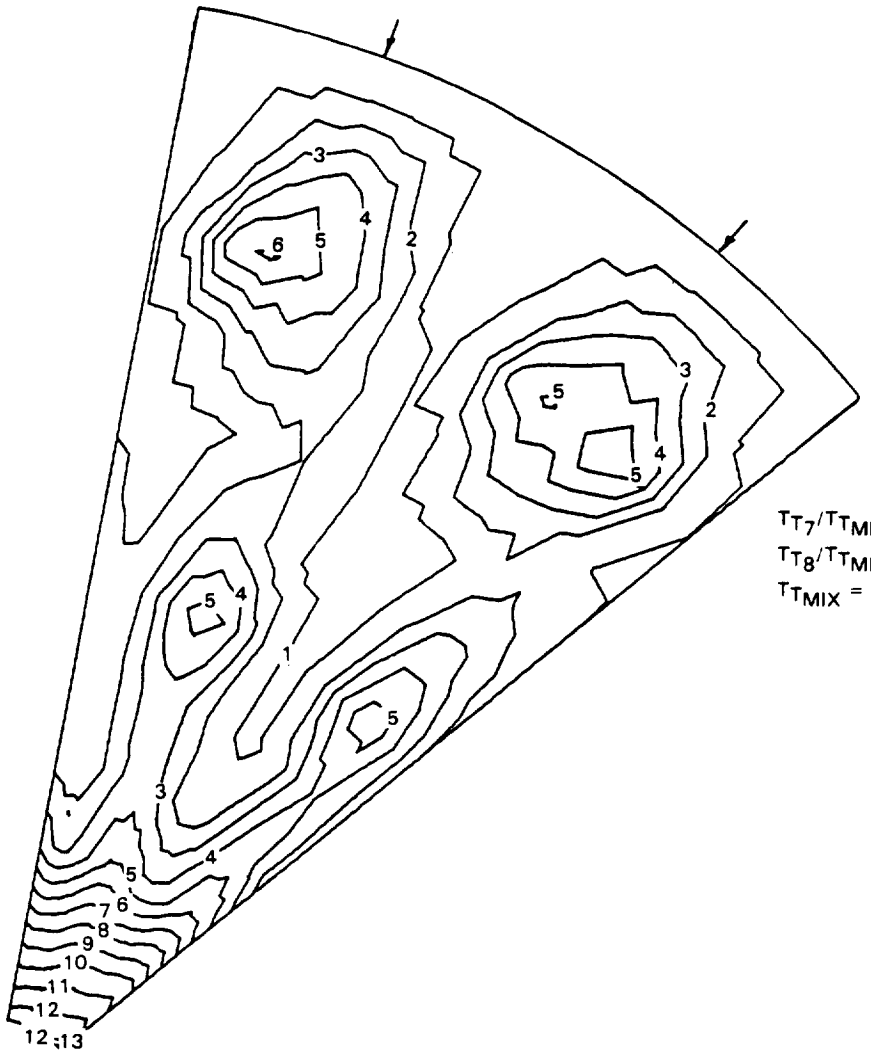

$T_T/T_{T_{MIX}}$

CURVE LABEL	CURVE VALUE
1	0.850000E+00
2	0.950000E+00
3	0.105000E+01
4	0.115000E+01
5	0.125000E+01
6	0.135000E+01
7	0.145000E+01
8	0.155000E+01
9	0.165000E+01
10	0.175000E+01
11	0.185000E+01
12	0.195000E+01
13	0.205000E+01

$T_{T_7}/T_{T_{MIX}} = 0.8294$

$T_{T_8}/T_{T_{MIX}} = 2.0725$

$T_{T_{MIX}} = 360.93°K\ (649.68°R)$

TEMPERATURE

CONFIGURATION 57

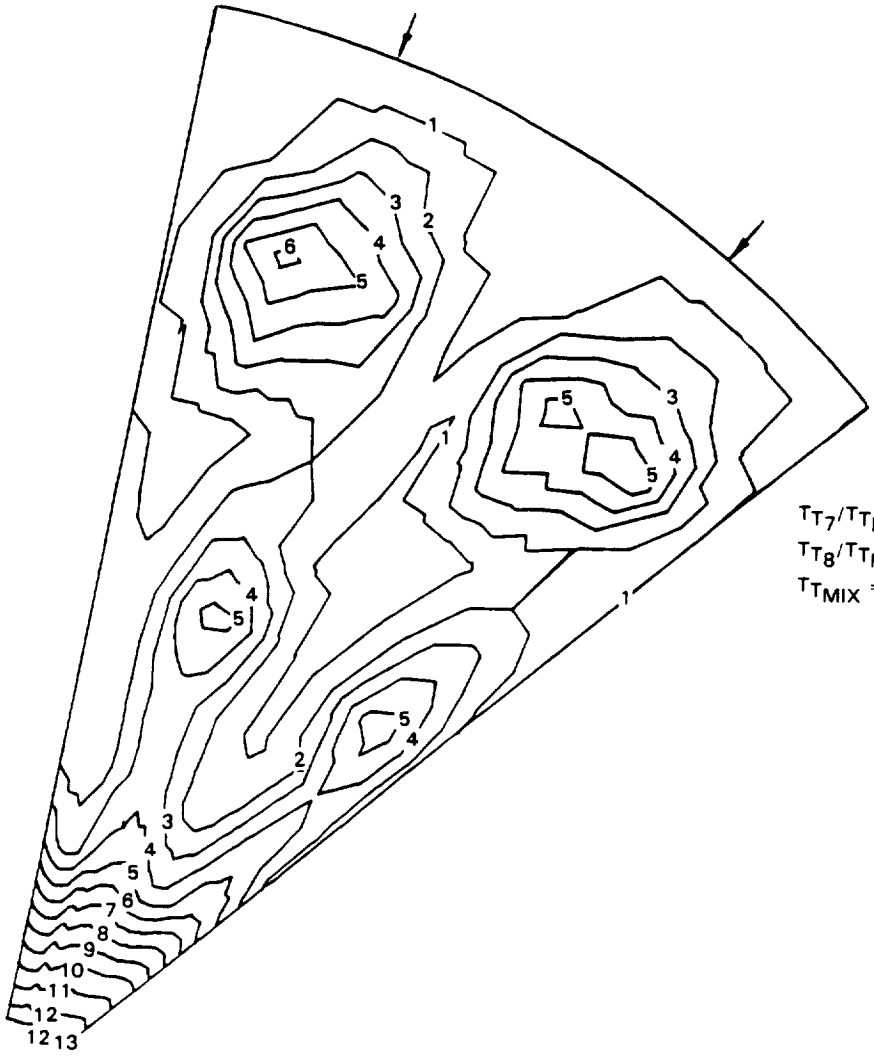

CURVE LABEL	$T_T/T_{T_{MIX}}$ CURVE VALUE
1	0.850000E+00
2	0.950000E+00
3	0.105000E+01
4	0.115000E+01
5	0.125000E+01
6	0.135000E+01
7	0.145000E+01
8	0.155000E+01
9	0.165000E+01
10	0.175000E+01
11	0.185000E+01
12	0.195000E+01
13	0.205000E+01

$T_{T_7}/T_{T_{MIX}} = 0.8299$

$T_{T_8}/T_{T_{MIX}} = 2.0715$

$T_{T_{MIX}} = 362.38°K\ (652.29°R)$

TEMPERATURE

CONFIGURATION 59

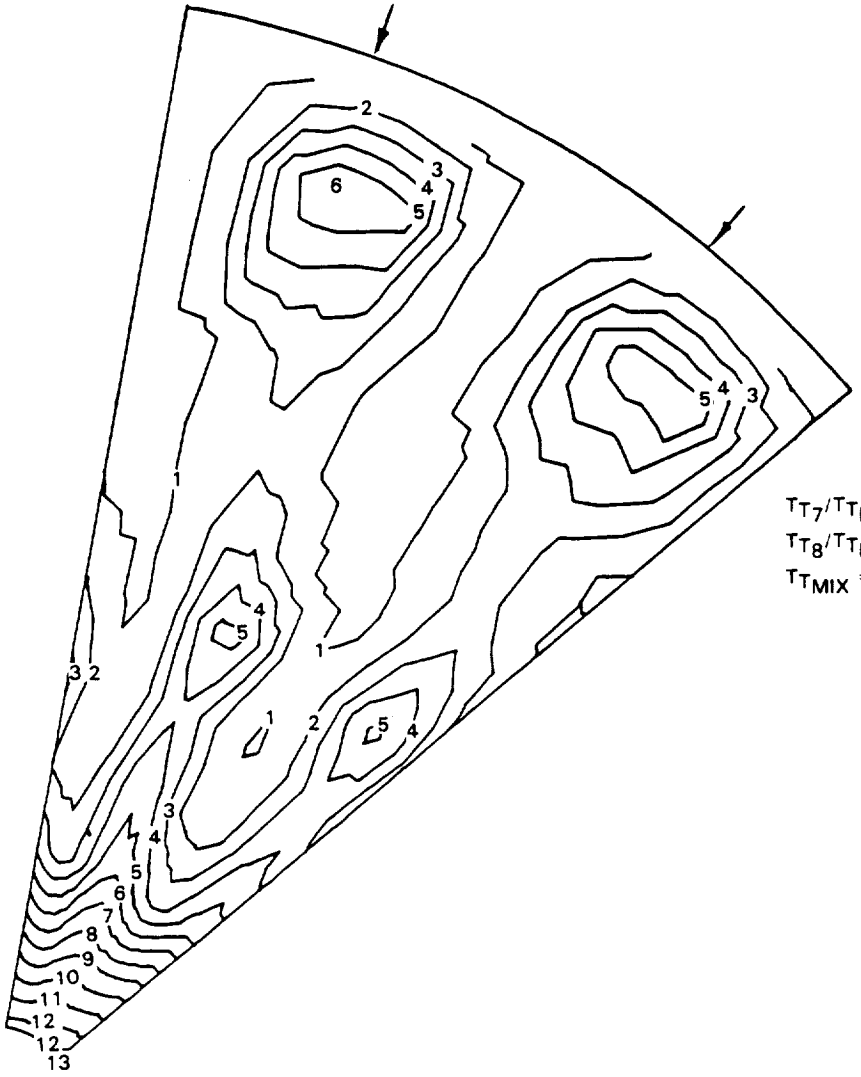

$T_T/T_{T_{MIX}}$

CURVE LABEL	CURVE VALUE
1	0.850000E+00
2	0.950000E+00
3	0.105000E+01
4	0.115000E+01
5	0.125000E+01
6	0.135000E+01
7	0.145000E+01
8	0.155000E+01
9	0.165000E+01
10	0.175000E+01
11	0.185000E+01
12	0.195000E+01
13	0.205000E+01

$T_{T_7}/T_{T_{MIX}} = 0.8326$

$T_{T_8}/T_{T_{MIX}} = 2.0794$

$T_{T_{MIX}} = 359.49°K\ (643.49°R)$

TEMPERATURE

CONFIGURATION 60

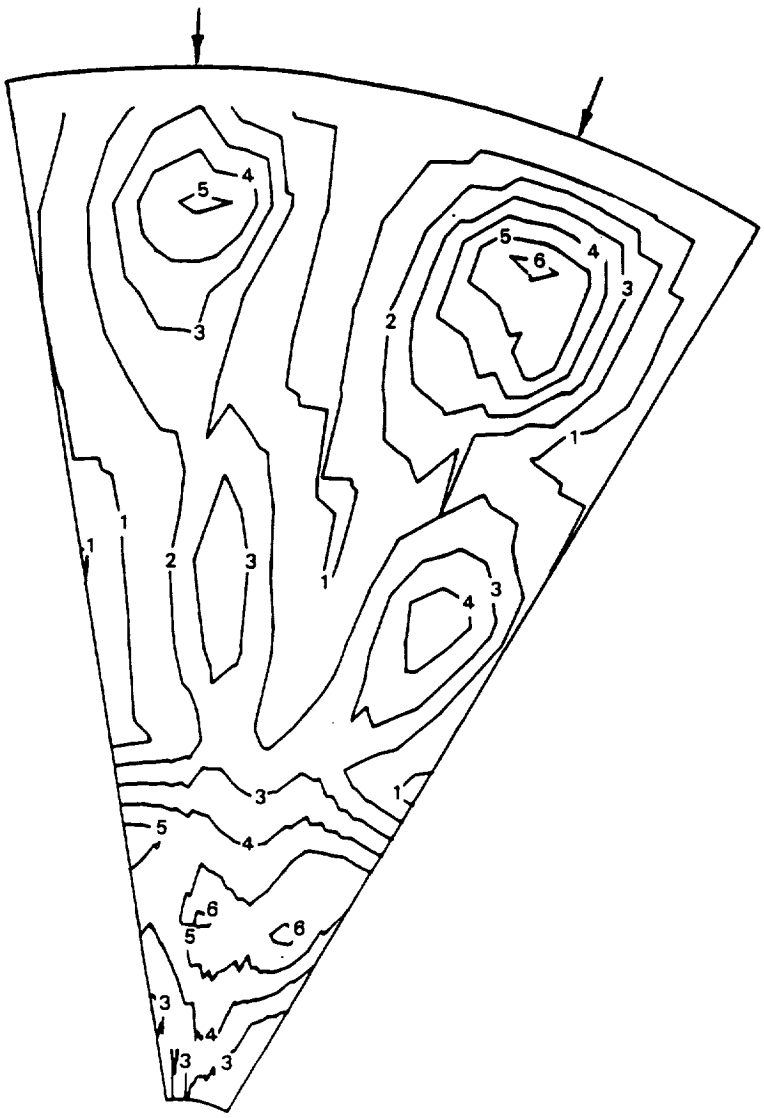

$T_T/T_{T_{MIX}}$

CURVE LABEL	CURVE VALUE
1	0.850000E+00
2	0.950000E+00
3	0.105000E+01
4	0.115000E+01
5	0.125000E+01
6	0.135000E+01

$T_{T_7}/T_{T_{MIX}} = 0.8377$

$T_{T_8}/T_{T_{MIX}} = 2.0888$

$T_{T_{MIX}} = 353.68°K\ (636.62°R)$

APPENDIX C

FLOW VISUALIZATION PHOTOGRAPHS

Flow visualization tests were made for all of the Phase III configurations. These tests were conducted with uniform cold flow at a nozzle pressure ratio of 2.5 to provide a general indication of the flow field through the exhaust system. The streaks shown on the photographs on the following pages resulted from placing an array of dots (using a lampblack/glycerine mixture) on the painted surface of the model prior to a test run.

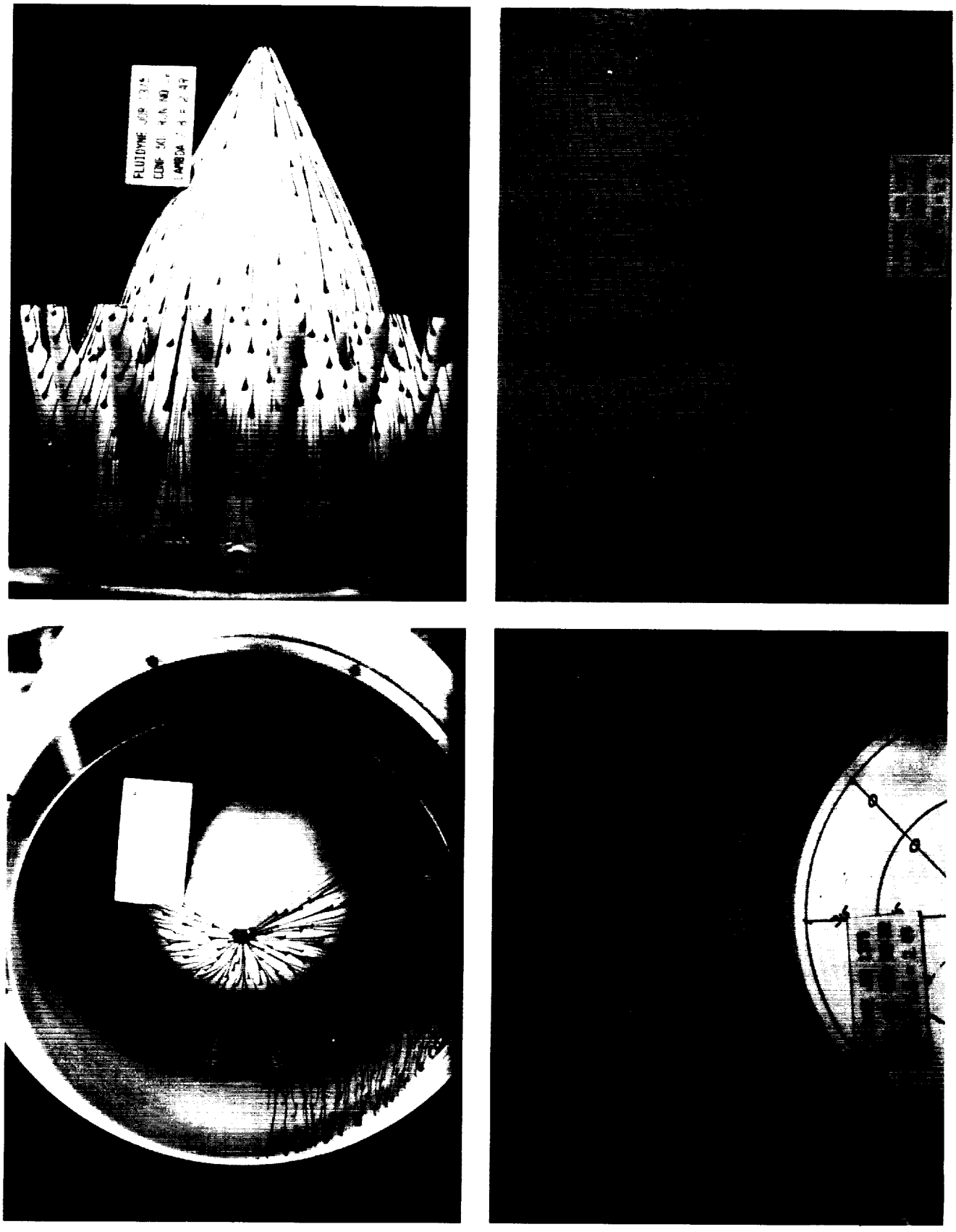

Flow Visualization Photographs, Configuration 50

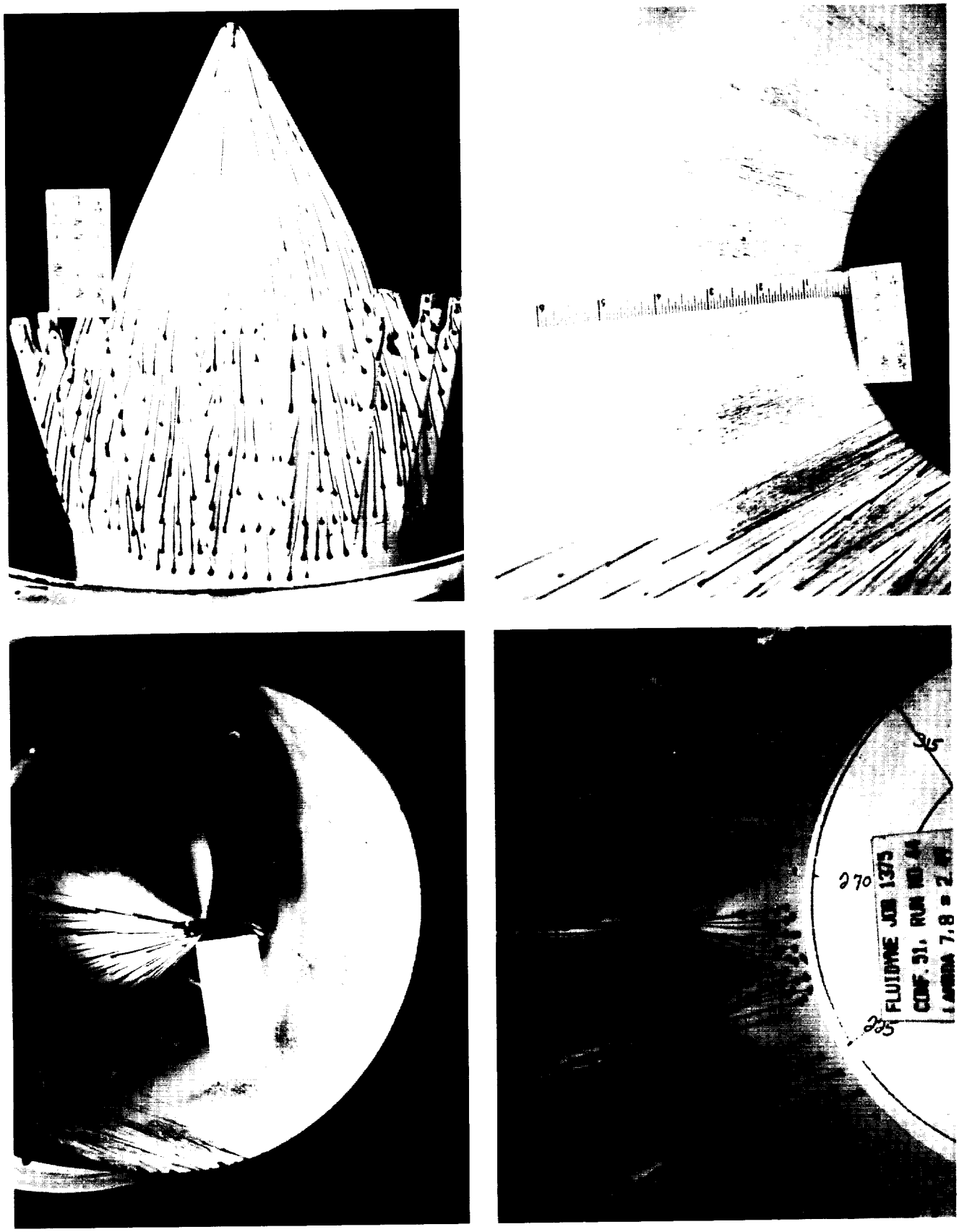

Flow Visualization Photographs, Configuration 51

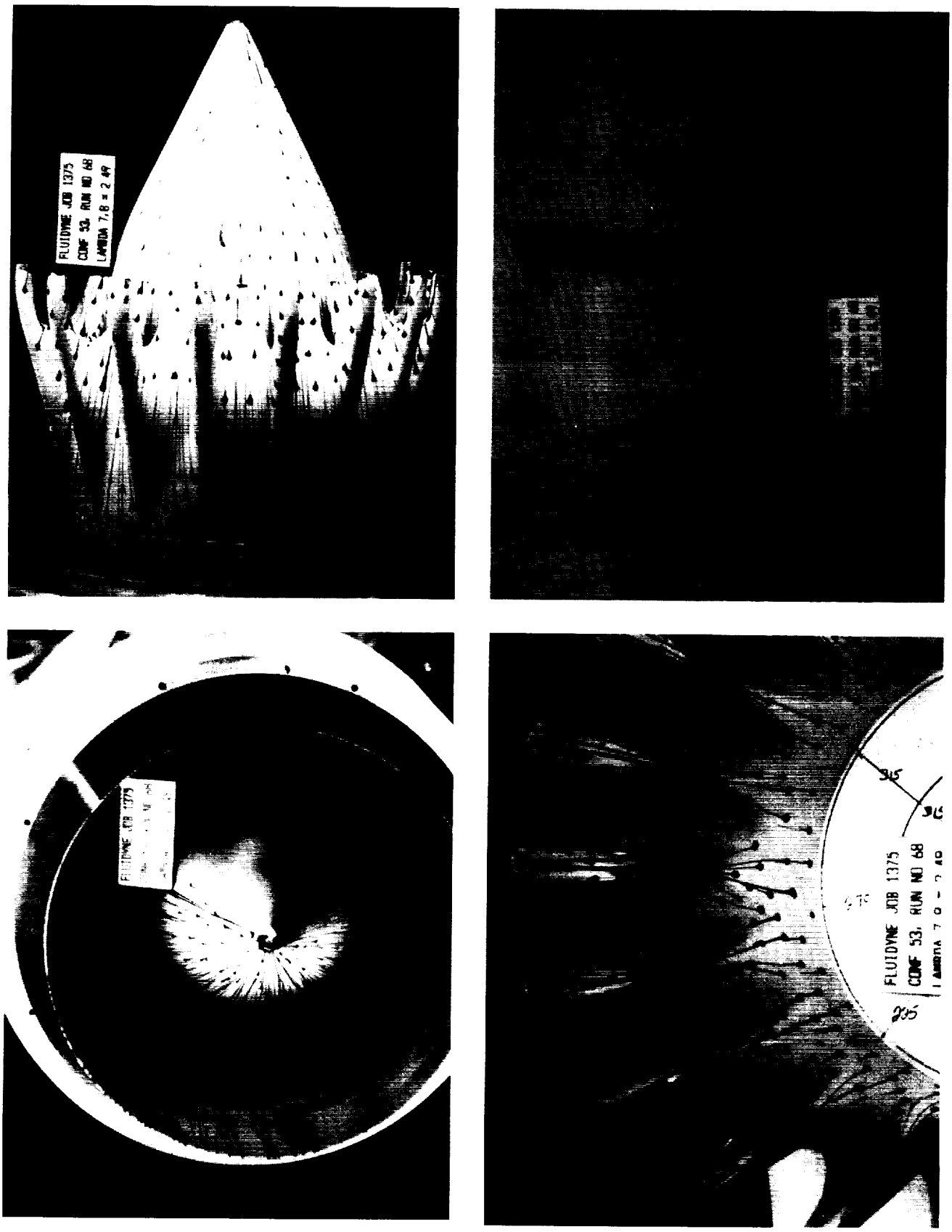

Flow Visualization Photographs, Configuration 53

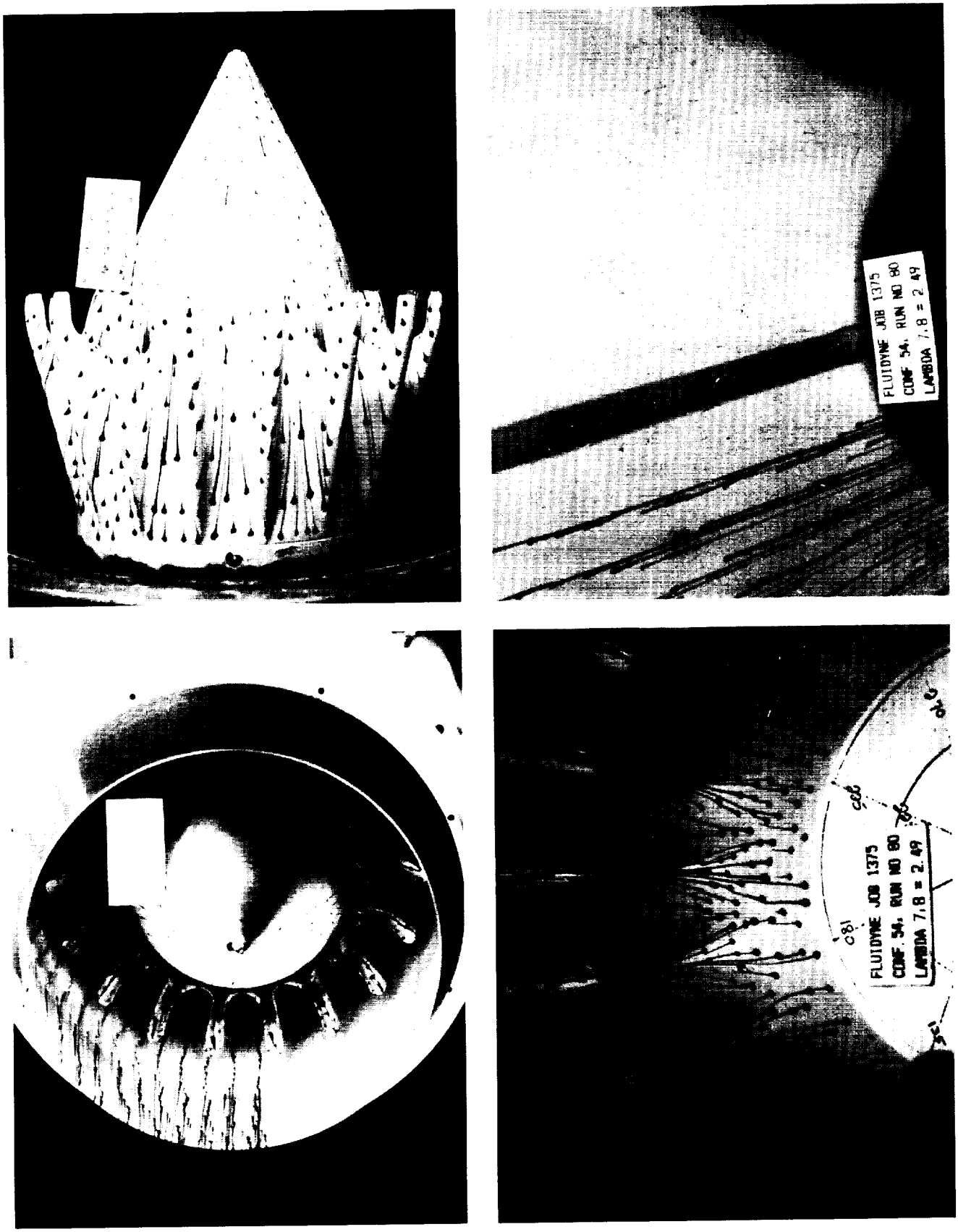

Flow Visualization Photographs, Configuration 54

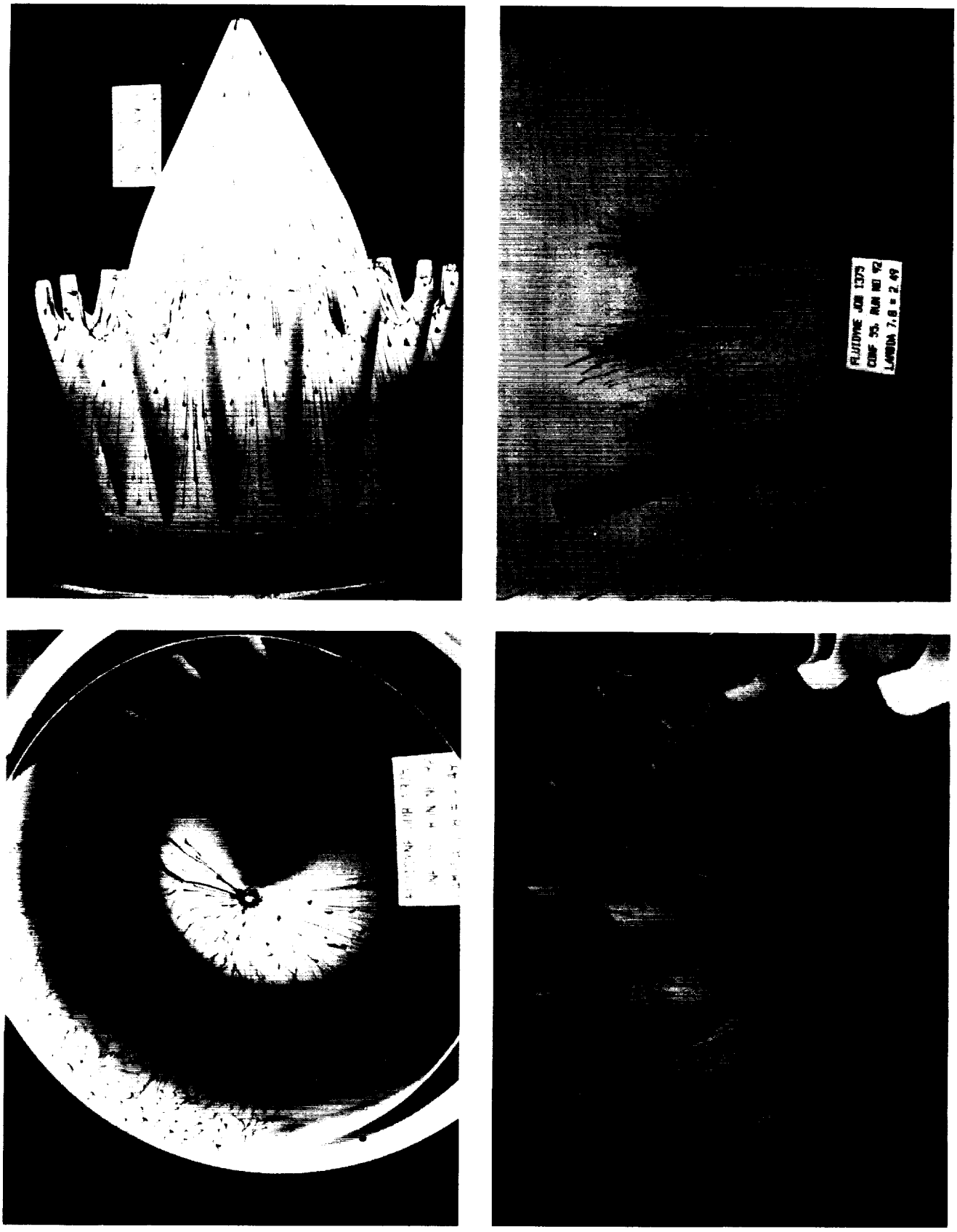

Flow Visualization Photographs, Configuration 55

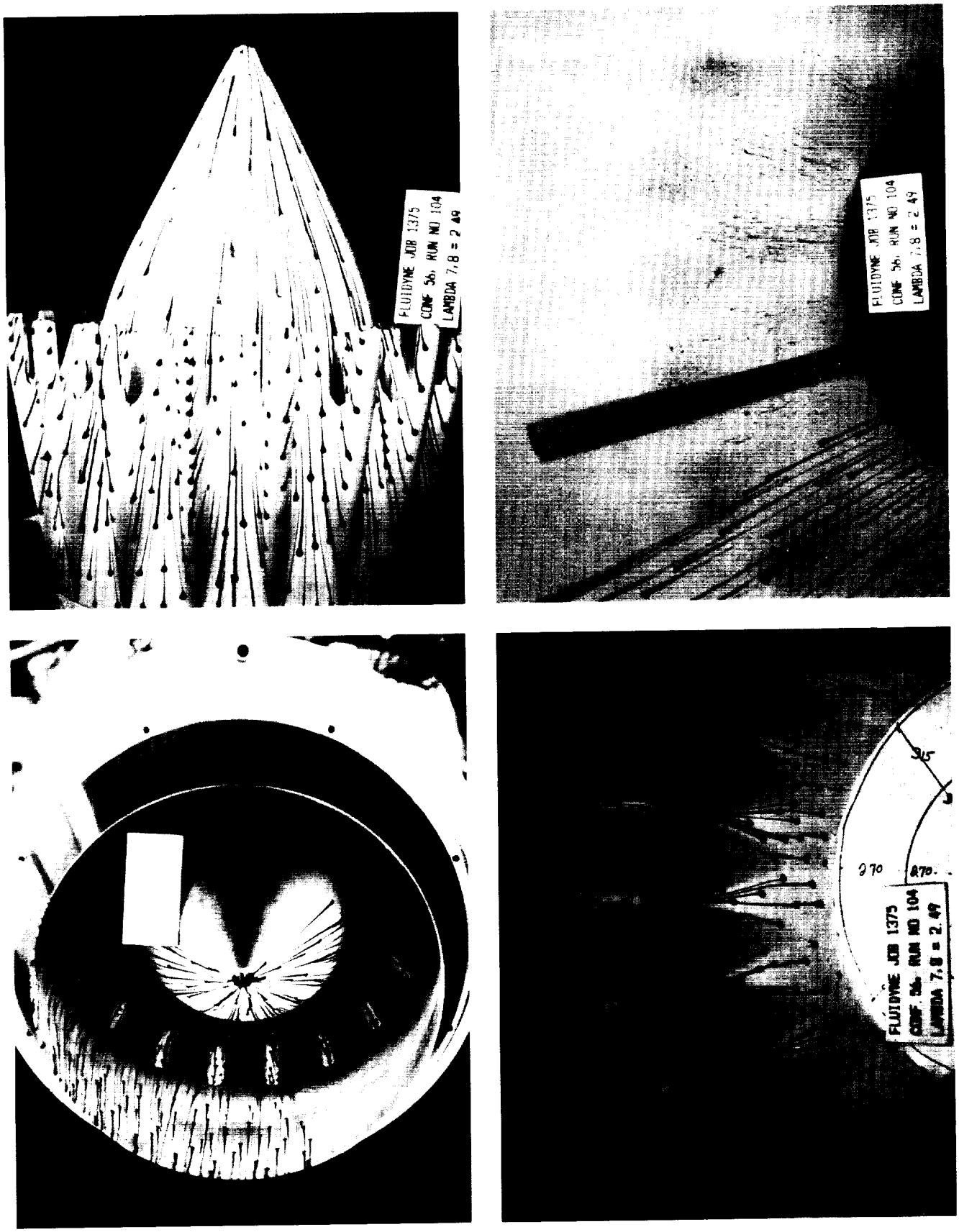

Flow Visualization Photographs, Configuration 56

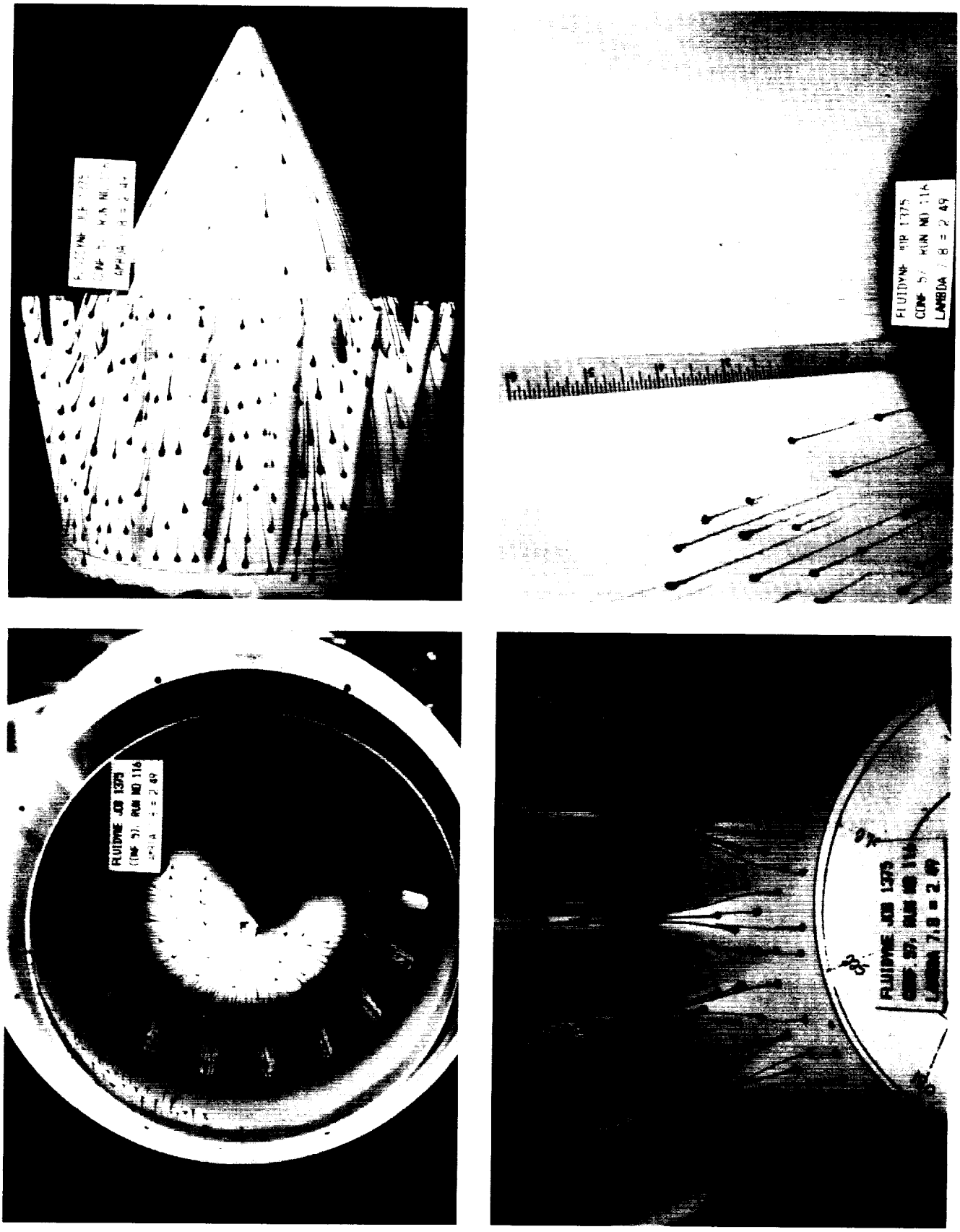

Flow Visualization Photographs, Configuration 57

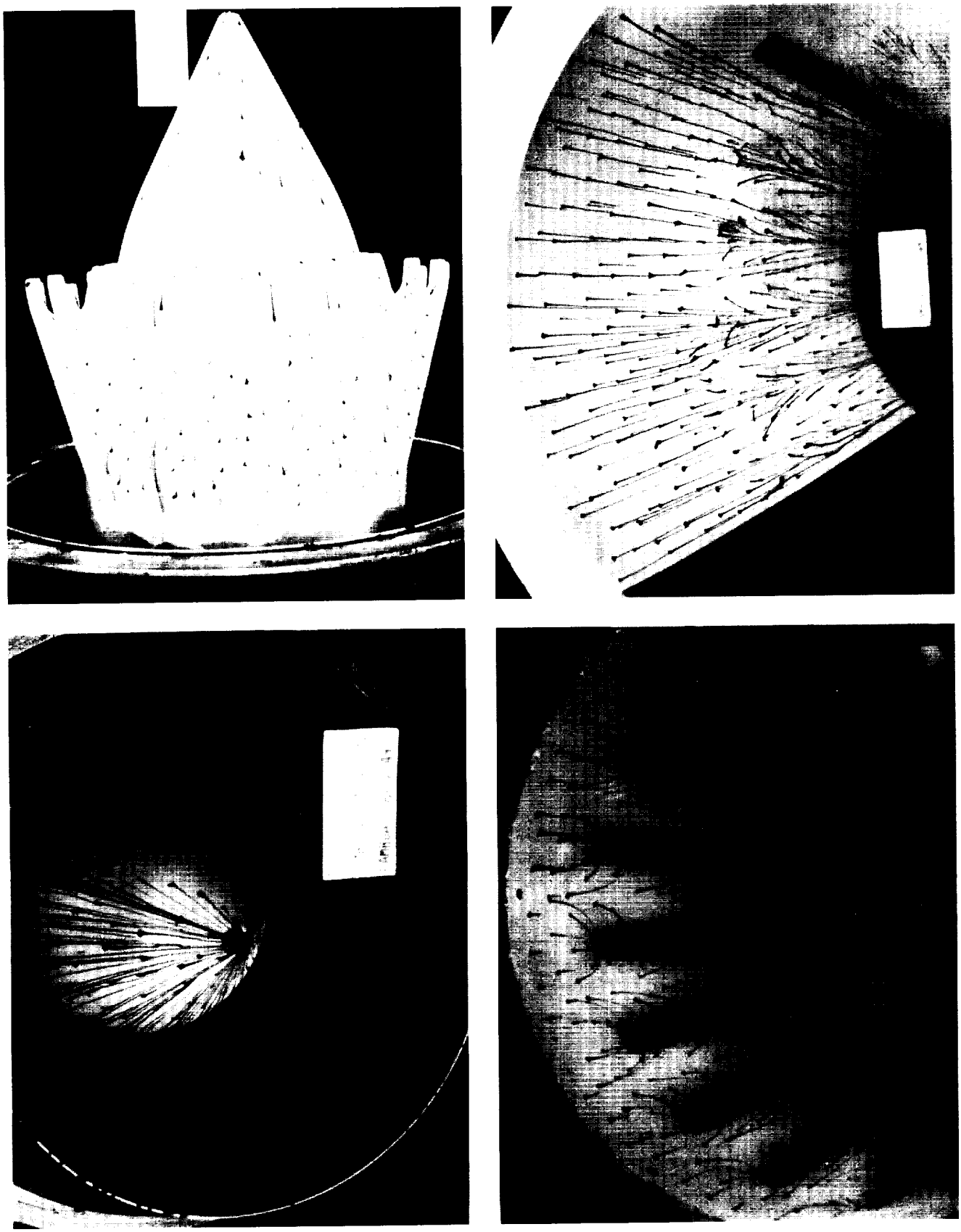

Flow Visualization Photographs, Configuration 59

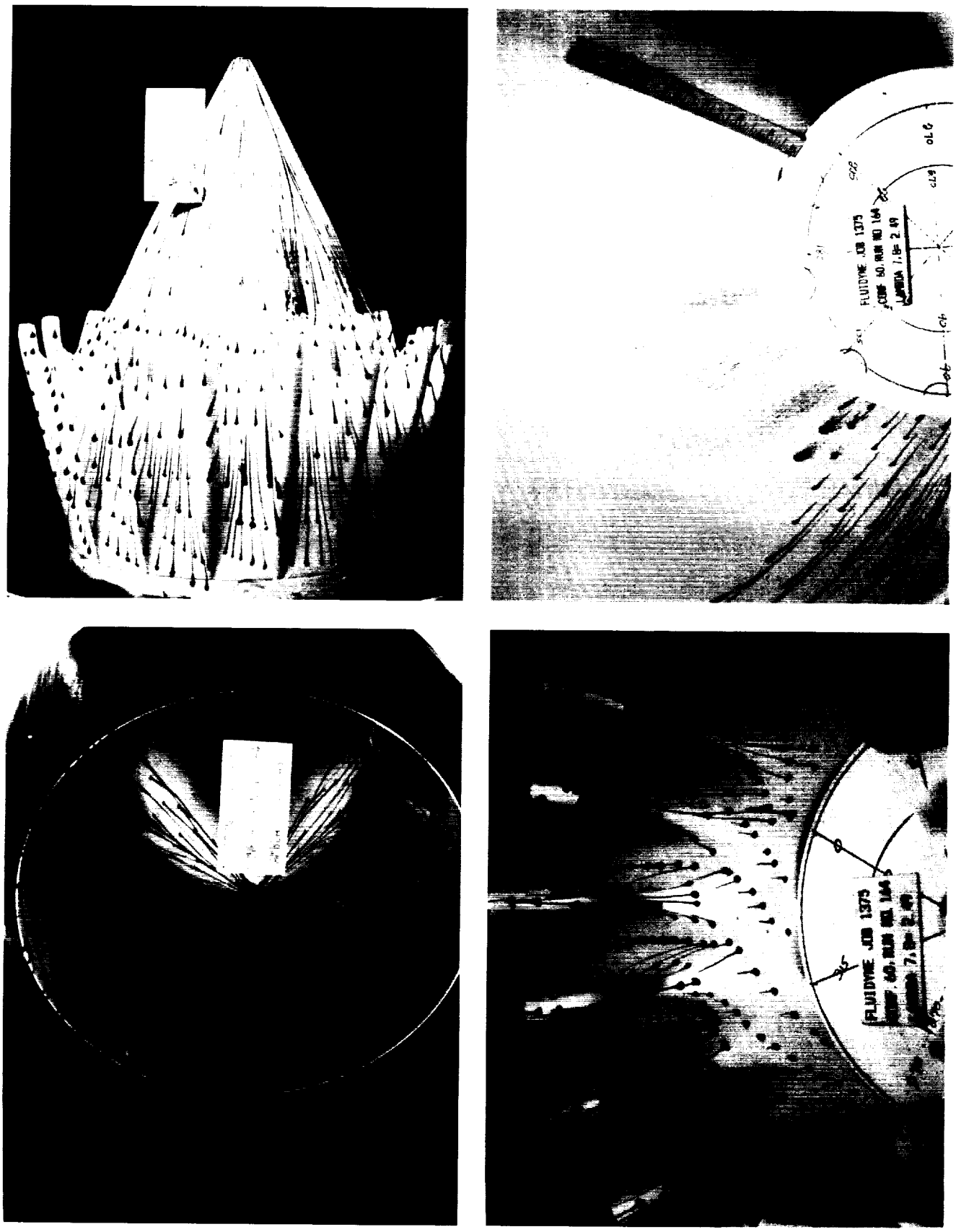

Flow Visualization Photographs, Configuration 60

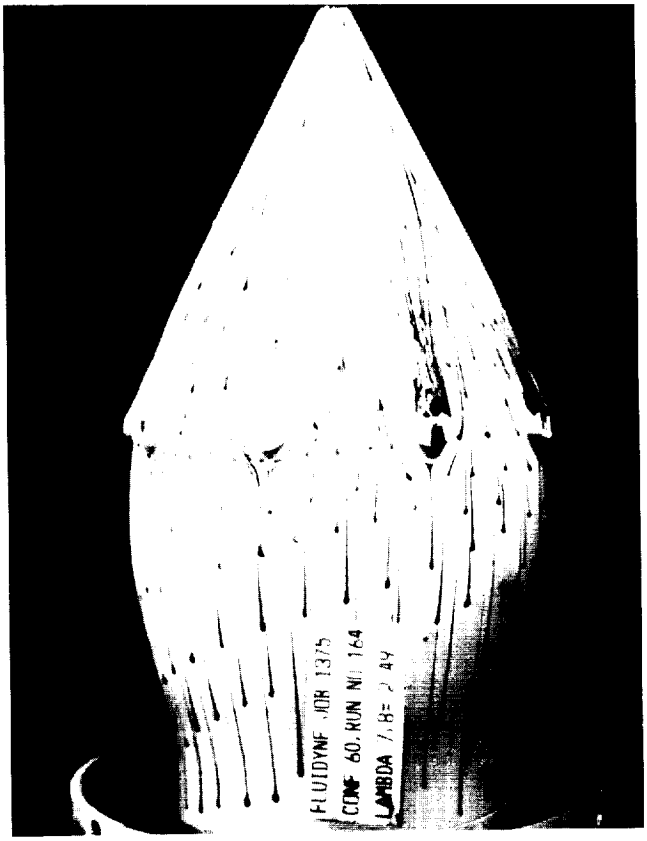

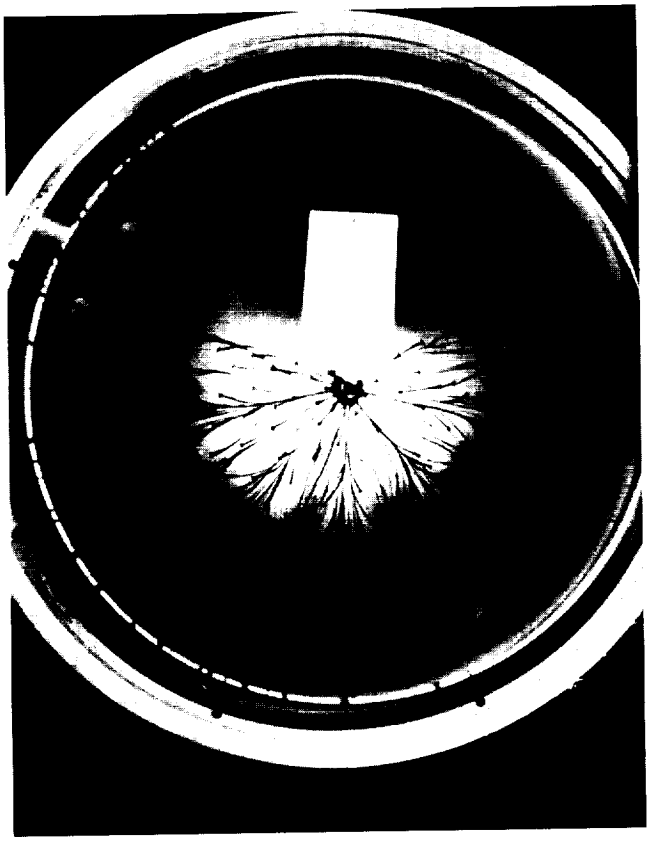

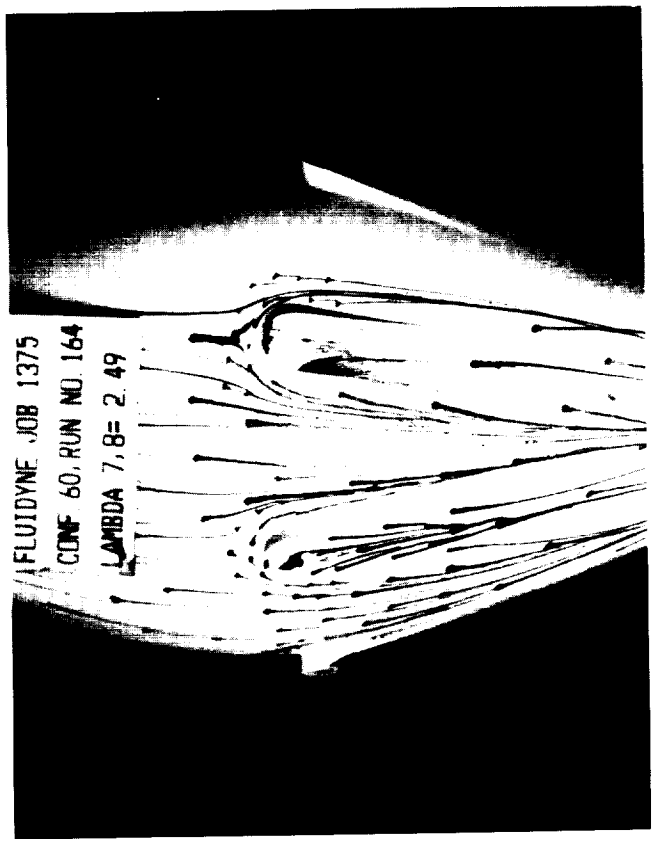

Flow Visualization Photographs, Configuration 60

APPENDIX D

MODEL GEOMETRY AND INSTRUMENTATION DATA

Tabulations of the key mixer instrumentation test data and detailed geometry definition of the tested configurations are presented in this appendix. Traverse test flow conditions, mixer plane velocity, total pressure and temperature data, along with model surface pressures are presented in tabular form. Also included are flow angle correlation curves (using second order, least squares fit).

It should be noted that one of the pressure tubes of pitch probe No. 2 and several plug surface pressures were blocked; therefore, these readings were disregarded. Also, several flow-angle probe readings resulted in flow angles that were too large to be considered. This result was believed to be due to part of the flow angle probe being located in the lobe wall wake region.

The subsections of this appendix are arranged as follows:

D.1 DEFINITION OF SYMBOLS

Defined at model Charging Station

Wa_{FAN}	Fan Stream Flow - lb/sec
Wa_{PRI}	Primary Stream Flow - lb/sec
T_{T7}	Fan Stream Total Temperature - °R
T_{T8}	Primary Stream Total Temperature - °R
P_{T7}	Fan Stream Total Pressure - $lb/in.^2$
P_{T8}	Primary Stream Total Pressure - $lb/in.^2$
A_7	Fan Stream Cross Sectional Area - $in.^2$
A_8	Primary Stream Cross Sectional Area - $in.^2$

Defined at Model Mixing Plane

$T_{T\ MIX}$	Fully Mixed Total Temperature - °R
$P_{T\ MIX}$	Fully Mixed Total Pressure - $lb/in.^2$

D.2 MIXER INSTRUMENTATION TRAVERSE TEST FLOW CONDITIONS

Parameter	Configuration Number 29	Configuration Number 34
Wa_{FAN}	19.953	20.093
T_{T7}	528.64	544.72
P_{T7}	36.48	36.162
A_7	34.94	34.94
Wa_{PRI}	3.0576	3.224
T_{T8}	1320.9	1357.8
P_{T8}	33.054	32.704
A_8	12.94	12.94
$T_{T\ MIX}$	637.08	660.74
$P_{T\ MIX}$	35.241	34.789
P_{AM}	14.268	14.138

Fan Stream Charging Station Total Pressure and Total Temperature Profiles:

Pressure Rake Radius meters	(inches)	P_T/P_{T7}
0.0737	2.903	0.97046
0.0788	3.104	1.00056
0.0825	3.249	1.00506
0.0861	3.388	1.00539
0.0895	3.523	1.00531
0.0928	3.652	1.00568
0.0959	3.776	1.00575
0.0990	3.897	1.00553
0.1020	4.014	1.00529
0.1049	4.128	1.00425
0.1077	4.239	1.00186
0.1109	4.368	0.97088

Temperature Rake Radius meters	(inches)	T_T/T_{T7}
0.0742	2.920	1.0104
0.0816	3.213	0.9952
0.0869	3.422	0.9972
0.0919	3.620	0.9947
0.0967	3.807	0.9981
0.1012	3.985	0.9956
0.1056	4.156	0.9980
0.1105	4.350	1.0003

Primary Stream Charging Station Total Pressure and Total Temperature Profiles:

Pressure Rake Radius meters	(inches)	P_T/P_{T8}
0.0491	1.933	0.99923
0.0540	2.126	1.00519
0.0573	2.254	1.00376
0.0605	2.381	1.00294
0.0635	2.501	1.00024
0.0664	2.616	0.99969
0.0698	2.748	0.98504

Temperature Rake Radius meters	(inches)	T_T/T_{T8}
0.0495	1.950	1.0135
0.0559	2.201	1.0140
0.0605	2.381	1.0038
0.0647	2.548	1.0095
0.0693	2.730	0.9797

D.3 NONAXIAL VELOCITY DATA AT MIXING PLANE

where:

R	=	Radius - in.
Θ	=	Circumferential Location - degrees
$V_{Nonaxial}$	=	Nonaxial Components of Velocity - m/sec
V_{ABS}	=	Absolute Velocity - m/sec
ω	=	Nonaxial Velocity Flow Angle - degrees
μ	=	Radial (Pitch) Flow Angle - degrees
ν	=	Circumferential (Yaw) Flow Angle - degrees
ϵ	=	Angle between Radial Axis (z) and Absolute Velocity

VELOCITY VECTOR DATA
CONFIGURATION 29

PROBE #	R	θ	$V_{MOM-AXIAL}$	ω	V_{RMS}	ϵ	μ	ν
1	1.59	10°	23	-57	182	84.0	6.0	-3.9
3	2.856		49	-86	187	75.0	15.0	-1.2
4	3.122		50	-86	190	74.6	15.4	-1.0
5	3.388		48	90	186	75.1	14.9	0
6	3.654		30	-89	181	80.6	9.4	-.2
7	3.920		15	-79	174	85.0	5.0	-1.0
8	4.053		19	-72	170	84.0	6.0	-2.0
9	4.186		20	-66	165	83.7	6.3	-2.8
10	4.319	↓	21	-62	161	83.3	6.7	-3.6

PROBE #	R	θ	$V_{MOM-AXIAL}$	ω	V_{RMS}	ϵ	μ	ν
1	2.590	14	35	-34	222	84.9	5.1	-7.5
3	2.856		54	-78	193	74.2	13.3	-3.5
4	3.122		52	-80	199	74.9	13.1	-2.7
5	3.388		51	90	189	74.4	15.6	0
6	3.654		28	80	185	81.5	8.5	1.5
7	3.920		15	90	175	85.2	4.8	0
8	4.053		19	-82	169	83.5	6.5	-0.9
9	4.186		21	-77	164	83.0	7.0	-1.6
10	4.319	↓	22	-68	158	82.6	7.4	-3.0

PROBE #	R	θ	$V_{MOM-AXIAL}$	ω	V_{RMS}	ϵ	μ	ν
1	2.590	16	28	-21	232	87.5	2.5	-6.5
3	2.856		—	—	—	—	—	—
4	3.122		—	—	—	—	—	—
5	3.388		—	-	—	—	—	—
6	3.654		23	69	185	83.4	6.6	2.5
7	3.920		12	84	176	86.0	4.0	0.4
8	4.053		17	-85	170	84.4	5.6	-0.5
9	4.186		17	-80	164	84.0	6.0	-1.1
10	4.319	↓	20	-74	156	83.1	6.9	-2.0

VELOCITY VECTOR DATA
CONFIGURATION 29

PROBE #	R	θ	$V_{MOM-AXIAL}$	W	V_{RES}	ε	μ	ν
1	2.590	18	25	-25	232	87.4	2.6	-5.5
3	2.856		-39	76	222	-80.2	-9.8	-2.4
4	3.122		-37	-87	218	-80.2	-9.8	0.5
5	3.388		-32	-83	205	-81.0	-9.0	1.2
6	3.654		14	61	190	86.4	3.6	2.0
7	3.920		9	82	186	87.2	2.8	0.4
8	4.053		14	-88	173	85.4	4.6	-0.2
9	4.186		15	-83	166	85.0	5.0	-0.6
10	4.319	↓	17	-79	157	83.8	6.2	-1.2

PROBE #	R	θ	$V_{MOM-AXIAL}$	W	V_{RES}	ε	μ	ν
1	2.590	20°	16	-42	226	87.3	2.7	-3.0
3	2.856		-26	81	225	-83.5	-6.5	-1.0
4	3.122		-35	-88	219	-80.8	-9.2	0.3
5	3.388		-29	-90	202	-81.8	-8.2	0
6	3.654		16	-70	190	85.4	4.6	-1.7
7	3.920		9	-57	181	87.7	2.3	-1.5
8	4.053		14	-68	176	85.9	4.1	-1.7
9	4.186		15	-72	169	85.1	4.9	-1.6
10	4.319	↓	17	-75	161	84.0	6.0	-1.6

VELOCITY VECTOR DATA
CONFIGURATION 34

PROBE #	R in	θ	$V_{MOM-AXIAL}$ m/sec	ω	V_{ABS} m/sec	ε	μ	ν
1	2.20	10°	55	−77	260	78.1	11.9°	−2.7°
3	2.486		69	−87	196	69.5	20.5°	−1.2°
4	2.752		69	−95	205	70.2	19.8°	−1.8°
5	3.018		66	90	203	70.9	19.1°	0°
6	3.284		61	−88	201	72.4	17.6°	−0.6°
7	3.550		51	−99	196	75.1	14.9°	−0.2°
8	3.683		52	−83	192	74.4	15.6	−0.5°
9	3.816		48	−86	191	75.4	14.6	−1.0°
10	3.949		42	−82	193	77.2	12.8°	−1.8°

PROBE #	R	θ	$V_{MOM-AXIAL}$	ω	V_{ABS}	ε	μ	ν
1	2.20	16°	58	−60	267	79.3	10.8°	−8.9
3	2.486		—	—	—		—	—
4	2.752		69	−82	226	72.5	17.5°	−2.6°
5	3.018		59	−86	221	74.5	15.5°	−1.0°
6	3.284		57	−85	216	74.7	15.3°	−1.4°
7	3.550		50	−87	212	76.5	13.5°	−0.7°
8	3.683		59	89	206	73.4	16.6°	0.2°
9	3.816		52	80	210	75.8	14.2°	2.6°
10	3.949		40	85	201	78.6	11.4°	1.1°

VELOCITY VECTOR DATA
CONFIGURATION 34

PROBE #	R	θ	V_{MOM} - AXIAL	ω	V_{ABS}	ε	μ	ν
1	2.2	18°	-53	-61	267	80.0	10	-5.6
3	2.486		-24	42	299	-86.9	-3.1	-3.5
4	2.752		41	-65	225	80.5	9.5	-4.4
5	3.018		-27	11	196	-88.5	-1.5	-7.8
6	3.284		-38	65	173	-78.5	-11.5	-5.5
7	3.550		-24	86	166	-81.9	-8.1	-0.6
8	3.683		-22	75	162	-82.5	-7.5	-2.0
9	3.816		52	88	214	76.0	14.0	0.6
10	3.949		33	75	203	81.0	9.0	2.4

PROBE #	R	θ	V_{MOM} - AXIAL	ω	V_{ABS}	ε	μ	ν
1	2.20	20°	-47	-72	262	80.11	9.9°	-3.2
3	2.486		-24	70	268	-85.2	-4.3	-1.9
4	2.752		-37	-88	257	-70.1	-19.9	0.9
5	3.018		-33	-87	251	-69.4	-20.6	1.2
6	3.284		-79	-88	249	-71.7	-18.3	0.7
7	3.550		-49	-88	243	-78.3	-11.7	0.5
8	3.683		-56	-90	236	-76.3	-13.7	0
9	3.816		-5	90	175	-88.4	-1.6	0
10	3.949		29	-81	203	82.0	8.0	-1.3

D.4 TOTAL PRESSURE/TOTAL TEMPERATURE TRAVERSE DATA

CONFIGURATION 29 THETA = 10.00

RADIUS	TT/TT MIX	PT/PT MIX
2.590	1.28922	0.94086
2.723	0.89408	0.95282
2.856	0.85922	0.98909
2.989	0.84143	1.01217
3.122	0.83103	1.01936
3.255	0.82784	1.02942
3.388	0.82465	1.02815
3.521	0.82486	1.03392
3.654	0.82417	1.03360
3.787	0.82443	1.03352
3.920	0.82402	1.03170
4.053	0.82429	1.03016
4.186	0.82417	1.02948
4.319	0.82451	1.02752
4.452	0.82443	1.02235

CONFIGURATION 29 THETA = 12.00

RADIUS	TT/TT MIX	PT/PT MIX
2.590	1.48095	0.94101
2.723	0.87635	0.97165
2.856	0.85293	0.99573
2.989	0.83940	1.01723
3.122	0.83064	1.02339
3.255	0.82785	1.03258
3.388	0.82506	1.02977
3.521	0.82499	1.03542
3.654	0.82387	1.03445
3.787	0.82463	1.03340
3.920	0.82443	1.03071
4.053	0.82477	1.02799
4.186	0.82477	1.02623
4.319	0.82520	1.02325
4.452	0.82540	1.01755

CONFIGURATION 29 THETA = 14.00

RADIUS	TT/TT MIX	PT/PT MIX
2.590	1.91876	0.93985
2.723	0.90767	0.96910
2.856	0.86985	1.00264
2.989	0.85171	1.02135
3.122	0.85728	1.02419
3.255	0.84179	1.03285
3.388	0.82627	1.02834
3.521	0.82573	1.03578
3.654	0.82452	1.03512
3.787	0.82523	1.03370
3.920	0.82486	1.02996
4.053	0.82529	1.02575
4.186	0.82550	1.02237
4.319	0.82607	1.01786
4.452	0.82719	1.01005

CONFIGURATION 29 THETA = 16.00

RADIUS	TT/TT MIX	PT/PT MIX
2.590	2.09232	0.93935
2.723	1.98949	0.93589
2.856	1.96445	0.97327
2.989	2.00573	0.96162
3.122	1.99760	0.96323
3.255	1.67916	0.95529
3.388	1.01058	0.93462
3.521	0.83194	1.03560
3.654	0.82678	1.03626
3.787	0.82572	1.03455
3.920	0.82566	1.03081
4.053	0.82629	1.02610
4.186	0.82635	1.02063
4.319	0.82713	1.01346
4.452	0.82798	1.00112

CONFIGURATION 29 THETA = 18.00

RADIUS	TT/TT MIX	PT/PT MIX
2.590	2.10487	0.93981
2.723	2.10080	0.93910
2.856	2.10080	0.93607
2.989	2.09809	0.93862
3.122	2.08928	0.93715
3.255	2.04427	0.93685
3.388	1.99924	0.93297
3.521	1.02573	0.92349
3.654	0.82754	1.03718
3.787	0.82506	1.03547
3.920	0.82513	1.03198
4.053	0.82583	1.02719
4.186	0.82634	1.02097
4.319	0.82698	1.01189
4.452	0.82775	0.99639

CONFIGURATION 29 THETA = 20.00

RADIUS	TT/TT MIX	PT/PT MIX
2.590	2.09720	0.93640
2.723	2.09720	0.93978
2.856	2.09737	0.93921
2.989	2.09523	0.93989
3.122	2.08736	0.93816
3.255	2.07356	0.93748
3.388	1.98462	0.93092
3.521	1.01075	0.90093
3.654	0.82641	1.03730
3.787	0.82382	1.03749
3.920	0.82382	1.03509
4.053	0.82395	1.03366
4.186	0.82545	1.02887
4.319	0.82641	1.02027
4.452	0.83214	1.00429

CONFIGURATION 29 THETA = 22.00

RADIUS	TT/TT MIX	PT/PT MIX
2.590	2.09725	0.93759
2.723	2.02456	0.93972
2.856	1.99544	0.93808
2.989	2.03449	0.93859
3.122	1.95375	0.93671
3.255	1.85297	0.93600
3.388	1.75219	0.93081
3.521	0.83399	0.91874
3.654	0.82590	1.03706
3.787	0.82413	1.03816
3.920	0.82419	1.03728
4.053	0.82447	1.03578
4.186	0.82564	1.03135
4.319	0.82638	1.02201
4.452	0.83099	1.00111

CONFIGURATION 29 THETA = 24.00

RADIUS	TT/TT MIX	PT/PT MIX
2.590	1.92036	0.93965
2.723	0.89207	0.93900
2.856	0.84064	0.92084
2.989	0.83404	0.89578
3.122	0.83033	0.90808
3.255	0.82837	0.90893
3.388	0.82640	1.02271
3.521	0.82557	1.03709
3.654	0.82585	1.03771
3.787	0.82426	1.03893
3.920	0.82426	1.03780
4.053	0.82434	1.03578
4.186	0.82557	1.03024
4.319	0.82634	1.01947
4.452	0.83046	0.98921

CONFIGURATION 29 THETA = 26.00

RADIUS	TT/TT MIX	PT/PT MIX
2.590	1.57378	0.93903
2.723	0.87725	0.91594
2.856	0.84494	1.00669
2.989	0.83058	1.02436
3.122	0.82727	1.02430
3.255	0.82693	1.03389
3.388	0.82657	1.03154
3.521	0.82630	1.03817
3.654	0.82553	1.03843
3.787	0.82574	1.03959
3.920	0.82533	1.03808
4.053	0.82547	1.03744
4.186	0.82602	1.03307
4.319	0.82565	1.02419
4.452	0.82914	1.00751

CONFIGURATION 29 THETA = 28.00

RADIUS	TT/TT MIX	PT/PT MIX
2.590	1.83264	0.94083
2.723	0.92406	0.96983
2.856	0.85383	0.99951
2.989	0.83208	1.02090
3.122	0.82688	1.02550
3.255	0.82640	1.03449
3.388	0.82591	1.03239
3.521	0.82597	1.03815
3.654	0.82528	1.03844
3.787	0.82542	1.03960
3.920	0.82465	1.03926
4.053	0.82465	1.03832
4.186	0.82534	1.03546
4.319	0.82528	1.02896
4.452	0.82709	1.01679

CONFIGURATION 29 THETA = 30.00

RADIUS	TT/TT MIX	PT/PT MIX
2.590	1.84307	0.93972
2.723	0.92700	0.95802
2.856	0.85932	0.98961
2.989	0.83624	1.01879
3.122	0.82880	1.02649
3.255	0.82738	1.03527
3.388	0.82595	1.03377
3.521	0.82601	1.03908
3.654	0.82507	1.03934
3.787	0.82493	1.04033
3.920	0.82392	1.04019
4.053	0.82364	1.03911
4.186	0.82453	1.03630
4.319	0.82439	1.02959
4.452	0.82669	1.01808

CONFIGURATION 29 THETA = 32.00

RADIUS	TT/TT MIX	PT/PT MIX
2.590	1.76176	0.93894
2.723	0.88679	0.96564
2.856	0.85606	0.99231
2.989	0.83924	1.01991
3.122	0.83277	1.02714
3.255	0.83002	1.03544
3.388	0.82726	1.03360
3.521	0.82740	1.03918
3.654	0.82616	1.03975
3.787	0.82582	1.04066
3.920	0.82598	1.04063
4.053	0.82660	1.03937
4.186	0.82582	1.03662
4.319	0.82592	1.03023
4.452	0.82815	1.01841

CONFIGURATION 29 THETA = 34.00

RADIUS	TT/TT MIX	PT/PT MIX
2.590	1.88569	0.93732
2.723	0.89438	0.96488
2.856	0.86027	0.99935
2.989	0.84618	1.02165
3.122	0.84141	1.02611
3.255	0.83534	1.03401
3.388	0.82924	1.03120
3.521	0.82822	1.03799
3.654	0.82774	1.03909
3.787	0.82643	1.04009
3.920	0.82567	1.04015
4.053	0.82555	1.03924
4.186	0.82643	1.03637
4.319	0.82671	1.02887
4.452	0.82951	1.01520

CONFIGURATION 29 THETA = 36.00

RADIUS	TT/TT MIX	PT/PT MIX
2.590	2.09563	0.93813
2.723	1.96172	0.92556
2.856	1.89604	0.99871
2.989	1.93385	1.01900
3.122	1.95045	1.02070
3.255	1.94315	1.02845
3.388	0.88344	1.02272
3.521	0.83275	1.03603
3.654	0.83035	1.03870
3.787	0.82615	1.03975
3.920	0.82533	1.03991
4.053	0.82531	1.03862
4.186	0.82643	1.03456
4.319	0.82634	1.02553
4.452	0.82898	1.00969

CONFIGURATION 29 THETA = 38.00

RADIUS	TT/TT MIX	PT/PT MIX
2.590	2.09604	0.93708
2.723	2.09138	0.93716
2.856	2.09272	0.93425
2.989	2.09739	0.93617
3.122	2.07808	0.93470
3.255	2.03210	0.93408
3.388	1.98611	0.93062
3.521	1.01675	0.92272
3.654	0.83053	1.03739
3.787	0.82678	1.03924
3.920	0.82644	1.03963
4.053	0.82664	1.03898
4.186	0.82735	1.03513
4.319	0.82761	1.02594
4.452	0.83018	1.00813

CONFIGURATION 29 THETA = 40.00

RADIUS	TT/TT MIX	PT/PT MIX
2.590	2.08916	0.93379
2.723	2.08852	0.93919
2.856	2.08916	0.93893
2.989	2.08461	0.93924
3.122	2.07548	0.93757
3.255	2.02677	0.93731
3.388	1.97806	0.93311
3.521	1.07024	0.90188
3.654	0.83111	0.97482
3.787	0.82508	1.03824
3.920	0.82434	1.03932
4.053	0.82448	1.03932
4.186	0.82637	1.03708
4.319	0.82719	1.02944
4.452	0.83374	1.01323

CONFIGURATION 29 THETA = 42.00

RADIUS	TT/TT MIX	PT/PT MIX
2.590	2.09798	0.93776
2.723	2.07645	0.94156
2.856	2.04766	0.94091
2.989	2.05093	0.94170
3.122	1.95977	0.94017
3.255	1.95948	0.93994
3.388	1.95918	0.93361
3.521	0.86616	0.92029
3.654	0.82772	1.03508
3.787	0.82432	1.03946
3.920	0.82364	1.03990
4.053	0.82357	1.03892
4.186	0.82472	1.03611
4.319	0.82500	1.02608
4.452	0.82981	1.00580

CONFIGURATION 29 THETA = 44.00

RADIUS	TT/TT MIX	PT/PT MIX
2.590	1.99138	0.93977
2.723	0.95584	0.93949
2.856	0.87874	0.93631
2.989	0.85454	0.90722
3.122	0.85026	0.91256
3.255	0.84180	0.90305
3.388	0.83332	0.96651
3.521	0.83093	1.03471
3.654	0.82868	1.03684
3.787	0.82724	1.03919
3.920	0.82669	1.03945
4.053	0.82676	1.03913
4.186	0.82738	1.03471
4.319	0.82744	1.02134
4.452	0.83065	0.99310

CONFIGURATION 29 THETA = 46.00

RADIUS	TT/TT MIX	PT/PT MIX
2.590	1.86797	0.94120
2.723	0.90330	0.93275
2.856	0.86991	1.00070
2.989	0.85171	1.02059
3.122	0.84074	1.02073
3.255	0.83289	1.02966
3.388	0.83124	1.02754
3.521	0.82947	1.03517
3.654	0.82776	1.03630
3.787	0.82660	1.03829
3.920	0.82604	1.03852
4.053	0.82611	1.03826
4.186	0.82660	1.03525
4.319	0.82652	1.02493
4.452	0.82748	1.00527

CONFIGURATION 29 THETA = 48.00

RADIUS	TT/TT MIX	PT/PT MIX
2.590	1.86214	0.93303
2.723	0.93978	0.9466:
2.856	0.87723	0.99703
2.989	0.85420	1.01724
3.122	0.84247	1.02144
3.255	0.83728	1.03010
3.388	0.83209	1.02899
3.521	0.83034	1.03527
3.654	0.83009	1.03643
3.787	0.82884	1.03839
3.920	0.82815	1.03890
4.053	0.82823	1.03881
4.186	0.82878	1.03671
4.319	0.82850	1.02916
4.452	0.82898	1.01375

CONFIGURATION 29 THETA = 50.00

RADIUS	TT/TT MIX	PT/PT MIX
2.590	1.89450	0.93810
2.723	0.94731	0.95215
2.856	0.87400	0.98402
2.989	0.84947	1.01515
3.122	0.83787	1.02145
3.255	0.83348	1.03005
3.388	0.82908	1.02917
3.521	0.82862	1.03487
3.654	0.82780	1.03598
3.787	0.82746	1.03754
3.920	0.82692	1.03768
4.053	0.82712	1.03669
4.186	0.82780	1.03376
4.319	0.82766	1.02641
4.452	0.82820	1.01381

CONFIGURATION 34 THETA = 10.00

RADIUS	TT/TT MIX	PT/PT MIX
2.220	1.94819	0.93956
2.353	0.97508	0.93540
2.486	0.87119	0.97056
2.619	0.84355	1.00726
2.752	0.82995	1.01396
2.885	0.84206	1.02925
3.018	0.82113	1.02568
3.151	0.82073	1.03638
3.284	0.82045	1.03364
3.417	0.82099	1.03798
3.550	0.82005	1.03501
3.683	0.81977	1.03022
3.816	0.82059	1.03296
3.949	0.81943	1.03239
4.082	0.81970	1.03016

CONFIGURATION 34 THETA = 12.00

RADIUS	TT/TT MIX	PT/PT MIX
2.220	1.95924	0.94206
2.353	0.99363	0.90390
2.486	0.87341	0.97631
2.619	0.84621	1.01028
2.752	0.82953	1.01859
2.885	0.82229	1.03409
3.018	0.81986	1.02983
3.151	0.81955	1.03369
3.284	0.81865	1.03403
3.417	0.81815	1.03691
3.550	0.81741	1.03256
3.683	0.81755	1.02563
3.816	0.81761	1.02762
3.949	0.81755	1.02664
4.082	0.81768	1.02503

CONFIGURATION 34 THETA = 14.00

RADIUS	TT/TT MIX	PT/PT MIX
2.220	2.00759	0.93944
2.353	1.41191	0.94111
2.486	0.87159	0.98215
2.619	0.84587	1.01420
2.752	0.82936	1.02195
2.885	0.82266	1.03700
3.018	0.82090	1.03172
3.151	0.81961	1.03987
3.284	0.81876	1.03436
3.417	0.81833	1.03783
3.550	0.81765	1.03301
3.683	0.81799	1.02500
3.816	0.81833	1.02709
3.949	0.81785	1.02514
4.082	0.81819	1.02178

CONFIGURATION 34 THETA = 16.00

RADIUS	TT/TT MIX	PT/PT MIX
2.220	2.06182	0.93930
2.353	1.81287	0.94384
2.486	0.87764	0.96867
2.619	0.84354	1.01567
2.752	0.83054	1.02210
2.885	0.81771	1.03710
3.018	0.81933	1.03161
3.151	0.81897	1.03991
3.284	0.81864	1.03454
3.417	0.81826	1.03808
3.550	0.81784	1.03431
3.683	0.81893	1.02457
3.816	0.81852	1.02808
3.949	0.81871	1.02604
4.082	0.81804	1.01972

CONFIGURATION 34 THETA = 18.00

RADIUS	TT/TT MIX	PT/PT MIX
2.220	2.07916	0.93820
2.353	2.08565	0.94413
2.486	2.01076	0.93990
2.619	1.72992	0.91110
2.752	1.03880	0.95751
2.885	1.67719	0.93449
3.018	1.24855	0.88505
3.151	1.02664	0.88050
3.284	1.00791	0.90532
3.417	1.00036	0.90975
3.550	0.95088	0.90710
3.683	0.95353	0.90423
3.816	0.86308	1.02432
3.949	0.81969	1.03114
4.082	0.81827	1.02107

CONFIGURATION 34 THETA = 20.00

RADIUS	TT/TT MIX	PT/PT MIX
2.220	2.06150	0.93342
2.353	2.08046	0.94176
2.486	2.08373	0.94299
2.619	2.08440	0.94282
2.752	2.07850	0.93374
2.885	2.07850	0.93995
3.018	2.07721	0.93955
3.151	2.07523	0.93960
3.284	2.06936	0.93259
3.417	2.06477	0.93394
3.550	2.05232	0.93092
3.683	2.02480	0.92696
3.816	1.69877	0.88623
3.949	0.83169	1.03631
4.082	0.82033	1.02775

CONFIGURATION 34 THETA = 22.00

RADIUS	TT/TT MIX	PT/PT MIX
2.220	2.07485	0.92932
2.353	2.08602	0.93927
2.486	2.03999	0.94194
2.619	1.98466	0.94157
2.752	1.83638	0.93165
2.885	1.86209	0.93778
3.018	1.96687	0.92883
3.151	1.98663	0.93708
3.284	2.00641	0.93079
3.417	2.02617	0.93599
3.550	2.02551	0.92791
3.683	2.00443	0.92757
3.816	1.60443	0.91146
3.949	0.82520	1.03862
4.082	0.82027	1.03382

CONFIGURATION 34 THETA = 24.00

RADIUS	TT/TT MIX	PT/PT MIX
2.220	2.06908	0.93337
2.353	1.79306	0.94109
2.486	0.87042	0.93914
2.619	0.83542	1.01225
2.752	0.82571	1.02083
2.885	0.82000	1.03699
3.018	0.81979	1.03042
3.151	0.81971	1.04078
3.284	0.81948	1.03545
3.417	0.81932	1.04113
3.550	0.81857	1.03820
3.683	0.81925	1.03062
3.816	0.81925	1.03308
3.949	0.81919	1.03932
4.082	0.81932	1.03458

CONFIGURATION 34 THETA = 26.00

RADIUS	TT/TT MIX	PT/PT MIX
2.220	1.99342	0.93766
2.353	1.18265	0.94240
2.486	0.85620	0.98235
2.619	0.83001	1.01903
2.752	0.82124	1.02520
2.885	0.82043	1.03876
3.018	0.81968	1.03304
3.151	0.81886	1.04177
3.284	0.81813	1.03790
3.417	0.81920	1.04241
3.550	0.81874	1.04051
3.683	0.81860	1.03675
3.816	0.81934	1.04126
3.949	0.81874	1.04051
4.082	0.81933	1.03509

CONFIGURATION 34 THETA = 28.00

RADIUS	TT/TT MIX	PT/PT MIX
2.220	1.96496	0.93890
2.353	0.97228	0.94157
2.486	0.86522	0.98327
2.619	0.83264	1.01688
2.752	0.81981	1.02572
2.885	0.81830	1.03930
3.018	0.81893	1.03448
3.151	0.81784	1.04274
3.284	0.81729	1.03936
3.417	0.81823	1.04364
3.550	0.81802	1.04229
3.683	0.81844	1.03861
3.816	0.81851	1.04157
3.949	0.81837	1.03936
4.082	0.81851	1.03324

CONFIGURATION 34 THETA = 30.00

RADIUS	TT/TT MIX	PT/PT MIX
2.220	1.96109	0.94085
2.353	0.99908	0.93700
2.486	0.87318	0.97448
2.619	0.83566	1.01509
2.752	0.82116	1.02505
2.885	0.81836	1.03092
3.018	0.81911	1.03438
3.151	0.81876	1.04265
3.284	0.81859	1.03929
3.417	0.81836	1.04383
3.550	0.81802	1.04271
3.683	0.81856	1.03921
3.816	0.81822	1.04211
3.949	0.81815	1.03993
4.082	0.81795	1.03587

CONFIGURATION 34 THETA = 32.00

RADIUS	TT/TT MIX	PT/PT MIX
2.220	1.96190	0.93951
2.353	0.96938	0.93427
2.486	0.87179	0.97449
2.619	0.83995	1.01491
2.752	0.82515	1.02518
2.885	0.82227	1.03875
3.018	0.82098	1.03432
3.151	0.82017	1.04263
3.284	0.81843	1.03933
3.417	0.82039	1.04384
3.550	0.81950	1.04274
3.683	0.81910	1.03889
3.816	0.81964	1.04138
3.949	0.81883	1.03924
4.082	0.81958	1.03239

CONFIGURATION 34 THETA = 34.00

RADIUS	TT/TT MIX	PT/PT MIX
2.220	1.99111	0.93786
2.353	1.19765	0.93883
2.486	0.87141	0.98139
2.619	0.84405	1.01738
2.752	0.82769	1.02604
2.885	0.82282	1.03916
3.018	0.82206	1.03435
3.151	0.82130	1.04269
3.284	0.82091	1.03934
3.417	0.82041	1.04383
3.550	0.82014	1.04269
3.683	0.82097	1.03859
3.816	0.82049	1.04160
3.949	0.82063	1.03876
4.082	0.81993	1.03114

CONFIGURATION 34 THETA = 36.00

RADIUS	TT/TT MIX	PT/PT MIX
2.220	2.04737	0.93964
2.353	1.77749	0.94309
2.486	0.87524	0.97739
2.619	0.84494	1.01866
2.752	0.82991	1.02513
2.885	0.82340	1.03938
3.018	0.82081	1.03335
3.151	0.81940	1.04166
3.284	0.81821	1.03810
3.417	0.81868	1.04272
3.550	0.81787	1.04152
3.683	0.81795	1.03646
3.816	0.81862	1.04120
3.949	0.81809	1.03973
4.082	0.81887	1.03249

CONFIGURATION 34 THETA = 38.00

RADIUS	TT/TT MIX	PT/PT MIX
2.220	2.07729	0.93782
2.353	2.03275	0.94251
2.486	1.85040	0.92664
2.619	0.89609	1.00242
2.752	0.89433	1.02170
2.885	0.86041	1.03366
3.018	0.84121	1.02596
3.151	0.84240	1.02182
3.284	0.84321	1.01825
3.417	0.84425	0.99466
3.550	0.83633	1.00412
3.683	0.86961	1.02156
3.816	0.83026	1.03837
3.949	0.82169	1.04164
4.082	0.82177	1.03397

CONFIGURATION 34 THETA = 40.00

RADIUS	TT/TT MIX	PT/PT MIX
2.220	2.06502	0.93428
2.353	2.08107	0.94118
2.486	2.08364	0.94006
2.619	2.08235	0.93934
2.752	2.07080	0.93112
2.885	2.07273	0.93664
3.018	2.07336	0.92856
3.151	2.06988	0.93641
3.284	2.05795	0.93026
3.417	2.05343	0.93589
3.550	2.03990	0.92851
3.683	2.01733	0.92121
3.816	1.81748	0.88976
3.949	0.84205	1.04218
4.082	0.82247	1.03218

CONFIGURATION 34 THETA = 42.00

RADIUS	TT/TT MIX	PT/PT MIX
2.220	2.07733	0.92809
2.353	2.08200	0.94046
2.486	2.07933	0.94279
2.619	2.05797	0.94279
2.752	1.98916	0.93581
2.885	1.96982	0.94052
3.018	2.04061	0.93246
3.151	2.04272	0.94040
3.284	2.04477	0.93432
3.417	2.04729	0.93956
3.550	2.03792	0.93105
3.683	2.02055	0.92763
3.816	1.90229	0.91033
3.949	0.84724	1.04266
4.082	0.82341	1.03645

CONFIGURATION 34 THETA = 44.00

RADIUS	TT/TT MIX	PT/PT MIX
2.220	2.07284	0.93650
2.353	1.92297	0.94405
2.486	0.93797	0.93822
2.619	0.85764	0.98108
2.752	0.83957	1.01500
2.885	0.82923	1.03212
3.018	0.82363	1.02906
3.151	0.82321	1.03971
3.284	0.82135	1.03776
3.417	0.82129	1.04201
3.550	0.81976	1.04006
3.683	0.82023	1.03276
3.816	0.81909	1.03933
3.949	0.81942	1.04074
4.082	0.81089	1.03468

CONFIGURATION 34 THETA = 46.00

RADIUS	TT/TT MIX	PT/PT MIX
2.220	2.01622	0.93733
2.353	1.46811	0.93936
2.486	0.87699	0.96570
2.619	0.85092	1.01388
2.752	0.83381	1.01996
2.885	0.82714	1.03403
3.018	0.82488	1.03007
3.151	0.88632	1.03929
3.284	0.81826	1.03725
3.417	0.81966	1.04184
3.550	0.81899	1.04067
3.683	0.81972	1.03667
3.816	0.81960	1.04110
3.949	0.81919	1.04058
4.082	0.81913	1.03467

CONFIGURATION 34 THETA = 48.00

RADIUS	TT/TT MIX	PT/PT MIX
2.220	1.96110	0.93411
2.353	0.97151	0.93589
2.486	0.87772	0.97794
2.619	0.85156	1.01201
2.752	0.83540	1.01956
2.885	0.82923	1.03363
3.018	0.82468	1.03010
3.151	0.82279	1.03909
3.284	0.82091	1.03714
3.417	0.82065	1.04199
3.550	0.81998	1.04142
3.683	0.82018	1.03817
3.816	0.82038	1.04211
3.949	0.82038	1.04099
4.082	0.81990	1.03524

CONFIGURATION 34 THETA = 50.00

RADIUS	TT/TT MIX	PT/PT MIX
2.220	1.96027	0.93576
2.353	0.97584	0.93672
2.486	0.87686	0.96950
2.619	0.85186	1.01040
2.752	0.83511	1.01876
2.885	0.82749	1.03255
3.018	0.82423	1.02872
3.151	0.93805	1.03736
3.284	0.81855	1.03547
3.417	0.82067	1.04047
3.550	0.81993	1.03973
3.683	0.82095	1.03662
3.816	0.82053	1.04016
3.949	0.82033	1.03881
4.082	0.81971	1.03335

CONFIGURATION 29 THETA = 20.00

RADIUS	TT/TT MIX	PT/PT MIX
0.260	1.35145	
0.520	1.11233	0.96184
0.780	0.90831	0.98809
1.040	0.83954	0.99571
1.300	0.83851	1.01152
1.560	1.07724	1.00136
1.820	1.26949	0.95704
2.080	1.20579	0.95308
2.340	0.89878	0.98470
2.600	0.82520	1.04258
2.860	0.82582	1.04258
3.120	0.82520	1.03157

CONFIGURATION 29 THETA = 22.50

RADIUS	TT/TT MIX	PT/PT MIX
0.260	1.35770	
0.520	1.15361	0.96133
0.780	0.93937	0.98481
1.040	0.85705	0.99385
1.300	0.83669	1.02067
1.560	1.06992	1.00147
1.820	1.13603	0.95178
2.080	0.94289	0.97380
2.340	0.83233	1.01531
2.600	0.82480	1.04269
2.860	0.82576	1.04269
3.120	0.82534	1.03168

CONFIGURATION 29 THETA = 25.00

RADIUS	TT/TT MIX	PT/PT MIX
0.260	1.34391	
0.520	1.19061	0.95978
0.780	0.99553	0.98180
1.040	0.90661	0.99281
1.300	0.85165	1.02894
1.560	1.03515	1.00128
1.820	1.14435	0.96599
2.080	0.99958	0.98462
2.340	0.83482	1.02612
2.600	0.82428	1.04249
2.860	0.82544	1.04249
3.120	0.82510	1.03148

CONFIGURATION 29 THETA = 27.50

RADIUS	TT/TT MIX	PT/PT MIX
0.260	1.31514	
0.520	1.21480	0.96113
0.780	1.06640	0.97977
1.040	0.97312	0.99841
1.300	0.88186	1.03484
1.560	1.05780	1.00519
1.820	1.32139	0.97214
2.080	1.35089	0.98513
2.340	0.91956	0.99954
2.600	0.82388	1.03484
2.860	0.82464	1.04303
3.120	0.82436	1.03202

CONFIGURATION 29 THETA = 30.00

RADIUS	TT/TT MIX	PT/PT MIX
0.260	1.26987	
0.520	1.21389	0.96088
0.780	1.11089	0.97443
1.040	1.01252	1.00493
1.300	0.91013	1.03401
1.560	0.99433	1.01255
1.820	1.47993	0.97585
2.080	1.43448	0.96342
2.340	1.12946	0.97387
2.600	0.82513	1.01533
2.860	0.82493	1.04023
3.120	0.82479	1.03034

CONFIGURATION 29 THETA = 32.50

RADIUS	TT/TT MIX	PT/PT MIX
0.260	1.23484	
0.520	1.18068	0.95736
0.780	1.09382	0.97204
1.040	0.99466	1.00932
1.300	0.90585	1.02937
1.560	0.96612	1.01553
1.820	1.37424	0.97967
2.080	1.31341	0.95492
2.340	1.28231	0.96018
2.600	0.82723	1.00452
2.860	0.82366	1.04038
3.120	0.82332	1.03191

CONFIGURATION 29 THETA = 35.00

RADIUS	TT/TT MIX	PT/PT MIX
0.260	1.20410	
0.520	1.13279	0.95471
0.780	1.03197	0.97391
1.040	0.92898	1.00695
1.300	0.87487	1.02078
1.560	1.11390	1.01259
1.820	1.25387	0.98068
2.080	1.26094	0.95527
2.340	1.34409	0.96007
2.600	0.82807	1.00977
2.860	0.82336	1.03801
3.120	0.82282	1.02925

CONFIGURATION 29 THETA = 37.50

RADIUS	TT/TT MIX	PT/PT MIX
0.260	1.19975	
0.520	1.08641	0.95212
0.780	0.96074	0.97557
1.040	0.87198	1.00183
1.300	0.85076	1.01822
1.560	1.27991	1.01235
1.820	1.33166	0.98234
2.080	1.29518	0.95354
2.340	1.20245	0.94851
2.600	0.82459	1.01906
2.860	0.82329	1.05629
3.120	0.82295	1.02584

CONFIGURATION 29 THETA = 40.00

RADIUS	TT/TT MIX	PT/PT MIX
0.260	1.20781	
0.520	1.03032	0.95162
0.780	0.91640	0.97646
1.040	0.84606	0.99348
1.300	0.84415	1.01852
1.560	1.28610	1.01231
1.820	1.39489	0.97928
2.080	1.30936	0.96686
2.340	0.98565	0.98747
2.600	0.82293	1.02614
2.860	0.82267	1.03292
3.120	0.82253	1.02050

CONFIGURATION 29 THETA = 42.50

RADIUS	TT/TT MIX	PT/PT MIX
0.260	1.22913	
0.520	0.95547	0.95203
0.780	0.89656	0.97688
1.040	0.84252	1.00173
1.300	0.84115	1.02235
1.560	1.25167	1.00992
1.820	1.23689	0.97688
2.080	1.08108	0.98507
2.340	0.84286	1.01134
2.600	0.82177	1.02856
2.860	0.82280	1.02376
3.120	0.82246	1.01134

CONFIGURATION 29 THETA = 45.00

RADIUS	TT/TT MIX	PT/PT MIX
0.260	1.25228	
0.520	1.05216	0.95232
0.780	0.90937	0.97059
1.040	0.86106	1.00602
1.300	0.85570	1.02868
1.560	1.24709	1.00486
1.820	1.18122	0.97718
2.080	0.95937	0.99017
2.340	0.82706	1.02605
2.600	0.82165	1.02831
2.860	0.82253	1.02103
3.120	0.82241	1.00825

CONFIGURATION 29 THETA = 47.50

RADIUS	TT/TT MIX	PT/PT MIX
0.260	1.29037	
0.520	1.08410	0.95223
0.780	0.94635	0.98245
1.040	0.91140	1.03872
1.300	0.89331	1.03217
1.560	1.21966	1.00194
1.820	1.29475	0.97426
2.080	1.30031	0.98523
2.340	0.92732	1.01833
2.600	0.82265	1.03217
2.860	0.82205	1.02630
3.120	0.82251	1.01296

CONFIGURATION 29 THETA = 50.00

RADIUS	TT/TT MIX	PT/PT MIX
0.260	1.32820	
0.520	1.12225	0.95217
0.780	1.01045	0.98465
1.040	0.97854	1.01826
1.300	0.93089	1.03493
1.560	1.11305	1.00188
1.820	1.44062	0.97137
2.080	1.47028	0.96799
2.340	1.24422	0.99906
2.600	0.82402	1.03493
2.860	0.82264	1.03210
3.120	0.82204	1.01628

CONFIGURATION 29 THETA = 52.50

RADIUS	TT/TT MIX	PT/PT MIX
0.260	1.35419	
0.520	1.11032	0.95486
0.780	1.07246	0.98790
1.040	1.02002	1.02660
1.300	0.93393	1.03196
1.560	1.01459	1.00372
1.820	1.35149	0.97548
2.080	1.39546	0.96023
2.340	1.46077	0.98452
2.600	0.82710	1.03479
2.860	0.82265	1.03761
3.120	0.82230	1.02095

CONFIGURATION 29 THETA = 55.00

RADIUS	TT/TT MIX	PT/PT MIX
0.260	1.37346	
0.520	1.10479	0.95520
0.780	1.11014	0.99303
1.040	1.01771	1.02635
1.300	0.89665	1.02353
1.560	1.04471	1.00630
1.820	1.31331	0.97524
2.080	1.40217	0.94399
2.340	1.36555	0.97101
2.600	0.82704	1.03256
2.860	0.82315	1.04075
3.120	0.82239	1.02635

CONFIGURATION 29 THETA = 57.50

RADIUS	TT/TT MIX	PT/PT MIX
0.260	1.37240	
0.520	1.00822	0.95711
0.780	1.10359	0.99862
1.040	0.97078	1.01866
1.300	0.86278	1.01527
1.560	1.10962	1.00680
1.820	1.43043	0.96812
2.080	1.45647	0.94328
2.340	1.18698	0.96553
2.600	0.82480	1.03447
2.860	0.82303	1.04153
3.120	0.82199	1.02911

CONFIGURATION 29 THETA = 60.00

RADIUS	TT/TT MIX	PT/PT MIX
0.260	1.35774	
0.520	1.01981	0.95781
0.780	1.05657	1.00128
1.040	0.90683	1.00664
1.300	0.84130	1.01031
1.560	1.12924	1.01229
1.820	1.41737	0.97079
2.080	1.36218	0.95442
2.340	0.93850	0.97644
2.600	0.82403	1.03770
2.860	0.82361	1.04249
3.120	0.82279	1.02951

CONFIGURATION 34 THETA = 10.00

RADIUS	TT/TT MIX	PT/PT MIX
0.260	1.64590	
0.520	1.33430	0.94010
0.780	1.01440	0.97350
1.040	0.89750	0.98450
1.300	0.84080	0.99410
1.560	0.82830	1.01230
1.820	0.82330	1.04000
2.080	0.83690	1.04480
2.340	0.84530	1.03720
2.600	0.91350	1.02610
2.860	0.87110	1.00800
3.120	0.84320	1.00320

CONFIGURATION 34 THETA = 12.50

RADIUS	TT/TT MIX	PT/PT MIX
0.260	1.67480	
0.520	1.35630	0.94450
0.780	1.05490	0.97080
1.040	0.94940	0.98190
1.300	0.87430	1.00340
1.560	0.85790	1.02630
1.820	0.83710	1.04020
2.080	0.86470	1.04560
2.340	0.88570	1.04020
2.600	1.06430	1.01250
2.860	1.11160	0.98810
3.120	0.92970	0.99010

CONFIGURATION 34 THETA = 15.00

RADIUS	TT/TT MIX	PT/PT MIX
0.260	1.70110	
0.520	1.37960	0.94580
0.780	1.13320	0.96500
1.040	1.04100	0.98740
1.300	0.96810	1.01480
1.560	0.93060	1.03010
1.820	0.87660	1.03430
2.080	0.88920	1.04000
2.340	0.90690	1.03430
2.600	1.11040	1.00380
2.860	1.39660	0.96500
3.120	1.09960	0.96580

CONFIGURATION 34 THETA = 17.50

RADIUS	TT/TT MIX	PT/PT MIX
0.260	1.71740	
0.520	1.40530	0.94270
0.780	1.19890	0.96140
1.040	1.11860	0.98570
1.300	1.04780	1.01460
1.560	0.97700	1.02310
1.820	0.89740	1.02310
2.080	0.88070	1.02980
2.340	0.91180	1.02310
2.600	1.05810	0.99820
2.860	1.38520	0.97040
3.120	1.16570	0.95030

CONFIGURATION 34 THETA = 20.00

RADIUS	TT/TT MIX	PT/PT MIX
0.260	1.72920	
0.520	1.43630	0.93340
0.780	1.22930	0.96180
1.040	1.13590	0.98530
1.300	1.07030	0.99730
1.560	0.97090	1.00460
1.820	0.89890	1.01420
2.080	0.87240	1.02120
2.340	0.91120	1.02270
2.600	1.08560	1.00880
2.860	1.23690	0.93610
3.120	1.14750	0.96180

CONFIGURATION 34 THETA = 22.50

RADIUS	TT/TT MIX	PT/PT MIX
0.260	1.74420	
0.520	1.43180	0.94260
0.780	1.23830	0.96130
1.040	1.09310	0.99010
1.300	1.01240	1.00660
1.560	0.90510	1.01250
1.820	0.86960	1.01730
2.080	0.85160	1.02410
2.340	0.89630	1.02210
2.600	1.16600	1.00540
2.860	1.25960	0.97650
3.120	1.05160	0.97400

CONFIGURATION 34 THETA = 25.00

RADIUS	TT/TT MIX	PT/PT MIX
0.260	1.75900	
0.520	1.23580	0.93470
0.780	1.19660	0.96500
1.040	0.98190	0.98740
1.300	0.91450	0.99840
1.560	0.84640	1.00520
1.820	0.83420	1.01770
2.080	0.82650	1.02470
2.340	0.86960	1.03150
2.600	1.06170	1.00950
2.860	1.05410	0.97630
3.120	0.87780	0.98510

CONFIGURATION 34 THETA = 27.50

RADIUS	TT/TT MIX	PT/PT MIX
0.260	1.76580	
0.520	1.07850	0.93460
0.780	1.13780	0.97260
1.040	0.90340	0.98980
1.300	0.85300	1.00110
1.560	0.82390	1.00740
1.820	0.82270	1.02600
2.080	0.81920	1.03340
2.340	0.83850	1.03760
2.600	0.92540	1.00650
2.860	0.87260	0.99690
3.120	0.83820	1.00930

CONFIGURATION 34 THETA = 30.00

RADIUS	TT/TT MIX	PT/PT MIX
0.260	1.76500	
0.520	0.96460	0.93890
0.780	1.10030	0.97730
1.040	0.87580	0.99260
1.300	0.83030	1.00510
1.560	0.82230	1.01690
1.820	0.84360	1.03480
2.080	0.82510	1.04100
2.340	0.83290	1.03990
2.600	0.95720	1.00650
2.860	1.02890	0.99830
3.120	0.90960	1.00360

CONFIGURATION 34 THETA = 32.50

RADIUS	TT/TT MIX	PT/PT MIX
0.260	1.76270	
0.520	0.96590	0.94390
0.780	1.12830	0.97840
1.040	0.91340	0.99630
1.300	0.83510	1.01580
1.560	0.83900	1.01580
1.820	0.89410	1.03500
2.080	0.84770	1.03250
2.340	0.84020	1.03450
2.600	1.10420	0.99290
2.860	1.35830	0.97700
3.120	1.14920	0.98470

CONFIGURATION 34 THETA = 35.00

RADIUS	TT/TT MIX	PT/PT MIX
0.260	1.75540	
0.520	1.00380	0.94780
0.780	1.17400	0.97330
1.040	0.98910	1.00320
1.300	0.86610	1.01990
1.560	0.87080	1.03350
1.820	0.91350	1.02810
2.080	0.86710	1.02250
2.340	0.84980	1.02670
2.600	1.13570	0.98990
2.860	1.39090	0.93960
3.120	1.25790	0.97890

CONFIGURATION 34 THETA = 37.50

RADIUS	TT/TT MIX	PT/PT MIX
0.260	1.74620	
0.520	1.14390	0.94720
0.780	1.20700	0.97410
1.040	1.08520	1.00470
1.300	0.94490	1.01430
1.560	0.92430	1.02960
1.820	0.89530	1.01290
2.080	0.89010	1.01570
2.340	0.87720	1.01770
2.600	1.04560	0.99650
2.860	1.23130	0.95630
3.120	1.28840	0.97270

CONFIGURATION 34 THETA = 40.00

RADIUS	TT/TT MIX	PT/PT MIX
0.260	1.72870	
0.520	1.00470	0.94680
0.780	1.22960	0.97400
1.040	1.14090	1.00180
1.300	1.03240	1.00910
1.560	0.98450	1.02100
1.820	0.95800	1.00430
2.080	0.91970	1.00180
2.340	0.91890	1.00430
2.600	1.02700	0.98990
2.860	1.34700	0.96010
3.120	1.25940	0.97400

CONFIGURATION 34 THETA = 42.50

RADIUS	TT/TT MIX	PT/PT MIX
0.260	1.69310	
0.520	1.14790	0.94680
0.780	1.21630	0.97450
1.040	1.14750	0.99550
1.300	1.08350	1.00600
1.560	0.99180	1.01900
1.820	0.82800	1.00910
2.080	0.89400	1.02440
2.340	0.94360	0.99890
2.600	1.02710	0.99320
2.860	1.17190	0.96010
3.120	1.07890	0.97940

CONFIGURATION 34 THETA = 45.00

RADIUS	TT/TT MIX	PT/PT MIX
0.260	1.65900	
0.520	1.23720	0.94310
0.780	1.16200	0.97290
1.040	1.06260	0.99350
1.300	1.03170	1.00600
1.560	0.93080	1.01450
1.820	0.81900	1.01790
2.080	0.84190	1.03320
2.340	0.89470	1.00460
2.600	0.93520	0.99920
2.860	0.92400	0.97970
3.120	0.86040	0.98590

CONFIGURATION 34 THETA = 47.50

RADIUS	TT/TT MIX	PT/PT MIX
0.260	1.63710	
0.520	1.10050	0.94170
0.780	1.09330	0.97570
1.040	0.96960	0.99630
1.300	0.93350	1.00880
1.560	0.85440	1.01360
1.820	0.81820	1.02270
2.080	0.82040	1.04080
2.340	0.83650	1.02180
2.600	0.84760	1.00260
2.860	0.83080	0.99970
3.120	0.83500	0.99970

CONFIGURATION 34 THETA = 50.00

RADIUS	TT/TT MIX	PT/PT MIX
0.260	1.63700	
0.520	1.00550	0.94190
0.780	1.07060	0.97840
1.040	0.92200	0.99660
1.300	0.86290	1.01870
1.560	0.82690	1.02010
1.820	0.82100	1.02830
2.080	0.81790	1.04500
2.340	0.81940	1.03880
2.600	0.84090	1.01950
2.860	0.86190	1.00710
3.120	0.89090	1.00080

D.5 SURFACE PRESSURE DATA

CONFIGURATION 29 AVERAGE VALUES

ROW 1 STATION 8

TAP	AXIAL STATION	MACH	PS/PT
101	11.900	0.2871	0.9459
102	12.195	0.2739	0.9506
103	12.490	0.2770	0.9495
104	12.785	0.3476	0.9221
105	13.080	0.3268	0.9306
106	13.375	0.3424	0.9241
107	13.670	0.3607	0.9163
108	13.965	0.3650	0.9143
109	14.260	0.3772	0.9089
110	14.555	0.4093	0.8938
111	14.850	0.4325	0.8824
112	15.000	0.4559	0.8704

ROW 2 STATION 8

TAP	AXIAL STATION	MACH	PS/PT
113	11.900	0.2882	0.9455
114	12.195	0.2751	0.9502
115	12.490	0.2775	0.9493
116	12.785	0.3002	0.9410
117	13.080	0.3261	0.9309
118	13.375	0.3490	0.9213
119	13.670	0.3584	0.9173
120	13.965	0.3646	0.9145
121	14.260	0.3917	0.9022
122	14.555	0.4189	0.8892
123	14.850	0.4315	0.8829
124	15.000	0.4410	0.8781

ROW 3 STATION 8

TAP	AXIAL STATION	MACH	PS/PT
125	11.900	0.2901	0.9448
126	12.195	0.2727	0.9510
127	12.490	0.2775	0.9493
128	12.785	0.2996	0.9413
129	13.080	0.3523	0.9157
130	13.375	0.5137	0.8396
131	13.670	0.3568	0.9180
132	13.965	0.3640	0.9148
133	14.260	0.3802	0.9075
134	14.555	0.4113	0.8928
135	14.850	0.4307	0.8833
136	15.000	0.4426	0.8773

ROW 4 STATION 8

TAP	AXIAL STATION	MACH	PS/PT
301	12.195	0.3564	0.9181
302	12.490	0.3791	0.9089
303	12.785	0.4040	0.8964
304	13.080	0.3595	0.9168
305	13.375	0.3667	0.9136
306	13.670	0.3684	0.9129
307	13.965	0.3590	0.9170
308	14.260	0.3638	0.9149
309	14.555	0.3695	0.9123
310	14.822	0.3957	0.9003

ROW 5 STATION 8

TAP	AXIAL STATION	MACH	PS/PT
311	14.260	0.3848	0.9054
312	14.555	0.3869	0.9044
313	14.822	0.4336	0.8818

ROW 6 STATION 8

TAP	AXIAL STATION	MACH	PS/PT
314	14.260	0.3962	0.9001
315	14.555	0.4055	0.8957
316	14.822	0.4560	0.8704

ROW 7 STATION 8

TAP	AXIAL STATION	MACH	PS/PT
317	12.195	0.3530	0.9196
318	12.490	0.3785	0.9083
319	12.785	0.4015	0.8976
320	13.080	0.3465	0.9224
321	13.375	0.3783	0.9084
322	13.670	0.3953	0.9005
323	13.965	0.3958	0.9003
324	14.260	0.4151	0.8910
325	14.555	0.4305	0.8834
326	14.822	0.4584	0.8691

ROW 8 STATION 8

TAP	AXIAL STATION	MACH	PS/PT
327	13.375	0.3660	0.9139
328	13.670	0.3817	0.9063
329	13.965	0.4091	0.8939
330	14.260	0.4209	0.8882
331	14.555	0.4350	0.8817
332	14.822	0.4728	0.8616

ROW 9 STATION 8

TAP	AXIAL STATION	MACH	PS/PT
333	12.195	0.3551	0.9187
334	12.490	0.3845	0.9055
335	12.785	0.4067	0.8941
336	13.080	0.3123	0.9364
337	13.375	0.2960	0.9418
338	13.670	0.3175	0.9343
339	13.965	0.3402	0.9251
340	14.260	0.3696	0.9123
341	14.555	0.4299	0.8837
342	14.822	0.4395	0.8789

ROW 10 STATION 7

TAP	AXIAL STATION	MACH	PS/PT
351	12.195	0.4165	0.8874
352	12.490	0.4213	0.8850
353	12.785	0.4088	0.8913
354	13.080	0.3677	0.9108
355	13.375	0.3619	0.9134
356	13.670	0.4088	0.8912
357	13.965	0.4625	0.8635
358	14.260	0.4999	0.8430
359	14.555	0.5182	0.8326
360	14.822	0.5703	0.8019

ROW 11 STATION 7

TAP	AXIAL STATION	MACH	PS/PT
361	13.375	0.4471	0.8717
362	13.670	0.5216	0.8307
363	13.965	0.5681	0.8033
364	14.260	0.5947	0.7872
365	14.555	0.6352	0.7621
366	14.822	0.5675	0.8037

ROW 12 STATION 7

TAP	AXIAL STATION	MACH	PS/PT
367	12.195	0.4169	0.8872
368	12.490	0.4192	0.8860
369	12.785	0.4127	0.8893
370	13.080	0.3921	0.8994
371	13.375	0.4462	0.8722
372	13.670	0.5666	0.8042
373	13.965	0.5926	0.7884
374	14.260	0.6166	0.7737
375	14.555	0.6367	0.7611
376	14.822	0.5802	0.7960

ROW 13 STATION 7

TAP	AXIAL STATION	MACH	PS/PT
377	14.260	0.5911	0.7893
378	14.555	0.6287	0.7661
379	14.822	0.6029	0.7821

ROW 14 STATION 7

TAP	AXIAL STATION	MACH	PS/PT
380	14.260	0.6063	0.7800
381	14.555	0.6255	0.7681
382	14.822	0.6062	0.7801

ROW 15 STATION 7

TAP	AXIAL STATION	MACH	PS/PT
383	12.195	0.4166	0.8874
384	12.490	0.4211	0.8851
385	12.785	0.4203	0.8855
386	13.080	0.4171	0.8871
387	13.375	0.4434	0.8736
388	13.670	0.5296	0.8261
389	13.965	0.5891	0.7936
390	14.260	0.6345	0.7685
391	14.555	0.6321	0.7640
392	14.822	0.6225	0.7739

ROW 16 STATION 7

TAP	AXIAL STATION	MACH	PS/PT
401	11.900	0.3985	0.8963
402	12.195	0.4051	0.8931
403	12.490	0.4107	0.8903
404	12.785	0.4078	0.8918
405	13.080	0.4173	0.8870
406	13.375	0.4269	0.8822
407	13.670	0.4349	0.8781
408	13.965	0.4426	0.8741
409	14.260	0.4525	0.8689
410	14.555	0.4675	0.8609
411	14.850	0.4812	0.8534
412	15.000	0.4643	0.8617

ROW 17 STATION 7

TAP	AXIAL STATION	MACH	PS/PT
413	11.900	0.3939	0.8985
414	12.195	0.3944	0.8983
415	12.490	0.3983	0.8964
416	12.785	0.4093	0.8910
417	13.080	0.4166	0.8874
418	13.375	0.4268	0.8822
419	13.670	0.4343	0.8784
420	13.965	0.4420	0.8744
421	14.260	0.4557	0.8672
422	14.555	0.4644	0.8625
423	14.850	0.4786	0.8548
424	15.000	0.4650	0.8513

ROW 18 STATION 7

TAP	AXIAL STATION	MACH	PS/PT
425	11.900	0.3952	0.8979
426	12.195	0.3917	0.8996
427	12.490	0.3986	0.8963
428	12.785	0.4061	0.8926
429	13.080	0.4191	0.8861
430	13.375	0.4250	0.8832
431	13.670	0.4316	0.8798
432	13.965	0.4376	0.8767
433	14.260	0.4494	0.8705
434	14.555	0.4605	0.8646
435	14.850	0.4743	0.8572
436	15.000	0.4802	0.8539

CONFIGURATION 34 AVERAGE VALUES

ROW 1 STATION 8

TAP	AXIAL STATION	MACH	PS/PT
101	11.900	0.3295	0.9295
102	12.195	0.3025	0.9402
103	12.490	0.3168	0.9346
104	12.785	0.3788	0.9082
105	13.080	0.4032	0.8968
106	13.375	0.4070	0.8950
107	13.670	0.4094	0.8943
108	13.965	0.4278	0.8848
109	14.260	0.4601	0.8683
110	14.555	0.5093	0.8417
111	14.850	0.5032	0.8451
112	15.000	0.4989	0.8474

ROW 2 STATION 8

TAP	AXIAL STATION	MACH	PS/PT
113	11.900	0.3260	0.9309
114	12.195	0.3196	0.9335
115	12.490	0.3165	0.9347
116	12.785	0.3617	0.9159
117	13.080	0.4003	0.8982
118	13.375	0.4134	0.8919
119	13.670	0.4086	0.8942
120	13.965	0.4277	0.8848
121	14.260	0.4636	0.8665
122	14.555	0.5068	0.8451
123	14.850	0.4994	0.8472
124	15.000	0.4963	0.8489

ROW 3 STATION 8

TAP	AXIAL STATION	MACH	PS/PT
125	11.900	0.3259	0.9310
126	12.195	0.3004	0.9410
127	12.490	0.3192	0.9337
128	12.785	0.3586	0.9172
129	13.080	0.3984	0.8991
130	13.375	0.4097	0.8945
131	13.670	0.4070	0.8950
132	13.965	0.4269	0.8852
133	14.260	0.4580	0.8694
134	14.555	0.5064	0.8433
135	14.850	0.4984	0.8477
136	15.000	0.4995	0.8471

ROW 4 STATION 8

TAP	AXIAL STATION	MACH	PS/PT
301	12.195	0.3808	0.9073
302	12.490	0.3936	0.9013
303	12.785	0.3902	0.9029
304	13.080	0.4226	0.8874
305	13.375	0.5147	0.8387
306	13.670	0.5771	0.8226
307	13.965	0.4994	0.8472
308	14.260	0.4488	0.8742
309	14.555	0.4290	0.8842
310	14.822	0.4656	0.8654

ROW 5 STATION 8

TAP	AXIAL STATION	MACH	PS/PT
311	13.670	0.5870	0.7967
312	13.965	0.5546	0.8159
313	14.260	0.4957	0.8492
314	14.555	0.4663	0.8650
315	14.822	0.5093	0.8417

ROW 6 STATION 8

TAP	AXIAL STATION	MACH	PS/PT
316	13.965	0.5655	0.8095
317	14.260	0.5651	0.8097
318	14.555	0.5463	0.8207
319	14.822	0.5261	0.8323

ROW 7 STATION 8

TAP	AXIAL STATION	MACH	PS/PT
320	12.195	0.3832	0.9062
321	12.490	0.3931	0.9016
322	12.785	0.3826	0.9064
323	13.080	0.4037	0.8962
324	13.375	0.4839	0.8529
325	13.670	0.5905	0.7946
326	13.965	0.6006	0.7895
327	14.260	0.6283	0.7716
328	14.555	0.6425	0.7629
329	14.822	0.5854	0.7976

ROW 8 STATION 8

TAP	AXIAL STATION	MACH	PS/PT
330	13.375	0.4242	0.8866
331	13.670	0.4870	0.8539
332	13.965	0.5212	0.8350
333	14.260	0.5528	0.8169
334	14.555	0.6038	0.7866
335	14.822	0.5778	0.8012

ROW 9 STATION 8

TAP	AXIAL STATION	MACH	PS/PT
336	12.195	0.3814	0.9070
337	12.490	0.3937	0.9013
338	12.785	0.3578	0.9175
339	13.080	0.3411	0.9247
340	13.375	0.3490	0.9214
341	13.670	0.3666	0.9137
342	13.965	0.3939	0.8988
343	14.260	0.4484	0.8743
344	14.555	0.4958	0.8492
345	14.822	0.5126	0.8399

ROW 10 STATION 7

TAP	AXIAL STATION	MACH	PS/PT
351	12.195	0.4621	0.8638
352	12.490	0.4417	0.8746
353	12.785	0.4223	0.8846
354	13.080	0.4031	0.8955
355	13.375	0.3517	0.9180
356	13.670	0.3228	0.9304
357	13.965	0.3580	0.9152
358	14.260	0.4675	0.8609
359	14.555	0.6067	0.7799
360	14.822	0.6168	0.7736

ROW 11 STATION 7

TAP	AXIAL STATION	MACH	PS/PT
361	13.375	0.5053	0.8400
362	13.670	0.6932	0.7253
363	13.965	0.7301	0.7015
364	14.260	0.7176	0.7095
365	14.555	0.6661	0.7426
366	14.822	0.6502	0.7527

ROW 12 STATION 7

TAP	AXIAL STATION	MACH	PS/PT
367	12.195	0.4633	0.8632
368	12.490	0.4427	0.8741
369	12.785	0.4267	0.8823
370	13.080	0.4409	0.8750
371	13.375	0.6023	0.7826
372	13.670	0.7564	0.6844
373	13.965	0.7788	0.6698
374	14.260	0.7277	0.7030
375	14.555	0.6028	0.7319
376	14.822	0.6323	0.7639

ROW 13 STATION 7

TAP	AXIAL STATION	MACH	PS/PT
377	13.965	0.6186	0.7785
378	14.260	0.6290	0.7660
379	14.555	0.6574	0.7481
380	14.822	0.6591	0.7471

ROW 14 STATION 7

TAP	AXIAL STATION	MACH	PS/PT
381	13.670	0.7219	0.7063
382	13.965	0.6239	0.7692
383	14.260	0.6343	0.7627
384	14.555	0.6725	0.7385
385	14.822	0.6977	0.7224

ROW 15 STATION 7

TAP	AXIAL STATION	MACH	PS/PT
386	12.195	0.4589	0.8655
387	12.490	0.4442	0.8733
388	12.785	0.4449	0.8729
389	13.080	0.4703	0.8594
390	13.375	0.5439	0.8177
391	13.670	0.5745	0.7995
392	13.965	0.6319	0.7642
393	14.260	0.6006	0.7837
394	14.555	0.6581	0.7477
395	14.822	0.6577	0.7479

ROW 16 STATION 7

TAP	AXIAL STATION	MACH	PS/PT
401	11.900	0.3962	0.8975
402	12.195	0.3889	0.9009
403	12.490	0.3982	0.8965
404	12.785	0.4071	0.8921
405	13.080	0.4207	0.8853
406	13.375	0.4294	0.8810
407	13.670	0.4511	0.8697
408	13.965	0.4858	0.8509
409	14.260	0.4934	0.8467
410	14.555	0.5199	0.8317
411	14.850	0.5534	0.8121
412	15.000	0.5583	0.8092

ROW 17 STATION 7

TAP	AXIAL STATION	MACH	PS/PT
413	11.900	0.3923	0.8993
414	12.195	0.3874	0.9017
415	12.490	0.3958	0.8977
416	12.785	0.4091	0.8911
417	13.080	0.4145	0.8884
418	13.375	0.4279	0.8817
419	13.670	0.4494	0.8712
420	13.965	0.4632	0.8642
421	14.260	0.4902	0.8495
422	14.555	0.5200	0.8316
423	14.850	0.5492	0.8146
424	15.000	0.5663	0.8044

ROW 18 STATION 7

TAP	AXIAL STATION	MACH	PS/PT
425	11.900	0.3922	0.8993
426	12.195	0.3863	0.9022
427	12.490	0.3931	0.8985
428	12.785	0.3997	0.8950
429	13.080	0.4141	0.8887
430	13.375	0.4377	0.8767
431	13.670	0.4439	0.8735
432	13.965	0.4637	0.8630
433	14.260	0.4930	0.8486
434	14.555	0.5230	0.8299
435	14.850	0.5457	0.8161
436	15.000	0.5575	0.8097

D.6 FLOW ANGLE CORRELATION; SECOND-ORDER FIT

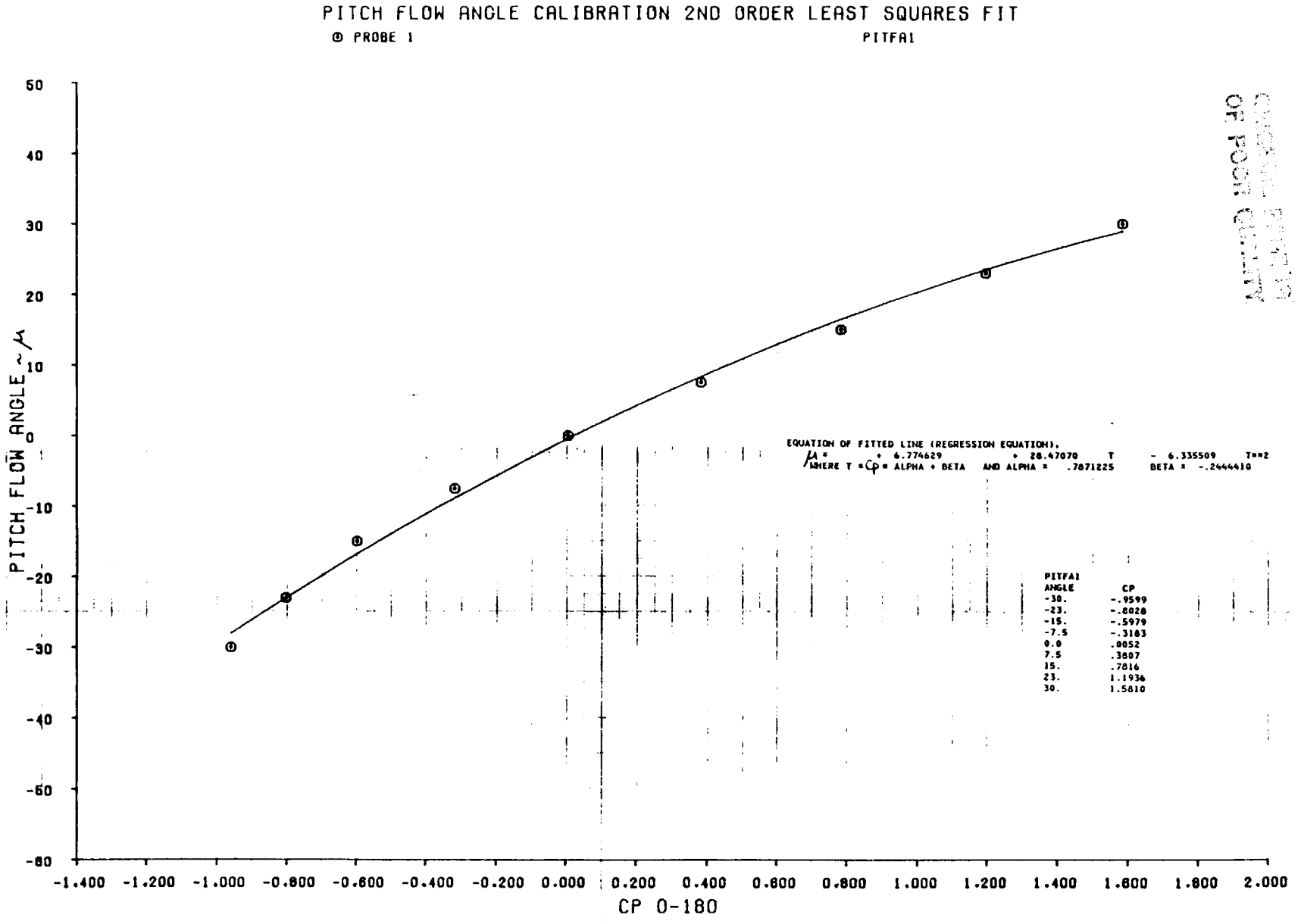

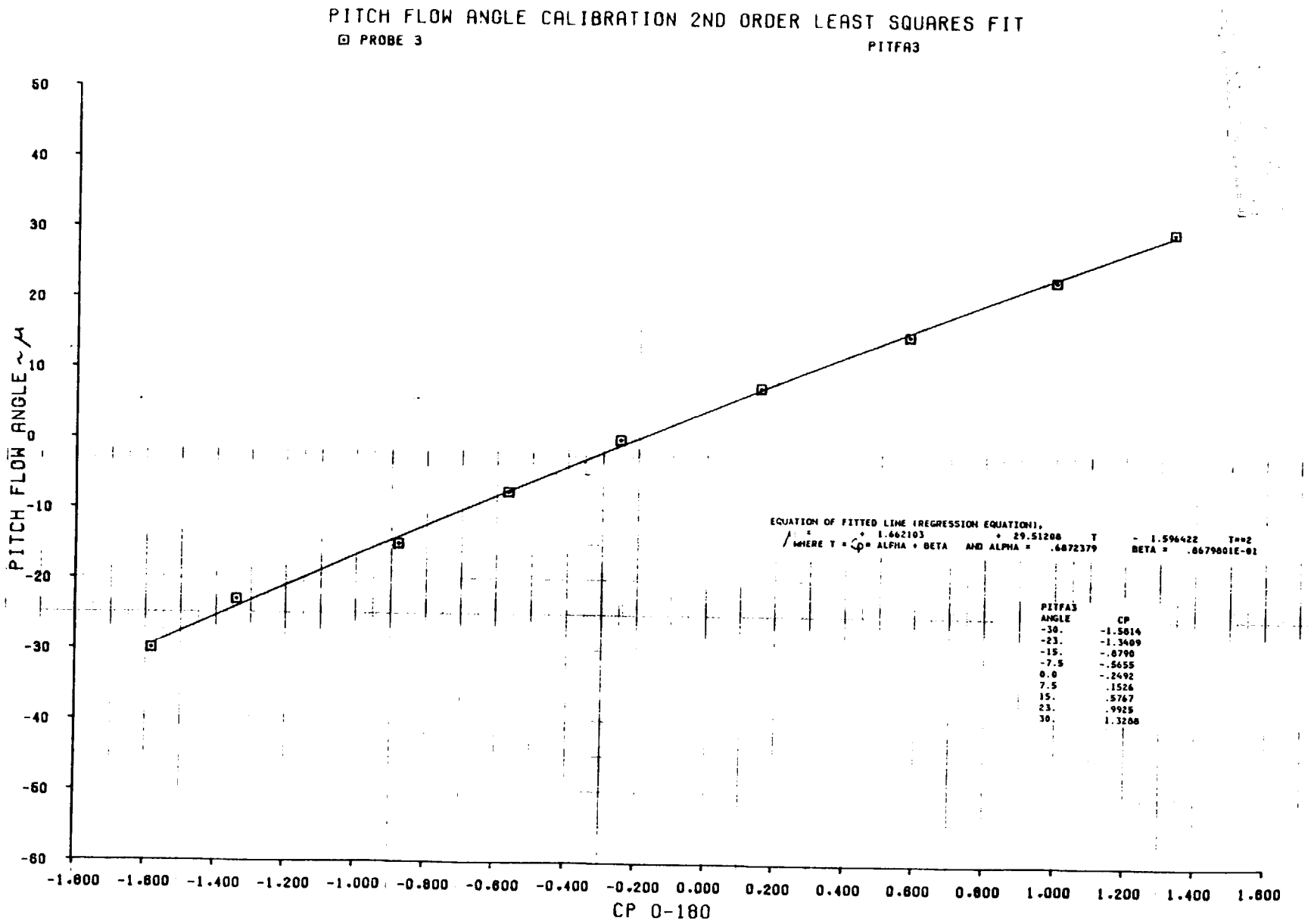
PITCH FLOW ANGLE CALIBRATION 2ND ORDER LEAST SQUARES FIT
PROBE 3
PITFA3
PITCH FLOW ANGLE ~μ
CP 0-180
EQUATION OF FITTED LINE (REGRESSION EQUATION).
WHERE T = φ= ALFHA + BETA AND ALPHA = .6872379
BETA = .8679801E-01
PITFA3
ANGLE CP
-30. -1.5814
-23. -1.3409
-15. -.8790
-7.5 -.5655
0.0 -.2492
7.5 .1526
15. .5767
23. .9925
30. 1.3268

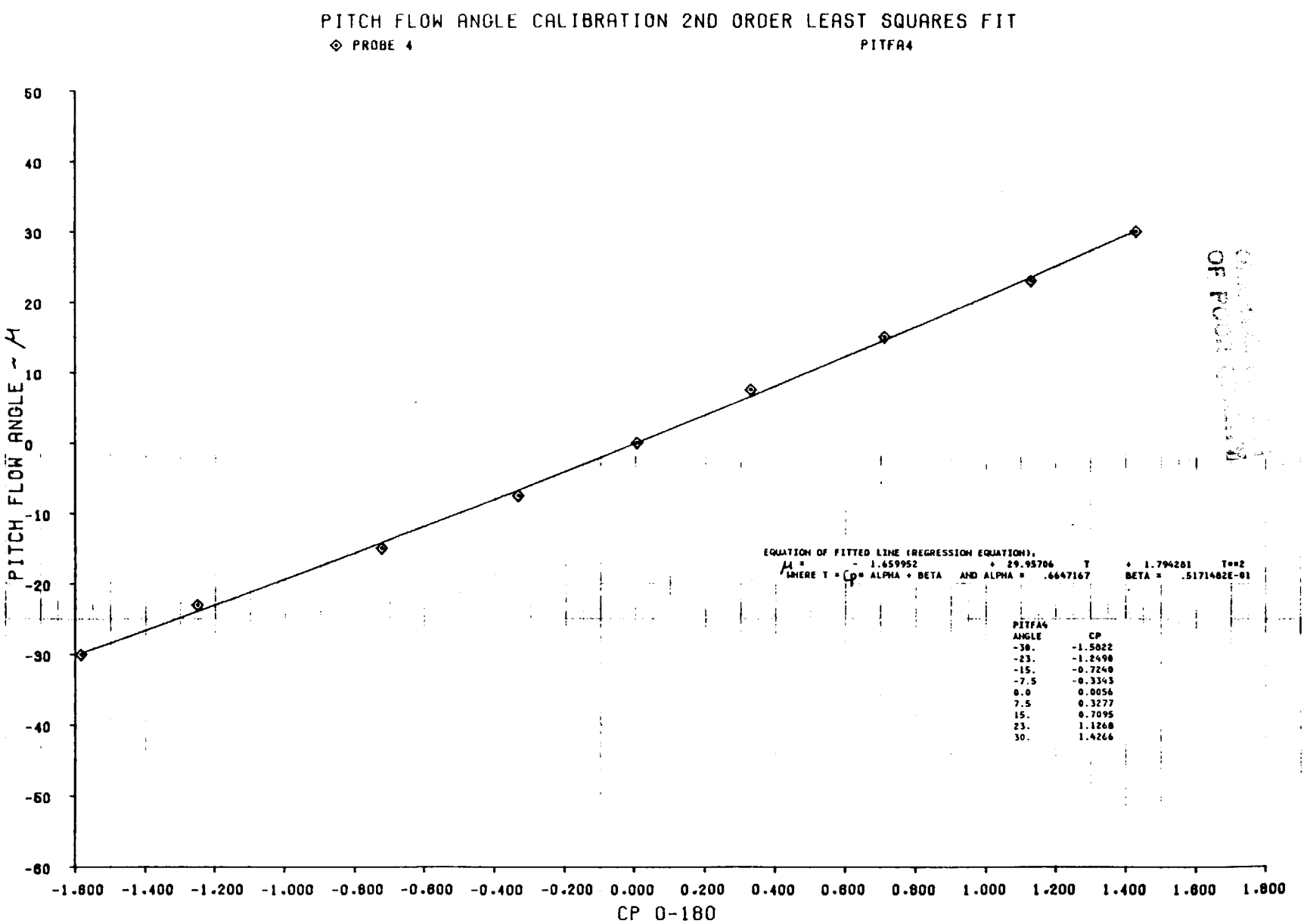
PITCH FLOW ANGLE CALIBRATION 2ND ORDER LEAST SQUARES FIT
PROBE 4
PITFA4
PITCH FLOW ANGLE ~ μ
CP 0-180
EQUATION OF FITTED LINE (REGRESSION EQUATION):
μ = - 1.659952 + 29.95706 T + 1.794281 T**2
WHERE T = Cp= ALPHA + BETA AND ALPHA = .6647167 BETA = .5171482E-01
PITFA4 ANGLE CP
-30. -1.5822
-23. -1.2490
-15. -0.7240
-7.5 -0.3343
0.0 0.0056
7.5 0.3277
15. 0.7095
23. 1.1268
30. 1.4266

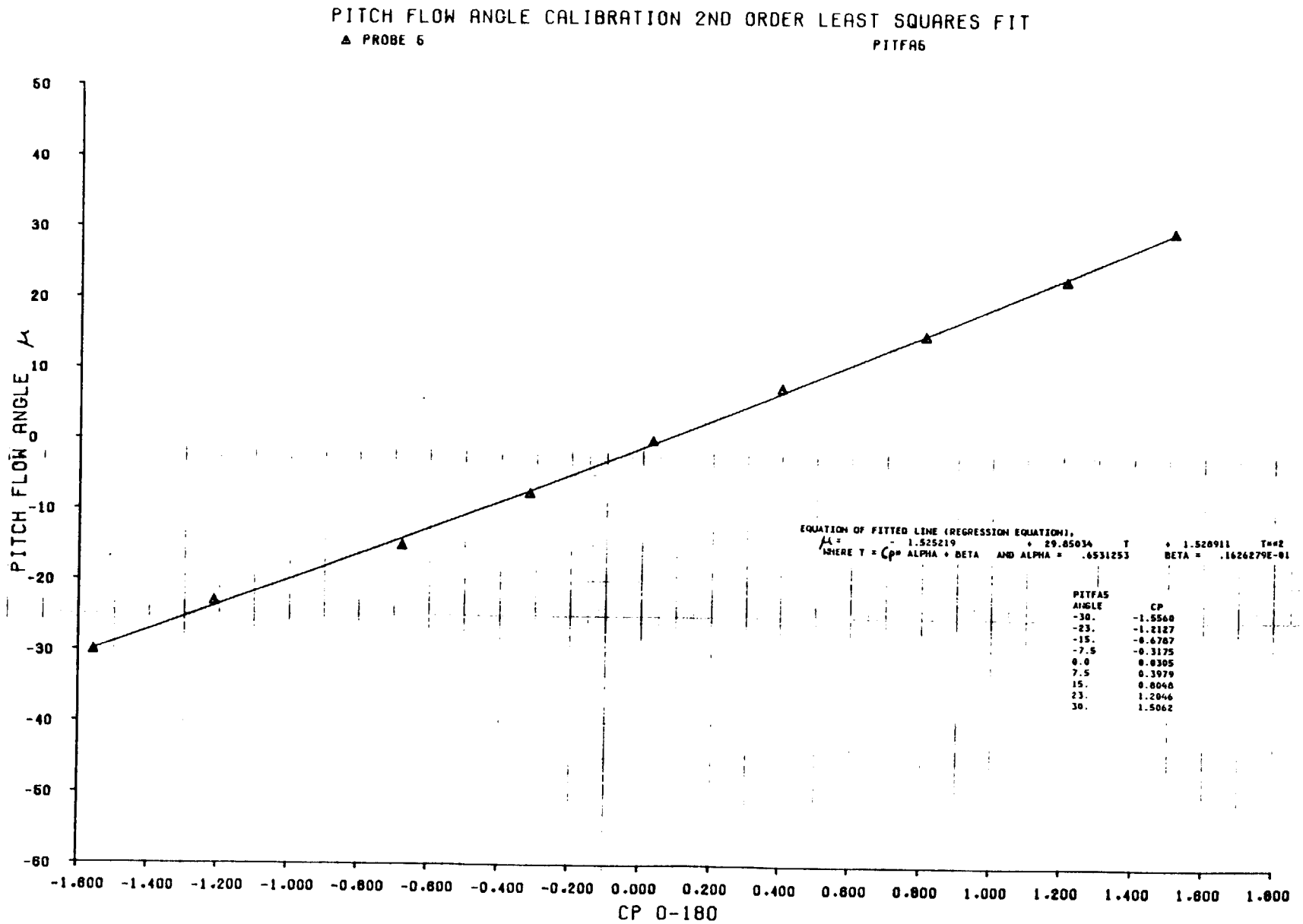

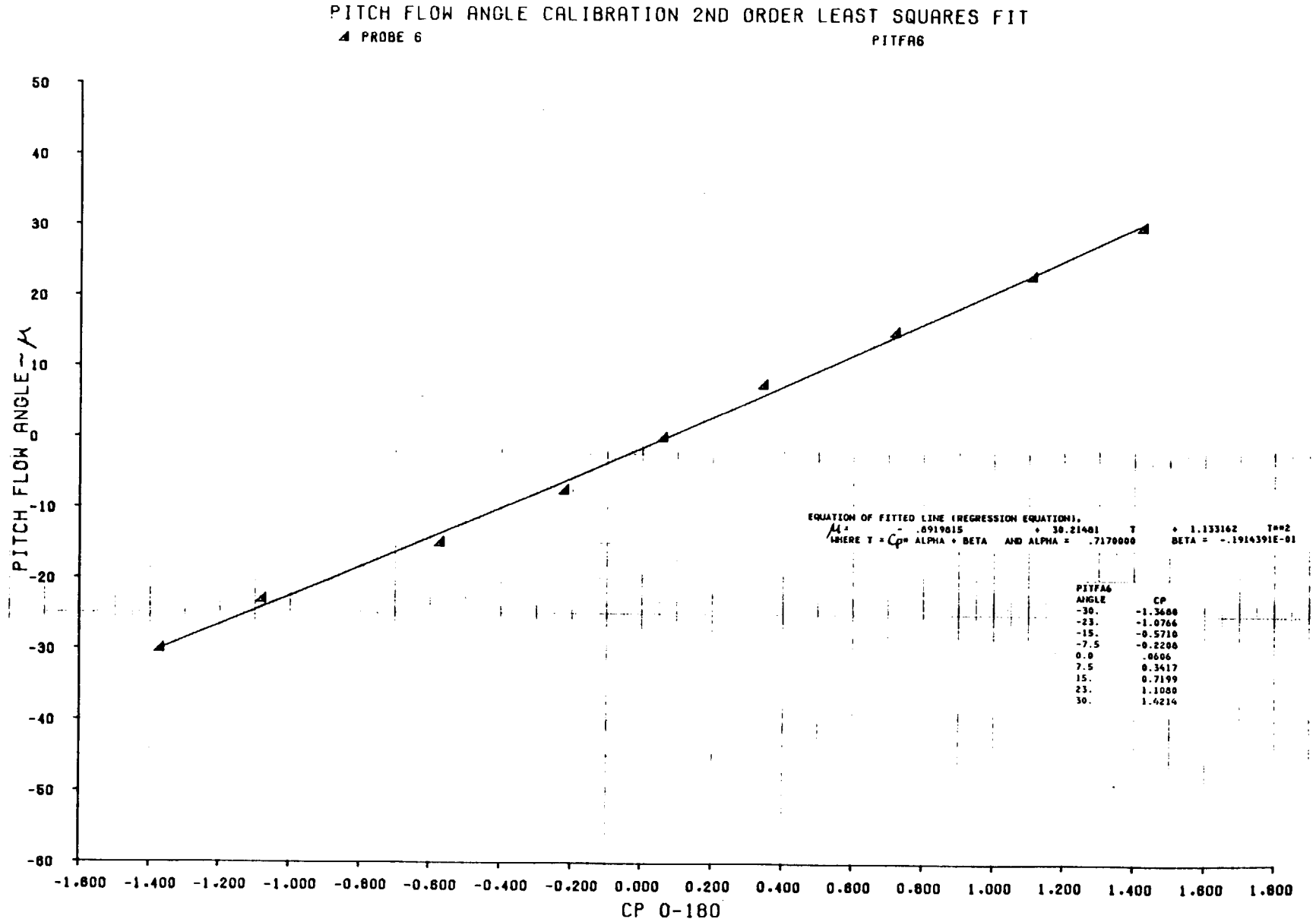

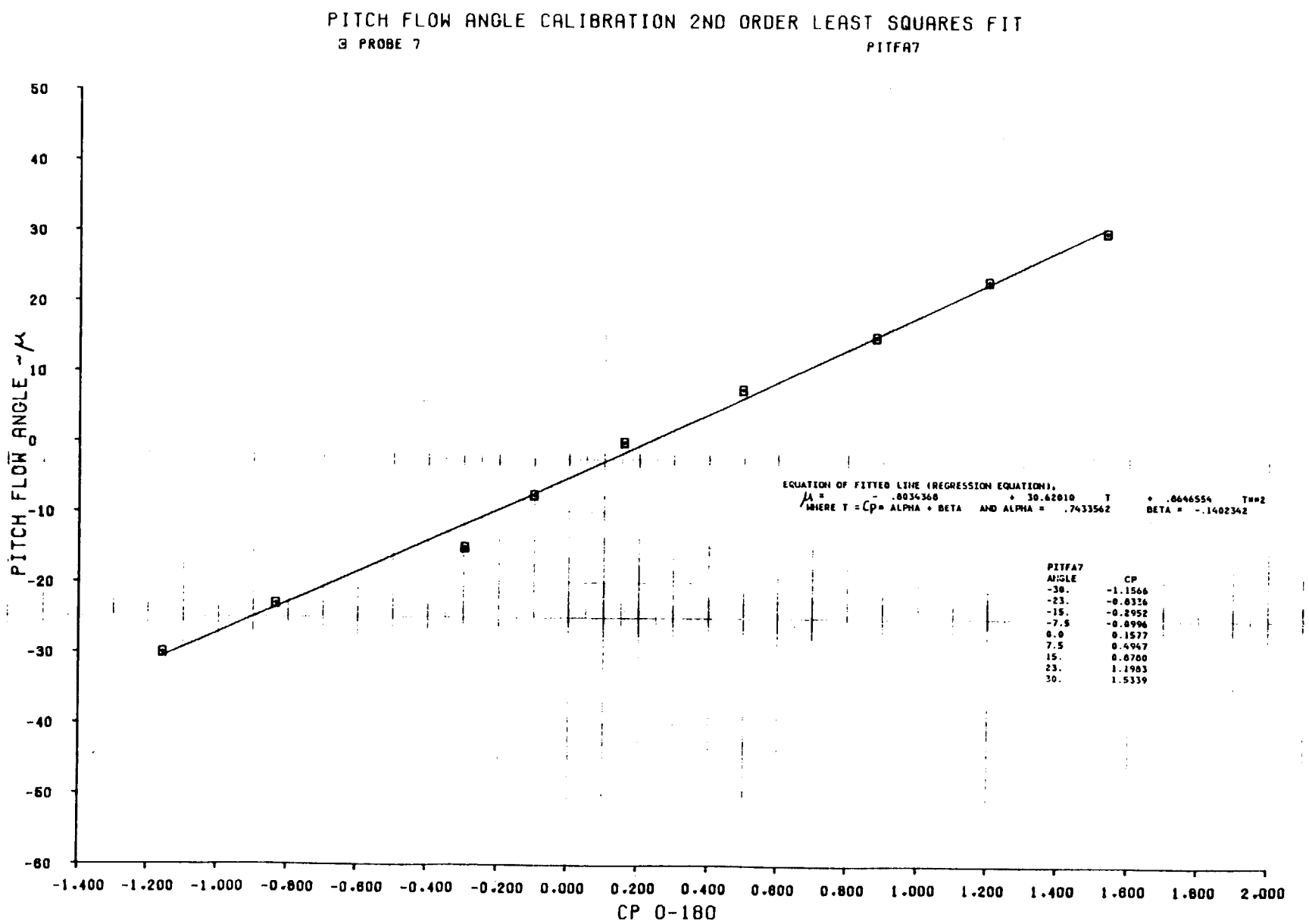

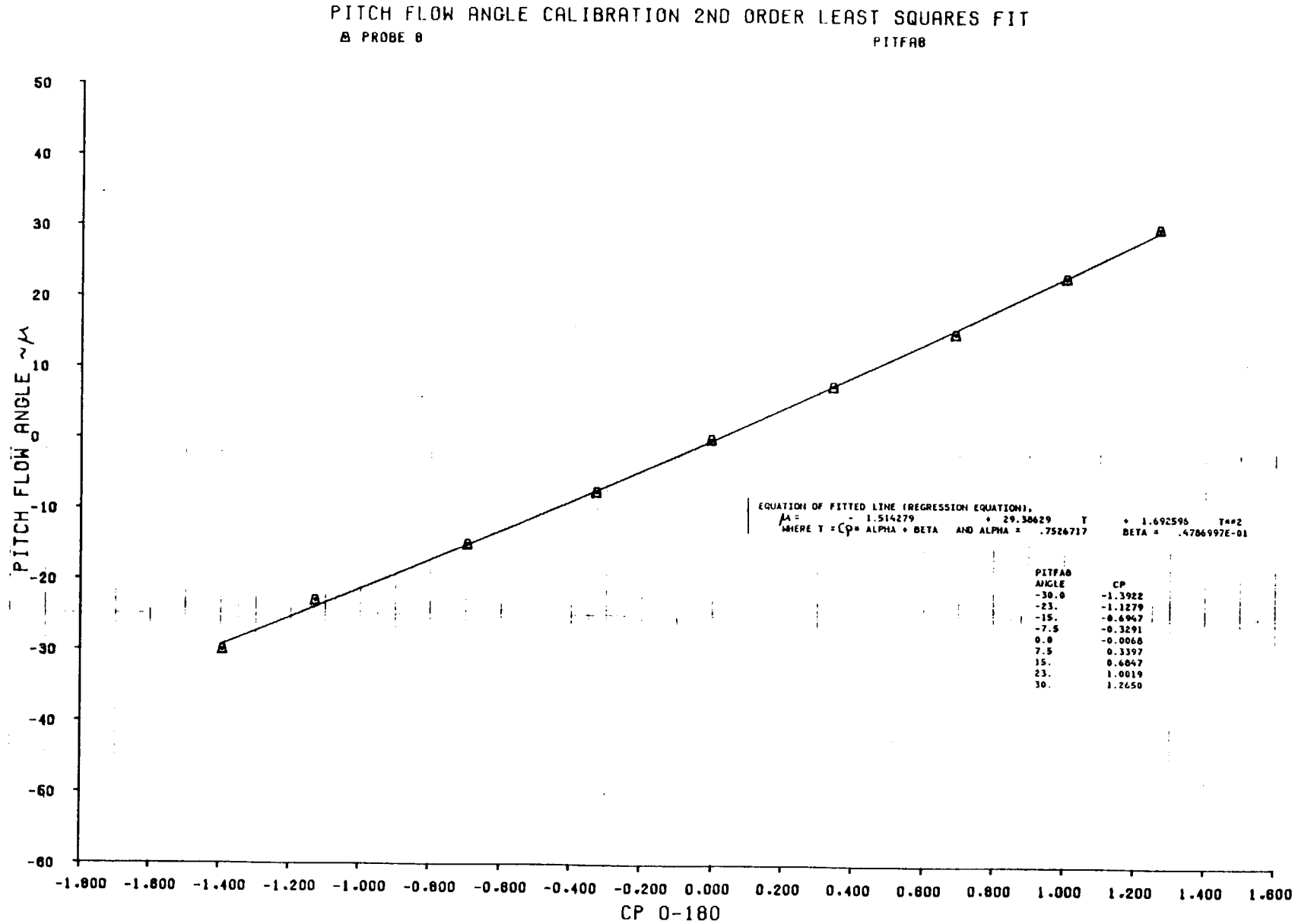

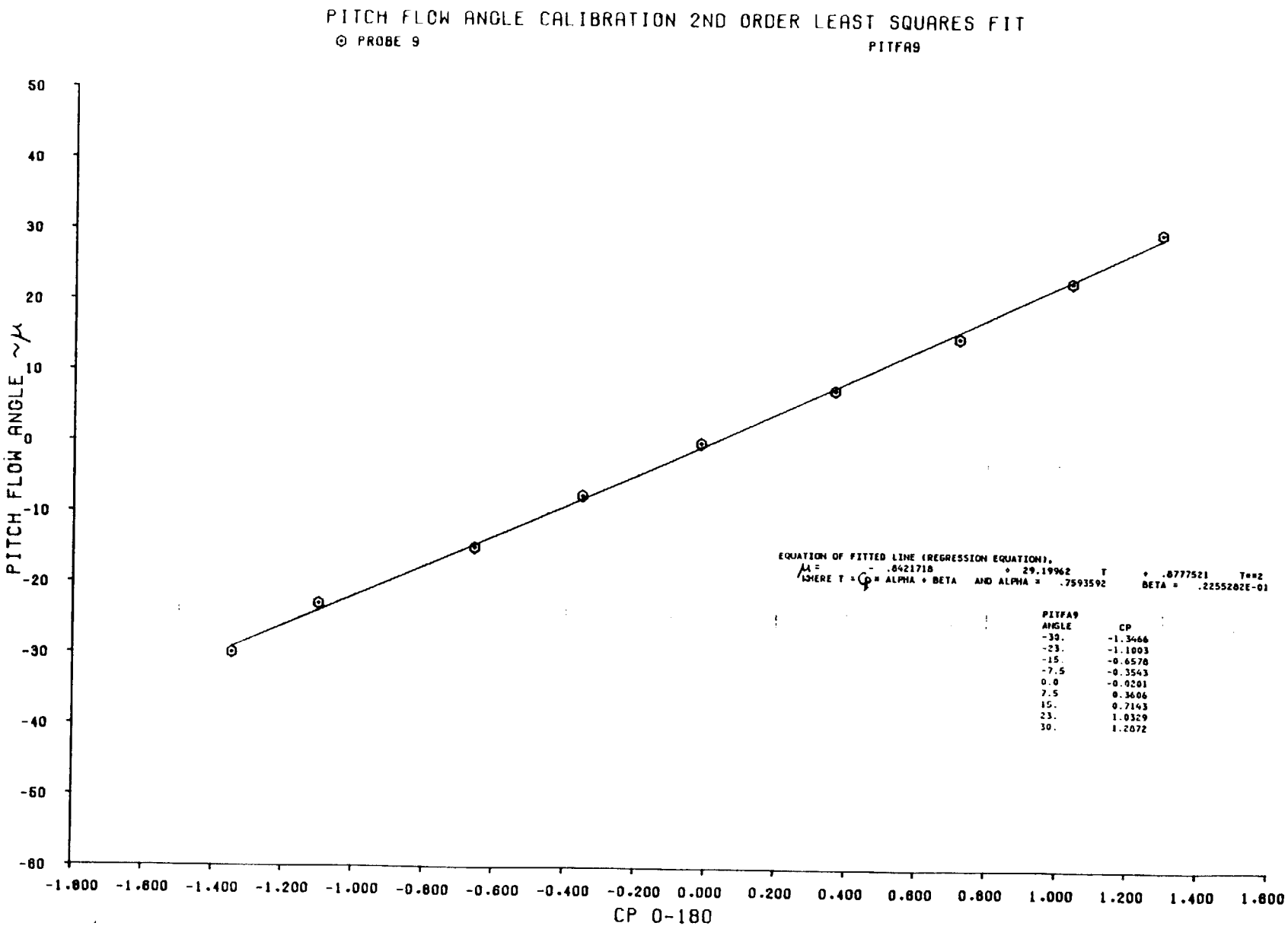

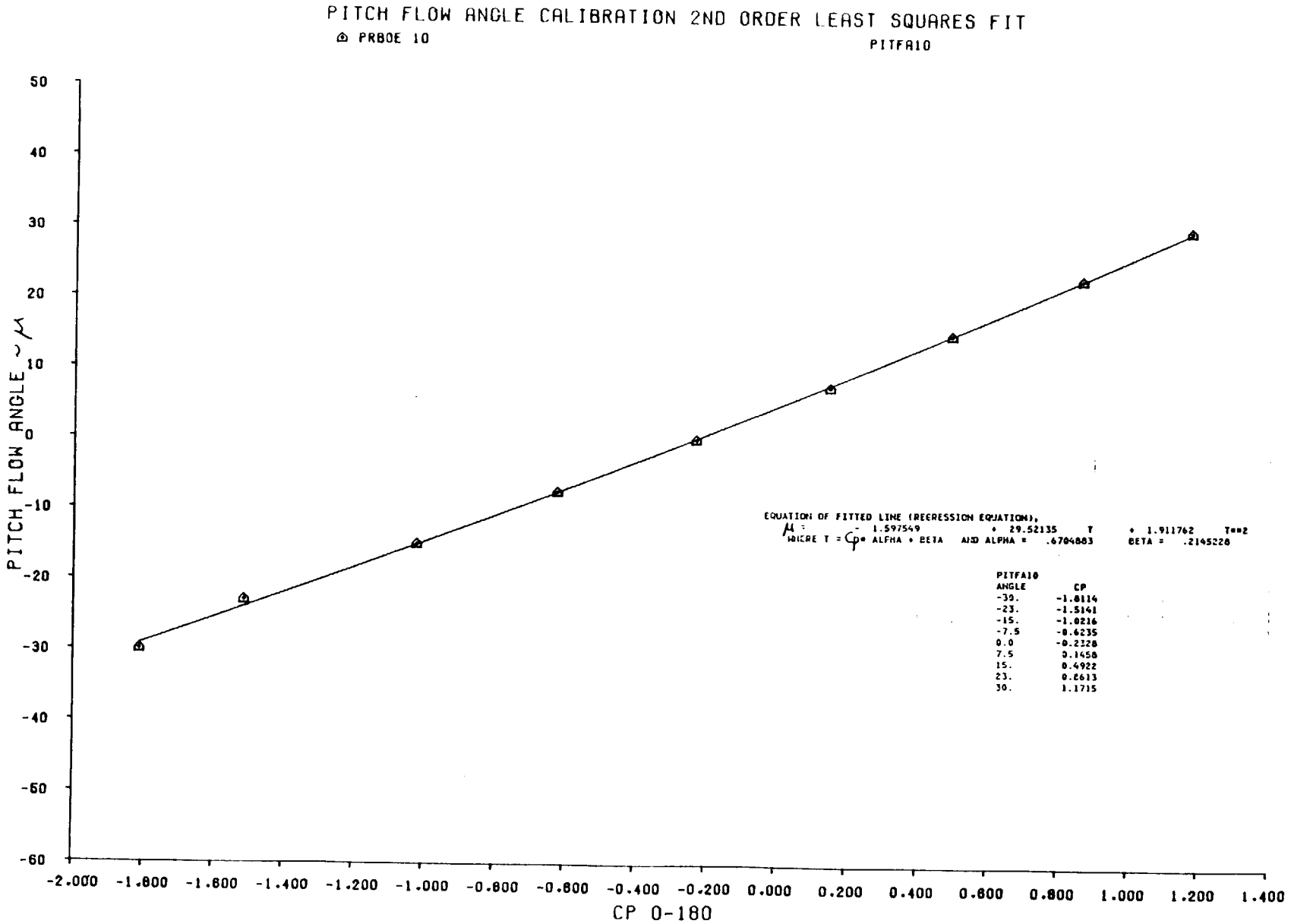

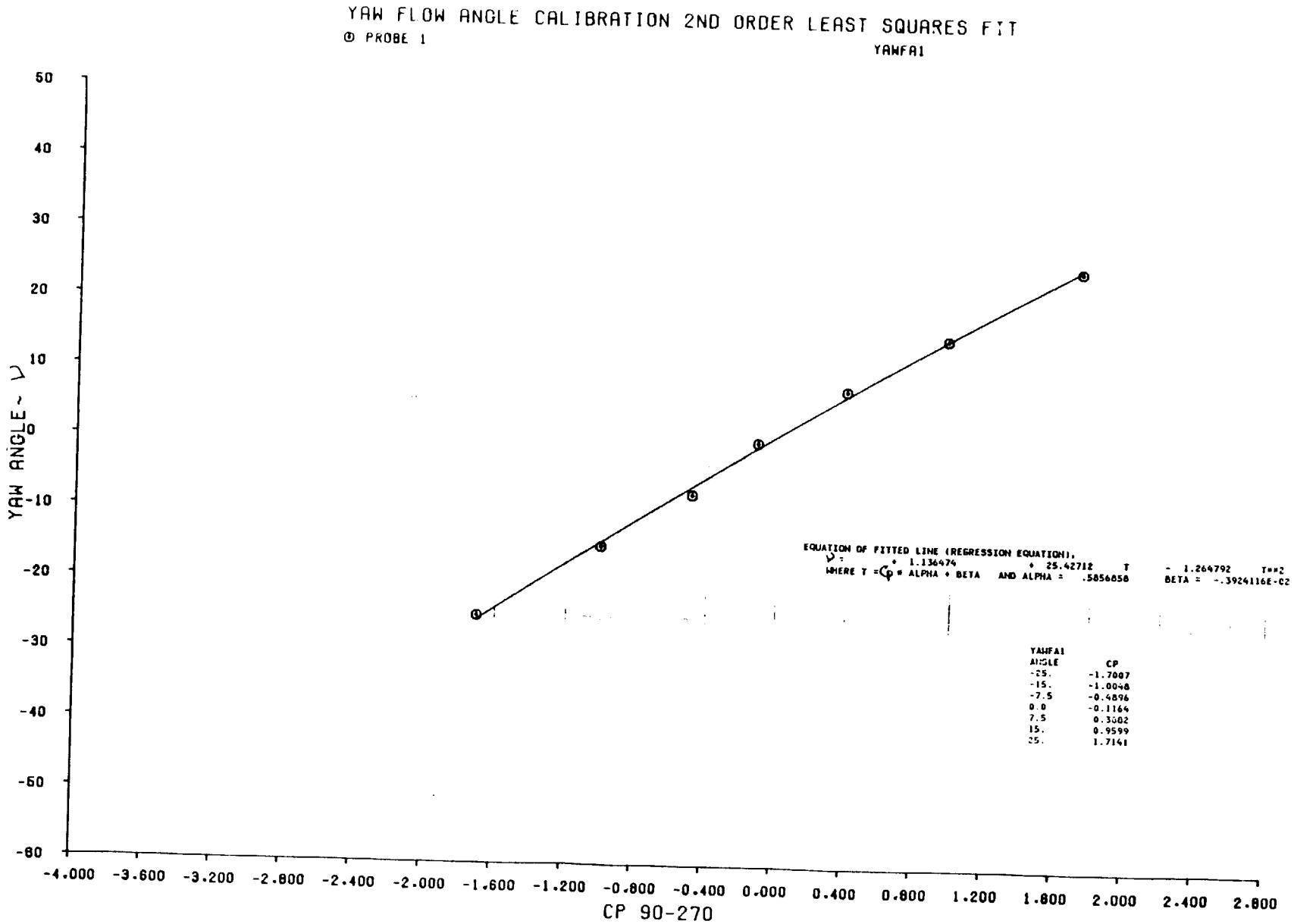
YAW FLOW ANGLE CALIBRATION 2ND ORDER LEAST SQUARES FIT
① PROBE 1
YAWFA1
YAW ANGLE ~ ν
CP 90-270
50
40
30
20
10
0
-10
-20
-30
-40
-50
-60
-4.000
-3.600
-3.200
-2.800
-2.400
-2.000
-1.600
-1.200
-0.800
-0.400
0.000
0.400
0.800
1.200
1.600
2.000
2.400
2.800
EQUATION OF FITTED LINE (REGRESSION EQUATION),
+ 1.136474 + 25.42712 T - 1.264792 T**2
WHERE T = Cp = ALPHA + BETA AND ALPHA = .5856858
BETA = -.3924116E-02
YAWFA1
ANGLE CP
-25. -1.7007
-15. -1.0048
-7.5 -0.4896
0.0 -0.1164
7.5 0.3002
15. 0.9599
25. 1.7141

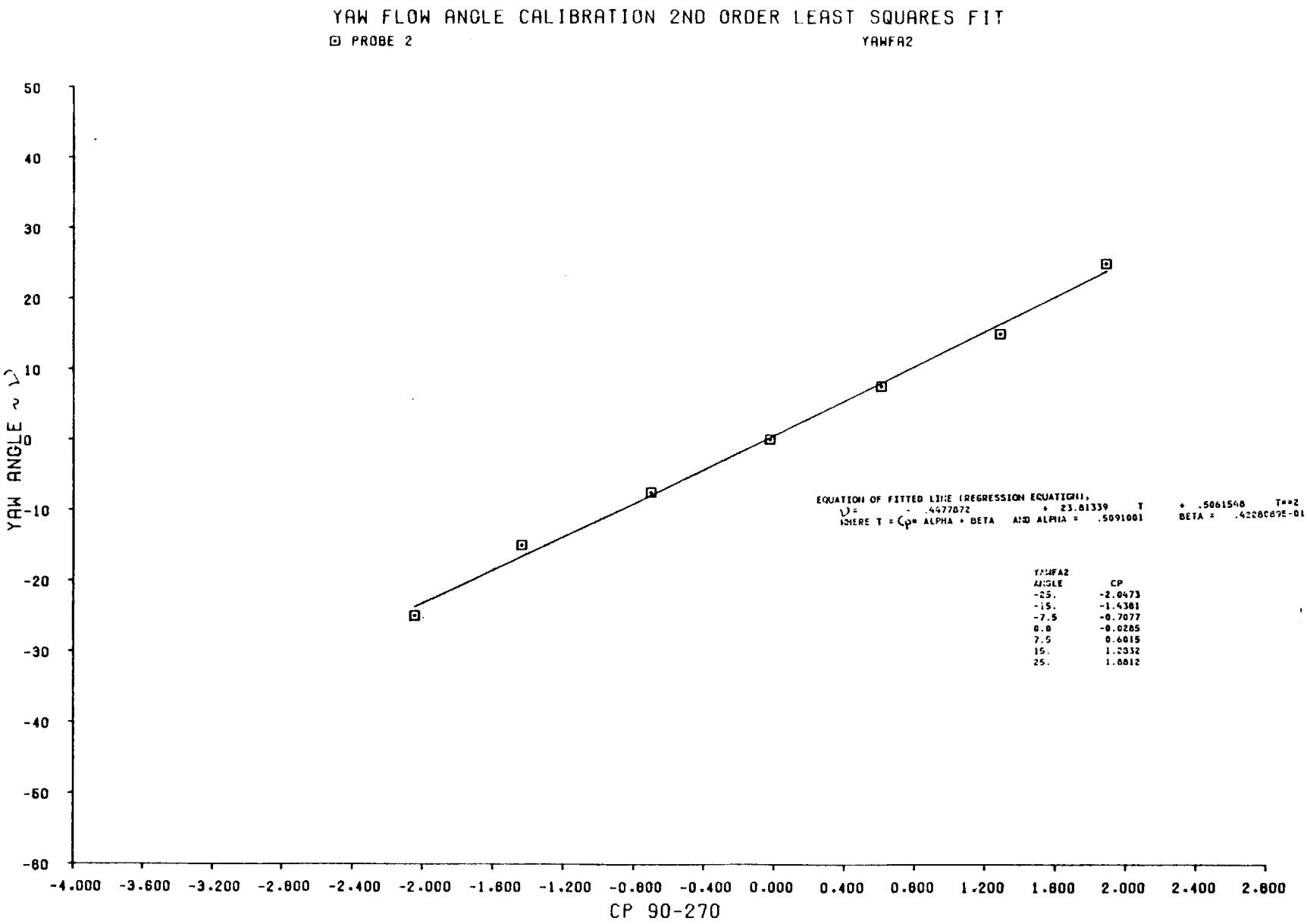

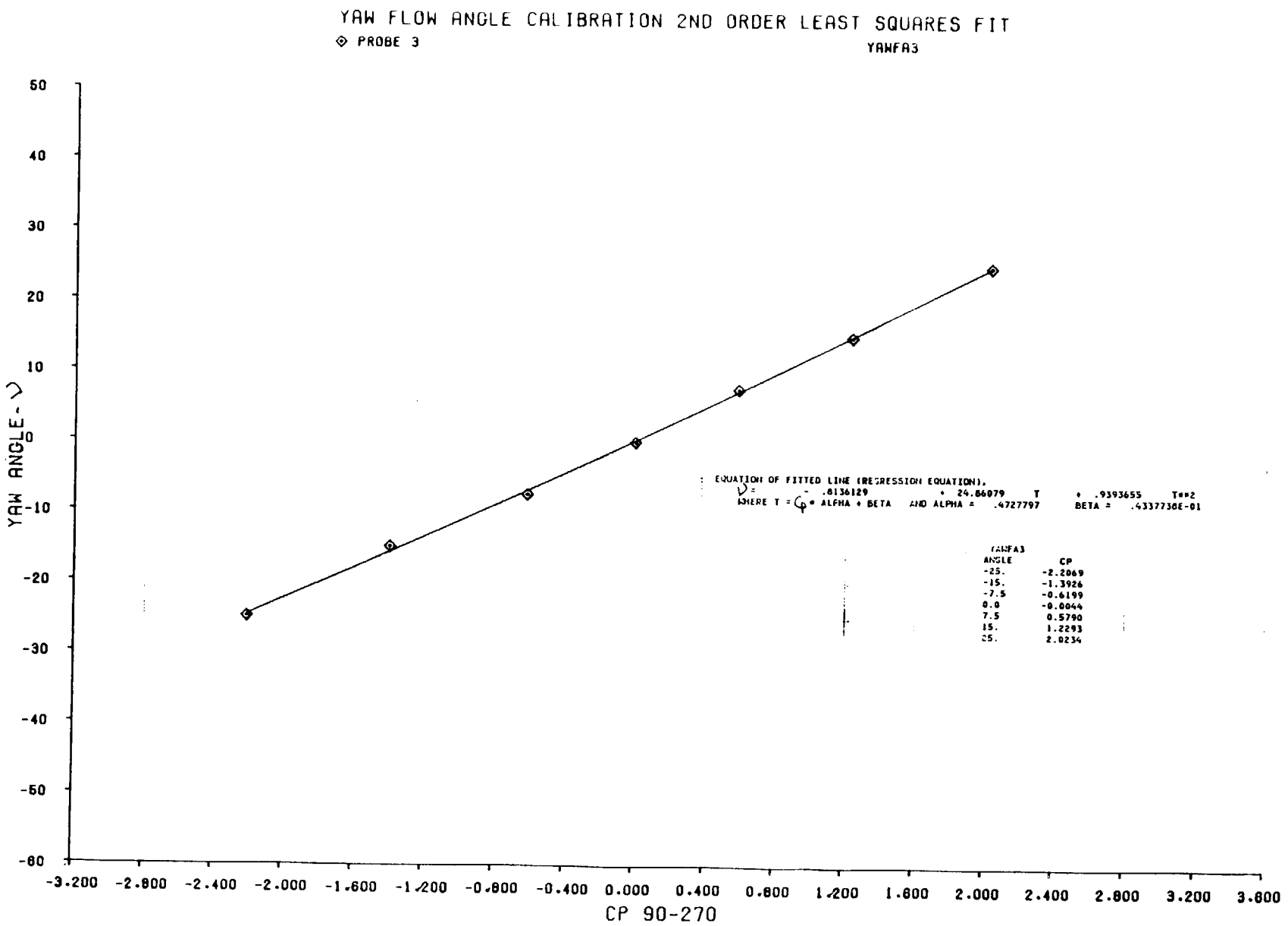

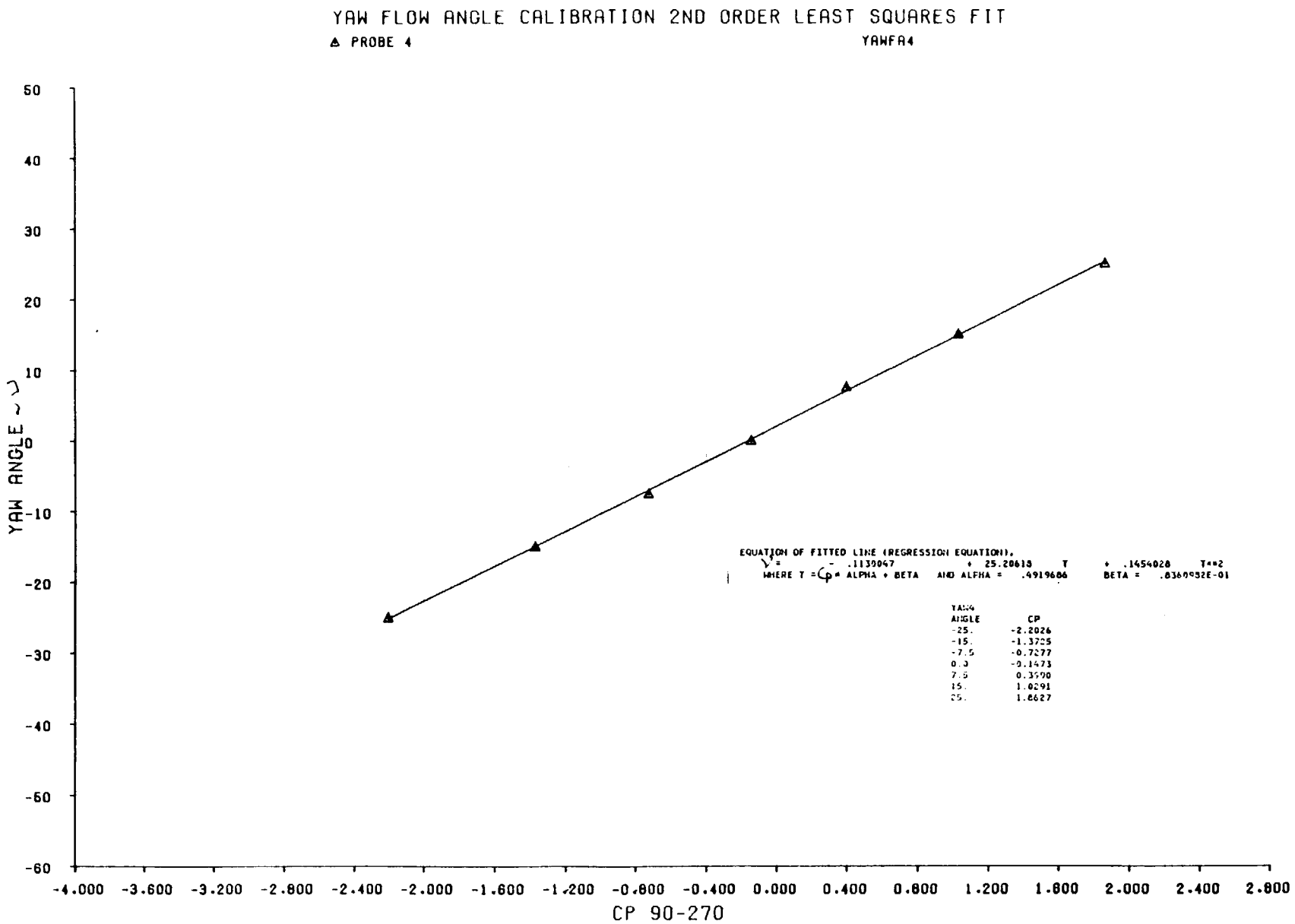

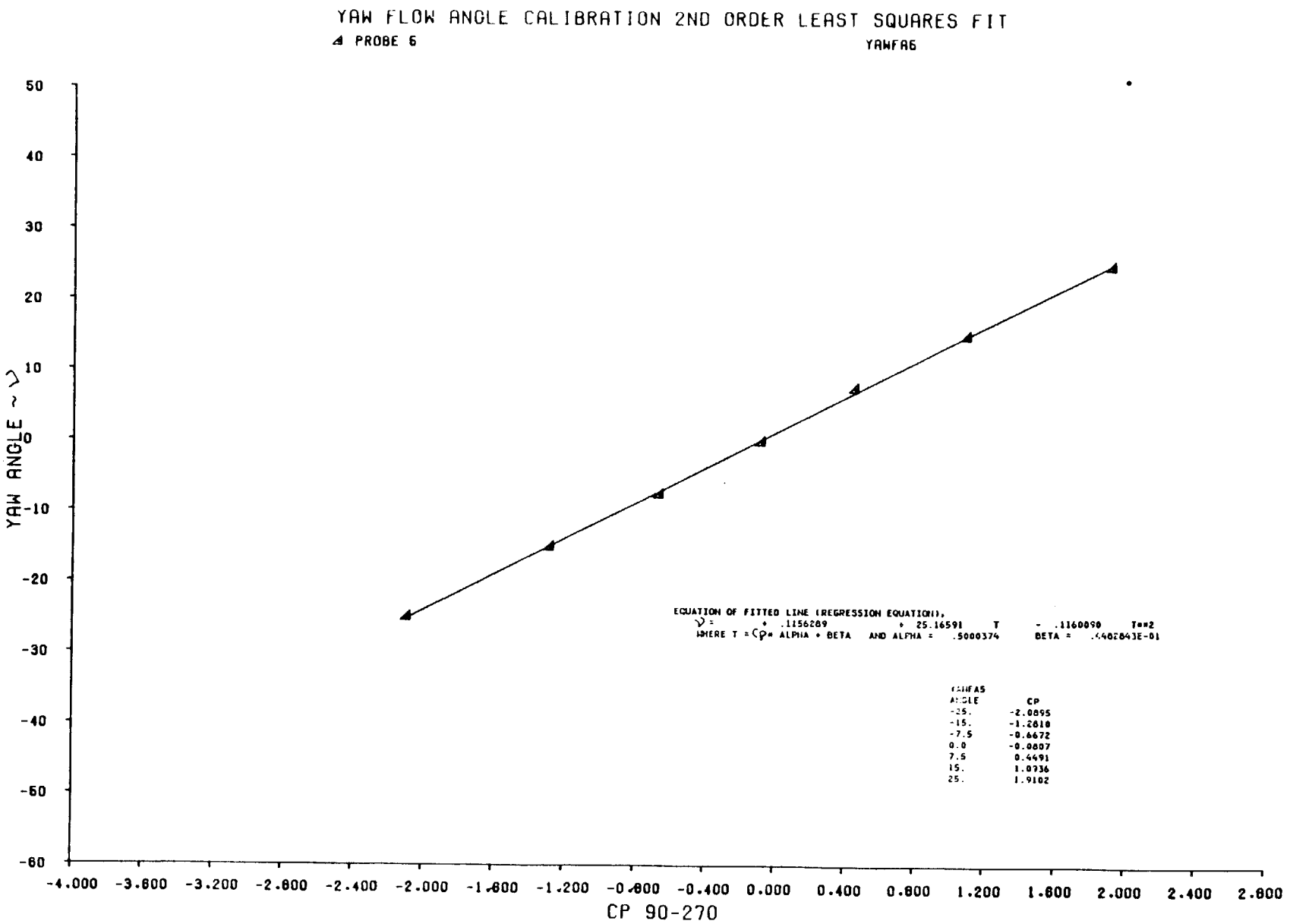
YAW FLOW ANGLE CALIBRATION 2ND ORDER LEAST SQUARES FIT
PROBE 6
YAWFA6
YAW ANGLE ~ ν
CP 90-270
50
40
30
20
10
0
-10
-20
-30
-40
-50
-60
-4.000
-3.600
-3.200
-2.800
-2.400
-2.000
-1.600
-1.200
-0.800
-0.400
0.000
0.400
0.800
1.200
1.600
2.000
2.400
2.800
EQUATION OF FITTED LINE (REGRESSION EQUATION),
ν = + .1156289 + 25.16591 T - .1160090 T**2
WHERE T = Cp* ALPHA + BETA AND ALPHA = .5000374 BETA = .4402843E-01
YAWFA5
ANGLE CP
-25. -2.0895
-15. -1.2818
-7.5 -0.6672
0.0 -0.0007
7.5 0.4491
15. 1.0736
25. 1.9102

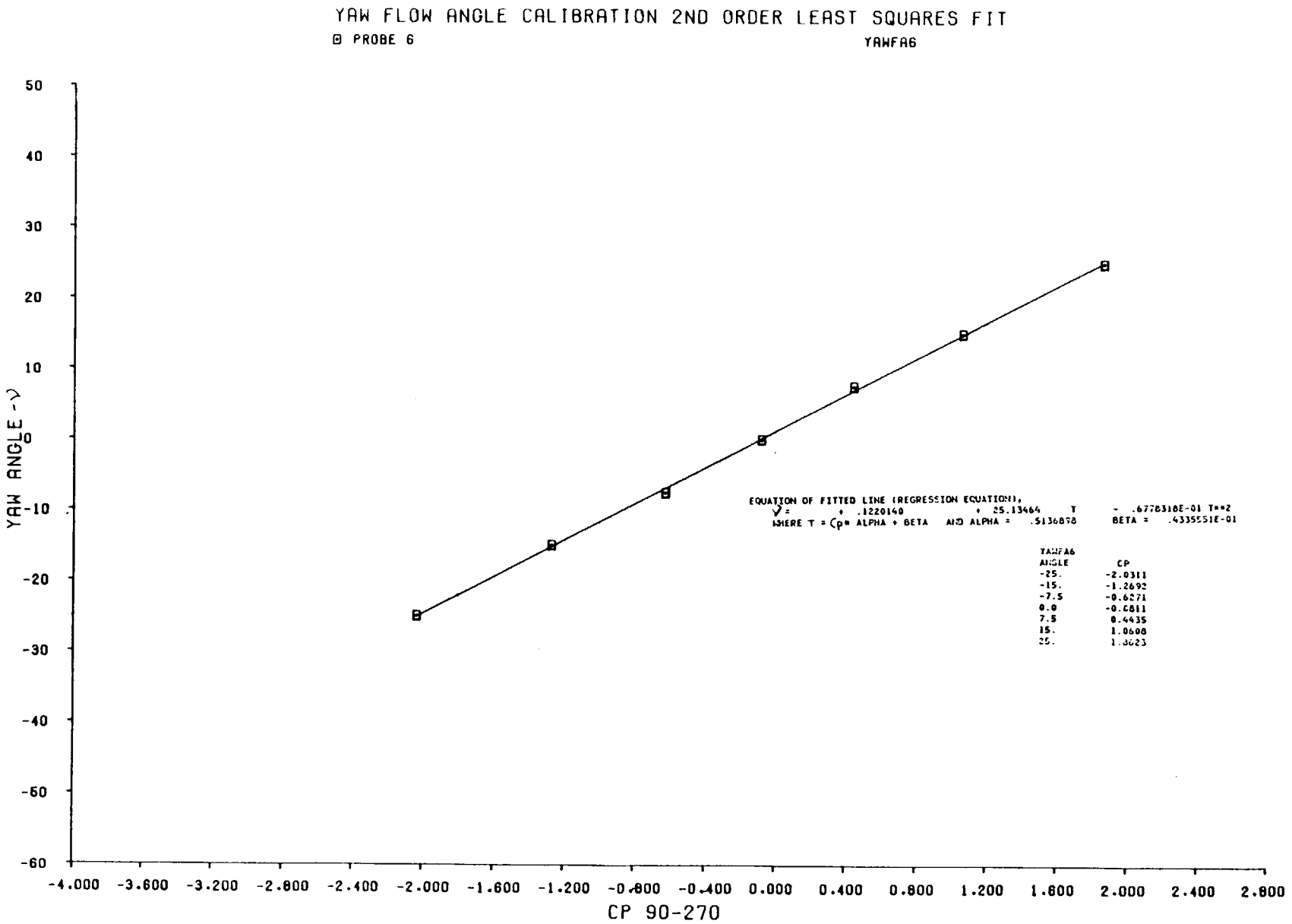

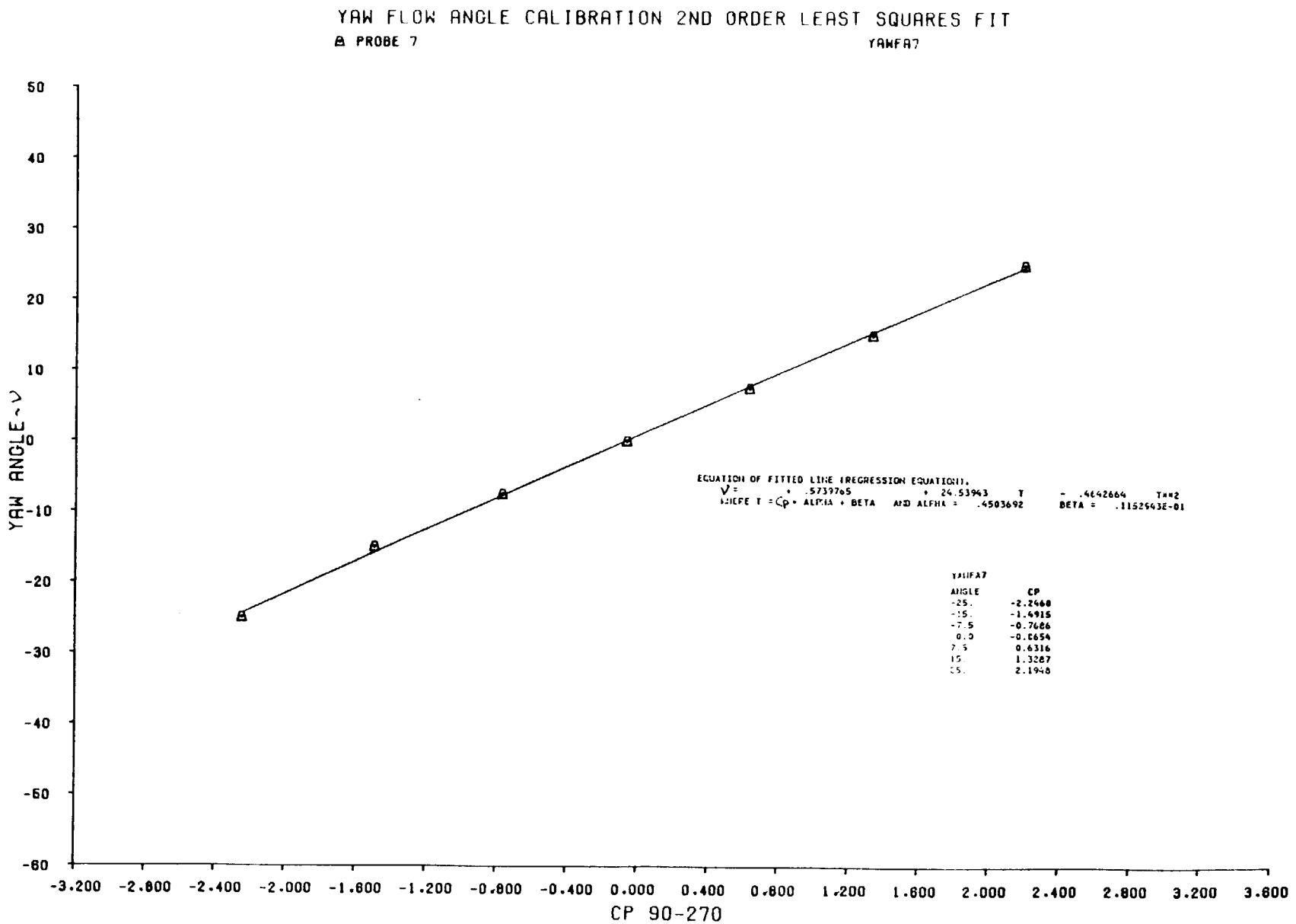
YAW FLOW ANGLE CALIBRATION 2ND ORDER LEAST SQUARES FIT
PROBE 7
YAWFA7
YAW ANGLE-ν
CP 90-270
50
40
30
20
10
0
-10
-20
-30
-40
-50
-60
-3.200
-2.800
-2.400
-2.000
-1.600
-1.200
-0.800
-0.400
0.000
0.400
0.800
1.200
1.600
2.000
2.400
2.800
3.200
3.600
EQUATION OF FITTED LINE (REGRESSION EQUATION).
ν = + .5739765 + 24.53943 T - .4642664 T**2
WHERE T = Cp + ALPHA + BETA AND ALPHA = .4503692 BETA = .1152643E-01
YAWFA7
ANGLE CP
-25. -2.2460
-15. -1.4915
-7.5 -0.7686
0.0 -0.0654
7.5 0.6316
15. 1.3287
25. 2.1948

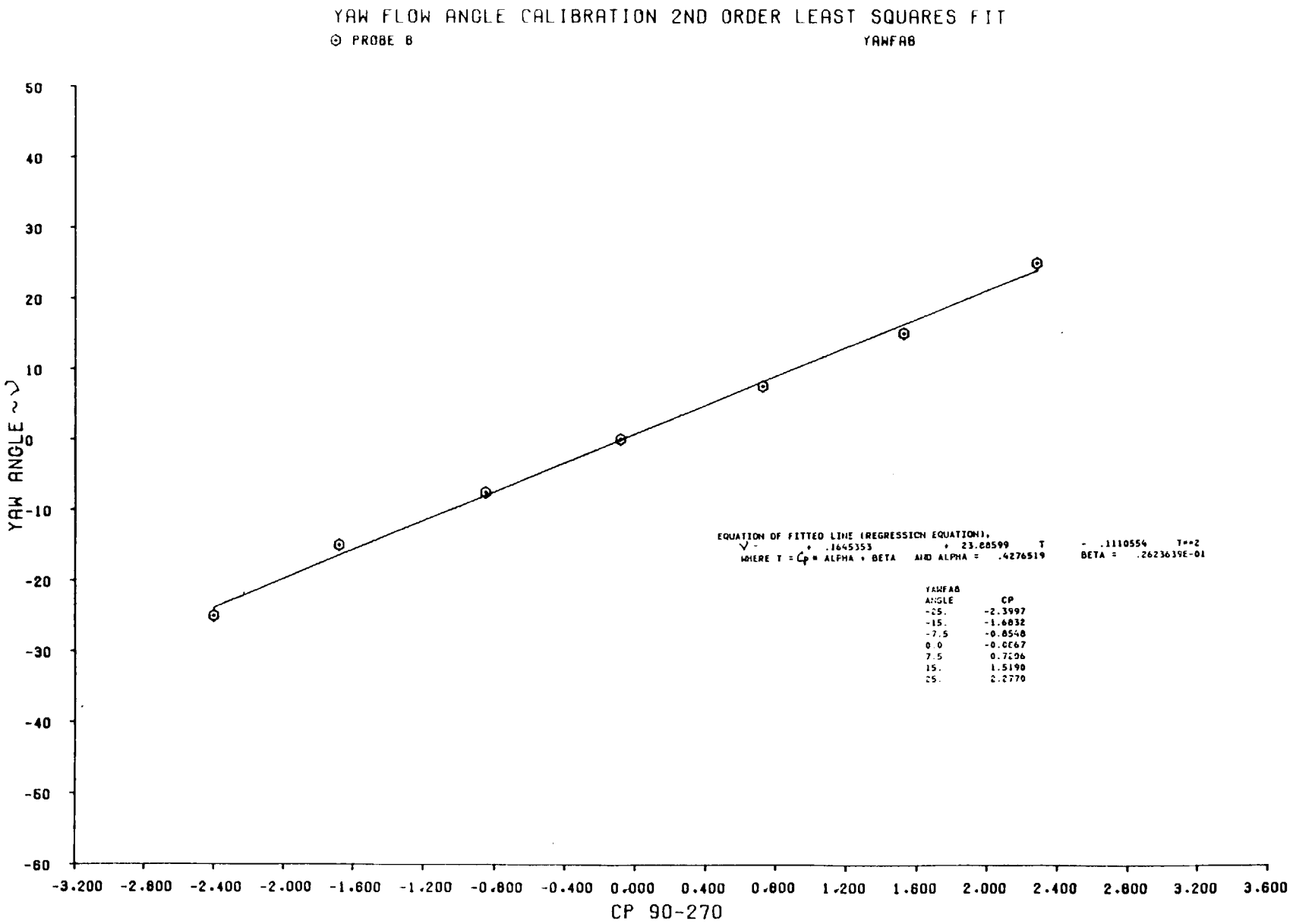

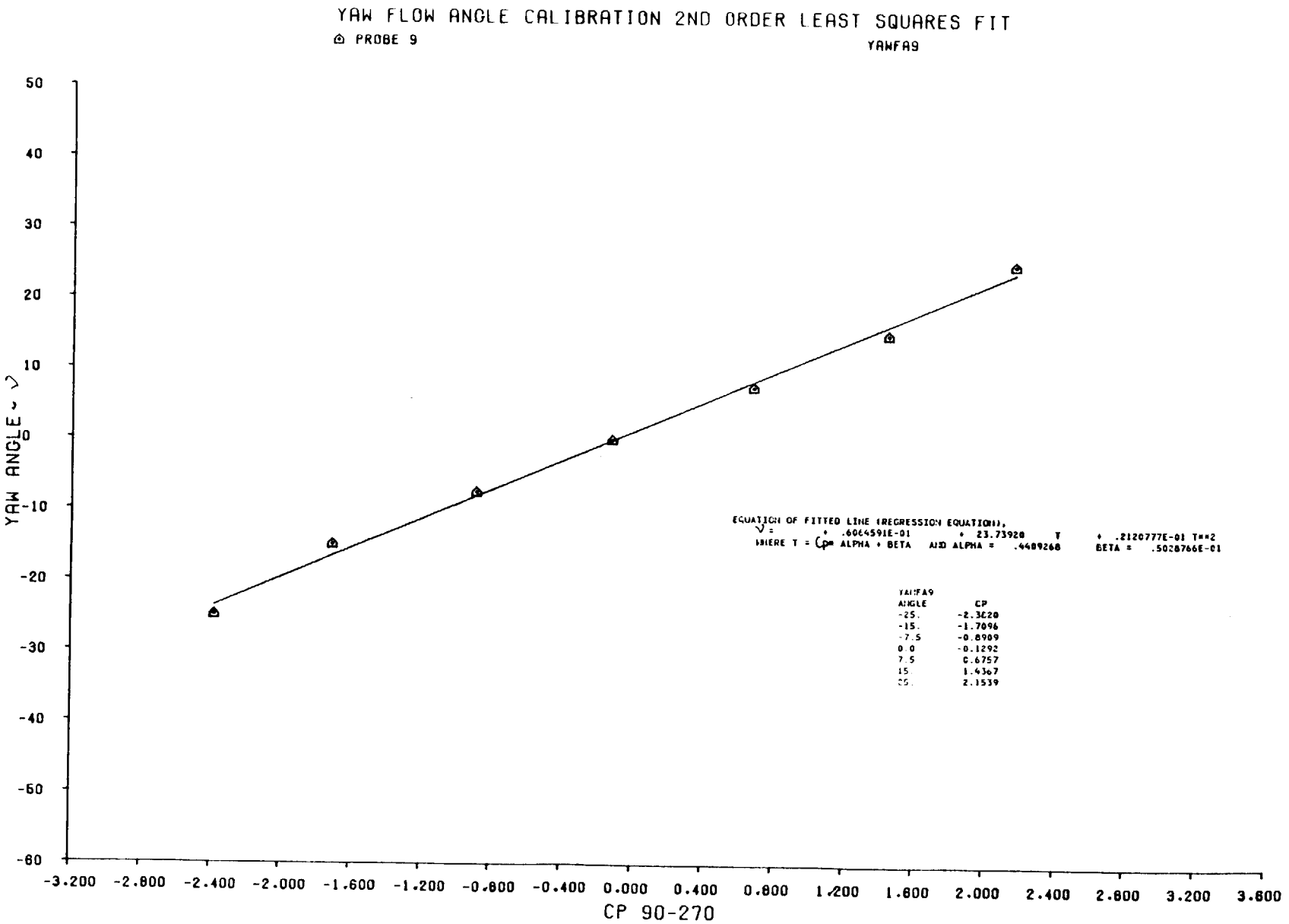

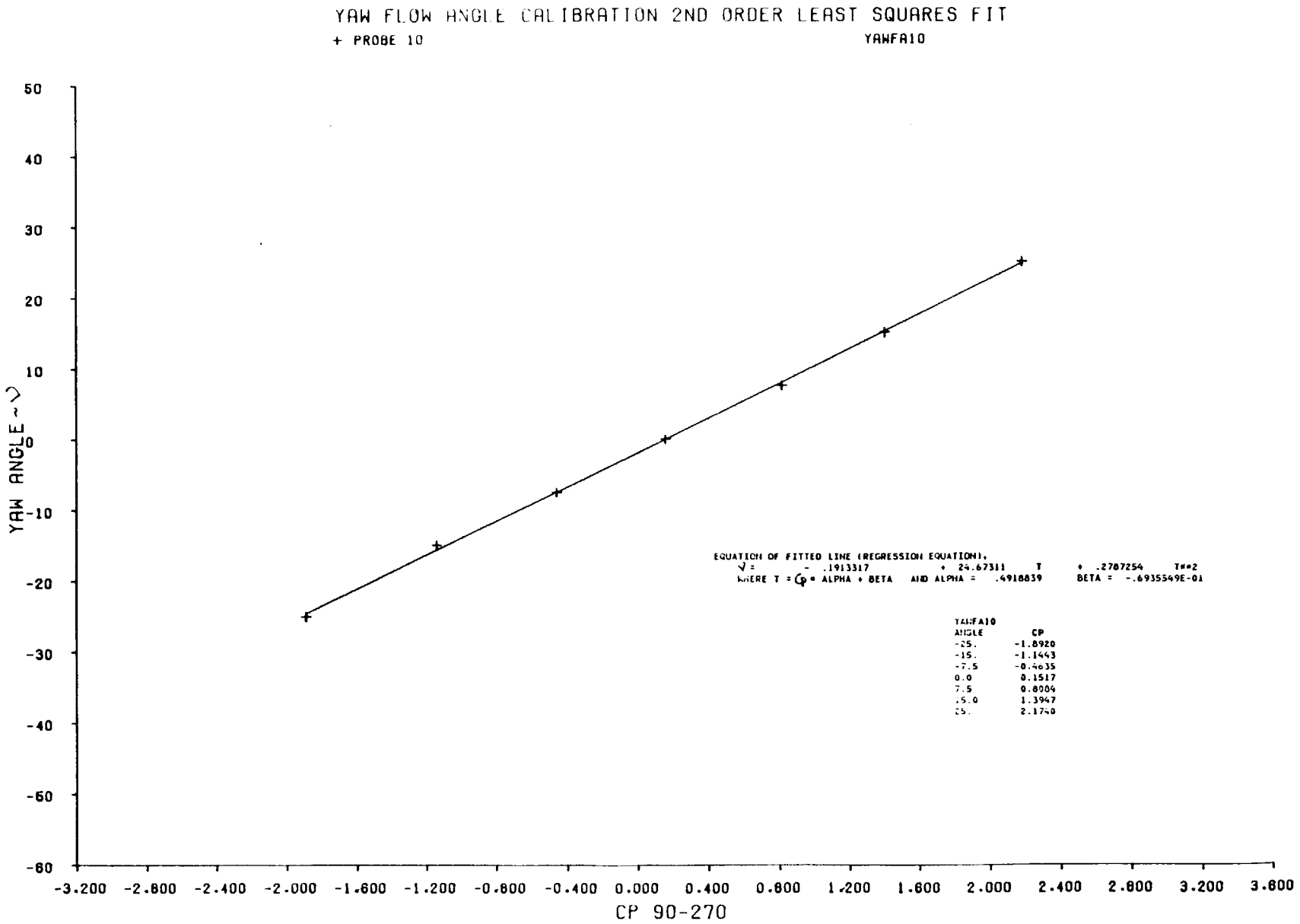

D.7 MODEL GEOMETRY DEFINITION

E^3 RADIAL WALL MIXER GEOMETRY DEFINITIONS END VIEW

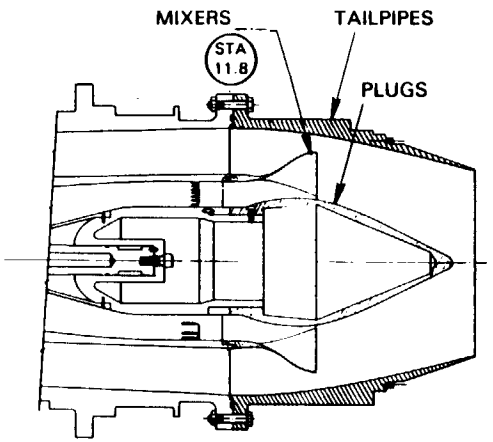

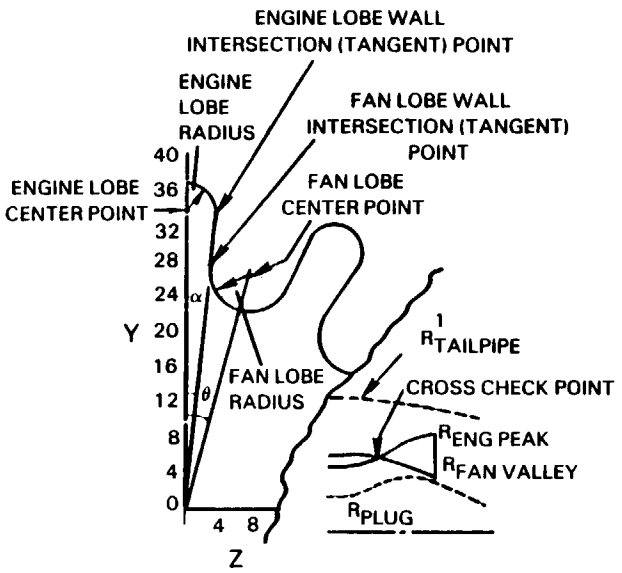

1 ALL DIMENSIONS ARE IN INCHES

CONFIGURATION 29 MIXER LOBE COORDINATES

AXIAL STA	R PLUG	R ENG PEAK	R TAILPIPE	R FAN VALLEY	ALPHA/THETA
11.800	1.900	2.780	4.690	3.048	0.493
11.950	1.900	2.780	4.690	3.052	0.493
12.100	1.901	2.781	4.690	3.055	0.493
12.250	1.915	2.788	4.686	3.059	0.493
12.400	1.942	2.799	4.680	3.060	0.493
12.550	1.980	2.819	4.673	3.058	0.493
12.700	2.027	2.849	4.667	3.052	0.493
12.850	2.082	2.890	4.659	3.040	0.493
13.000	2.139	2.943	4.651	3.025	0.493
13.150	2.195	3.009	4.644	3.010	0.493
13.300	2.252	3.083	4.637	2.992	0.493
13.450	2.309	3.170	4.630	2.972	0.493
13.600	2.359	3.258	4.623	2.952	0.493
13.750	2.404	3.339	4.616	2.929	0.493
13.900	2.440	3.410	4.608	2.901	0.493
14.050	2.473	3.470	4.599	2.872	0.493
14.200	2.501	3.518	4.588	2.840	0.493
14.350	2.524	3.557	4.575	2.807	0.493
14.500	2.539	3.590	4.560	2.773	0.493
14.650	2.545	3.619	4.543	2.738	0.493
14.800	2.543	3.644	4.525	2.700	0.493
14.850	2.541	3.651	4.519	2.689	0.493

CONFIGURATION 29 MIXER LOBE COORDINATES

AXIAL STATION	ALPHA (DEG)	THETA(DEG)	FAN CENTER POINT Y	FAN CENTER POINT Z	FAN LOBE RADIUS	FAN LOBE INTERSECTION POINT Y	FAN LOBE INTERSECTION POINT Z
13.300	4.935	10.000	4.010	0.707	1.080	3.027	0.261
13.450	4.935	10.000	3.386	0.597	0.467	3.059	0.264
13.600	4.935	10.000	3.241	0.572	0.339	3.092	0.267
13.750	4.935	10.000	3.177	0.560	0.297	3.118	0.269
13.900	4.935	10.000	3.134	0.553	0.282	3.137	0.271
14.050	4.935	10.000	3.102	0.547	0.278	3.126	0.270
14.200	4.935	10.000	3.068	0.541	0.275	3.091	0.267
14.350	4.935	10.000	3.032	0.535	0.272	3.055	0.264
14.500	4.935	10.000	2.995	0.528	0.269	3.018	0.261
14.650	4.935	10.000	2.958	0.521	0.265	2.980	0.257
14.800	4.935	10.000	2.916	0.514	0.261	2.939	0.254
14.850	4.935	10.000	2.905	0.512	0.260	2.927	0.253

CONFIGURATION 29 MIXER LOBE COORDINATES

AXIAL STATION	ALPHA (DEG)	THETA(DEG)	ENG CENTER POINT Y	ENG CENTER POINT Z	ENG LOBE RADIUS	ENG LOBE INTERSECTION POINT Y	ENG LOBE INTERSECTION POINT Z
13.300	4.935	10.000	2.450	0.0	0.633	3.027	0.261
13.450	4.935	10.000	2.800	0.0	0.370	3.059	0.264
13.600	4.935	10.000	2.961	0.0	0.297	3.092	0.267
13.750	4.935	10.000	3.064	0.0	0.275	3.118	0.269
13.900	4.935	10.000	3.139	0.0	0.271	3.137	0.271
14.050	4.935	10.000	3.195	0.0	0.275	3.171	0.274
14.200	4.935	10.000	3.239	0.0	0.279	3.215	0.278
14.350	4.935	10.000	3.275	0.0	0.282	3.251	0.281
14.500	4.935	10.000	3.306	0.0	0.284	3.281	0.283
14.650	4.935	10.000	3.332	0.0	0.287	3.308	0.286
14.800	4.935	10.000	3.355	0.0	0.289	3.331	0.288
14.850	4.935	10.000	3.362	0.0	0.289	3.337	0.288

CONFIGURATION 34 MIXER LOBE COORDINATES

AXIAL STA	R PLUG	R ENG PEAK	R TAILPIPE	R FAN VALLEY	ALPHA/THETA
11.800	1.900	2.780	4.690	3.048	0.261
11.950	1.900	2.780	4.690	3.052	0.261
12.100	1.900	2.780	4.686	3.050	0.261
12.250	1.907	2.783	4.678	3.038	0.261
12.400	1.937	2.794	4.666	3.020	0.261
12.550	1.979	2.811	4.651	2.999	0.261
12.700	2.026	2.840	4.634	2.973	0.261
12.850	2.072	2.879	4.628	2.945	0.261
13.000	2.113	2.927	4.598	2.915	0.261
13.150	2.147	2.983	4.576	2.881	0.261
13.300	2.172	3.059	4.552	2.846	0.261
13.450	2.192	3.145	4.530	2.809	0.261
13.600	2.210	3.245	4.505	2.768	0.261
13.750	2.225	3.354	4.480	2.723	0.261
13.900	2.234	3.470	4.454	2.677	0.261
14.050	2.240	3.579	4.428	2.629	0.261
14.200	2.241	3.673	4.402	2.569	0.261
14.350	2.239	3.748	4.376	2.527	0.261
14.500	2.230	3.804	4.348	2.473	0.261
14.650	2.213	3.839	4.320	2.420	0.261
14.800	2.189	3.850	4.289	2.365	0.261
14.850	2.180	3.851	4.279	2.347	0.261

CONFIGURATION 34 MIXER LOBE COORDINATES

AXIAL STATION	ALPHA (DEG)	THETA(DEG)	FAN CENTER POINT Y	FAN CENTER POINT Z	FAN LOBE RADIUS	FAN LOBE INTERSECTION POINT Y	FAN LOBE INTERSECTION POINT Z
13.150	2.610	10.000	4.271	0.753	1.456	2.953	0.135
13.300	2.610	10.000	3.428	0.604	0.635	2.999	0.137
13.450	2.610	10.000	3.221	0.568	0.461	3.051	0.139
13.600	2.610	10.000	3.130	0.552	0.411	3.110	0.142
13.750	2.610	10.000	3.077	0.543	0.402	3.096	0.141
13.900	2.610	10.000	3.025	0.533	0.395	3.043	0.139
14.050	2.610	10.000	2.971	0.524	0.368	2.989	0.136
14.200	2.610	10.000	2.903	0.512	0.379	2.921	0.133
14.350	2.610	10.000	2.856	0.504	0.373	2.873	0.131
14.500	2.610	10.000	2.795	0.493	0.365	2.812	0.128
14.650	2.610	10.000	2.735	0.482	0.357	2.751	0.125
14.800	2.610	10.000	2.673	0.471	0.349	2.689	0.123
14.850	2.610	10.000	2.653	0.468	0.346	2.668	0.122

CONFIGURATION 34 MIXER LOBE COORDINATES

AXIAL STATION	ALPHA (DEG)	THETA(DEG)	ENG CENTER POINT Y	ENG CENTER POINT Z	ENG LOBE RADIUS	ENG LOBE INTERSECTION POINT Y	ENG LOBE INTERSECTION POINT Z
13.150	2.610	10.000	2.666	0.0	0.317	2.953	0.135
13.300	2.610	10.000	2.873	0.0	0.186	2.999	0.137
13.450	2.610	10.000	2.995	0.0	0.150	3.051	0.139
13.600	2.610	10.000	3.103	0.0	0.142	3.110	0.142
13.750	2.610	10.000	3.208	0.0	0.146	3.201	0.146
13.900	2.610	10.000	3.319	0.0	0.151	3.312	0.151
14.050	2.610	10.000	3.423	0.0	0.156	3.416	0.156
14.200	2.610	10.000	3.513	0.0	0.160	3.506	0.160
14.350	2.610	10.000	3.585	0.0	0.163	3.577	0.163
14.500	2.610	10.000	3.638	0.0	0.166	3.631	0.166
14.650	2.610	10.000	3.672	0.0	0.167	3.664	0.167
14.800	2.610	10.000	3.682	0.0	0.168	3.675	0.168
14.850	2.610	10.000	3.683	0.0	0.168	3.676	0.168

TAILPIPE COORDINATES

CONFIGURATION 29

AXIAL STA	R	
118	4.690 REF	STA LINE
121	4.690	
124	4.680	
127	4.667	
130	4.631	
133	4.637	
136	4.613	
139	4.608	
142	4.588	
145	4.560	
148	4.525	
151	4.489	
154	4.444	
157	4.393	
160	4.341	
163	4.281	
166	4.215	
169	4.147	
172	4.078	
175	4.009	
178	3.940	
181	3.870	
184	3.796	
187	3.715	
190	3.630	
193	3.540	
196	3.445	
199	3.347	
201	3.280	
201.5	3.267	
202	3.255	
202.23	3.250	
202.5	3.249	
202.85	3.246 MIN	

CONFIGURATION 34

AXIAL STA.	R	
118.00	4.690	REF
121.00	4.686	
124.00	4.666	
127.00	4.634	
130.00	4.598	
133.00	4.552	
136.00	4.503	
139.00	4.454	
142.00	4.402	
145.00	4.348	
148.00	4.289	
151.00	4.229	ST. LINE
154.10	3.273	
154.50	3.263	
155.00	3.257	
155.50	3.251	
200.00	3.247	
200.57	3.246	THROAT REF

PLUG COORDINATES

AXIAL STA	R	
118.0	1.900	REF
121	1.901	
124	1.942	
127	2.027	
130	2.139	
133	2.252	
136	2.359	
139	2.440	
142	2.501	
145	2.539	
148	2.543	
151	2.514	
154	2.458	
157	2.378	
160	2.276	
163	2.155	
166	2.026	
169	1.890	
172	1.749	
175	1.600	
178	1.445	
181	1.285	
184	1.115	
187	.948	
190	.779	
193	.604	
196	.419	
196.55	.305	
198.60	0	REF — .46 R. (REF)

AXIAL STA	R	
118.0	1.900	REF.
121.7	1.900	
124.0	1.937	
127.0	2.026	
130.0	2.113	
133.0	2.172	
136.0	2.210	
139.0	2.234	
142.0	2.241	
145.0	2.230	
148.0	2.169	
151.0	2.129	
154.0	2.050	
157.0	1.956	
160.0	1.847	
163.0	1.728	
166.0	1.595	
169.0	1.450	
172.0	1.300	
175.0	1.150	
178.0		
181.0	STR. LINE	
184.0		
193.6	0.207	— 0.23 R
194.73	0	

APPENDIX E

FLOW ANGLE CALIBRATION

Flow angle measurements were made downstream of the mixer plane at 10 radial locations and 21 circumferential locations as part of the "multisurvey" on configurations 29 and 34. These angles were measured in the radial and circumferential directions (denoted pitch μ , and yaw ν , respectively) using five-hole pyramid probes shown in the sketch below.

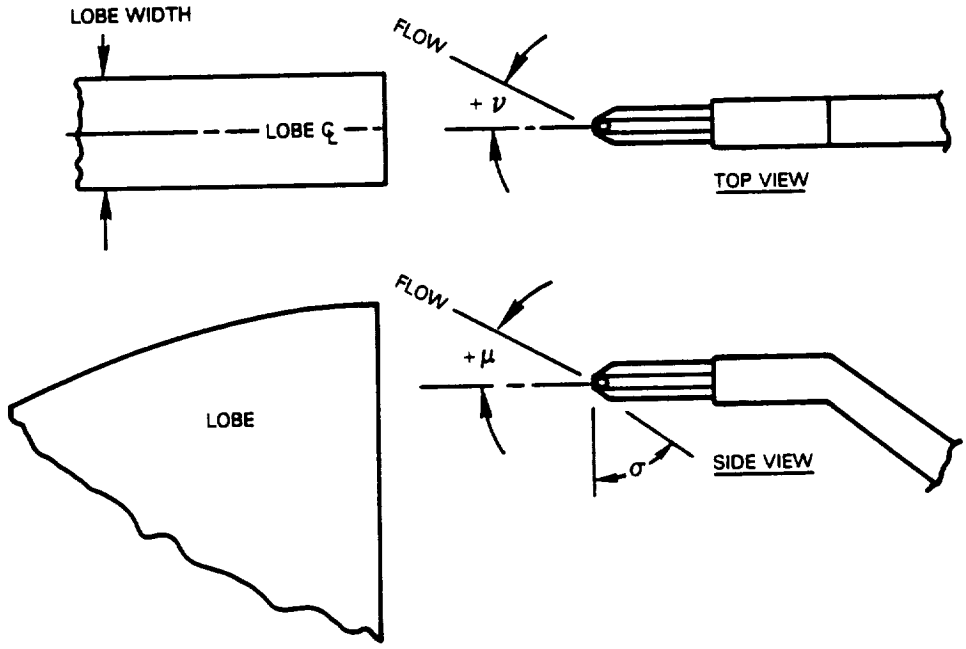

Each probe consists of five tubes, silver soldered together; a center pilot probe and two probes each in the horizontal and veratical planes which are bevel machined in assembly to an angle σ . The probe assembly was calibrated in the free-jet exhaust of a 5.5-inch diameter standard ASME long-radius flow nozzle. Calibration results presented herein were made at a Mach number of 0.5 at pitch angles of 0, $\pm$7.5, and $\pm$15 degrees.

Measured pressures from the calibration tests were reduced to pressure coefficients, defined as the ΔP between taps on opposite sides of the probe, divided by the free stream dynamic pressure (Q).

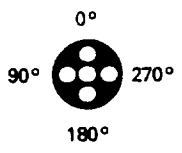

$$C_{P\ pitch} = (P_{0°} - P_{180°}) / Q \quad vs \quad \mu$$

$$C_{P\ yaw} = (P_{90°} - P_{270°}) / Q \quad vs \quad \nu$$

$$\text{where } Q = (\gamma/2)\ P_{AMB}\ Mn^2$$

Pressure coefficients (shown in tabular form from pages 169 through 171) in the pitch and yaw planes were then correlated as functions of pitch and yaw angles and were curve fitted with straight lines, that is,

$$C_p = (\Delta P/Q) = a + b\ (\text{angle})$$

where coefficients a and b were determined for each of the ten probes and are presented in the tabulations below.

PITCH DATA

PROBE	a	b_1	b_2
001 DATA	.0062.	.0508.	.0418
002 DATA	.4556.	.0214.	.0184
003 DATA	-.2479.	.0542.	.0422
004 DATA	.006.	.0449.	.0470
005 DATA	.0304.	.0503.	.0468
006 DATA	.0605.	.0408.	.0398
007 DATA	.1612.	.0462.	.0326
008 DATA	-.0102.	.0465.	.0441
009 DATA	-.0216.	.0501.	.0434
010 DATA	-.2429.	.0504.	.0513

YAW DATA

PROBE	a	b_1	b_2
001 DATA	-.1133.	.0669.	.0501
002 DATA	-.0294.	.0841.	.0904
003 DATA	-.0032.	.0776.	.0822
004 DATA	-.1475.	.0729.	.0774
005 DATA	-.0807.	.0706.	.0782
006 DATA	-.0810.	.0699.	.0728
007 DATA	-.0641.	.0928.	.0939
008 DATA	-.0864.	.1076.	.1025
009 DATA	-.1279.	.1071.	.1017
010 DATA	.1519.	.0875.	.0821

where:

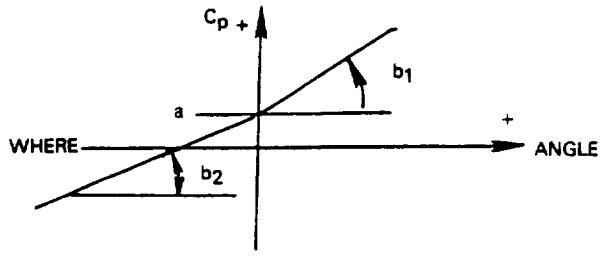

Flow angles at the mixer plane were then calculated from the multisurvey pressure data as:

$$\text{angle} = [(\Delta P/Q) - a] / b$$

where ΔP is the measured pressure difference at the model exit plane in either the pitch or yaw direction, and Q is the model free stream dymanic pressure. A complete tabulation of Q, C_p, and flow angle data for both configurations is presented from pages 172 through 185.

ANGLE (DEG) 0
YAW (DEG) -7.5

(DELTA P)/Q

RAKE	0-180	90-270
1	0.0056	-0.4896
2	0.0000	-0.7077
3	-0.2073	-0.6199
4	0.0357	-0.7277
5	0.0217	-0.6672
6	0.0634	-0.6271
7	0.1431	-0.7686
8	-0.0405	-0.8548
9	-0.0345	-0.8909
10	-0.2253	-0.4635

ANGLE (DEG) 0
YAW (DEG) 0

(DELTA P)/Q

RAKE	0-180	90-270
1	0.0052	-0.1164
2	0.0000	-0.0285
3	-0.2492	-0.0044
4	0.0056	-0.1473
5	0.0305	-0.0607
6	0.0606	-0.0811
7	0.1577	-0.0654
8	-0.0068	-0.0867
9	-0.0201	-0.1292
10	-0.2428	0.1517

ANGLE (DEG) 0
YAW (DEG) 7.5

(DELTA P)/Q

RAKE	0-180	90-270
1	0.0742	0.3882
2	0.0000	0.6015
3	-0.2703	0.5790
4	-0.0048	0.3990
5	0.0160	0.4491
6	0.0481	0.4435
7	0.1981	0.6316
8	-0.0569	0.7206
9	-0.0834	0.6757
10	-0.3180	0.8084

ANGLE (DEG)-15
YAW (DEG) 0

(DELTA P)/Q

RAKE	0-180	90-270
1	-0.5979	-0.0940
2	0.0000	-0.0265
3	-0.8790	-0.0056
4	-0.7240	-0.1257
5	-0.6787	-0.1016
6	-0.5710	-0.0582
7	-0.2952	-0.0141
8	-0.6947	-0.0586
9	-0.6578	-0.1048
10	-1.0216	0.1410

ANGLE (DEG)-7.5
YAW (DEG) 0

(DELTA P)/Q

RAKE	0-180	90-270
1	-0.3183	-0.1096
2	0.0000	-0.0312
3	-0.5655	-0.0020
4	-0.3343	-0.1336
5	-0.3175	-0.0912
6	-0.2208	-0.0908
7	-0.0996	-0.0460
8	-0.3291	-0.0804
9	-0.3543	-0.1036
10	-0.6235	0.1676

ANGLE (DEG) 7.5
YAW (DEG) 0

(DELTA P)/Q

RAKE	0-180	90-270
1	0.3807	-0.1116
2	0.0000	0.0028
3	0.1526	0.0080
4	0.3277	-0.1626
5	0.3979	-0.0827
6	0.3417	-0.0731
7	0.4947	-0.0542
8	0.3397	-0.0683
9	0.3606	-0.1132
10	0.1458	0.1357

ANGLE (DEG) 15
YAW (DEG) 0
(DELTA P)/Q

RAKE	0-180	90-270
1	0.7816	-0.1221
2	0.0000	0.0252
3	0.5767	-0.0048
4	0.7095	-0.2081
5	0.8048	-0.0292
6	0.7199	-0.0900
7	0.8780	-0.0456
8	0.6847	-0.0764
9	0.7143	-0.0660
10	0.4922	0.1024

CONFIGURATION 29
THETA(DEG)= 10.0

PROBE	Q	CP 0-180	PITCH ANGLE	CP 90-270	YAW ANGLE
1	2.4750	0.4251	8.25	-0.5042	-7.79
2	5.6210	~~0.4062~~	~~2.69~~	-0.1523	-1.36
3	5.6210	0.5960	15.57	-0.1400	-1.66
4	5.6210	0.8732	19.31	-0.2774	-1.68
5	5.6210	0.9046	17.38	-0.1094	-0.37
6	5.6210	0.5437	11.84	-0.1272	-0.63
7	5.6210	0.4499	6.25	-0.1765	-1.20
8	5.6210	0.2708	6.04	-0.2565	-1.66
9	5.6210	0.2736	5.89	-0.3610	-2.29
10	5.6210	0.0841	6.49	-0.1276	-3.40

CONFIGURATION 29
THETA(DEG)= 12.0

PROBE	Q	CP 0-180	PITCH ANGLE	CP 90-270	YAW ANGLE
1	2.4750	0.4897	9.52	-0.7697	-13.09
2	2.4750	~~1.1107~~	~~30.61~~	-0.4352	-4.49
3	5.6210	0.6289	16.18	-0.2496	-3.00
4	5.6210	0.9025	19.97	-0.3768	-2.96
5	5.6210	0.9356	18.00	-0.1140	-0.43
6	5.6210	0.5549	12.12	-0.0569	0.34
7	5.6210	0.4631	6.53	-0.1151	-0.54
8	5.6210	0.2930	6.52	-0.2037	-1.14
9	5.6210	0.2944	6.31	-0.3115	-1.81
10	5.6210	0.1027	6.86	-0.1059	-3.14

CONFIGURATION 29
THETA(DEG)= 14.0

PROBE	Q	CP 0-180	PITCH ANGLE	CP 90-270	YAW ANGLE
1	2.4750	0.3794	7.35	-0.8695	-15.08
2	2.4750	~~0.9774~~	~~24.38~~	-1.2089	-13.05
3	5.6210	0.6732	16.99	-0.3656	-4.41
4	5.6210	0.9148	20.24	-0.4663	-4.12
5	5.6210	0.9811	18.90	-0.1071	-0.34
6	5.6210	0.5198	11.26	0.0347	1.66
7	5.6210	0.4499	6.25	-0.0667	-0.03
8	5.6210	0.2889	6.43	-0.1560	-0.68
9	5.6210	0.2943	6.30	-0.2597	-1.30
10	5.6210	0.1087	6.98	-0.0701	-2.70

CONFIGURATION 29
THETA(DEG)= 16.0

PROBE	Q	CP 0-180	PITCH ANGLE	CP 90-270	YAW ANGLE
1	2.4750	0.2004	3.82	-0.7867	-13.43
2	2.4750	~~-0.2469~~	~~-11.34~~	-0.7071	-7.50
3	2.4750	1.2630	27.88	-1.4238	-17.28
4	2.4750	1.1156	24.71	-1.3325	-15.31
5	2.4750	1.3984	27.20	-0.9337	-10.91
6	5.6210	0.4264	8.97	0.1238	2.93
7	5.6210	0.4151	5.49	-0.0395	0.27
8	5.6210	0.2530	5.66	-0.1142	-0.27
9	5.6210	0.2596	5.61	-0.2055	-0.76
10	5.6210	0.0874	6.55	-0.0100	-1.97

CONFIGURATION 29
THETA(DEG)= 18.0

PROBE	Q	CP 0-180	PITCH ANGLE	CP 90-270	YAW ANGLE
1	2.4750	0.2069	3.95	-0.6655	-11.01
2	2.4750	~~-0.2897~~	~~-9.02~~	-0.7923	-8.44
3	2.4750	-0.9507	-16.65	-0.3224	-3.88
4	2.4750	-0.6731	-14.45	-0.1774	-0.39
5	2.4750	-0.5188	-11.73	0.0044	1.21
6	5.6210	0.2839	5.48	0.0929	2.49
7	5.6210	0.3782	4.70	-0.0560	0.09
8	5.6210	0.2154	4.85	-0.1030	-0.16
9	5.6210	0.2240	4.90	-0.1727	-0.44
10	5.6210	0.0633	6.08	0.0464	-1.28

CONFIGURATION 29
THETA(DEG)= 20.0

PROBE	Q	CP 0-180	PITCH ANGLE	CP 90-270	YAW ANGLE
1	2.4750	0.2020	3.85	-0.3984	-5.68
2	2.4750	~~-0.3713~~	~~-4.58~~	-0.3564	-3.62
3	2.4750	-0.7568	-12.06	-0.1511	-1.80
4	2.4750	-0.6323	-13.58	-0.1956	-0.62
5	2.4750	-0.4493	-10.25	-0.1208	-0.51
6	5.6210	0.3402	6.85	-0.2649	-2.53
7	5.6210	0.3571	4.24	-0.2514	-1.99
8	5.6210	0.2012	4.55	-0.2487	-1.58
9	5.6210	0.2231	4.88	-0.2688	-1.39
10	5.6210	0.0548	5.91	0.0125	-1.70

CONFIGURATION 29
THETA(DEG)= 22.0

PROBE	Q	CP 0-180	PITCH ANGLE	CP 90-270	YAW ANGLE
1	2.4750	0.1968	3.75	-0.1374	-0.47
2	2.4750	~~0.3556~~	~~-5.44~~	0.0323	0.73
3	2.4750	-0.7964	-13.00	0.1014	1.35
4	2.4750	-0.6404	-13.75	-0.2097	-0.80
5	2.4750	-0.5257	-11.88	-0.2024	-1.56
6	5.6210	0.3021	5.92	-0.5657	-6.66
7	5.6210	0.3499	4.09	-0.3921	-3.49
8	5.6210	0.1845	4.19	-0.3729	-2.79
9	5.6210	0.2049	4.52	-0.3724	-2.40
10	5.6210	0.0342	5.50	-0.0566	-2.54

CONFIGURATION 29
THETA(DEG)= 24.0

PROBE	Q	CP 0-180	PITCH ANGLE	CP 90-270	YAW ANGLE
1	2.4750	0.1426	2.69	0.1063	3.29
2	2.4750	~~0.3285~~	~~-6.91~~	0.1442	2.06
3	2.4750	-0.6432	-9.37	0.4028	5.23
4	2.4750	0.4259	9.35	0.4190	7.77
5	5.6210	0.9891	19.06	0.0324	1.60
6	5.6210	0.4021	8.37	-0.5072	-5.85
7	5.6210	0.3579	4.26	-0.4051	-3.63
8	5.6210	0.1824	4.14	-0.3930	-2.99
9	5.6210	0.1946	4.32	-0.3939	-2.62
10	5.6210	0.0253	5.32	-0.0875	-2.92

CONFIGURATION 29
THETA(DEG)= 26.0

PROBE	Q	CP 0-180	PITCH ANGLE	CP 90-270	YAW ANGLE
1	2.4750	0.3192	6.16	0.1382	3.77
2	2.4750	~~0.0614~~	~~21.42~~	0.5887	7.35
3	5.6210	0.7385	18.20	0.2092	2.74
4	5.6210	0.9714	21.50	-0.1585	-0.14
5	5.6210	0.9370	18.02	-0.2179	-1.75
6	5.6210	0.4821	10.33	-0.4010	-4.40
7	5.6210	0.4099	5.38	-0.3594	-3.14
8	5.6210	0.2272	5.11	-0.3501	-2.57
9	5.6210	0.2364	5.15	-0.3501	-2.19
10	5.6210	0.0578	5.97	-0.0466	-2.42

CONFIGURATION 29
THETA(DEG)= 28.0

PROBE	Q	CP 0-180	PITCH ANGLE	CP 90-270	YAW ANGLE
1	2.4750	0.4804	9.33	-0.0105	1.54
2	5.6210	~~0.4739~~	~~0.86~~	0.0181	0.57
3	5.6210	0.6908	17.32	-0.0116	-0.10
4	5.6210	0.9393	20.79	-0.2608	-1.46
5	5.6210	0.8927	17.14	-0.2167	-1.74
6	5.6210	0.5257	11.40	-0.3142	-3.20
7	5.6210	0.4579	6.42	-0.3138	-2.66
8	5.6210	0.2750	6.13	-0.3149	-2.23
9	5.6210	0.2804	6.03	-0.3225	-1.91
10	5.6210	0.0890	6.58	-0.0265	-2.17

CONFIGURATION 29
THETA(DEG)= 30.0

PROBE	Q	CP 0-180	PITCH ANGLE	CP 90-270	YAW ANGLE
1	2.4750	0.4901	9.53	-0.3632	-4.98
2	5.6210	~~0.4232~~	~~1.76~~	-0.2140	-2.04
3	5.6210	0.6602	16.75	-0.1101	-1.30
4	5.6210	0.9159	20.26	-0.3428	-2.52
5	5.6210	0.8781	16.85	-0.2062	-1.60
6	5.6210	0.5389	11.72	-0.2393	-2.17
7	5.6210	0.4791	6.88	-0.2610	-2.10
8	5.6210	0.3042	6.76	-0.2786	-1.88
9	5.6210	0.2937	6.29	-0.2989	-1.68
10	5.6210	0.0978	6.76	-0.0164	-2.05

CONFIGURATION 29
THETA(DEG)= 32.0

PROBE	Q	CP 0-180	PITCH ANGLE	CP 90-270	YAW ANGLE
1	2.4750	0.4396	8.53	-0.7099	-11.90
2	2.4750	~~1.1006~~	~~30.14~~	-0.2287	-2.20
3	5.6210	0.6682	16.90	-0.2138	-2.56
4	5.6210	0.9160	20.27	-0.4366	-3.73
5	5.6210	0.8941	17.17	-0.1968	-1.48
6	5.6210	0.5401	11.76	-0.1649	-1.15
7	5.6210	0.4743	6.78	-0.2062	-1.51
8	5.6210	0.3005	6.68	-0.2425	-1.52
9	5.6210	0.2903	6.23	-0.2814	-1.51
10	5.6210	0.0966	6.74	-0.0109	-1.98

CONFIGURATION 29
THETA(DEG)= 34.0

PROBE	Q	CP 0-180	PITCH ANGLE	CP 90-270	YAW ANGLE
1	2.4750	0.3964	7.68	-0.8699	-15.09
2	2.4750	~~0.9200~~	~~21.70~~	-0.9588	-10.28
3	5.6210	0.7122	17.71	-0.3117	-3.75
4	5.6210	0.9126	20.19	-0.5090	-4.67
5	5.6210	0.9319	17.92	-0.1523	-0.92
6	5.6210	0.5170	11.19	-0.0744	0.09
7	5.6210	0.4474	6.20	-0.1582	-1.00
8	5.6210	0.2765	6.16	-0.2074	-1.18
9	5.6210	0.2733	5.89	-0.2581	-1.28
10	5.6210	0.0856	6.52	0.0087	-1.74

CONFIGURATION 29
THETA(DEG)= 36.0

PROBE	Q	CP 0-180	PITCH ANGLE	CP 90-270	YAW ANGLE
1	2.4750	0.2307	4.42	-0.8154	-14.00
2	2.4750	~~0.1034~~	~~19.14~~	-0.6954	-7.37
3	2.4750	1.6905	35.76	-1.2893	-15.65
4	2.4750	1.8040	40.05	-1.6089	-18.88
5	2.4750	2.0703	40.55	-1.0283	-12.12
6	5.6210	0.4408	9.32	0.0541	1.93
7	5.6210	0.4038	5.25	-0.1007	-0.39
8	5.6210	0.2334	5.24	-0.1564	-0.68
9	5.6210	0.2377	5.18	-0.2172	-0.88
10	5.6210	0.0644	6.10	0.0436	-1.32

CONFIGURATION 29
THETA(DEG)= 38.0

PROBE	Q	CP 0-180	PITCH ANGLE	CP 90-270	YAW ANGLE
1	2.4750	0.2602	5.00	-0.7180	-12.06
2	2.4750	~~0.3014~~	~~8.38~~	-0.8889	-9.51
3	2.4750	-0.8966	-15.37	-0.3438	-4.14
4	2.4750	-0.6295	-13.52	-0.1543	-0.09
5	2.4750	-0.4982	-11.29	-0.0242	0.80
6	5.6210	0.3400	6.85	0.1192	2.86
7	5.6210	0.3716	4.56	-0.0857	-0.23
8	5.6210	0.2023	4.57	-0.1379	-0.50
9	5.6210	0.2169	4.76	-0.2010	-0.72
10	5.6210	0.0463	5.74	0.0726	-0.97

CONFIGURATION 29
THETA(DEG)= 40.0

PROBE	Q	CP 0-180	PITCH ANGLE	CP 90-270	YAW ANGLE
1	2.4750	0.2570	4.94	-0.4925	-7.56
2	2.4750	-0.4012	-2.96	-0.5095	-5.31
3	2.4750	-0.6954	-10.60	-0.2800	-3.37
4	2.4750	-0.6174	-13.26	-0.2105	-0.81
5	2.4750	-0.4683	-10.66	-0.1168	-0.46
6	5.6210	0.5896	12.97	-0.1622	-1.12
7	5.6210	0.3435	3.95	-0.2581	-2.07
8	5.6210	0.1925	4.36	-0.2864	-1.95
9	5.6210	0.2275	4.97	-0.3240	-1.93
10	5.6210	0.0521	5.85	-0.0167	-2.05

CONFIGURATION 29
THETA(DEG)= 42.0

PROBE	Q	CP 0-180	PITCH ANGLE	CP 90-270	YAW ANGLE
1	2.4750	0.2283	4.37	-0.2497	-2.71
2	2.4750	-0.3919	-3.46	-0.1172	-0.97
3	2.4750	-0.7390	-11.64	0.0117	0.19
4	2.4750	-0.6897	-14.80	-0.1628	-0.20
5	2.4750	-0.5640	-12.70	-0.2400	-2.04
6	5.6210	0.2987	5.84	-0.5355	-6.24
7	5.6210	0.3362	3.79	-0.4220	-3.81
8	5.6210	0.1866	4.23	-0.4261	-3.31
9	5.6210	0.2130	4.68	-0.4394	-3.06
10	5.6210	0.0242	5.30	-0.1041	-3.12

CONFIGURATION 29
THETA(DEG)= 44.0

PROBE	Q	CP 0-180	PITCH ANGLE	CP 90-270	YAW ANGLE
1	2.4750	0.2020	3.85	0.0246	2.07
2	2.4750	-0.3576	-5.33	0.2428	3.24
3	2.4750	-0.7406	-11.68	0.0525	0.72
4	2.4750	-0.1277	-2.84	0.3543	6.88
5	2.4750	1.7527	34.24	0.1725	3.59
6	5.6210	0.3944	8.18	-0.5270	-6.13
7	5.6210	0.3508	4.10	-0.4755	-4.38
8	5.6210	0.1889	4.28	-0.4871	-3.91
9	5.6210	0.1959	4.34	-0.4910	-3.57
10	5.6210	0.0059	4.94	-0.1461	-3.63

CONFIGURATION 29
THETA(DEG)= 46.0

PROBE	Q	CP 0-180	PITCH ANGLE	CP 90-270	YAW ANGLE
1	2.4750	0.3022	5.83	0.0719	2.78
2	2.4750	~~-0.2586~~	~~10.71~~	0.1519	2.16
3	5.6210	0.7714	18.81	0.2830	3.69
4	5.6210	0.8870	19.62	-0.1007	0.64
5	5.6210	0.9096	17.48	-0.2407	-2.05
6	5.6210	0.4535	9.63	-0.4051	-4.45
7	5.6210	0.3891	4.93	-0.4167	-3.75
8	5.6210	0.2222	5.00	-0.4280	-3.33
9	5.6210	0.2316	5.05	-0.4373	-3.04
10	5.6210	0.0343	5.50	-0.1055	-3.14

CONFIGURATION 29
THETA(DEG)= 48.0

PROBE	Q	CP 0-180	PITCH ANGLE	CP 90-270	YAW ANGLE
1	2.4750	0.4267	8.28	-0.0283	1.28
2	5.6210	~~-0.2854~~	~~-9.25~~	0.1329	1.93
3	5.6210	0.6936	17.37	-0.0059	-0.03
4	5.6210	0.8577	18.97	-0.1969	-0.64
5	5.6210	0.8525	16.34	-0.1930	-1.44
6	5.6210	0.4944	10.63	-0.3133	-3.19
7	5.6210	0.4352	5.93	-0.3659	-3.21
8	5.6210	0.2645	5.91	-0.3861	-2.92
9	5.6210	0.2713	5.85	-0.4079	-2.75
10	5.6210	0.0637	6.08	-0.0863	-2.90

CONFIGURATION 29
THETA(DEG)= 50.0

PROBE	Q	CP 0-180	PITCH ANGLE	CP 90-270	YAW ANGLE
1	2.4750	0.3770	7.30	-0.3814	-5.34
2	5.6210	~~-0.3503~~	~~-5.72~~	-0.2019	-1.91
3	5.6210	0.6127	15.88	-0.1041	-1.23
4	5.6210	0.8605	19.03	-0.2777	-1.68
5	5.6210	0.8276	15.85	-0.1662	-1.09
6	5.6210	0.5248	11.38	-0.2341	-2.10
7	5.6210	0.4629	6.53	-0.3104	-2.62
8	5.6210	0.2921	6.50	-0.3421	-2.49
9	5.6210	0.2880	6.18	-0.3674	-2.35
10	5.6210	0.0809	6.43	-0.0747	-2.76

CONFIGURATION 34
THETA(DEG)= 10.0

PROBE	Q	CP 0-180	PITCH ANGLE	CP 90-270	YAW ANGLE
1	3.4303	0.7620	14.88	-0.3402	-4.52
2	3.4303	~~0.4927~~	~~1.73~~	-0.2434	-2.37
3	6.5491	0.7766	18.90	-0.1232	-1.46
4	6.5491	1.0279	22.76	-0.3199	-2.23
5	6.5491	1.0919	21.10	-0.0927	-0.15
6	6.5491	0.9368	21.48	-0.1440	-0.87
7	6.5491	0.9065	16.13	-0.1040	-0.42
8	6.5491	0.6871	15.00	-0.1338	-0.46
9	6.5491	0.6547	13.50	-0.2014	-0.72
10	6.5491	0.3788	12.34	0.0046	-1.79

CONFIGURATION 34
THETA(DEG)= 12.0

PROBE	Q	CP 0-180	PITCH ANGLE	CP 90-270	YAW ANGLE
1	3.4303	0.7448	14.54	-0.5376	-8.46
2	3.4303	~~0.0670~~	~~21.12~~	-0.2662	-2.62
3	6.5491	0.7680	18.74	-0.1654	-1.97
4	6.5491	1.0356	22.93	-0.3604	-2.75
5	6.5491	1.0733	20.73	-0.1099	-0.37
6	6.5491	0.9355	21.45	-0.1603	-1.09
7	6.5491	0.9143	16.30	-0.0852	-0.22
8	6.5491	0.7039	15.36	-0.0838	0.02
9	6.5491	0.6729	13.86	-0.1040	0.22
10	6.5491	0.3947	12.65	0.0632	-1.08

CONFIGURATION 34
THETA(DEG)= 14.0

PROBE	Q	CP 0-180	PITCH ANGLE	CP 90-270	YAW ANGLE
1	3.4303	0.6909	13.48	-0.6588	-10.88
2	3.4303	~~0.4947~~	~~1.83~~	-0.5842	-6.14
3	6.5491	0.8261	19.81	-0.2019	-2.42
4	6.5491	1.0582	23.43	-0.4074	-3.36
5	6.5491	1.0873	21.01	-0.1455	-0.83
6	6.5491	0.9418	21.60	-0.1832	-1.40
7	6.5491	0.9623	17.34	-0.0883	-0.26
8	6.5491	0.7477	16.30	-0.0421	0.41
9	6.5491	0.6911	14.23	-0.0024	1.17
10	6.5491	0.3895	12.55	0.1414	-0.13

CONFIGURATION 34
THETA(DEG)= 16.0

PROBE	Q	CP 0-180	PITCH ANGLE	CP 90-270	YAW ANGLE
1	3.4303	0.6880	13.42	-0.6889	-11.48
2	3.4303	~~0.4877~~	~~1.50~~	-0.9798	-10.51
3	3.4303	1.5923	33.95	-0.7632	-9.25
4	6.5491	1.0863	24.06	-0.4657	-4.11
5	6.5491	1.0400	20.07	-0.2138	-1.70
6	6.5491	0.9241	21.17	-0.2387	-2.17
7	6.5491	0.9522	17.12	-0.1623	-1.05
8	6.5491	0.8209	17.87	-0.0626	0.22
9	6.5491	0.7421	15.24	0.1496	2.59
10	6.5491	0.3440	11.65	0.2715	1.37

CONFIGURATION 34
THETA(DEG)= 18.0

PROBE	Q	CP 0-180	PITCH ANGLE	CP 90-270	YAW ANGLE
1	3.4303	0.6346	12.37	-0.6049	-9.80
2	3.4303	~~0.4559~~	~~0.02~~	-0.8160	-8.70
3	3.4303	-0.6134	-8.66	-0.5536	-6.70
4	3.4303	0.9005	19.92	-0.9699	-10.63
5	3.4303	-0.0300	-1.29	-0.8597	-9.96
6	3.4303	-0.5478	-15.28	-0.6107	-7.28
7	3.4303	-0.1513	-9.59	-0.1586	-1.01
8	3.4303	-0.3632	-8.01	-0.3035	-2.12
9	3.4303	1.3768	27.91	-0.1356	-0.08
10	6.5491	0.2223	9.23	0.3826	2.64

CONFIGURATION 34
THETA(DEG)= 20.0

PROBE	Q	CP 0-180	PITCH ANGLE	CP 90-270	YAW ANGLE
1	3.4303	0.6061	11.81	-0.3723	-5.16
2	3.4303	~~0.4828~~	~~1.27~~	-0.3822	-3.90
3	3.4303	-0.6034	-8.43	-0.2370	-2.84
4	3.4303	-1.2999	-27.78	-0.1061	0.57
5	3.4303	-1.2579	-27.53	-0.0041	1.09
6	3.4303	-0.9565	-25.55	-0.0356	0.65
7	3.4303	-0.3452	-15.53	-0.0458	0.20
8	3.4303	-0.7008	-15.66	-0.0738	0.12
9	3.4303	-0.0437	-0.51	-0.0965	0.29
10	6.5491	0.1745	8.28	0.0531	-1.20

CONFIGURATION 34
THETA(DEG)= 22.0

PROBE	Q	CP 0-180	PITCH ANGLE	CP 90-270	YAW ANGLE
1	3.4303	0.5693	11.09	-0.2189	-2.10
2	3.4303	-0.5082	-2.22	-0.1149	-0.95
3	3.4303	-0.5102	-6.21	0.0726	0.98
4	3.4303	-1.3028	-27.85	0.0105	2.17
5	3.4303	-1.2250	-26.82	0.0050	1.21
6	3.4303	-0.9084	-24.34	-0.0740	0.10
7	3.4303	-0.3592	-15.96	-0.1525	-0.94
8	3.4303	-0.7101	-15.87	-0.2216	-1.32
9	3.4303	-0.1306	-2.51	-0.1965	-0.67
10	6.5491	0.2635	10.05	-0.2373	-4.74

CONFIGURATION 34
THETA(DEG)= 24.0

PROBE	Q	CP 0-180	PITCH ANGLE	CP 90-270	YAW ANGLE
1	3.4303	0.5795	11.29	0.0012	1.72
2	3.4303	-0.5093	-2.51	0.2758	3.63
3	6.5491	-0.1188	2.38	0.1976	2.59
4	6.5491	1.0464	23.17	0.1177	3.64
5	6.5491	1.0808	20.88	0.1819	3.72
6	6.5491	0.9623	22.10	-0.0444	0.52
7	6.5491	0.9818	17.76	-0.1750	-1.18
8	6.5491	0.8271	18.01	-0.3628	-2.70
9	6.5491	0.7561	15.52	-0.6021	-4.66
10	6.5491	0.2965	10.70	-0.2014	-4.30

CONFIGURATION 34
THETA(DEG)= 26.0

PROBE	Q	CP 0-180	PITCH ANGLE	CP 90-270	YAW ANGLE
1	3.4303	0.7151	13.95	0.0915	3.07
2	3.4303	-0.5070	-2.40	0.3647	4.69
3	6.5491	0.8415	20.10	0.1006	1.34
4	6.5491	1.0747	23.80	-0.2148	-0.87
5	6.5491	1.0844	20.95	-0.0570	0.34
6	6.5491	0.9340	21.41	-0.1878	-1.47
7	6.5491	0.9108	16.23	-0.2495	-1.97
8	6.5491	0.7274	15.86	-0.3533	-2.60
9	6.5491	0.6879	14.16	-0.4323	-2.99
10	6.5491	0.3477	11.72	-0.1090	-3.18

CONFIGURATION 34
THETA(DEG)= 28.0

PROBE	Q	CP 0-180	PITCH ANGLE	CP 90-270	YAW ANGLE
1	3.4303	0.7154	13.96	0.0274	2.11
2	3.4303	~~0.5358~~	~~3.75~~	0.1219	1.80
3	6.5491	0.8053	19.43	-0.0658	-0.76
4	6.5491	1.0545	23.35	-0.2608	-1.46
5	6.5491	1.0766	20.80	-0.0818	-0.01
6	6.5491	0.9250	21.19	-0.2006	-1.64
7	6.5491	0.8868	15.71	-0.2321	-1.79
8	6.5491	0.6857	14.97	-0.2884	-1.97
9	6.5491	0.6802	14.01	-0.3384	-2.07
10	6.5491	0.3833	12.42	-0.0453	-2.40

CONFIGURATION 34
THETA(DEG)= 30.0

PROBE	Q	CP 0-180	PITCH ANGLE	CP 90-270	YAW ANGLE
1	3.4303	0.7093	13.84	-0.1702	-1.13
2	6.5491	~~0.2361~~	~~11.93~~	-0.1205	-1.01
3	6.5491	0.7277	18.00	-0.1110	-1.31
4	6.5491	1.0340	22.90	-0.3095	-2.09
5	6.5491	1.0783	20.83	-0.1096	-0.37
6	6.5491	0.9111	20.85	-0.2124	-1.80
7	6.5491	0.8850	15.67	-0.2051	-1.50
8	6.5491	0.6842	14.93	-0.2266	-1.37
9	6.5491	0.6777	13.96	-0.2608	-1.31
10	6.5491	0.3842	12.44	0.0070	-1.76

CONFIGURATION 34
THETA(DEG)= 32.0

PROBE	Q	CP 0-180	PITCH ANGLE	CP 90-270	YAW ANGLE
1	3.4303	0.7081	13.82	-0.4000	-5.71
2	3.4303	~~0.4262~~	~~1.60~~	-0.2411	-2.34
3	6.5491	0.7442	18.30	-0.1307	-1.55
4	6.5491	1.0466	23.17	-0.3571	-2.71
5	6.5491	1.0685	20.64	-0.1298	-0.63
6	6.5491	0.9046	20.69	-0.2167	-1.86
7	6.5491	0.8954	15.89	-0.1780	-1.21
8	6.5491	0.6964	15.20	-0.1727	-0.84
9	6.5491	0.6751	13.91	-0.1845	-0.56
10	6.5491	0.3773	12.31	0.0644	-1.07

CONFIGURATION 34
THETA(DEG)= 34.0

PROBE	Q	CP 0-180	PITCH ANGLE	CP 90-270	YAW ANGLE
1	3.4303	0.6615	12.90	-0.5521	-8.75
2	3.4303	~~-0.4962~~	~~1.90~~	-0.4956	-5.16
3	6.5491	0.8097	19.51	-0.1732	-2.07
4	6.5491	1.0698	23.69	-0.3941	-3.19
5	6.5491	1.0765	20.80	-0.1519	-0.91
6	6.5491	0.9020	20.62	-0.2280	-2.02
7	6.5491	0.9017	16.03	-0.1553	-0.97
8	6.5491	0.7033	15.34	-0.1185	-0.31
9	6.5491	0.6778	13.96	-0.1084	0.18
10	6.5491	0.3639	12.04	0.1203	-0.38

CONFIGURATION 34
THETA(DEG)= 36.0

PROBE	Q	CP 0-180	PITCH ANGLE	CP 90-270	YAW ANGLE
1	3.4303	0.6857	13.38	-0.6102	-9.91
2	3.4303	~~-0.4790~~	~~1.09~~	-0.9098	-9.74
3	3.4303	1.6850	35.66	-0.6104	-7.39
4	6.5491	1.0977	24.31	-0.4349	-3.71
5	6.5491	1.0415	20.10	-0.1849	-1.33
6	6.5491	0.8896	20.32	-0.2406	-2.19
7	6.5491	0.9181	16.38	-0.1596	-1.02
8	6.5491	0.7451	16.24	-0.0841	0.02
9	6.5491	0.6943	14.29	0.0218	1.40
10	6.5491	0.3210	11.19	0.2125	0.69

CONFIGURATION 34
THETA(DEG)= 38.0

PROBE	Q	CP 0-180	PITCH ANGLE	CP 90-270	YAW ANGLE
1	3.4303	0.6437	12.55	-0.5574	-8.85
2	3.4303	~~-0.4539~~	~~0.09~~	-0.7932	-8.45
3	3.4303	-0.1367	2.05	-0.5927	-7.17
4	3.4303	1.9322	42.90	-1.1859	-13.42
5	3.4303	1.5209	29.63	-1.0361	-12.22
6	3.4303	1.2139	28.27	-1.0285	-13.01
7	3.4303	1.1786	22.02	-1.1229	-11.28
8	3.4303	1.5555	33.67	-0.9874	-8.79
9	3.4303	1.7159	34.68	0.1367	2.47
10	6.5491	0.2666	10.11	0.3353	2.10

CONFIGURATION 34
THETA(DEG)= 40.0

PROBE	Q	CP 0-180	PITCH ANGLE	CP 90-270	YAW ANGLE
1	3.4303	0.5816	11.33	-0.3731	-5.18
2	3.4303	~~-0.4656~~	~~-0.47~~	-0.4186	-4.31
3	3.4303	-0.6685	-9.97	-0.2979	-3.59
4	3.4303	-1.2054	-25.78	-0.0880	0.82
5	3.4303	-1.1705	-25.66	0.0146	1.35
6	3.4303	-0.8979	-24.08	-0.0055	1.08
7	3.4303	-0.2863	-13.73	0.0367	1.09
8	3.4303	-0.6588	-14.71	0.0096	0.89
9	3.4303	0.0309	1.05	-0.1688	-0.40
10	6.5491	0.1927	8.64	0.1312	-0.25

CONFIGURATION 34
THETA(DEG)= 42.0

PROBE	Q	CP 0-180	PITCH ANGLE	CP 90-270	YAW ANGLE
1	3.4303	0.5329	10.37	-0.1854	-1.43
2	3.4303	~~-0.5151~~	~~-2.78~~	-0.1023	-0.81
3	3.4303	-0.4903	-5.74	0.0507	0.69
4	3.4303	-1.2011	-25.68	-0.0449	1.41
5	3.4303	-1.2016	-26.33	0.0332	1.61
6	3.4303	-0.9262	-24.79	-0.0204	0.87
7	3.4303	-0.3306	-15.09	-0.0426	0.23
8	3.4303	-0.7460	-16.68	-0.1076	-0.21
9	3.4303	-0.3574	-7.74	-0.0464	0.76
10	6.5491	0.2939	10.65	-0.2295	-4.65

CONFIGURATION 34
THETA(DEG)= 44.0

PROBE	Q	CP 0-180	PITCH ANGLE	CP 90-270	YAW ANGLE
1	3.4303	0.5982	11.65	0.0329	2.19
2	3.4303	~~-0.5344~~	~~-3.68~~	0.2781	3.66
3	6.5491	-0.2077	0.74	0.2237	2.92
4	6.5491	0.9969	22.07	0.1391	3.93
5	6.5491	1.0024	19.32	0.2385	4.52
6	6.5491	0.8792	20.07	0.0353	1.66
7	6.5491	0.9349	16.75	-0.1193	-0.59
8	6.5491	0.8168	17.78	-0.3017	-2.10
9	6.5491	0.8058	16.51	-0.6233	-4.87
10	6.5491	0.3110	10.99	-0.2532	-4.93

CONFIGURATION 34
THETA(DEG)= 46.0

PROBE	Q	CP 0-180	PITCH ANGLE	CP 90-270	YAW ANGLE
1	3.4303	0.6842	13.35	0.0997	3.19
2	3.4303	0.4979	1.98	0.3781	4.85
3	6.5491	0.8184	19.67	0.1674	2.20
4	6.5491	1.0863	24.06	-0.2135	-0.85
5	6.5491	1.0438	20.15	-0.0510	0.42
6	6.5491	0.8855	20.22	-0.1805	-1.37
7	6.5491	0.8792	15.54	-0.2530	-2.01
8	6.5491	0.7148	15.59	-0.3677	-2.74
9	6.5491	0.7120	14.64	-0.4762	-3.43
10	6.5491	0.3568	11.90	-0.1599	-3.80

CONFIGURATION 34
THETA(DEG)= 48.0

PROBE	Q	CP 0-180	PITCH ANGLE	CP 90-270	YAW ANGLE
1	3.4303	0.6798	13.26	0.0536	2.50
2	3.4303	0.5105	2.56	0.2218	2.99
3	6.5491	0.8394	20.06	-0.0424	-0.48
4	6.5491	1.0447	23.13	-0.2365	-1.15
5	6.5491	1.0412	20.10	-0.0687	0.17
6	6.5491	0.8844	20.19	-0.1925	-1.53
7	6.5491	0.8806	15.57	-0.2471	-1.95
8	6.5491	0.6948	15.16	-0.3123	-2.20
9	6.5491	0.6983	14.37	-0.3816	-2.49
10	6.5491	0.3794	12.35	-0.0939	-2.99

CONFIGURATION 34
THETA(DEG)= 50.0

PROBE	Q	CP 0-180	PITCH ANGLE	CP 90-270	YAW ANGLE
1	3.4303	0.5720	11.14	-0.1580	-0.88
2	6.5491	0.2709	10.04	-0.0771	-0.53
3	6.5491	0.7667	18.72	-0.1028	-1.21
4	6.5491	1.0316	22.84	-0.2661	-1.53
5	6.5491	1.0371	20.01	-0.0838	-0.04
6	6.5491	0.8873	20.26	-0.2043	-1.69
7	6.5491	0.8688	15.32	-0.2391	-1.86
8	6.5491	0.6773	14.79	-0.2765	-1.85
9	6.5491	0.6871	14.15	-0.3171	-1.86
10	6.5491	0.3970	12.70	-0.0429	-2.37

LIST OF DISTRIBUTION

NASA Headquarters
600 Independence Ave. SW
Washington, D. C. 20546
Attention: R/R.S. Colladay RT-6

NASA Headquarters
600 Independence Ave. SW
Washington, D. C. 20546
Attention: RT/C.C. Rosen RTP-6

NASA-Lewis Research Center
21000 Brookpark Road
Cleveland, Ohio 44135
Attention: RJP/L. Wright

NASA Headquarters
600 Independence Ave. SW
Washington, D. C. 20546
Attention: J. Facey RTP-6

NASA-Lewis Research Center
21000 Brookpark Road
Cleveland, Ohio 44135
Attention: J.A. Ziemianski MS 49-6

NASA-Lewis Research Center
21000 Brookpark Road
Cleveland, Ohio 44135
Attention: C.C. Ciepluch MS 100-3

NASA-Lewis Research Center
21000 Brookpark Road
Cleveland, Ohio 44135
Attention: P.G. Batterton MS 301-4

NASA-Lewis Research Center
21000 Brookpark Road
Cleveland, Ohio 44135
Attention: G.M. Sievers MS 301-2

NASA-Lewis Research Center
21000 Brookpark Road
Cleveland, Ohio 44135
Attention: E.T. Meleason MS 49-6
(10 Copies)

NASA-Lewis Research Center
21000 Brookpark Road
Cleveland, Ohio 44135
Attention: M.A. Beheim MS-3-5

NASA-Lewis Research Center
21000 Brookpark Road
Cleveland, Ohio 44135
Attention: N.T. Saunders MS-3-8

NASA-Lewis Research Center
21000 Brookpark Road
Cleveland, Ohio 44135
Attention: M.J. Hartmann MS-3-7

NASA-Lewis Research Center
21000 Brookpark Road
Cleveland, Ohio 44135
Attention: J.C. Williams MS-500-211

NASA-Lewis Research Center
21000 Brookpark Road
Cleveland, Ohio 44135
Attention: L.J. Kaszubinski MS-86-2

NASA-Lewis Research Center
21000 Brookpark Road
Cleveland, Ohio 44135
Attention: L.J. Kiraly MS 23-2

NASA-Lewis Research Center
21000 Brookpark Road
Cleveland, Ohio 44135
Attention: D.C. Mikkelson MS 86-1

NASA-Lewis Research Center
21000 Brookpark Road
Cleveland, Ohio 44135
Attention: L.J. Thomas MS 500-305

NASA-Lewis Research Center
21000 Brookpark Road
Cleveland, Ohio 44135
Attention: J.F. Groeneweg MS 54-3

NASA-Lewis Research Center
21000 Brookpark Road
Cleveland, Ohio 44135
Attention: R.L. Davies MS 105-1

NASA-Lewis Research Center
21000 Brookpark Road
Cleveland, Ohio 44135
Attention: R. H. Johns MS 49-6

NASA-Lewis Research Center
21000 Brookpark Road
Cleveland, Ohio 44135
Attention: J.R. Mihaloew MS 100-1

NASA-Lewis Research Center
21000 Brookpark Road
Cleveland, Ohio 44135 MS 5-9
Attention: L. Reid

NASA-Lewis Research Center
21000 Brookpark Road
Cleveland, Ohio 44135 MS 86-2
Attention: D.W.Drier

NASA-Lewis Research Center
21000 Brookpark Road
Cleveland, Ohio 44135
Attention: R.W. Niedzwiecki MS 86-6

NASA-Lewis Research Center
21000 Brookpark Road
Cleveland, Ohio 44135
Attention: AFSC Liaison Office
MS 501-3

NASA-Lewis Research Center
21000 Brookpark Road
Cleveland, Ohio 44135 MS 302-2
Attention: Army R&T Propulsion

NASA Ames Research Center
Moffett Field, CA 94035
Attention: 202-7/M. H. Waters
(2)

NASA Langley Research Center
Langley Field, VA 23365
Attention: Bob James
Neil Driver
L.J. Williams (3)

NASA Dryden Flight Research Center
P.O. Box 273
Edwards, CA 93523
Attention: J. A. Albers

Department of Defense
Washington, D.C. 20301
Attention: R. Standahar 3D1089 Pentagon

Wright-Patterson Air Force Base
Dayton, Ohio 45433
Attention: APL Chief Scientist AFWAL/PS

Wright-Patterson Air Force Base
Dayton, Ohio 45433
Attention: E.E. Abell ASD/YZE

Wright-Patterson Air Force Base
Dayton, Ohio 45433
Attention: H.I. Bush AFWAL/POT

Wright-Patterson Air Force Base
Dayton, Ohio 45433
Attention: E.E. Bailey (NASA Liaison)
AFWAL/NASA

Wright-Patterson Air Force Base
Dayton, Ohio 45433
Attention: R.P. Carmichael ASD/XRHI

Wright-Patterson Air Force Base
Dayton, Ohio 45433
Attention: R. Ellis ASD/YZN

Wright-Patterson Air Force Base
Dayton, Ohio 45433
Attention: W.H. Austin, Jr. ASD/ENF

Eustis Directorate
U.S. Army Air Mobility
R&D Laboratory
Fort Eustis, VA 23604
Attention: J. Lane, SAVDL-EU-Tapp

Navy Department
Naval Air Systems Command
Washington, D. C. 20361
Attention: W. Koven AIR-03E

Navy Department
Naval Air Systems Command
Washington, D. C. 20361
Attention: J.L. Byers AIR-53602

Navy Department
Naval Air Systems Command
Washington, D. C. 20361
Attention: E.A. Lichtman AIR-330E

Navy Department
Naval Air Systems Command
Washington, D. C. 20361
Attention: G. Derderian AIR-5362C

NAVAL AIR Propulsion Test Center
Trenton, NJ 08628
Attention: J. J. Curry
A. A. Martino (2)

USAVRAD Command
PO Box 209
St. Louis, MO 63166
Attention: Robert M. Titus (ASTIO)

Department of Transportation
NASA/DOT Joint Office of Noise Abatement
Washington, D.C. 20590
Attention: C. Foster

Federal Aviation Administration
12 New England Executive Park
Burlington, MA 18083
Attention: Jack A. Sain, ANE-200

Curtiss Wright Corporation
Woodridge, NJ 07075
Attention: S. Lombardo
S. Moskowitz (2)

Detroit Diesel Allison Div. G.M.C.
P.O. Box 894
Indianapolis, IN 46206
Attention: W. L. McIntire

AVCO/Lycoming
550 S. Main Street
Stratford, CT 06497
Attention: H. Moellmann

The Garrett Corporation
AIResearch Manufacturing Co.
Torrance, CA 90509
Attention: F. E. Faulkner

The Garrettt Corportion
AIResearch Manufacturing Co.
402 S. 36 Street
Phoenix, AZ 85034
Attention: Library

General Electric Co./AEG
One Jimson Road
Evendale, Ohio 45215
Attention: R.W. Bucy (3 copies)
T. F. Donohue
(4)

Pratt & Whitney Aircraft Group/UTC
Government Products Division
P.O. Box 2691
West Palm Beach, Fl 33402
Attention: B. A. Jones

AIResearch Manufacturing Co.
111 South 34th Street
P.O. Box 5217
Phoenix, AZ 85010
Attention: C. E. Corrigan
(93-120/503-4F)

Williams Research Co.
2280 W. Maple Road
Walled Lake, MI 48088
Attention: R. VanNimwegen
R. Horn (3)
Library

Teledyne CAE, Turbine Engines
1330 Laskey Road
Tolendo, Ohio 43612
Attention: R. H. Gaylord

General Electric Co./AEG
1000 Western Ave.
Lynn, MA 01910
Attention: R. E. Neitzel

Pratt & Whitney Aircraft Group/UTC
Commercial Products Division
East Hartford, Ct 06108
Attention: D. Gray

MS-118-26

LIST OF DISTRIBUTION (continued)

Douglas Aircraft Company
McDonnell Douglas Corp.
3855 Lakewood Boulevard
Long Beach, CA 90846
Attention: R. T. Kawai Code 36-41
M. Klotzsche (2)

Lockheed California Co.
Burbank, CA 91502
Attention: J. F. Stroud, Dept. 75-42
R. Tullis, Dept. 75-21 (2)

Federal Aviation Administration
Noise Abatement Division
Washington, D. C. 20590
Attention: E. Sellman AEE-120

Detroit Diesel Allison Div. G.M.C.
333 West First St.
Dayton, OH 45402
Attention: F.H. Walters

Boeing Commercial Airplane Co.
P.O. Box 3707
Seattle, WA 98124
Attention: P.E. Johnson MS-9H-46

Boeing Commercial Airplane Co.
P.O. Box 3707
Seattle, WA 98124
Attention: D.C. Nordstrom MS-73-4F

Drexel University
College of Engineering
Philadelphia, PA 19104
Attention: A.M. Mellor

Brunswick Corporation
2000 Brunswick Lane
Deland, FL 32720
Attention: A. Erickson